Copyright is owned by the Author of the thesis. Permission is given for a copy to be downloaded by an individual for the purpose of research and private study only. The thesis may not be reproduced elsewhere without the permission of the Author.

Beyond endogenous enzymes: A microbial oxidoreductase platform for tea (*Camellia sinensis* (L.) Kuntze) catechin biotransformation

A thesis presented in partial fulfillment of the requirements for the degree of

Doctor of Philosophy

in

Food Technology

At Massey University, Manawatū, New Zealand

Prishanthini Muthulingam

2026



MASSEY UNIVERSITY
TE KUNENGA KI PŪREHUROA
UNIVERSITY OF NEW ZEALAND

“To my beloved Amma and Appa, my dear husband and son, and my two sisters —

this work is a testament to your unwavering love and sacrifices.”

Abstract

Black tea quality depends on the enzymatic oxidation of catechins into theaflavins, thearubigins, and related oxidation-associated metabolites; however, conventional processing relies on endogenous intracellular plant polyphenol oxidases that are difficult to regulate and highly susceptible to batch-to-batch variation. This thesis developed, optimized, and evaluated a microbial enzymatic platform using extracellular microbial polyphenol-oxidizing-like oxidoreductase (MPLO) activity from *Alcaligenes faecalis* NZRM 836 as a controllable biocatalytic system for tea catechin oxidation. Culture-dependent screening of tea-associated microorganisms identified multiple isolates exhibiting extracellular MPLO-associated activities, with *A. faecalis* selected for subsequent optimization and biotransformation studies. Response surface methodology was used to optimize fermentation conditions, yielding an extracellular enzyme preparation with 3.7–3.9-fold higher substrate oxidation activities.

Application of this preparation to green tea aqueous extract produced MPLO-treated tea (MPLO-T). Comparative HPLC-DAD and untargeted LC–MS/MS analyses demonstrated that MPLO-T exhibited an intermediate chemical profile positioned between minimally oxidized green tea and conventionally processed orthodox black tea. EGCG decreased markedly from 83.97 ± 5.87 mg/g DW in green tea to 18.24 ± 1.28 mg/g DW in MPLO-T, accompanied by the formation of oxidation-associated metabolites, including theaflavins, catechin dimers, and thearubigin-associated pigments, while retaining higher residual monomeric catechins than conventional black tea. Untargeted LC–MS metabolomics further identified multiple putative oxidation-associated intermediates consistent with controlled catechin biotransformation pathways. Functionally, MPLO-T retained strong antioxidant activity and exhibited significantly greater inhibitory activity against α-glucosidase and α-amylase than both green tea and black tea *in vitro*. Simulated INFOGEST gastrointestinal digestion further demonstrated improved *in vitro* phenolic bioaccessibility in MPLO-T relative to green tea. These outcomes were achieved through externally controlled enzyme dosage and a defined 5 h reaction window, thereby partially decoupling catechin biotransformation from variability associated with endogenous leaf enzymes.

Overall, this study provides quantitative evidence that extracellular MPLO preparations from *A. faecalis* can mediate experimentally controlled transformation of tea catechins and generate a tea product with an intermediate oxidative profile with promising functional properties. The findings

improve mechanistic understanding of microbial contributions to tea polyphenol transformation and establish a practical framework for potentially tunable oxidation-based tea bioprocessing. Future work should focus on genomic and proteomic characterization of MPLO-associated activities, pilot-scale validation, sensory evaluation, and regulatory assessment for industrial translation.

Acknowledgements

This thesis represents not only years of research and learning, but also the encouragement, kindness, and support of many individuals and institutions who accompanied me throughout this journey.

I deeply appreciate my primary supervisor, Asso. Prof. Ali Rashidinejad, for his outstanding guidance, insightful feedback, and unwavering support throughout my research. His expertise was crucial from start to finish. I am especially thankful to him for becoming my primary supervisor after Dr. Popovich left Massey University. His encouragement during my health and financial difficulties was invaluable, and his kindness and reassurance made him a constant source of support throughout my PhD journey.

I am sincerely grateful to Dr. David Popovich for accepting my research proposal and initiating this research. I also thank my co-supervisors, Asso. Prof. Carl H. Mesarich, Prof. Chandrika M. Nanayakkara, and Prof. P. A. Nimal Punyasiri, for their advice, constructive criticism, and steady encouragement. I am especially grateful to Prof. Nanayakkara and Prof. Punyasiri for introducing me to tea factories, helping me build industry connections, and supporting my research while I worked offshore during the COVID-19 lockdown and the closure of New Zealand's borders. The combined expertise of my supervisory team greatly enriched this multidisciplinary study.

I owe a special word of thanks to Prof. Carl H. Mesarich, who joined my supervisory team midway through my PhD and became a tremendous source of support. His thoughtful insights into revising manuscripts and reviewing this thesis strengthened my work considerably, and his kind words and steady encouragement kept me motivated when I needed it most. I am deeply grateful for the time, care, and generosity he gave so willingly.

My sincere thanks go to the technical staff whose assistance was essential to the successful completion of this work. I am particularly grateful to Maggie Zou for her patience and guidance during HPLC training in the Te Rourou Laboratory, Massey University, Palmerston North. I also thank Ann-Marie and Baizura from the Microbiology Laboratory; the late David Lun, Milson Fransis, Dr. Daniel Bernstein, and Dr. Karl Fraser for their assistance with LC-MS work; Jack for training in SDS-PAGE; and Peter Zhu for his assistance with GC-MS. Their expertise and willingness to help were invaluable.

I gratefully acknowledge my employer, Eastern University, Sri Lanka, for granting me three years of paid leave, which allowed me to dedicate myself fully to this PhD journey. I also acknowledge with gratitude the financial support provided by the AHEAD PhD Grant (AHEAD/PhD/R3/Tech/406) from the Government of Sri Lanka, and I thank the Riddet Institute, Massey University, for supporting my fourth year of tuition. I further acknowledge the School of Food Technology and Natural Sciences at Massey University, together with the Riddet Institute, for providing excellent research facilities and a stimulating academic environment. I am also thankful to the Department of Plant Sciences at the University of Colombo for supporting the initial phase of this research in Sri Lanka.

I am deeply thankful to Dr. Roshan Rajadurai, Managing Director of the Hayleys Plantation Sector (Talawakelle Tea Estates and Kelani Valley Plantations, Sri Lanka), for granting access to tea estates and facilitating the collection of the high-quality samples essential for this study. I gratefully acknowledge the support and assistance of the managers and staff of Summerset and Radella Tea Factories. I am also deeply thankful to my cousin Jegathees, whose help with transport and companionship during sampling visits to the tea factories was greatly appreciated.

I owe a special word of thanks to Sheba and Kaushi, who are very close to my heart. We shared the laboratories, the long days of experiments, and the companionship that made the hardest stretches of this journey bearable. Their constant support, patience, and kindness meant more to me than I can express, and I will always treasure the friendship we built along the way.

I am also grateful to Wasana, Dilushi, and Hansani, who have been like sisters to me; their unwavering support and heartfelt conversations were truly invaluable. I extend my gratitude to my fellow postgraduate students, Srinithi, Crisline, Suji, Farah, Krisha, Ili, Maru, Linda, Yalda, Faruk, Reza, Maryam, and Gloria, whose support enriched this journey. My sincere thanks also go to the Palmerston North Tamil School community for their love and support, especially my childhood friend Laura and her family.

On a personal note, I extend my deepest gratitude to my beloved husband, Pushpakanth, and our son, Tejonidh. Pushpa, thank you for your unwavering love and patience and for being my rock. Tejo, my little teddy bear, you were my daily stress reliever and brought peace after every hard day. Your innocent questions about my research often became unexpected eye-openers, bringing clarity and joy. I am profoundly grateful to my parents, Mr. and Mrs. Muthulingam, for their

sacrifices and belief in me; fulfilling their dreams through this achievement fills me with a deep sense of honor. My thanks also go to my sisters, Priya and Yali, for their constant encouragement. My father's advice, never to step backward once a decision is made, remains my guiding principle. Finally, I acknowledge the resilience that carried me through, and I thank all who supported me, directly or indirectly. In each of you, I see God's kindness.

List of publications

A) Published peer-reviewed journal articles from this PhD research

- **Muthulingam, P**., Popovich, D. G., Nimal Punyasiri, P. A., Nanayakkara, C. M., Mesarich, C. H., & Rashidinejad, A. (2025). Development of a validated efficient HPLC-DAD analysis for assessing polyphenol transformation during black tea processing. *Journal of Food Composition and Analysis*, 148, 108330. https://10.1016/j.jfca.2025.108330 **(Chapter 3)**
- **Muthulingam, P**., Rashidinejad, A., Popovich, D., Punyasiri, P. A. N., Nanayakkara, C. M., & Mesarich, C. H. (2025). Microbial polyphenol oxidases in tea catechin oxidation: A novel approach to tea biotransformation. *Food and Bioproducts Processing*, 154, 731-740. https://10.1016/j.fbp.2025.11.012 **(Part of Chapter 4)**

B) Submitted manuscripts (under review) and manuscripts in preparation

- **Muthulingam, P.,** Popovich, D. G., Nimal Punyasiri, P. A., Nanayakkara, C. M., Mesarich, C. H., & Rashidinejad, A (2026). Extracellular polyphenol oxidase–producing fungi in Sri Lankan black tea processing: Culture-dependent screening and phylogenetic characterization. *Journal of Food Science and Technology* (Springer) - Under review **(Part of Chapter 4)**
- **Muthulingam, P**., Popovich, D. G., Nimal Punyasiri, P. A., Nanayakkara, C. M., Mesarich, C. H., & Rashidinejad, A (2026). Optimization and characterization of a bacterial polyphenol-oxidizing enzyme preparation for enhanced green tea functionality. *Food Research International* - In preparation **(Chapter 5)**
- **Muthulingam, P**., Popovich, D. G., Nimal Punyasiri, P. A., Nanayakkara, C. M., Mesarich, C. H., & Rashidinejad, A (2026). Controlled biotransformation of tea catechins using microbial polyphenol oxidizing-like enzymes: Comparative metabolomic and functional evaluation against green and black tea (2026). *Food Chemistry* - In preparation- **(Chapter 6)**

Conference proceedings and presentations

- Isolation and screening of microorganisms involved in black tea processing with polyphenol oxidase activity — Oral/poster presentation, Food Structure, Digestion and

Health International Conference 2023, Queenstown, New Zealand (14–17 November 2023).

- Exploring the culturable microorganisms of industrial black tea (*Camellia sinensis*) processing and their potential to oxidize tea polyphenols — 3-Minute Thesis (3MT) video presentation, Riddet Institute student colloquium 2023, Queenstown, New Zealand (14–17 November 2023).
- Exploring the culturable microorganisms of industrial black tea (*Camellia sinensis*) processing and their potential to oxidize tea polyphenols — 3-Minute Thesis (3MT) presentation, Riddet Institute student colloquium, Palmerston North, New Zealand (30 August 2024).
- Understanding the dynamic changes of non-volatile metabolites in black tea during industrial processing — 3-Minute Thesis (3MT) presentation, New Zealand Institute of Food Science and Technology Annual Conference 2024, Hamilton, New Zealand (2–4 July 2024).
- The role of oxidative reactions in key compound transformations during black tea manufacture — Oral presentation, Nutrition Society of New Zealand Conference 2024, University of Otago, Christchurch, New Zealand (28–29 November 2024).
- The microbial touch: unveiling the enzymatic power of *Alcaligenes faecalis* in tea (*Camellia sinensis*) — Poster presentation, New Zealand Institute of Food Science and Technology Annual Conference 2025, Palmerston North, New Zealand (24–26 June 2025).
- Boosting tea quality: optimizing laccase-like enzymatic production from *Alcaligenes faecalis* for enhanced polyphenol oxidation — Oral presentation, Riddet Institute student colloquium 2025, Wellington, New Zealand (8–10 September 2025).
- Optimized phenol-oxidizing enzyme cocktail from *Alcaligenes faecalis* for controlled catechin biotransformation and theaflavin generation-Poster presentation, New Zealand Institute of Food Science and Technology Annual Conference 2026, Auckland, New Zealand (30 June-2 July 2026)

Table of contents

Abstract ..... **i**

Acknowledgements ..... **iii**

List of publications ..... **vi**

Table of contents ..... **viii**

List of figures ..... **xvi**

List of tables ..... **xxiii**

List of abbreviations ..... **xxv**

1 Chapter 1 ..... **1**

1.1 Background and context 2

1.1.1 Terminology clarification: Polyphenol oxidase (PPO) and PPO-like oxidoreductases 2

1.1.2 Limitations of endogenous enzyme-driven oxidation and the emerging role of microbial polyphenol-oxidizing-like oxidoreductases (MPLOs) as complementary catalysts… 3

1.2 Research gaps and rationale for a microbial enzymatic approach 4

1.3 Research aim, objectives, and hypotheses 4

1.3.1 Research aim 4

1.3.2 Specific research objectives 5

1.3.3 Research hypotheses 5

1.4 Research questions 6

1.5 Scope and limitations 7

1.6 Conceptual framework and structure of the thesis 8

2 Chapter 2 ..... **10**

Abstract 11

2.1 Introduction to tea as a global beverage and its significance 12

2.2 Introduction to tea biochemistry 15

2.2.1 Native polyphenols 16

2.2.2 Non-polyphenolic constituents of tea 18

2.3 Black tea processing and the biochemistry of catechin oxidation 19

2.3.1 Overview of black tea processing 21
2.3.2 Enzymatic initiation of catechin oxidation 23
2.3.3 Early quinone reactions and intermediate formation 23
2.3.4 Formation of benzotropolone structures and theaflavins 24
2.3.5 Higher order benzotropolone oligomers 24
2.3.6 Formation of theasinensins, oolongtheanins, and theacitrins 25
2.3.7 Pathways leading to thearubigins and theabrownins 27
2.3.8 Factors influencing dynamics of oxidation 28
2.4 Endogenous PPOs: Role and limitations 29
2.4.1 Role of endogenous PPOs in black tea oxidation 29
2.4.2 Biochemical and environmental limitations 30
2.4.3 Implications and opportunities for innovation 31
2.5 Microbial contributions to tea processing and quality 32
2.5.1 Microbial presence during black tea manufacturing 32
2.5.2 Microbial succession and enzymatic activity in black tea 33
2.5.3 Microbial fermentation in dark and post-fermented teas 34
2.5.4 MPLOs as biotechnological tools 34
2.5.5 Bacterial extracellular enzymes as biocatalysts 35
2.6 Advances in production, purification, and application of MPLOs 37
2.6.1 Screening and identification of PPO-producing microorganisms 37
2.6.2 Analytical methods for polyphenol oxidizing enzymatic activity measurement 40
2.6.3 Screening of related MPLO and associated oxidoreductases 40
2.6.4 Optimization of enzyme production 43
2.6.5 Purification strategies for MPLOs 44
2.6.6 Applications of MPLOs in tea biotransformation and beyond 45
2.7 Analytical approaches for tea chemical and functional evaluation 47
2.7.1 Sample preparation and extraction techniques 47
2.7.2 Traditional analytical methods 49
2.7.3 High-performance liquid chromatography with diode array detection (HPLC–DAD) for targeted polyphenol quantification 50

2.7.4 LC-MS/MS and LC-HRMS for structural confirmation and intermediate detection 51

2.7.5 Gas chromatography–mass spectrometry (GC–MS) for volatile and semi-volatile profiling 52

2.7.6 Analytical challenges in thearubigin characterization 52

2.7.7 Antioxidant capacity assays for functional evaluation..... 53

2.7.8 Integrated multi-method frameworks for comprehensive evaluation 54

2.8 Synthesis of literature and identification of research gaps..... 55

3 Chapter 3..... 58

Abstract 59

3.1 Introduction 60

3.2 Materials and methods 61

3.2.1 Chemicals and instrumentation 61

3.2.2 Preparation of standard solutions 62

3.2.3 HPLC analysis..... 63

3.2.4 Calibration and validation 63

3.2.5 Extraction procedure and optimization 64

3.2.6 Dynamics of the major tea polyphenols during black tea processing 64

3.2.7 Statistical and data analysis..... 66

3.3 Results and discussion 66

3.3.1 Separation of tea compounds 66

3.3.1.1 Method validation and performance 67

3.3.1.2 Method comparison with published methods 70

3.3.2 Optimization of extraction methods..... 72

3.3.3 Dynamics of the major tea polyphenols during black tea processing 76

3.3.3.1 Polyphenol dynamics 76

3.3.3.2 Correlation and clustering analysis 79

3.4 Conclusions 82

4 Chapter 4..... 84

Abstract 85

4.1 Introduction 86

4.2 Materials and methods 87
4.2.1 Chemicals, media, and instruments 87
4.2.2 Sample collection 88
4.2.3 Isolation of bacteria and fungi from tea and processing environments 88
4.2.3.1 Bacterial isolation 89
4.2.3.2 Fungal isolation 90
4.2.3.3 Preservation and morphological characterization 90
4.2.4 Screening for extracellular MPLO activity 90
4.2.5 Molecular identification of MPLO-positive isolates 91
4.2.6 Enzyme activity profiling of *A. faecalis* 92
4.2.6.1 Catechol-like oxidase activity 92
4.2.6.2 Laccase-like activity 92
4.2.6.3 Peroxidase-associated activity 93
4.2.7 EGCG oxidation by *A. faecalis* crude enzymes 93
4.2.7.1 HPLC analysis of EGCG oxidation-associated metabolites 93
4.2.7.2 Quantification of tea pigments (TFs, TRs, and TBs) 94
4.2.8 Statistical analysis 95
4.3 Results and discussion 95
4.3.1 Microbial diversity across tea processing stages 95
4.3.2 Molecular identification and taxonomic composition of MPLO-positive isolates 97
4.3.3 MPLO activity of the identified bacterial and fungal isolates 99
4.3.3.1 MPLO-positive bacterial isolates 99
4.3.3.2 MPLO-positive fungal isolates 99
4.3.4 Phylogenetic relationships and association with MPLO activity 101
4.3.5 Biochemical and molecular characterization of *Alcaligenes faecalis* NZRM 836 105
4.3.6 Profiling of *Alcaligenes faecalis* NZRM 836 crude enzyme preparations 106
4.3.7 Oxidation of EGCG by *A. faecalis* enzyme filtrate 109
4.3.7.1 Proposed mechanism of EGCG oxidation 115
4.4 Conclusions 117
5 Chapter 5 118

Abstract 119
5.1 Introduction 120
5.2 Materials and methods 121
5.2.1 Chemicals and reagents 121
5.2.2 Culture media 122
5.2.3 Instruments and analytical equipment 122
5.2.4 Microorganism and inoculum preparation 123
5.2.5 Preliminary media screening and inoculum size optimization 123
5.2.6 Culture conditions and addition of inducer/cofactor for response surface methodology (RSM) optimization 124
5.2.7 Enzyme activity assays 124
5.2.8 Experimental design and statistical analysis 125
5.2.8.1 Central composite design 125
5.2.8.2 Response surface modeling 126
5.2.8.3 Multi-objective optimization by desirability function application 126
5.2.8.4 Verification of the predicted optimum 127
5.2.9 Production and partial purification of the MPLO enzyme preparation 127
5.2.10 Sodium dodecyl sulfate–polyacrylamide gel electrophoresis (SDS-PAGE) 128
5.2.11 *In silico* genome mining of reference *Alcaligenes faecalis* genomes associated with extracellular MPLO-associated activities 128
5.2.12 Characterization of the partially purified MPLO enzyme preparation 128
5.2.12.1 Optimum temperature and pH 129
5.2.12.2 Thermal stability 129
5.2.12.3 pH stability 129
5.2.12.4 Substrate specificity 129
5.2.12.5 Effect of inhibitors and metal ions 130
5.2.12.6 Enzyme kinetics 130
5.2.13 *In-vitro* oxidation of EGCG (model system) using MPLO preparation 130
5.2.14 Application of the MPLO preparation on green tea matrix 131
5.2.14.1 Preparation of green tea extract 131
5.2.14.2 Time–dose optimization of MPLO-mediated oxidation 131

5.2.14.3 Kinetic evaluation under optimized conditions 132
5.2.15 HPLC analysis of key polyphenols and spectrophotometric quantification of tea pigments. 132
5.2.16 Statistical data analysis 133
5.3 Results and discussion 134
5.3.1 Preliminary media screening: Growth kinetics and MPLO activity profiling 134
5.3.2 RSM model fitting and statistical evaluation 137
5.3.3 Response surface analysis and effect of culture duration 140
5.3.4 Partial purification and concentration 143
5.3.5 SDS-PAGE analysis of the partially purified MPLO enzyme preparation 144
5.3.6 Characterization of *Alcaligenes faecalis* NZRM 836 MPLO preparation 145
5.3.6.1 pH and temperature profiles 145
5.3.6.2 Thermal and pH stability 146
5.3.6.3 Substrate oxidation profiles 148
5.3.6.4 Apparent kinetic behavior 149
5.3.6.5 Effects of inhibitors and metal ions 150
5.3.7 *In-silico* genome mining of reference *Alcaligenes faecalis* genomes associated with extracellular MPLO-associated activities 152
5.3.8 *In-vitro* oxidation of EGCG and green tea extract using the MPLO enzyme preparation of *Alcaligenes faecalis* NZRM 836 154
5.3.8.1 *In-vitro* oxidation of the EGCG model system 154
5.3.8.2 *In-vitro* oxidation of green tea matrix 157
5.4 Conclusions 163
6 Chapter 6 165
Abstract 166
6.1 Introduction 167
6.2 Materials and methods 168
6.2.1 Chemicals and reagents 168
6.2.2 Instruments and analytical equipment 169
6.2.3 Microorganism and enzyme preparation 170
6.2.4 Preparation of tea samples 170

6.2.5 Chemical composition analysis 172
6.2.5.1 Determination of tea polyphenols 172
6.2.5.2 Determination of free amino acids 172
6.2.5.3 Determination of total reducing sugars 173
6.2.6 Chromatographic and metabolomic analysis 173
6.2.6.1 HPLC-DAD analysis of non-volatile compounds and spectrophotometric quantification of tea pigments 173
6.2.6.2 LC–MS/MS metabolite profiling 174
6.2.6.3 Data processing and multivariate chemometric analysis 175
6.2.7 Antioxidant activity evaluation 176
6.2.7.1 DPPH free radical scavenging activity 176
6.2.7.2 FRAP antioxidant activity 176
6.2.8 *In vitro* enzyme inhibition assays 177
6.2.8.1 Alpha-glucosidase inhibition assay 177
6.2.8.2 Alpha-amylase inhibition assay 178
6.2.8.3 Calculation of inhibitory activity 179
6.2.9 Simulated gastrointestinal digestion 179
6.2.10 Statistical analysis 181
6.3 Results and discussion 182
6.3.1 Changes in bulk chemical composition (total phenolics, amino acids, and reducing sugars) 182
6.3.2 MPLO-induced biotransformation of tea metabolites 184
6.3.2.1 Quantitative profiling of major tea metabolites by HPLC–DAD 184
6.3.2.2 Transformation of tea pigments (thearubigins and theabrownins) 187
6.3.2.3 Non-targeted LC–MS metabolomics 189
6.3.3 Functionality assessment 197
6.3.3.1 Antioxidant activity (DPPH and FRAP assays) 197
6.3.3.2 Enzyme inhibitory activity (α-glucosidase and α-amylase) 199
6.3.3.3 *In vitro* gastrointestinal digestion and bioaccessibility 201
6.3.4 Integrative multivariate analysis and overall insights 206
6.4 Conclusions 209

7 Chapter 7 211
7.1 Synthesis of key findings 212
7.2 Broader implications for tea biotechnology 215
7.3 Limitations and critical evaluation 216
7.4 Potential industrial and research applications 219
7.5 Summary of outcomes and answers to research questions 220
7.6 Recommendations for future work 224
7.7 Contribution to knowledge 225
7.8 Closing Statement 227
8 Bibliography 229
Appendices 258
Appendix A: Declaration on AI Usage in the thesis 259
Appendix B: Supplementary data for Chapter 3 260
Appendix C: Supplementary data for Chapter 4 265
Appendix D: Supplementary data for Chapter 5 267
Appendix E: Supplementary data for Chapter 6 274

List of figures

Figure 1.1: Integrated conceptual and experimental framework illustrating the alignment of research gaps, research questions, objectives, and corresponding thesis chapters. 9
Figure 2.1: Representative imagery of the Sri Lankan tea industry, illustrating the transition from raw harvest to the final consumer product. 13
Figure 2.2: Overview of global tea production and per-capita consumption (2024 estimates). Generated from the sources: FAO (2024); ITC Annual Bulletin of Statistics (2024); Tea & Coffee Trade Journal (2024/2025 Global Tea Reports). 14
Figure 2.3: Tea biotransformation pathways, illustrating the formation of distinct metabolites in green, oolong, black, and Pu-erh teas, with notes on analytical challenges. 14
Figure 2.4: Chemical structures of major tea catechins and their gallated derivatives. The figure illustrates the stereochemical variants of non-gallated catechins, including (+)-catechin, (−)-epicatechin, (+)-gallocatechin, and (−)-epigallocatechin, alongside their corresponding gallated forms: (−)-catechin gallate, (−)-epicatechin gallate, (+)-gallocatechin gallate, and (−)-epigallocatechin gallate. 16
Figure 2.5: Chemical structures of representative flavonols and phenolic acids identified in tea. (A) Flavonols, including quercetin, myricetin, and kaempferol, highlight variations in hydroxylation patterns on the flavonoid backbone. (B) Phenolic acids, comprising hydroxybenzoic acids (salicylic acid, gallic acid, vanillic acid, and dihydroxybenzoic acid) and hydroxycinnamic acids (caffeic acid, p-coumaric acid, and ferulic acid), along with chlorogenic acid. 17
Figure 2.6: Chemical structures of major tea alkaloids: caffeine, theobromine, and theophylline. 18
Figure 2.7: Integrated biochemical pathways of catechin oxidation during black tea processing (schematic representation without chemical structures). 22
Figure 2.8: Chemical structures of the major theaflavins and their derivatives formed during the oxidative polymerization of tea catechins. The figure is organized into three groups: (A) primary theaflavins and their gallated forms, including theaflavin (TF), theaflavin-3-gallate (TF3G), theaflavin-3′-gallate (TF3′G), and theaflavin 3-3′gallate (TFDG), as well as the structural isomers neotheaflavin and isotheaflavin and their gallates; (B) higher-order oxidation-associated metabolites, including theaflavates A and B and neotheaflavate A; and (C) theaflavic acid, epitheaflavic acid, and epitheaflavic acid-3′-gallate. R groups indicate sites of galloylation (R = H or galloyl). 25
Figure 2.9: Representative structures of theacitrinins (A–C) and theasinensin (A-F) derivatives identified in tea. These compounds are oxidative dimerization products of catechins formed during enzymatic or microbial oxidation. Colored highlighting distinguishes the two aromatic rings joined by the central biaryl bond, one positioned above and one below the

plane of rotation, reflecting the restricted-rotation, non-coplanar conformation characteristic of theasinensin-type biaryl linkages. 26
Figure 2.10: Flow chart of PPO-like enzyme production, purification and application pipeline. 38
Figure 2.11: Representative tertiary structures and reactions of microbial polyphenol-oxidizing-like oxidoreductases (MPLOs). (A) CotA laccase from *Bacillus subtilis* (PDB ID: 1GSK): a thermostable multicopper oxidase containing the T1/T2/T3 copper cluster; functions as a model for bacterial laccases and related multicopper oxidases. (B) Tyrosinase from *Streptomyces castaneoglobisporus* in the oxy form (PDB ID: 1WX2): shown with its caddie protein; features the conserved CuA–CuB dinuclear center; catalyses monophenol hydroxylation and diphenol oxidation. (C) Catechol oxidase from *Aspergillus oryzae* (PDB ID: 4J3P): a polyphenol oxidase with the canonical dinuclear copper active site; represents catechol-oxidase-type diphenolases. (D) Catechol oxidase reaction: catechol is oxidized to o-quinone; produces brown pigments. (E) Tyrosinase pathway: L-tyrosine is converted to L-DOPA; L-DOPA is further oxidized to dopaquinone; forms melanin-like intermediates. (F) Laccase reaction: ABTS is oxidized to the green-blue radical cation $ABTS^{+}$; it serves as a chromogenic reporter for multicopper oxidase activity. 41
Figure 2.12: Conceptual overview of literature synthesis and research gaps in microbial enzyme-mediated tea biotransformation. 57
Figure 3.1: Black tea processing stages, including plucking (A), withering (B), Rolling (C), Rotovane cutting (D), Oxidation (E), and Firing (F). 65
Figure 3.2: HPLC-DAD chromatograms of a mixed standard of 12 compounds (A), Green tea extract using 70% methanol by ultrasonication (B), and Black tea extract using 70% methanol by ultrasonication (C) at 210 nm. Peaks shown are gallic acid (3.75 min), theobromine (4.75 min), EGC (10.22 min), caffeine (11.35 min), catechin (11.83 min), EC (14.08 min), EGCG (14.86 min), ECG (19.12 min), TF (29.69 min), TF3G (31.05 min), TF3'G (31.72 min), and TF3-3'G (32.50 min). 67
Figure 3.3: Radar plot comparing the normalized analytical performance of the present HPLC method with previously reported methods. 72
Figure 3.4: Analytical visualization of bioactive compound profiles in green tea (GT) and black tea (BT) across 22 extraction methods. (A) Clustered heatmap of standardized concentrations (z-scores) for catechins, alkaloids, phenolic acids, and theaflavins across hot-water, ultrasonication-assisted solvent extractions, and ISO methods. Blue indicates below-average and red indicates above-average concentrations. (B) Principal component analysis (PCA) biplot showing sample clustering and compound loadings based on standardized concentrations. (C) Scree plot showing the proportion of variance explained by principal components. 75
Figure 3.5: Major catechins (A), theaflavins (B), gallic acid and theobromine (C1), caffeine (C2), and TPC (D) across eight black tea processing stages (FTL–FBT). 77
Figure 3.6: Correlogram of Pearson correlation coefficients among bioactive compounds during black tea processing. Compounds include catechins (Catechin, EC, EGC, EGCG, ECG),

theaflavins (Theaflavin, TF3G, TF3'G, TF3-3'G), and others (Gallic acid, Theobromine, Caffeine), assessed across processing stages: FTL, WTL, ROL, RTL, OTL 1, OTL 2, OTL 3, and FBT..... 80
Figure 3.7: Clustered heatmap of normalized z-scores for 12 bioactive compounds across black tea processing stages. Compounds are grouped into catechins, theaflavins, and others. Processing stages include FTL, WTL, ROL, RTL, OTL 1, OTL 2, OTL 3, and FBT. Z-scores are normalized per compound to highlight relative concentration trends. Color scale: blue = low z-scores (low concentrations), red = high z-scores (high concentrations). Dashed lines separate compound categories. 81
Figure 4.1: Black tea manufacturing process: Plucking of tea leaves (A); spreading of leaves on withering trays (B); withering of tea leaves (C); feeding withered leaves into rollers (D); rolling (E); cutting rolled leaves using a rotovane (F); oxidation (fermentation) of leaves on fermentation beds (G); drying and sorting of leaves for packing (H). 89
Figure 4.2: Relative frequency of isolates with detectable extracellular MPLO-associated activity (>0 U/mL) by isolation source in bacterial (A) and fungal (B) communities from tea processing. Abbreviations: FTL = fresh tea leaves; FTL-En = endophytes from fresh tea leaves; FTL-Ep = epiphytes from fresh tea leaves; WTL = withered leaves; RS = roller surfaces; RE = rolling equipment; RTL= rotovaned leaves; OTL = oxidized leaves; FB = fermentation beds; FBT = fired black tea; WT = withering trays; RT = Rotovane surfaces; AB = airborne/environmental. 97
Figure 4.3: Taxonomic compositions of microbial isolates with extracellular MPLO activity, displaying bacteria at the phylum (A) and genus (B) levels, and fungi at the phylum (C) and genus (D) levels..... 98
Figure 4.4: Macroscopic and microscopic morphology (scale bars = 10 µm) of the fungal isolate *Aspergillus fumigatus* EP09 grown on potato dextrose agar (PDA) medium for 168 h. Colonies arising from surface-sterilized leaf blocks (A). Colonies exhibit rapid growth, initially white, turning blue-green to grey-green with a powdery texture due to conidia development (B). Microscopic morphology shows conidia (c), conidiophores (cn), and vesicles (vs) (C). Conidiophores are uniseriate with a smooth stipe widening into a globular vesicle (20–30 µm) bearing phialides over the upper two-thirds. Conidia are globose to subglobose (2.5–3 µm), green, and arranged in chains. Hyphae are septate, hyaline, branched, and 2–4 µm in diameter. 100
Figure 4.5: Maximum Likelihood phylogenetic analysis of bacterial (A) and fungal (B) isolates recovered from orthodox black tea fermentation. Trees were inferred using the Maximum Likelihood method with 1,000 bootstrap replicates, and branches supported by <50% bootstrap values were collapsed. Bootstrap percentages (>50%) are shown below the corresponding nodes. Initial heuristic trees were generated using the Neighbor-Joining method with p-distance estimates. The final bacterial dataset included 27 nucleotide sequences with 970 aligned positions. All evolutionary analyses were performed in MEGA12 using parallel computing. 102

Figure 4.6: Comparative hierarchical clustering (Ward's method, Euclidean distance) of extracellular MPLO-associated activity in fungal and bacterial isolates from tea processing stages. (A, B) Fungal isolates: dendrogram with black leaf labels (A) and aligned MPLO activity bars colored by isolation source (B); clustering threshold 50 U/mL. (C, D) Bacterial isolates: dendrogram with black leaf labels (C) and aligned MPLO activity bars colored by isolation source (D); clustering threshold 40 U/mL. Isolation source color key: FTL (blue), FBT (pink), RS (green), RE (olive), OTL (purple), FB (brown), WTL (orange), WT (red), RTL (cyan). 104
Figure 4.7: *Alcaligenes faecalis* NZRM 836: Colony morphology on nutrient agar (left) and Gram-stained rods (right; Gram-negative bacilli, scale bar = 5 µm). 105
Figure 4.8: Trend of extracellular MPLO-associated activities during growth of *Alcaligenes faecalis* NZRM 836 in nutrient broth medium. 107
Figure 4.9: HPLC-DAD chromatograms showing the effect of different crude enzyme volumes on EGCG degradation, along with the appearance of oxidation-associated metabolites in the sample vials. Detection at 280 nm. (1) Mixed standard of 13 compounds; (2) Control (EGCG) before incubation; (3) 31.25 µL; (4) 62.5 µL; (5) 125 µL; (6) 250 µL; (7) 500 µL enzyme treatment; and (8) Control (EGCG) with inactivated enzyme preparation at the end of the reaction. 110
Figure 4.10: EGCG oxidation by *Alcaligenes faecalis* crude enzyme filtrate at 0, 31.25, 62.5, 125, 250, 500 µL, major products GA/GCG (A), and other catechins (GC, EGC, C, EC, ECG, CG) (B), SD error bars and letters denoting Tukey's HSD pairwise comparison results ($p < 0.05$). 112
Figure 4.11: Relative concentrations (%) of total theaflavins, thearubigins, and theabrownins formed at different crude extracellular enzyme preparation volumes. 114
Figure 4.12: Pathway of epigallocatechin gallate biotransformation into oxidation-associated tea polyphenols, proposed by the authors as a modification of existing literature pathways (Lei et al., 2021) to reflect the extracellular oxidoreductase activities characterized in this study. E1 represents esterase-associated activity; E2 represents catechol oxidase-like, peroxidase-like, or laccase-like activity; and E3 represents peroxidase-like or laccase-like activity. Peroxide species generated during oxidation may include hydrogen peroxide. 116
Figure 5.1: Growth of *Alcaligenes faecalis* NZRM 836 in lysogeny broth (LB), tryptic soy broth (TSB), and minimal broth (MB) supplemented with catechin, $CuSO_4$, or both. The upper panel shows the final OD_{600} at 60 h; the lower panel shows lag phase duration. Error bars = SD of mean (n=3). Hatching denotes additives (see legend). Values for longer lag phases in MB are indicated as >60 h or >40 h. 135
Figure 5.2: Time-course profiles of *Alcaligenes faecalis* NZRM 836 growth (OD_{600}) and extracellular MPLO-associated substrate oxidation activities during cultivation in Tryptic soy broth (TSB). Panels (A)–(D) show the production of ABTS-oxidizing activity (A), Catechol_oxidizing_activity (B), L_DOPA_oxidizing_activity (C), and Pyrogallol_oxidizing_activity (D), respectively, in relation to cell growth (OD_{600}, grey

line). Enzyme activities are expressed in U/mL, while optical density at 600 nm reflects biomass accumulation. 136
Figure 5.3: Effect of *Alcaligenes faecalis* NZRM 836 inoculum concentration (0.5–20% v/v) on extracellular MPLO-associated substrate oxidation activities in tryptic soy broth supplemented with (+)-catechin and $CuSO_4$ after 60 h cultivation. Curves show ABTS-, catechol-, pyrogallol-, and L-DOPA-oxidizing activities. 137
Figure 5.4: Experimental extracellular MPLO-associated substrate oxidation activities and model validation for *A. faecalis* NZRM 836 in the central composite design. Left panels (A, C, E, G): Mean ± SD of experimental ABTS-, pyrogallol-, catechol-, and L-DOPA-oxidizing activities, respectively, across all 20 design runs. Right panels (B, D, F, H): Actual versus predicted plots from the quadratic models. The dashed red line indicates the 1:1 reference. R^2 values are 0.841 (B), 0.840 (D), 0.811 (F), and 0.787 (H). 139
Figure 5.5: Response surface methodology (RSM) and contour plots illustrating the combined effects of catechin stock addition (X_1) and $CuSO_4$ stock addition (X_2) on the four MPLO-associated enzymatic activities of *Alcaligenes faecalis* NZRM 836 at a fixed culture duration of 54 h. Top row: 3D surfaces; bottom row: contour plots. The red star (★) indicates the X_1/X_2 position of the overall global optimum (occurring at 74 h; Table 5.3), projected onto this 54 h-fixed surface for visual reference; it does not represent a point directly calculated on this specific surface. Blue represents low activity; red represents high activity. 140
Figure 5.6: Effect of *Alcaligenes faecalis* NZRM 836 culture duration (12–96 h) on extracellular ABTS-, pyrogallol-, catechol-, and L-DOPA-oxidizing activities. Values represent mean ± SD (n = 3) with fitted linear trend lines. The red dashed line indicates the predicted global optimum at 74 h. 141
Figure 5.7: Derringer's desirability-based multi-objective optimization of extracellular MPLO-associated substrate oxidation activities from *Alcaligenes faecalis* NZRM 836. (A) Overall desirability surface showing the predicted global optimum at 74 h (101 µM catechin and 245 µM $CuSO_4$), indicated by a white star. (B) Individual desirability profiles for each substrate oxidation activity. (C) Comparison of substrate oxidation activities (U/mL) between the best experimental run and the globally optimized cultivation condition, with percentage improvements shown above bars. 142
Figure 5.8: SDS-PAGE profile of the partially purified extracellular MPLO preparation from *Alcaligenes faecalis* NZRM 836. Lane M: molecular weight marker; lanes 1–4: partially purified extracellular enzyme preparations from independent production batches. Multiple protein bands were observed, including prominent bands within the ~60–70 kDa and ~35–40 kDa regions, supporting the heterogeneous composition of the extracellular oxidoreductase preparation. 145
Figure 5.9: Effect of temperature (A) and pH (B) on the activity of the partially purified enzyme preparation from *Alcaligenes faecalis* NZRM 836 using ABTS and L-DOPA as substrates. Thermal stability of ABTS (C) and L-DOPA (D) after pre-incubation at different

temperatures (40–80 °C) for 0–24 h. pH stability of ABTS (E) and L-DOPA (F) after pre-incubation at pH 3, 5, and 7 for 0–24 h. Relative residual activity (%) is expressed as a percentage of the initial activity at 0 h. 147
Figure 5.10: Michaelis–Menten kinetic profiles of extracellular ABTS- and L-DOPA-oxidizing activities of the partially purified MPLO preparation from *Alcaligenes faecalis* NZRM 836. Enzyme activity (U/mL) is plotted against substrate concentration (mM). 150
Figure 5.11: Time-course profiles of EGCG biotransformation by the partially purified MPLO preparation in the model system over 60 minutes. (A) Depletion of EGCG and formation of major catechin products (catechin, EC, ECG). (B) Gallic acid formation and minor catechin products (EGC, GCG, CG). (C) Formation of individual theaflavins. 155
Figure 5.12: Effect of enzyme dose and incubation time on MPLO-mediated oxidation in a green tea matrix. (A) TF/TC ratio heatmap showing the time–dose dependence of oxidation efficiency. (B) Correlation matrix of major catechins, theaflavins, and derived indices, with circle size and color indicating Pearson correlation coefficients. 158
Figure 5.13: Time-course profiles of enzymatic oxidation using the MPLO preparation from *Alcaligenes faecalis* in green tea matrix over 10 hours. (A) Degradation of major catechins, (B) Trend of gallic acid, (C) Formation of individual theaflavins, and (D) Residual ABTS and L-DOPA activities with corresponding pH changes. 160
Figure 5.14: Visual progression of enzymatic oxidation of green tea infusion by the MPLO enzyme preparation from *Alcaligenes faecalis* NZRM 836. (A) The initial reaction mixture at 0 h, showing a pale-yellow color. (B) Time-dependent color development from 1 to 5 h, illustrating the transition from yellow to orange-brown associated with the formation of theaflavins and related oxidation-associated metabolites. (C) Proposed reaction network showing major substrates (blue circles), intermediates/side products (light blue), oxidation-associated metabolites (red diamonds), positive correlations (solid blue lines), negative correlations (dashed grey lines), and proposed pathway directions. 161
Figure 6.1: Integrated compositional comparison of green tea (GT), MPLO-treated tea (MPLO-T), and black tea (BT). Panels show (A) total phenolic content (TPC), (B) total free amino acids (TFAA), (C) total reducing sugars (TRS), and (D) normalized compositional heatmap expressed relative to GT (GT = 100). Bars in panels A–C represent mean ± SD (n = 3), and different letters indicate significant differences among samples within each parameter at $p < 0.05$. 183
Figure 6.2: Multivariate analysis of green tea (GT) and microbial polyphenol-oxidizing-like oxidoreductase-treated tea (MPLO-T) metabolite profiles showing (A) clustered heatmap of Z-score-normalized data, (B) PCA score plot with loading vectors, and (C) correlogram illustrating metabolite correlations. The analyses collectively demonstrate catechin depletion and formation of oxidation-associated metabolites during MPLO treatment. 186
Figure 6.3: Thearubigin (TR) and theabrownin (TB) contents (%) of green tea (GT), MPLO-treated tea (MPLO-T), and black tea (BT). Values are expressed as mean ± SD (n = 3). Different letters indicate significant differences within each parameter ($p < 0.05$). 188

Figure 6.4: Distribution of metabolite classes identified in green tea (GT), MPLO-treated tea (MPLO-T), and black tea (BT) based on untargeted LC–MS profiling. Compounds are grouped into major chemical classes, including catechins, flavonoids, phenolic acids, alkaloids, and oxidation-associated metabolites. 190
Figure 6.5: Multivariate analysis of LC–MS metabolomic profiles of green tea (GT), MPLO-treated tea (MPLO-T), and black tea (BT). Principal component analysis (PCA) score plot showing unsupervised separation of samples based on major sources of variance. 191
Figure 6.6: Clustered heatmap illustrating relative changes in catechin biotransformation-associated metabolites among minimally oxidized green tea (GT), MPLO-treated tea (MPLO-T), and black tea (BT) based on normalized LC–MS peak areas..... 192
Figure 6.7: Representative total ionization chromatogram (TIC) profiles and corresponding infusion colors of (A) green tea (GT), (B) MPLO-treated tea (MPLO-T), and (C) black tea (BT). 195
Figure 6.8: Proposed catechin biotransformation pathway in MPLO-treated tea (MPLO-T) based on LC–MS metabolomic profiling and the inferred activity of extracellular microbial polyphenol-oxidizing-like oxidoreductase (MPLO) components. The pathway illustrates the progression from native catechins to catechin dimers, theaflavins, thearubigin-associated intermediates, and downstream oxidation-associated metabolites detected during enzymatic treatment. Solid boxes represent metabolites detected in MPLO-T, whereas dashed boxes indicate putative or non-confirmed intermediates inferred from accurate mass and known tea oxidation systems. Proposed transformations include oxidative coupling, hydroxylation, ester hydrolysis, polymerization, and secondary oxidative degradation mediated by possible oxidoreductase-, hydroxylase-, esterase-, and peroxidase-associated activities. 196
Figure 6.9: Comparison of antioxidant activities of GT, BT, and MPLO-T aqueous tea extracts using DPPH (left axis) and FRAP (right axis) assays. 198
Figure 6.10: Inhibitory activity of tea infusions against α-glucosidase and α-amylase. 200
Figure 6.11: Phase-wise changes in phenolic compounds during simulated gastrointestinal digestion of green tea (GT), black tea (BT), and MPLO-treated tea (MPLO-T, 0.2% v/v). Panels show (A) total phenolic content (TPC), (B) epigallocatechin gallate (EGCG), (C) caffeine, (D) total catechins and (E) bioaccessibility heatmap. 204
Figure 6.12: Integrative multivariate analysis combining chemical and functional data of green tea (GT), microbial polyphenol-oxidizing-like oxidoreductase-treated tea (MPLO-T), and black tea (BT). (A) Pearson correlation heatmap between chemical and functional parameters. (B) Principal component analysis (PCA) score plot with loading vectors. PC1 accounts for 66.2%, and PC2 accounts for 33.8% of the total variance. 207

List of tables

Table 2.1: Major metabolites in tea: Composition, sensory attributes, and health benefits. 20
Table 2.2: Conceptual comparison of endogenous PPOs and microbial oxidoreductases (synthesized from literature discussed in Sections 2.3 and 2.4). 32
Table 2.3: Common screening assays, substrates, and references for catechol oxidase, laccase and tyrosinase. 42
Table 2.4: Applications of PPOs in tea biotransformation and other industries 46
Table 2.5: Summary of extraction techniques used for tea and biotransformed tea metabolites, including mechanisms, advantages, limitations, and typical operating parameters. 48
Table 2.6: Overview of analytical methods, including their strengths, limitations, and challenges in analyzing biotransformed teas. 50
Table 3.1: Calibration parameters for standard compounds analyzed by HPLC, including retention times, linearity ranges, regression equations, correlation coefficients (r^2), limits of detection (LOD), and limits of quantification (LOQ). 68
Table 3.2: Intra-day and inter-day precision expressed as relative standard deviations (RSD) of the HPLC method in terms of the retention time and peak areas of the 12 standards; n = 6 per day, 3 days. 69
Table 3.3: Recovery analysis of key analytes of tea using blank (ultrapure water) and black tea extract (n=3). 70
Table 3.4: Comparison of analytical performance parameters between the present HPLC method and previously reported methods. 71
Table 3.5: The comparison of different extraction methods and the yield of gallic acid, caffeine, total catechins, and total theaflavins (values denote mean ± SD, 6 replicates of each). 74
Table 3.6: Major polyphenolic content during black tea processing (mg/g DW ± SD, n=18). 78
Table 4.1: Morphological, biochemical, and growth characteristics of *Alcaligenes faecalis* NZRM 836. 106
Table 4.2: Concentrations of oxidation-associated metabolites across enzyme volumes (mg/L, mean ± SD, n = 3) using HPLC quantification. 111
Table 5.1: Assay conditions, wavelengths, and molar extinction coefficients used for the determination of substrate oxidation activities associated with the extracellular MPLO system. 125
Table 5.2: Statistical parameters of the quadratic models 138
Table 5.3: Global optimum conditions, predicted activities, and experimental verification results. 141
Table 5.4: Partial purification of the enzyme preparation produced by *Alcaligenes faecalis* NZRM 836 143
Table 5.5: Substrate specificity of the enzyme preparation expressed by *Alcaligenes faecalis* NZRM 836 as activity (U/mL) at different substrate concentrations. 148

Table 5.6: Effect of metal ions, inhibitors, and caffeine on the activity of the partially purified enzyme preparation from *Alcaligenes faecalis* NZRM 836 (residual activity % of control). 151
Table 5.7: Representative putative blue copper-containing multicopper oxidases and related oxidoreductases identified in reference *Alcaligenes faecalis* genomes. 152
Table 5.8: Changes in EGCG and associated catechin and oxidation products during treatment of a 1.00 mM EGCG model system with 0.5% (v/v) partially purified extracellular MPLO preparation from *Alcaligenes faecalis* NZRM 836 at 50 °C for 0, 10, 30, and 60 min, compared with a boiled-enzyme control at 60 min. 155
Table 5.9: Changes in major catechins, theaflavins, caffeine, color development (A_{420}), and Briskness Index during the initial 0–6 h of enzymatic oxidation of green tea infusion by the MPLO enzyme preparation. 159
Table 6.1: Statistical analysis of compositional parameters. 182
Table 6.2: Quantitative profiling of major tea metabolites with ANOVA statistics. 185
Table 6.3: Thearubigin (TR) and theabrownin (TB) content of tea samples. 188
Table 6.4: Oxidation-associated metabolites detected by LC–MS in green tea (GT), MPLO-treated tea (MPLO-T), and black tea (BT). 193
Table 6.5: Antioxidant activity of aqueous tea extracts (DPPH and FRAP). 198
Table 6.6: α-Glucosidase and α-Amylase inhibitory activity of tea infusions. 199
Table 6.7: Changes in (A) total phenolic content, (B) Epigallocatechin gallate (EGCG), (C) caffeine, and (D) total catechins during simulated gastrointestinal digestion of green tea (GT), black tea (BT), and MPLO-treated tea (MPLO-T). Values are expressed on a dry weight basis. 203
Table 6.8: Summary of key parameters and effect sizes (η^2) from one-way ANOVA. 208
Table 7.1: Key differences between the MPLO-mediated and conventional black tea oxidation systems. 214

List of abbreviations

Abbreviation	Full term
AB	Airborne/environmental
ABTS	2,2′-Azinobis(3-ethylbenzothiazoline-6-sulfonic acid)
AOAC	Association of Official Analytical Collaboration
ANOVA	Analysis of variance
BSA	Bovine serum albumin
BT	Black tea
C	(+)-Catechin
CCD	Central composite design
CG	Catechin gallate
$CuSO_4$	Copper(II) sulfate
CV	Coefficient of variation
DLLME	Dispersive liquid–liquid microextraction
DNA	Deoxyribonucleic acid
DPPH	2,2-Diphenyl-1-picrylhydrazyl
DW	Dry weight
EC	(−)-Epicatechin
ECG	(−)-Epicatechin gallate
EGC	(−)-Epigallocatechin
EGCG	(−)-Epigallocatechin gallate
EDTA	Ethylenediaminetetraacetic acid
FAO	Food and Agriculture Organization
FB	Fermentation bed
FBT	Fired black tea
FC	Folin–Ciocalteu
FRAP	Ferric reducing antioxidant power
FTIR	Fourier transform infrared spectroscopy
FTL	Fresh tea leaves
FTL-En	Endophytes from fresh tea leaves
FTL-Ep	Epiphytes from fresh tea leaves
GA	Gallic acid
GAE	Gallic acid equivalents
GC	(+)-Gallocatechin
GC–MS	Gas chromatography–mass spectrometry
GCG	(+)-Gallocatechin gallate

Abbreviation	Full term
GRAS	Generally Recognized as Safe
GT	Green tea
HBT	1-Hydroxybenzotriazole
HESI	Heated electrospray ionization
HPLC-DAD	High-performance liquid chromatography with diode array detection
HRMS	High-resolution mass spectrometry
INFOGEST	International consensus *in vitro* digestion method
ISO	International Organization for Standardization
ITS	Internal Transcribed Spacer
Km	Michaelis constant
L-DOPA	L-3,4-Dihydroxyphenylalanine
LB	Lysogeny broth
LC–MS	Liquid chromatography–mass spectrometry
LC–MS/MS	Liquid chromatography–tandem mass spectrometry
LOQ	Limit of quantification
LOD	Limit of detection
MAE	Microwave-assisted extraction
MB	Minimal broth
MCPT	Mechanochemical pretreatment
MEA	Malt extract agar
MEPS	Microextraction by packed sorbent
ML	Maximum Likelihood
MPLO	Microbial polyphenol oxidizing-like oxidoreductase
MPLO-T	MPLO-treated tea
MS	Mass spectrometry
MS^1	Full scan mass spectrometry
MWCO	Molecular weight cut-off
NA	Nutrient agar
NB	Nutrient broth
NIRS	Near-infrared spectroscopy
OD_{600}	Optical density at 600 nm
OTL	Oxidized tea leaves
PAGE	Polyacrylamide gel electrophoresis
PCA	Principal component analysis
PDB	Potato dextrose broth
PDA	Potato dextrose agar

Abbreviation	Full term
PFE	Pressurized fluid extraction
PLE	Pressurized liquid extraction
POD	Peroxidase
PPO	Polyphenol oxidase
QC	Quality control
RSD	Relative standard deviation
RSM	Response surface methodology
RS	Roller surfaces
RTL	Rotovaned leaves
SD	Standard deviation
SGF	Simulated gastric fluid
SIF	Simulated intestinal fluid
SSF	Simulated salivary fluid
TB	Theabrownin/Brightness (context-dependent)
TBI	Tea Board India
TBS	Tris-buffered saline
TC	Total color
TFAA	Total free amino acids
TF	Theaflavin
TF3G	Theaflavin-3-gallate
TF3′G	Theaflavin-3′-gallate
TF3-3′G / TFDG	Theaflavin-3,3′-digallate
TFs	Theaflavins
TR	Thearubigin
TRS	Total reducing sugars
TSA	Tryptic soy agar
TSB	Tryptic soy broth
TPC	Total phenolic content
UAE	Ultrasound-assisted extraction
UHPLC	Ultra-high-performance liquid chromatography
U/mL	Units per milliliter
UV	Ultraviolet
UV–Vis	Ultraviolet–visible spectroscopy
VOC	Volatile organic compound
WT	Withering trays
WTL	Withered tea leaves

Chapter 1

Introduction to thesis

Preface

This chapter introduces tea polyphenol biotransformation and the limitations of endogenous enzyme-driven oxidation in conventional tea processing. It outlines the emerging role of microbial polyphenol-oxidizing-like oxidoreductases (MPLOs) as complementary biocatalysts and presents the research objectives, hypotheses, and overall conceptual framework guiding this thesis.

1.1 Background and context

Tea (*Camellia sinensis* L.) is one of the most widely consumed beverages worldwide. Global production reached approximately 7.05 million metric tonnes in 2024 and continues to grow steadily, driven in part by increasing demand for functional and health-promoting products (FAO, 2024; Kumbasaroglu, 2026; TBI, 2024). Black tea remains the dominant category in production and trade, prized for its brisk flavor, bright reddish-brown liquor, and strong mouthfeel (Chen et al., 2023c). These characteristic attributes develop primarily during the enzymatic catechin oxidation stage of orthodox black tea processing. Mechanical disruption releases endogenous polyphenol oxidases (PPOs) and peroxidases (PODs), initiating oxidative catechin transformation reactions leading to the formation of theaflavins, thearubigins, and complex polymeric pigments (Cisneros-Yupanqui & Lante, 2020; Takemoto & Takemoto, 2018; Zou et al., 2024). These oxidation-associated metabolites contribute substantially to black tea color, briskness, astringency, and antioxidant properties (Akuli et al., 2012; Bhuyan et al., 2015; Tang et al., 2018). Thearubigins, in particular, remain structurally heterogeneous and poorly resolved, presenting persistent challenges for precise quality prediction (Zhu et al., 2021).

1.1.1 Terminology clarification: Polyphenol oxidase (PPO) and PPO-like oxidoreductases

In tea science, the term polyphenol oxidase (PPO) is frequently applied inconsistently. In this thesis, PPO refers exclusively to the endogenous, copper-containing catechol oxidase of tea leaves, which catalyzes the oxygen-dependent oxidation of o-diphenols during black tea manufacture (Obanda et al., 1997; Roberts & Smith, 1961; Tanaka & Matsuo, 2020). This enzyme initiates the formation of o-quinones that subsequently polymerize into theaflavins, thearubigins, and related pigments.

By contrast, microbial or exogenous systems often employ the term “PPO” more broadly to encompass phenolic-oxidizing enzymes such as tyrosinases, laccases, catechol oxidases, and peroxidases. These enzymes differ from plant PPO both structurally and mechanistically, despite catalyzing functionally analogous oxidation reactions of tea polyphenols (Claus, 2004; Claus, 2010; Mayer, 2006).

To ensure terminological precision, this thesis reserves the term 'PPO' exclusively for the endogenous plant enzyme. The term microbial polyphenol-oxidizing-like oxidoreductases (MPLOs) refers to microbial extracellular or cell-associated oxidoreductase systems that catalyze oxidation of tea polyphenols through mechanisms analogous to plant polyphenol oxidases, generating reactive quinone intermediates that drive catechin transformation, pigment formation, and polyphenol polymerization. The term MPLO is operational and activity-based rather than structurally or taxonomically defined and encompasses laccase-like multicopper oxidases, tyrosinase-like oxidoreductases, catechol oxidase-like activities, peroxidase-associated phenol-oxidizing systems, and related oxidative activities inferred from substrate-based assays.

1.1.2 Limitations of endogenous enzyme-driven oxidation and the emerging role of microbial polyphenol-oxidizing-like oxidoreductases (MPLOs) as complementary catalysts

Endogenous PPOs are central to the orthodox black tea oxidation reactions yet impose inherent constraints. These intracellular enzymes are sensitive to oxygen levels, mechanical shear, temperature fluctuations, and moisture loss, and they undergo rapid inactivation under processing stresses (Zhang et al., 2022; Zou et al., 2024). Once activated by tissue disruption, they are difficult to regulate under industrial processing conditions, resulting in substantial batch-to-batch variation in theaflavin–thearubigin ratios, pigment intensity, and residual catechin levels, and overall product consistency (Li et al., 2025b; Liu et al., 2023c; Mayer, 2006).

Tea-associated microorganisms originating from the phyllosphere, processing environments, and equipment surfaces may contribute to oxidation-associated chemistry during tea processing (Assad et al., 2023; Lin et al., 2022; Mondal et al., 2025; Tang et al., 2023). Some surviving microbial communities may remain metabolically active during early processing stages and secrete extracellular MPLOs capable of interacting with released catechins and related substrates. Unlike plant PPO, many microbial enzymes exhibit broader substrate specificity, operate via one-electron oxidation mechanisms, and tolerate wider environmental ranges (Murugesan et al., 2002; Verloop et al., 2016). Consequently, these systems may generate alternative quinone intermediates and oxidative coupling pathways that influence pigment formation, chemical composition, flavor development, and functional properties and coupling patterns, potentially yielding alternative

pigment structures, flavor, chemical profiles, and functional outcomes (Jia et al., 2022; Wang et al., 2023c).

This mechanistic diversity, combined with the ability to control enzyme dosage, reaction time, oxygen availability, and other process parameters, positions MPLO systems as complementary biocatalysts that decouple oxidation from the intrinsic variability of leaf enzymes.

1.2 Research gaps and rationale for a microbial enzymatic approach

Despite growing recognition of microbial contributions to phenolic oxidation, the deliberate use of MPLOs as controlled biocatalysts in black tea processing remains largely unexplored. Existing research has primarily focused on endogenous plant PPOs or complex fungal fermentation systems, while bacterial or fungal enzymes have received comparatively limited systematic investigation in tea-related contexts (Assad et al., 2023).

Extracellular bacterial MPLO systems offer several potential advantages for controlled biotransformation applications. They are frequently extracellular, readily produced in scalable cultures, and mechanistically distinct from endogenous plant PPO systems. A microbial enzymatic approach may therefore provide opportunities to improve process controllability, reduce variability associated with endogenous oxidation, and enable targeted modulation of tea chemical profiles and functional attributes. This thesis focuses primarily on extracellular MPLO from bacteria while recognizing that fungal enzymes also warrant future investigation.

1.3 Research aim, objectives, and hypotheses

1.3.1 Research aim

To develop, optimize, and evaluate a microbial enzyme-mediated catechin oxidation platform based on extracellular MPLOs from a selected bacterial isolate, and to assess its potential for controlled tea polyphenol biotransformation compared to conventional black tea oxidation systems.

1.3.2 Specific research objectives

1. To establish a comparative metabolite baseline profile of traditionally processed Sri Lankan orthodox black tea using HPLC-DAD as a reference framework for evaluating microbial tea biotransformation
2. To isolate, screen, and phylogenetically characterize MPLO-active microorganisms from tea-associated environments, and select a high-performing bacterial strain for further study.
3. To assess the polyphenol-oxidizing potential of crude extracellular enzyme extracts from the selected bacterial strain and evaluate their biotransformation of major tea catechins, including the disappearance of parent catechins, the formation of known oxidation-associated metabolites (e.g., theaflavins), and overall redox changes.
4. To optimize the production and reaction conditions of a bacterial extracellular MPLO preparation using response surface methodology to maximize enzyme yield and green tea biotransformation efficiency.
5. To partially purify and biochemically characterize the extracellular MPLO components from the selected strain, including pH/temperature optima, substrate oxidation profiles toward tea-relevant catechins, kinetic parameters, and stability.
6. To perform Liquid Chromatography coupled with tandem mass spectrometry untargeted LC-MS/MS polyphenolic profiling of microbially oxidized green tea, comparing it with traditional black tea and unoxidized green tea.
7. To evaluate selected functional properties of the microbial enzyme-oxidized product as comparative indicators, including total phenolics, antioxidant capacity, and *in vitro* bio-accessibility relative to traditional black tea and unoxidized green tea.

1.3.3 Research hypotheses

This research tests the central hypothesis that extracellular bacterial MPLO systems can mediate controlled oxidation of tea catechins and generate oxidation-associated chemical and functional changes comparable, in selected respects, to those occurring during orthodox black tea processing. Supporting this central hypothesis are the following sub-hypotheses:

1. Traditionally processed orthodox black tea exhibits characteristic metabolite profiles that can serve as analytical reference benchmarks for evaluating microbial catechin biotransformation.
2. Tea-associated environments contain microorganisms capable of producing extracellular MPLO systems with catechin-oxidizing activity.
3. Crude extracellular enzyme extracts from selected bacterial strains can catalyze oxidative transformation of major tea catechins, resulting in catechin depletion and formation of black tea-related oxidation-associated metabolites under controlled laboratory conditions.
4. Optimization of microbial enzyme production and reaction conditions using response surface methodology can significantly influence extracellular oxidoreductase activity and tea catechin biotransformation efficiency.
5. Partially purified extracellular MPLO preparations from the selected bacterial strain exhibit distinct biochemical characteristics, including substrate specificity, apparent kinetic behavior, and operational stability relevant to tea catechin oxidation.
6. MPLO-mediated oxidation of green tea alters selected functional properties, including total phenolic content, antioxidant capacity, and *in vitro* bioaccessibility, relative to unoxidized green tea and traditional black tea.

1.4 Research questions

1. Can traditionally processed Sri Lankan orthodox black tea provide a suitable analytical and metabolite reference framework for evaluating microbial tea catechin biotransformation?
2. Can MPLO-active microorganisms be isolated from tea-associated environments, and does the selected bacterial strain exhibit extracellular catechin-oxidizing activity relevant to tea biotransformation?
3. Can crude extracellular enzyme preparations from selected bacterial strains catalyze oxidative transformation of major tea catechins and generate black tea-related oxidation-associated metabolites under controlled laboratory conditions?
4. How do culture conditions and reaction parameters influence microbial oxidoreductase production and tea catechin biotransformation efficiency?

5. What biochemical characteristics, substrate preferences, apparent kinetic behavior, and operational stability properties are exhibited by partially purified MPLO from the selected bacterial strain?
6. How does the polyphenolic composition of microbially oxidized green tea compare with that of traditionally processed black tea and unoxidized green tea?
7. How does MPLO-mediated oxidation influence selected functional properties, including total phenolic content, antioxidant capacity, and *in vitro* bioaccessibility, relative to traditional black tea and unoxidized green tea?

1.5 Scope and limitations

This thesis investigates microbial enzyme-mediated tea catechin oxidation at laboratory scale through microbial isolation and screening, extracellular MPLO production and optimization, partial enzyme purification, controlled *in vitro* oxidation assays, targeted chemical profiling using HPLC-DAD and LC-MS/MS, and selected functional evaluations. Functional assessments include total phenolic content, antioxidant capacity, α-amylase and α-glucosidase inhibitory activities, and simulated gastrointestinal bioaccessibility using the INFOGEST digestion model. Enzyme characterization and kinetic analyses therefore reflect collective activity profiles of partially purified extracellular oxidoreductase systems rather than individually purified enzymes. Comprehensive screening and quantification of other extracellular enzyme classes potentially contributing to secondary catechin transformation reactions, including hydrolases, esterases, and dioxygenases, were beyond the scope of this study. Pilot-scale processing, industrial-scale validation, and process commercialization were beyond the scope of this study.

The study also excluded volatile compound profiling due to time constraints, sensory evaluation (requiring formulated products and consumer panels), long-term stability testing, and *in vivo* studies. The persistent analytical challenges in quantifying thearubigins owing to their structural heterogeneity are acknowledged (Zhu et al., 2021; Zou et al., 2025a).

Finally, biosecurity regulations prevented transport of microbial isolates obtained in Sri Lanka to New Zealand. Therefore, downstream experiments were conducted using a locally sourced *Alcaligenes faecalis* strain, with the study focusing on species-level MPLO-associated biotransformation potential rather than direct comparison of geographically distinct strains.

1.6 Conceptual framework and structure of the thesis

This thesis progresses from endogenous enzyme-dependent oxidation toward a controlled microbial biocatalytic approach. It advances through three main phases: foundational characterization, bioprocess development and enzymatic characterization, and comparative validation of chemical and functional outcomes.

This thesis is structured into seven chapters. **Chapter 1** introduces the research background, defines key terminology, and outlines the research aims, objectives, and hypotheses. **Chapter 2** reviews relevant literature on tea biochemistry, oxidation systems, and microbial oxidoreductases. **Chapter 3** establishes baseline profiles of traditional black tea. **Chapter 4** details microbial isolation and screening. **Chapter 5** presents optimization of extracellular MPLO production and biochemical characterization. **Chapter 6** evaluates biotransformation outcomes and functional properties. **Chapter 7** synthesizes findings, discusses implications, and proposes future directions. Figure 1.1 illustrates the integrated conceptual and experimental framework linking research gaps, questions, objectives, and chapters.



Figure 1.1: Integrated conceptual and experimental framework illustrating the alignment of research gaps, research questions, objectives, and corresponding thesis chapters.

Chapter 2

Literature review

Preface

This chapter reviews current knowledge on tea polyphenols, enzymatic oxidation pathways, microbial oxidoreductases, and analytical approaches used in tea research. It critically examines the biochemical and technological relevance of microbial oxidoreductase systems and identifies key knowledge gaps that form the basis for the present study.

Abstract

Tea, derived from *Camellia sinensis*, is a globally significant beverage whose quality is largely determined by the biochemical transformation of polyphenols during processing. Central to this transformation is the oxidation of catechins into key pigments such as theaflavins, thearubigins, and theabrownins through complex quinone-mediated pathways. These reactions are primarily initiated by endogenous polyphenol oxidases and peroxidases, whose catalytic activity, substrate specificity, and environmental sensitivity strongly influence oxidation dynamics and are associated with variability in black tea quality under industrial processing conditions.

The biochemical pathways underlying catechin oxidation involve sequential quinone formation, co-oxidation, benzotropolone generation, and progressive polymerization, resulting in structurally diverse and often poorly resolved products, particularly within the thearubigin fraction. This structural complexity presents significant analytical challenges and limits the extent to which these pathways can be fully resolved or quantitatively described.

In addition to plant-derived enzymes, increasing evidence suggests that microorganisms and their microbial polyphenol-oxidizing-like oxidoreductase (MPLO) systems contribute to tea polyphenol transformation. These functionally inferred oxidoreductase activities include laccase-like multicopper oxidases, tyrosinase-like oxidoreductases, catechol oxidase-like activities, and peroxidase-associated phenol-oxidizing systems capable of generating reactive quinone intermediates involved in catechin oxidation and pigment formation. Although microbial contributions are limited in conventional orthodox black tea manufacture, they play central roles in post-fermented teas and may provide a basis for developing externally controlled biocatalytic systems for tea oxidation. However, the application of microbial extracellular oxidoreductase systems as controllable platforms for tea catechin biotransformation remains relatively underexplored.

Advances in enzyme screening, production, purification, and analytical characterization, particularly chromatographic and mass spectrometric approaches, have improved the resolution of tea metabolite profiling. However, key gaps remain in mechanistic understanding, comparative enzymology, and process-level control, particularly regarding the deliberate and systematic use of microbial oxidoreductases in tea processing contexts.

This chapter critically reviews the existing literature on tea polyphenol chemistry, black tea oxidation biochemistry, polyphenol oxidases, microbial contributions to tea processing, and analytical approaches for evaluating tea composition and functionality. The review establishes the scientific foundation for the present study and culminates in the identification of clear research gaps addressed in subsequent chapters.

Keywords: Tea polyphenols; catechin oxidation; theaflavins; thearubigins; polyphenol oxidase; microbial oxidoreductases; enzymatic browning; tea biochemistry; biocatalysis; LC-MS/MS profiling.

2.1 Introduction to tea as a global beverage and its significance

Tea, derived from the leaves of *Camellia sinensis* (L.) Kuntze, is the world's second most consumed beverage after water and holds enduring cultural, economic, and health significance across societies (Hong et al., 2024; Kumar et al., 2025). Despite extensive processing innovation, tea manufacture still relies heavily on endogenous enzymatic oxidation systems that remain difficult to control consistently. This limitation provides a strong rationale for investigating alternative biocatalytic approaches for controlled catechin oxidation.

Although tea has a longstanding cultural importance across Asia and Europe, this thesis focuses primarily on tea biochemistry and oxidation chemistry. Major tea categories, including green, oolong, black, white, and Pu-erh teas, arise from differences in processing conditions and the extent of polyphenol oxidation, which determine their chemical composition and sensory properties (Adak & Abdel-Gabbar, 2011; Gascoyne et al., 2018).

As of 2024, global tea production reached approximately 7.05 million tonnes annually, with China contributing around 3.74 million tonnes and India between 1.28 and 1.37 million tonnes, together accounting for more than half of global output (FAO, 2022, 2024; Steffany et al., 2024; TBI, 2024). Other major producers include Kenya, Türkiye, Sri Lanka, Vietnam, and Indonesia (Koros et al., 2023). Figure 2.1 presents representative imagery of the Sri Lankan tea industry associated with this study, while Figure 2.2 summarizes global production and per capita consumption patterns (FAO, 2024; Koros et al., 2023).



Figure 2.1: Representative imagery of the Sri Lankan tea industry, illustrating the transition from raw harvest to the final consumer product.

Tea quality is strongly influenced by processing-dependent biochemical transformations. Green tea remains largely unoxidized, oolong tea is partially oxidized, black tea is fully oxidized, and dark teas such as Pu-erh undergo additional microbial fermentation (Figure 2.3). These processing-dependent differences primarily reflect variation in catechin oxidation systems, which govern pigment formation, flavor development, and sensory quality. Black tea remains the dominant product in international trade, representing approximately 38–42% of the global market (Adak & Abdel-Gabbar, 2011; Huda et al., 2024).

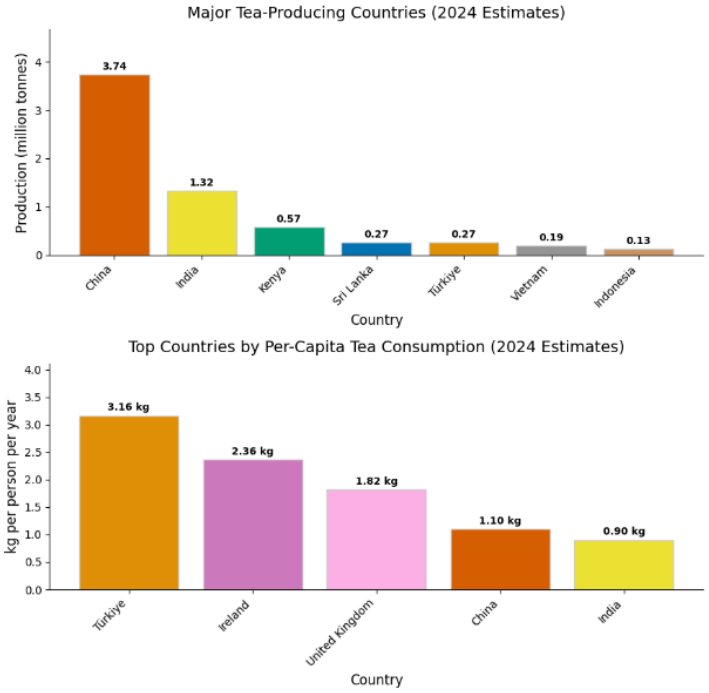

Figure 2.2: Overview of global tea production and per-capita consumption (2024 estimates). Generated from the sources: FAO (2024); ITC Annual Bulletin of Statistics (2024); Tea & Coffee Trade Journal (2024/2025 Global Tea Reports).

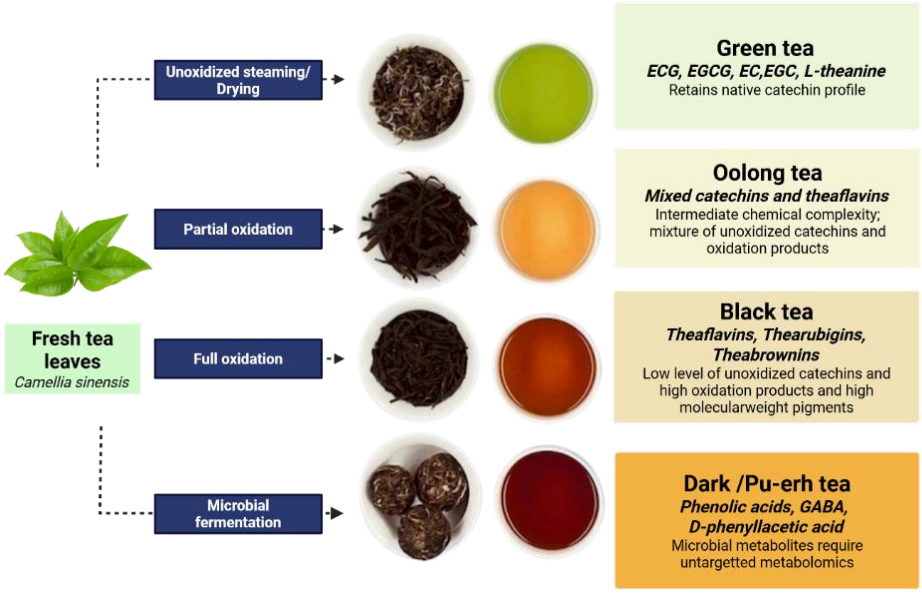

Figure 2.3: Tea biotransformation pathways, illustrating the formation of distinct metabolites in green, oolong, black, and Pu-erh teas, with notes on analytical challenges.

Tea production also supports millions of smallholder farmers worldwide, and emerging enzymatic and microbial technologies may provide opportunities for more controlled and value-added processing (Cabrera et al., 2006). Collectively, these factors highlight the importance of developing controllable oxidation systems capable of modulating tea polyphenol transformations under defined conditions.

2.2 Introduction to tea biochemistry

Tea quality is governed by multiple metabolite classes, but polyphenols and their oxidation-associated metabolites largely define the color–astringency characteristics that differentiates green versus black teas. In contrast, alkaloids and amino acids often modulate bitterness/umami but are less directly diagnostic of oxidation state. Accordingly, this thesis focuses primarily on polyphenol transformation chemistry and its controllability during black tea processing.

The chemical composition of tea derived from *C. sinensis* underpins its sensory qualities (flavor, color, aroma) and functional properties (antioxidant capacity, health benefits). Key metabolites include polyphenols, volatile organic compounds (VOCs), alkaloids, amino acids, carbohydrates, and minor components such as lipids, proteins, vitamins, minerals, saponins, and organic acids. These metabolites vary with cultivar, leaf maturity, agronomic conditions, and processing method. During withering, rolling, oxidation, fermentation, steaming, and drying, they undergo substantial biochemical transformation, altering substrate availability and redox conditions within the leaf matrix.

Among these metabolites, catechins are particularly important because they function as the primary substrates for oxidative pigment formation. Their structural differences, including galloylation and hydroxylation patterns, strongly influence quinone formation, benzotropolone generation, and subsequent polymerization reactions. These substrate-dependent differences contribute substantially to variability in endogenous oxidation systems and provide a biochemical basis for exploring externally controllable microbial oxidoreductases as alternative catalysts. Although multiple metabolite classes contribute to overall tea quality, the following sections emphasize pathways directly relevant to catechin oxidation, pigment formation, and controlled polyphenol biotransformation, which form the central focus of this thesis.

2.2.1 Native polyphenols

Native polyphenols constitute the major phenolic fraction in fresh *C. sinensis* leaves, which are central to tea's sensory qualities and antioxidant properties. Catechins (Figure 2.4) account for roughly 10–25% of leaf dry weight, with epigallocatechin gallate (EGCG) typically the most abundant, followed by Epigallocatechin (EGC), Epicatechin gallate (ECG), and EC. These flavan-3-ols contribute astringency and bitterness and provide strong free-radical-scavenging activity (Engelhardt, 2010; Goncalves et al., 2021; Ho et al., 2001). Catechin concentrations are generally highest in young shoots, which influences both raw material selection and subsequent oxidation behavior during processing (Lee et al., 2016).

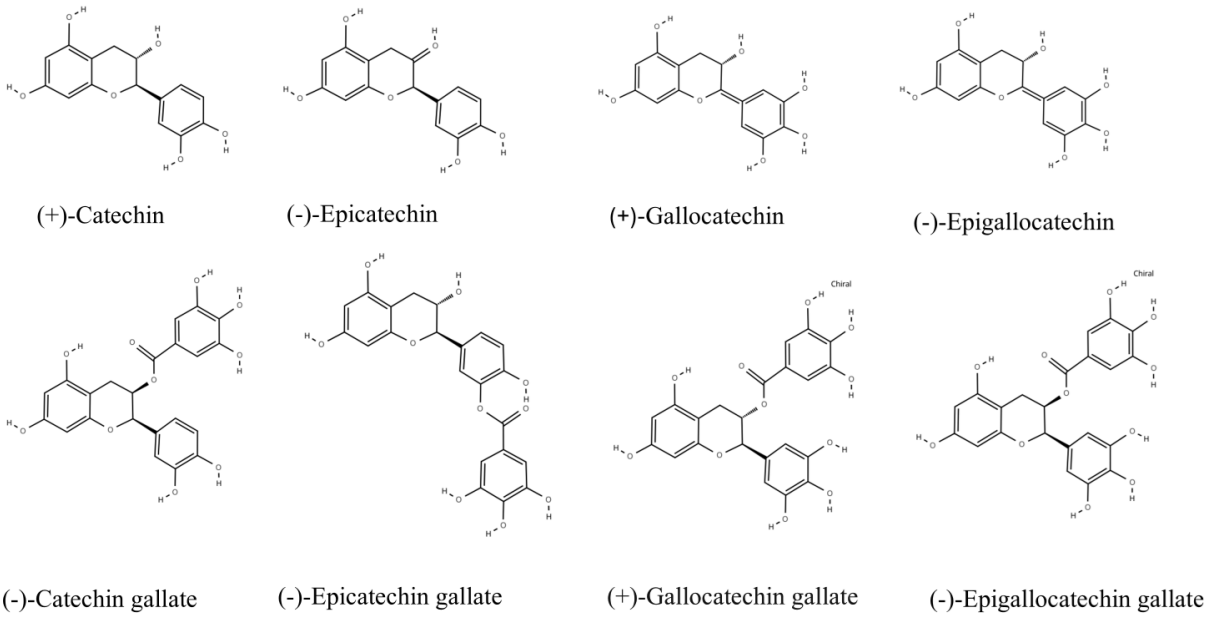

Figure 2.4: Chemical structures of major tea catechins and their gallated derivatives. The figure illustrates the stereochemical variants of non-gallated catechins, including (+)-catechin, (−)-epicatechin, (+)-gallocatechin, and (−)-epigallocatechin, alongside their corresponding gallated forms: (−)-catechin gallate, (−)-epicatechin gallate, (+)-gallocatechin gallate, and (−)-epigallocatechin gallate.

Processing strongly influences the retention or loss of these native catechins. Heat treatments used in green tea production rapidly inactivate oxidative enzymes, preserving monomeric catechins and maintaining the characteristic sharpness and high antioxidant potential (Aboulwafa et al., 2019; Adhikary et al., 2024). Partial oxidation in oolong tea and full oxidation in black tea progressively

reduce catechin levels, while post-fermented teas undergo additional microbial transformations that further diminish monomeric catechins and increase phenolic complexity (Kidist, 2019; Li et al., 2022d; Lu et al., 2023).

Several other polyphenol classes complement the catechin profile. Flavonols (Figure 2.5 A), such as quercetin, kaempferol, and myricetin, occur mainly as glycosides and contribute to antioxidant capacity, bitterness modulation, and color stability, while also serving as precursors for aroma-releasing reactions during thermal processing (Engelhardt, 2010; Yang et al., 2013). Phenolic acids (Figure 2.5B), including gallic, chlorogenic, and caffeic acids, provide mild astringency and participate in esterification reactions that generate gallated catechins such as EGCG and ECG (Haslam, 2003).

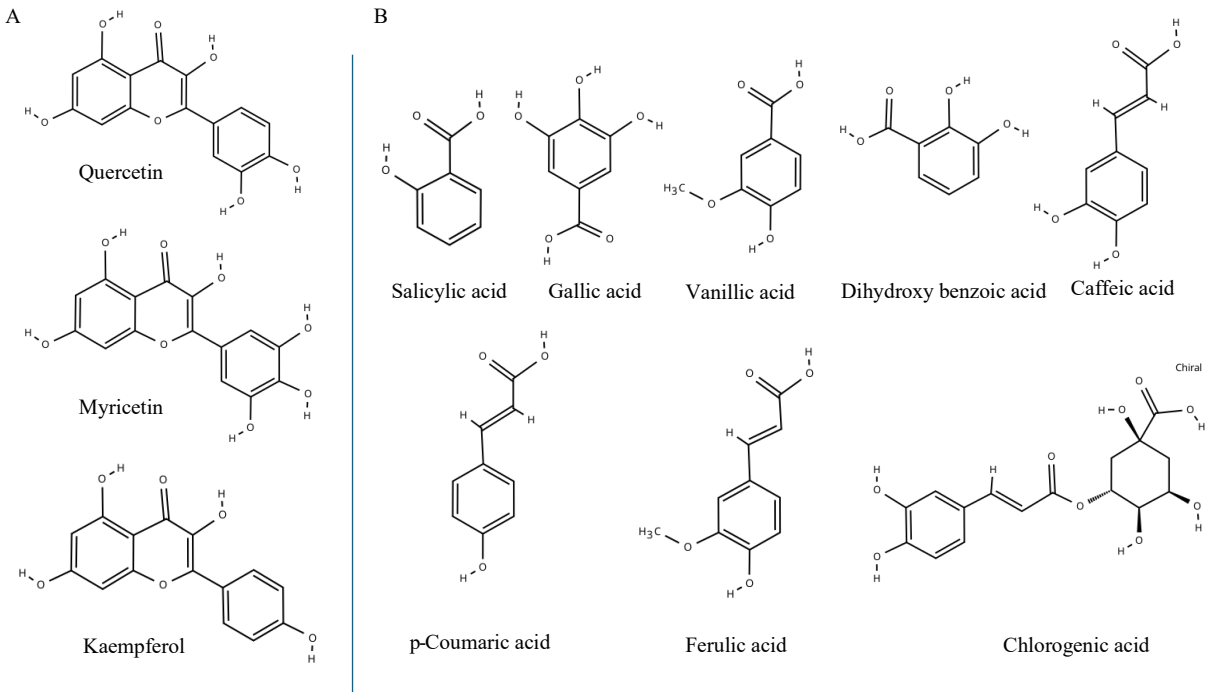

Figure 2.5: Chemical structures of representative flavonols and phenolic acids identified in tea. (A) Flavonols, including quercetin, myricetin, and kaempferol, highlight variations in hydroxylation patterns on the flavonoid backbone. (B) Phenolic acids, comprising hydroxybenzoic acids (salicylic acid, gallic acid, vanillic acid, and dihydroxybenzoic acid) and hydroxycinnamic acids (caffeic acid, p-coumaric acid, and ferulic acid), along with chlorogenic acid.

Proanthocyanidins, although present at lower levels than in many fruits, add further phenolic diversity and may undergo limited transformations during processing, influencing both taste and antioxidant behavior (Goncalves et al., 2021).

Tea catechins differ substantially in galloylation and hydroxylation patterns, which strongly influence their redox behavior and susceptibility to enzymatic oxidation. Consequently, catechin composition represents a major determinant of oxidation behavior and provides an important biochemical basis for evaluating controllable microbial oxidoreductase systems in this thesis.

2.2.2 Non-polyphenolic constituents of tea

Beyond polyphenols, tea contains several additional metabolite classes that contribute to flavor, aroma and bioactivity. Tea alkaloids (Figure 2.6), mainly caffeine, theobromine, and theophylline, are purine compounds that contribute to bitterness and physiological activity. Caffeine typically comprises 2 to 5% of dry weight, and contributes bitterness and interacts non-covalently with polyphenols, thereby modulating perceived astringency (Engelhardt, 2010; Harbowy et al., 2010).

However, because alkaloid concentrations remain relatively stable during processing and oxidation, they are considered secondary to polyphenol transformations in the chemistry of tea manufacture.

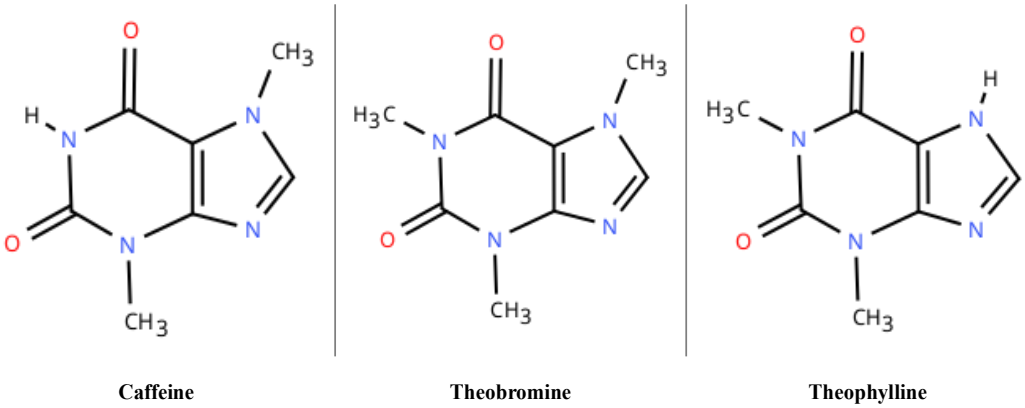

Figure 2.6: Chemical structures of major tea alkaloids: caffeine, theobromine, and theophylline.

Carbohydrates, typically 5 to 11% dry weight, provide mild sweetness and participate in Maillard and caramelization reactions during thermal processing (Aminianfar et al., 2024). Minor

constituents, including lipids, proteins, vitamins, minerals, saponins, and organic acids, contribute to nutritional value, color stability, and subtle flavor nuances (Engelhardt, 2010).

Volatile organic compounds (VOCs) form another key group of constituents and are responsible for the characteristic aroma profiles of different teas. Although present at only 0.01 to 0.05% of dry weight, more than 600 VOCs have been identified (Feng et al., 2019; Yang et al., 2013). These include terpenes such as linalool, geraniol, and nerolidol, aldehydes such as hexenal and benzaldehyde, and alcohols such as 2-phenylethanol.

VOCs originate from glycosidic and lipid precursors released during withering and rolling and are further diversified by enzymatic cleavage, oxidation, and thermal reactions during drying (Parveen et al., 2023; Yang et al., 2013). Microbial metabolism in fermented teas produces additional earthy and woody volatiles, contributing to their distinctive aroma profiles (Zhang et al., 2016). These VOC pathways further illustrate the interplay between plant and microbial metabolism during tea processing. Table 2.1 summarizes quantitative data for selected major compounds across tea types (values are approximate and vary by cultivar, origin, and processing).

2.3 Black tea processing and the biochemistry of catechin oxidation

The metabolites described in Section 2.2, particularly the native catechins, undergo extensive enzymatic transformation during black tea manufacture. This section outlines the processing steps that create the conditions for catechin oxidation and describes the biochemical pathways that convert these substrates into theaflavins, thearubigins, and related pigments. Because these pathways involve multiple competing enzymatic and non-enzymatic reactions, relatively small variations in processing conditions can substantially alter the final chemical composition and sensory quality of black tea.

Table 2.1: Major metabolites in tea: Composition, sensory attributes, and health benefits.

Metabolite	Subclasses	Approximate % in Tea	Quality Attributes	References
Phenolic compounds	Catechins (EGCG, EGC, ECG, EC)	10–30% (green tea: 20–30%; black tea: 2–10%; oolong: 10–20%; Pu-erh: <5%)	Contribute astringency and bitterness; hydrolysis of galloylated catechins yields sweetness; influence liquor color	Jiang et al. (2019b); Mukhtar and Ahmad (2000); Tounekti et al. (2013); He (2017)
	Flavonols (quercetin, kaempferol, myricetin)	1–5% (higher in herbal/green teas)	Enhance color stability and astringency; contribute floral and fruity notes	He (2017); Tounekti et al. (2013)
	Phenolic acids (gallic, chlorogenic, caffeic acids)	0.5–3% (higher in black/Pu-erh)	Add mild bitterness and astringency; contribute to aged tea flavor	Jiang et al. (2019b); He (2017)
	Theaflavins	1–5% (black tea only)	Impart reddish-orange color and brisk taste; reduce bitterness and enhance smoothness	He (2017); Jiang et al. (2019b) (Mukhtar & Ahmad, 2000)
	Thearubigins	10–20% (black tea only)	Provide dark brown and intense flavor; contribute body and reduce astringency	He (2017); Jiang et al. (2019b)
	Theabrownins	5–15% (Pu-erh: 10–15%; black tea: 5–10%; negligible in green/oolong)	Impart dark color and mellow flavor; contribute to smooth mouthfeel	He (2017)
Amino acids	L-Theanine	1–3% (higher in green tea)	Enhances umami and sweetness; balances bitterness	Kakuda (2011); Juneja et al. (1999)
	Other amino acids (glutamic acid, aspartic acid, arginine, alanine, etc.)	0.05–0.5% (varies with tea type; generally higher in green/shaded teas)	Contribute umami, mild sweetness, slight sourness, smooth mouthfeel, and overall flavor complexity; help reduce astringency	Juneja et al. (1999); Jiang et al. (2019b)
Alkaloids	Caffeine	2–5% (green tea: 2–4%; black tea: 3–5%; oolong: 2–4%; Pu-erh: 1–3%	Contributes bitterness, astringency, and stimulating mouthfeel	Juneja et al. (1999); Jiang et al. (2019b); He (2017)
	Theobromine	0.1–0.5% (higher in black/green teas)	Provides mild bitterness and subtle stimulation	Juneja et al. (1999) Jiang et al. (2019b)
	Theophylline	0.01–0.1% (higher in black tea)	Slight bitterness contributes to a brisk taste	Jiang et al. (2019b); He (2017)

2.3.1 Overview of black tea processing

"Orthodox" and "CTC" (crush-tear-curl) are the two principal commercial methods for manufacturing black tea; both produce a fully oxidized product meeting the general definition of "black tea," but differ fundamentally in how the leaf is physically processed. Orthodox manufacture preserves the leaf structure through gentle rolling, producing whole or twisted leaves, whereas CTC mechanically shreds the leaf into small, uniform granules to accelerate oxidation and standardize particle size for tea-bag production. This thesis focuses specifically on orthodox processing, the traditional method still used for higher-grade, whole-leaf black teas.

Orthodox black tea manufacturing involves a sequence of physical operations, that prepare leaf tissues for enzymatic oxidation. These steps disrupt cellular compartmentalization, allowing endogenous polyphenol oxidases (PPOs), peroxidases (PODs), oxygen, and catechin substrates to interact and initiate oxidative biotransformation. Withering reduces leaf moisture from approximately 70–80% to 55–70%, increasing pliability and concentrating catechins and oxidative enzymes. Subsequent rolling or maceration breaks open cells and exposes the leaf contents to oxygen, initiating the biochemical reactions that define black tea quality. The rolled leaves are then held under cool, humid, and oxygen-rich conditions for 45 minutes to several hours, during which the major oxidative transformations occur. Drying at 80 to 120 °C halts enzymatic activity and stabilizes the oxidized compounds (Chen et al., 2025b; Kong et al., 2022).

Despite this relatively standardized processing sequence, oxidation outcomes remain highly variable. Factors such as leaf moisture heterogeneity, maceration intensity, oxygen availability, cultivar, and processing conditions collectively influence PPO/POD activity and quinone reactivity. As a result, the balance between desirable theaflavins and higher-order polymeric pigments can differ substantially even under apparently similar manufacturing conditions. These limitations highlight the challenges of achieving precise control over endogenous enzyme-driven oxidation and provide a strong rationale for investigating externally controllable microbial oxidoreductase systems. Figure 2.7 summarizes the major pathways of catechin oxidation and pigment formation mediated by endogenous PPOs and PODs.

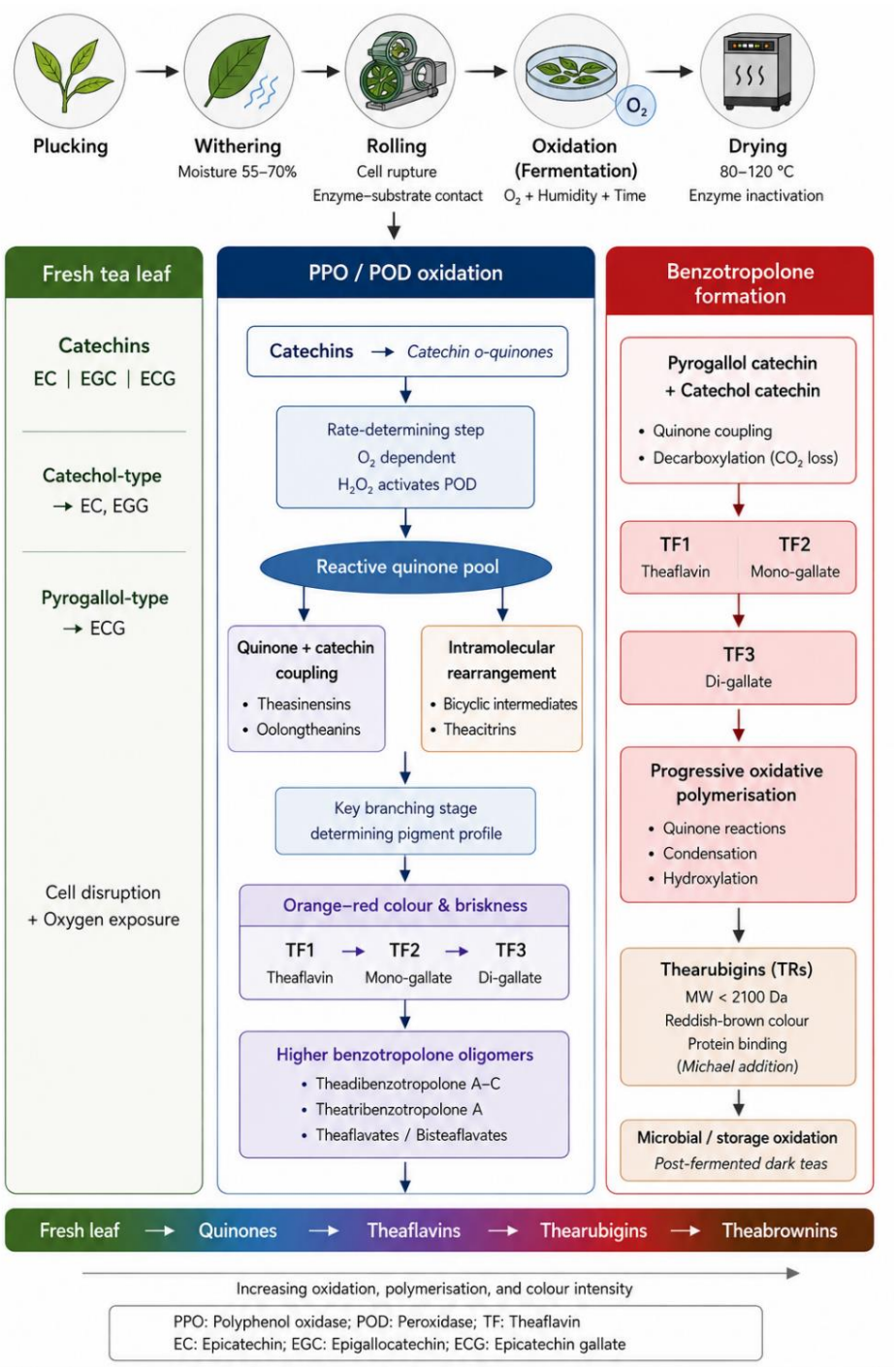

Figure 2.7: Integrated biochemical pathways of catechin oxidation during black tea processing (schematic representation without chemical structures).

2.3.2 Enzymatic initiation of catechin oxidation

The biochemical basis of black tea manufacture lies in the enzymatic oxidation of catechins, PPOs catalyze the initial two-electron oxidation of o-biphenolic and pyrogallol-type catechins (EC, EGC, ECG, and EGCG) to highly reactive o-quinones (Abudureheman et al., 2022; Subramanian et al., 1999). These quinones subsequently undergo rapid non-enzymatic coupling, rearrangement, and polymerization reactions that generate theaflavins, thearubigins, and other characteristic pigments.

Under typical processing conditions, PPOs preferentially oxidize catechol- and pyrogallol-type catechins because of their lower redox potentials and greater susceptibility to oxidation. As oxidation progresses and hydrogen peroxide accumulates, PODs increasingly contribute to quinone turnover and downstream polymerization reactions (Abudureheman et al., 2022; Subramanian et al., 1999).

Although the initial catechin-to-quinone conversion is mechanistically well established, the downstream distribution of oxidation-associated metabolites remains difficult to predict because multiple competing reactions occur simultaneously. Consequently, quinone formation alone does not reliably determine whether oxidation proceeds toward desirable theaflavins or toward higher-order polymeric pigments such as thearubigins and theabrownins. These limitations contribute substantially to variability in endogenous plant enzyme-mediated oxidation systems.

2.3.3 Early quinone reactions and intermediate formation

Once formed, catechin quinones enter several competing pathways. They may couple with unoxidized catechins to form B-ring–B-ring-linked dimers such as theasinensins, or they may undergo quinone–quinone coupling and intramolecular rearrangements that generate bicyclic intermediates. These intermediates serve as precursors to benzotropolone structures, which underpin the formation of theaflavins. Quinones may also react with water or other nucleophiles, forming oxygenated catechins that feed into later oxidation pathways (Abudureheman et al., 2022; Tanaka & Matsuo, 2020). The diversity of these early reactions contributes substantially to the chemical complexity of black tea and helps explain why oxidation outcomes remain highly sensitive to substrate composition and reaction conditions. These competing pathways also

highlight the importance of controlled model systems for the mechanistic evaluation of catechin oxidation.

2.3.4 Formation of benzotropolone structures and theaflavins

Theaflavin formation requires co-oxidation of two catechins, one containing a trihydroxylated B-ring (e.g., EGC, EGCG) and one containing an o-dihydroxy B-ring (e.g., EC, ECG). The mechanism involves oxidation of both catechins to quinones, coupling between the two quinones, decarboxylation with loss of one carbon atom as CO_2, and rearrangement to form the benzotropolone core (Abudureheman et al., 2022; Hashiguchi et al., 2023; Tanaka & Kouno, 2003). This pathway accounts for the four major theaflavins and numerous minor derivatives such as neo-theaflavins, iso-theaflavins, theaflavates, and theaflavic acids. Galloyl ester groups can also participate in oxidative coupling, producing galloyl-linked benzotropolone dimers and trimers that function as early precursors to higher-molecular-weight pigments. These mechanistic requirements illustrate why substrate ratios and redox environment strongly influence theaflavin yields. Figure 2.8 illustrates the structures of major theaflavins, and representative benzotropolone derivatives formed during catechin oxidation.

2.3.5 Higher order benzotropolone oligomers

Beyond theaflavins, catechin quinones can form a wide range of higher order benzotropolone structures. These include theadibenzotropolone A, B, and C (trimers), theatribenzotropolone A (a tetramer), theaflavate C, and bistheaflavates, all of which arise from oxidative coupling between benzotropolone units (Abudureheman et al., 2022; Hashiguchi et al., 2023).

Such oligomers represent transitional species between structurally defined theaflavins and the chemically heterogeneous thearubigins. Their formation demonstrates that benzotropolone-containing molecules remain chemically reactive throughout black tea oxidation and continue to participate in downstream polymerization pathways.

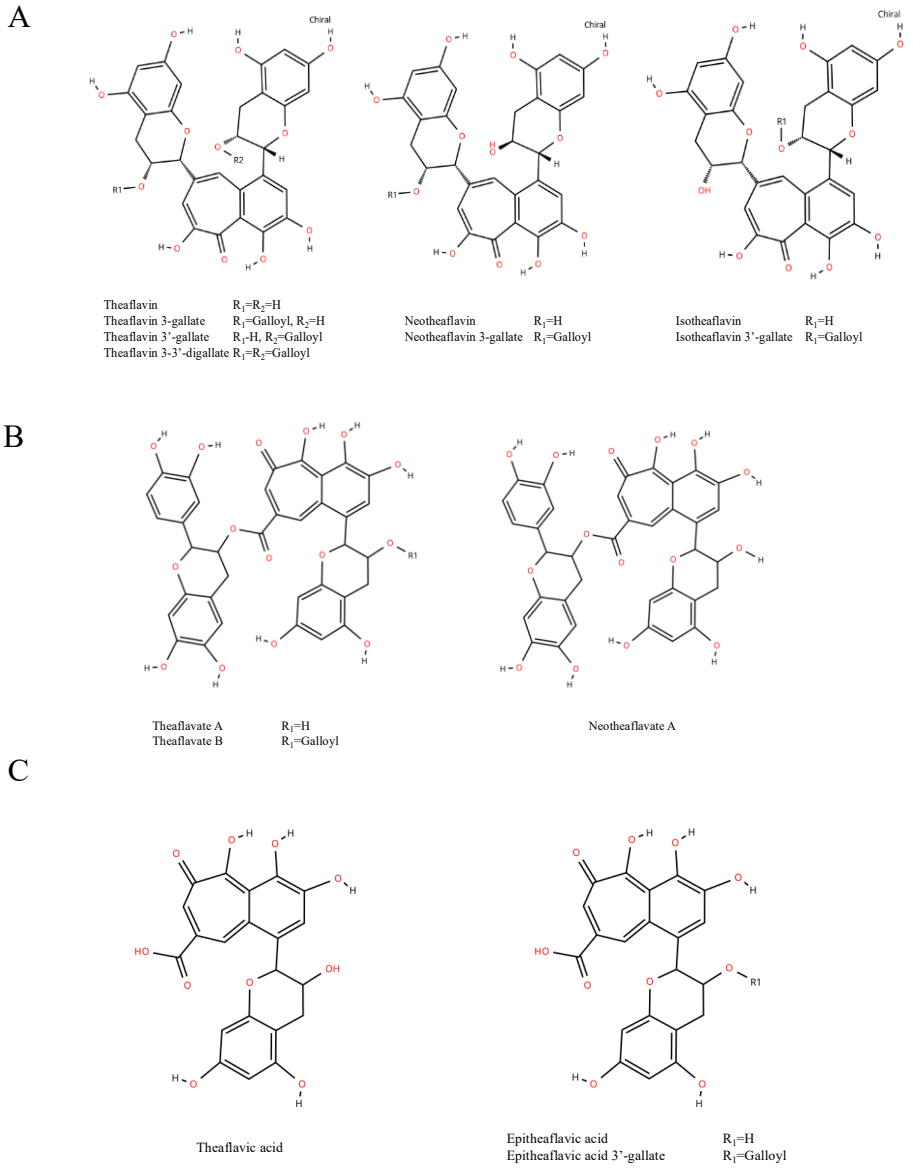

Figure 2.8: Chemical structures of the major theaflavins and their derivatives formed during the oxidative polymerization of tea catechins. The figure is organized into three groups: (A) primary theaflavins and their gallated forms, including theaflavin (TF), theaflavin-3-gallate (TF3G), theaflavin-3′-gallate (TF3′G), and theaflavin 3-3′gallate (TFDG), as well as the structural isomers neotheaflavin and isotheaflavin and their gallates; (B) higher-order oxidation-associated metabolites, including theaflavates A and B and neotheaflavate A; and (C) theaflavic acid, epitheaflavic acid, and epitheaflavic acid-3′-gallate. R groups indicate sites of galloylation (R = H or galloyl**).**

2.3.6 Formation of theasinensins, oolongtheanins, and theacitrins

Parallel pathways generate theasinensins and oolongtheanins through quinone–catechin coupling, redox-mediated dismutation, and hydration reactions. Theacitrins, another class of intermediates,

form through oxidation of the B-ring to a quinone, followed by 1,4-addition, intramolecular cyclisation, and rearrangement to bicyclo-octane structures. These intermediates can degrade into theacitrinins under acidic or thermal conditions, reflecting the instability of mid-stage oxidation-associated metabolites (Abudureheman et al., 2022; Matsuo et al., 2011). These branching pathways highlight the chemical sensitivity of mid-stage intermediates and the difficulty of capturing them in traditional leaf-based systems. Figure 2.9 presents representative structures of theacitrinins, and theasinensin derivatives formed during catechin oxidation.

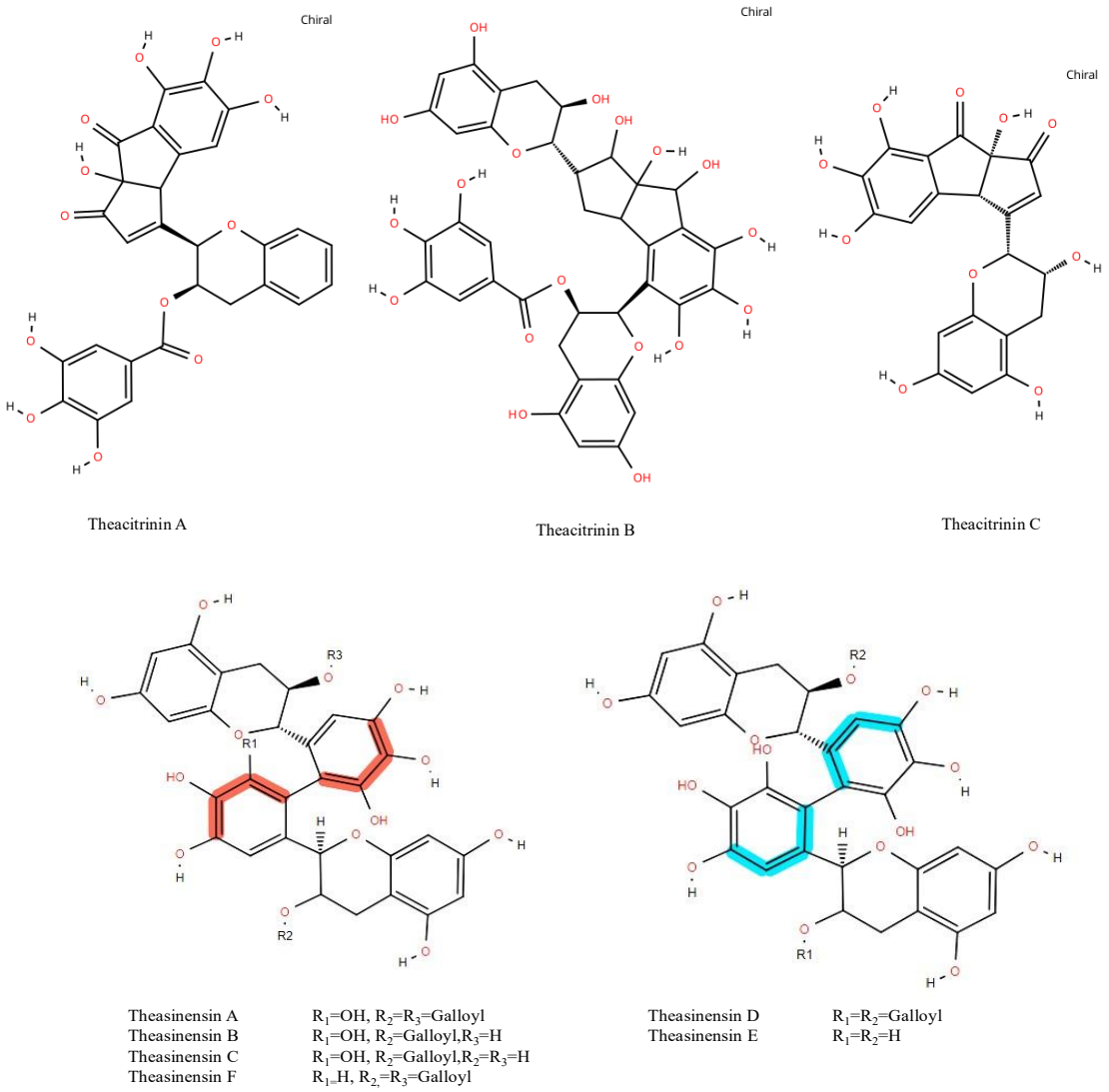

Figure 2.9: Representative structures of theacitrinins (A–C) and theasinensin (A-F) derivatives identified in tea. These compounds are oxidative dimerization products of catechins formed during enzymatic or microbial oxidation. Colored highlighting distinguishes the two aromatic rings joined by the central biaryl bond, one positioned above and one below the plane of rotation, reflecting the restricted-rotation, non-coplanar conformation characteristic of theasinensin-type biaryl linkages.

2.3.7 Pathways leading to thearubigins and theabrownins

Thearubigins (TRs) arise through progressive oxidation and polymerization of catechin-derived quinones and benzotropolone intermediates during black tea oxidation. Unlike theaflavins, TRs do not represent structurally discrete compounds but rather a structurally heterogeneous continuum of oligomeric products (Abudureheman et al., 2022; Hashiguchi et al., 2023; Kuhnert et al., 2010a). Their molecular weights generally remain below 2100 Da and are characterized by elevated O/C and reduced H/C ratios, reflecting extensive oxidative modification.

TR formation entails the incorporation of multiple intermediate classes, including theaflavins, theasinensins, theacitrins, oolongtheanins, and related quinone-derived products. Continued oxidative coupling yields diverse linkage types, including C–C, C–O–C, quinone–quinone, and quinone–methide interactions, leading to structurally complex oligomeric assemblies (Long et al., 2023; Yassin et al., 2014). Quinones may also react with amino acids and proteins via nucleophilic addition, forming protein-associated TR complexes in tea infusions (Bittner, 2006).

Mass spectrometric studies reveal polyhydroxylated oligomers connected mainly through B-type proanthocyanidin linkages, while acid depolymerization experiments frequently release catechins, theaflavins, and theasinensins, indicating that these compounds serve as important structural precursors within TR assemblies (Kuhnert et al., 2010a; Tanaka & Matsuo, 2020). Although the A- and C-rings are generally relatively conserved, extensive B-ring oxidation, condensation, hydroxylation, decarboxylation, and rearrangement reactions introduce considerable TR heterogeneity (Jiang et al., 2019a).

TRs are primarily responsible for the reddish-brown to deep-amber coloration and the reduced astringency characteristic of black tea infusions. As oxidation progresses, the bright orange red theaflavins gradually convert into darker, more polymerized TR fractions, producing increased liquor color intensity and modified mouthfeel characteristics (Kuhnert et al., 2010a; Tanaka & Matsuo, 2020). Despite extensive investigation, the structural heterogeneity of TRs remains a major analytical challenge, leading many studies to rely on operationally defined fractions rather than on full structural characterization. This analytical limitation restricts mechanistic comparisons between oxidation systems. Therefore, in this thesis, targeted catechin and theaflavin markers are combined with multivariate metabolomic profiling to address this challenge.

Unlike black tea TRs, theabrownins (TBs) mainly appear in post-fermented dark teas such as Pu-erh. Arising from further microbial oxidation and polymerization of TRs and related polyphenols during pile fermentation, these darker, high-molecular-weight polymers also form through additional interactions with microbial enzymes, polysaccharides, proteins, and oxidative condensation pathways. Together, these processes generate the characteristic dark color and mellow sensory profile of post-fermented teas (Chen et al., 2022b; Wang et al., 2011).

Overall, these pathways show that black tea oxidation involves highly interconnected, difficult-to-control enzymatic and non-enzymatic reactions. This complexity justifies investigating externally controllable microbial oxidoreductase systems for targeted catechin biotransformation and supports comparative evaluation against endogenous plant enzyme-mediated oxidation.

2.3.8 Factors influencing dynamics of oxidation

Catechin oxidation depends on a complex interplay of environmental and biochemical factors. Whereas Section 2.4.1 discusses the intrinsic catalytic properties of PPOs, this section focuses on the influence of processing conditions on oxidation kinetics and product distribution. Temperature, pH, humidity, and oxygen availability affect enzyme activity, quinone stability, nucleophilic addition rates, and the balance between competing coupling pathways (Kong et al., 2022; Yu et al., 2022). For example, limited oxygen diffusion within rolled leaf masses can promote uneven pigment formation, whereas pH fluctuations alter the balance between intramolecular rearrangements and intermolecular coupling reactions (Jayasinghe et al., 2020; Liu et al., 2022a).

Leaf maturity further modulates oxidation behavior by altering catechin composition, antioxidant content, moisture levels, and cell wall permeability. Young leaves generally contain higher concentrations of gallated catechins and exhibit greater oxidative reactivity than mature leaves (Lee et al., 2016; Yu et al., 2022). Together, these variables contribute substantially to the batch-to-batch variability characteristic of black tea manufacture (Jayasinghe et al., 2020; Liu et al., 2022a; Yu et al., 2022).

Although the major pathways of black tea oxidation are well established, most mechanistic understanding derives from traditional processing systems in which enzyme-mediated reactions occur within complex and poorly controlled leaf matrices (Abudureheman et al., 2022; Tanaka & Matsuo, 2020). Consequently, the ability to systematically modulate catechin oxidation under

defined conditions remains limited. In addition, the structural heterogeneity of thearubigins continues to constrain mechanistic interpretation of downstream polymerization pathways (Hashiguchi et al., 2023; Kuhnert, 2010). These limitations support the investigation of alternative oxidation systems that provide greater experimental control over catechin biotransformation.

In the microbial enzyme-mediated platform investigated in this thesis, many traditionally variable processing parameters become experimentally controllable factors. Oxygen availability can be regulated through aeration and headspace control; pH through buffered systems; temperature through controlled incubation; and substrate exposure through enzyme dosage and catechin concentration. This conversion of processing variables into tunable experimental parameters provides a more controlled framework for investigating oxidation kinetics, product distribution, and catechin biotransformation pathways.

2.4 Endogenous PPOs: Role and limitations

2.4.1 Role of endogenous PPOs in black tea oxidation

Endogenous PPOs, which are copper-containing metalloenzymes abundant in *C. sinensis* leaves, serve as the primary catalyst initiating the oxidative cascade that defines black tea quality. Localized mainly in chloroplasts and bound to organelle membranes in an inactive form, PPOs remain compartmentalized from vacuolar catechins until mechanical disruption (withering, rolling, maceration) enables contact with atmospheric oxygen. Once activated, PPOs, predominantly catecholase-type (diphenol oxidase) with both catecholase and limited monophenolase activities, rapidly oxidize o-diphenolic B-rings (EC, ECG) and trihydroxylic B-rings (EGC and EGCG) to reactive o-quinones.

Tea leaves contain multiple PPO isoenzymes, conventionally designated PPO1 and PPO2, that differ in catalytic properties. PPO1 catalyzes the formation of simple TF from mixed catechin substrates, while PPO2 exhibits broader specificity and can synthesize multiple TF derivatives, including gallated TFs such as TFDG. This indicates isoform-dependent contributions to TF profiles during fermentation (for example, PPO1 produces simpler TF, whereas PPO2 produces TF, TF3G, and TF3-3'DG) (Teng et al., 2017). Because PPO nomenclature varies across studies,

these designations should be interpreted as functional groupings rather than universally standardized isoform names.

These quinones drive non-enzymatic coupling to form TFs via benzotropolone structures from catechol–pyrogallol pairings, while PODs, which become active in the presence of hydrogen peroxide generated during broader oxidative metabolism, promote further oxidation of TFs into TRs, shaping the TF/TR ratio that influences brightness, brisk astringency, body, and overall sensory profile (Abudureheman et al., 2022; Drynan et al., 2010; Tanaka & Matsuo, 2020). Molecular studies have also identified multiple PPO gene family members (e.g., CsPPO1, CsPPO2, CsPPO4, etc.), which exhibit differential expression patterns and likely encode isoforms with variable regulatory responses and catalytic efficiencies relevant to oxidation activity in leaves (Aaqil et al., 2024; Kong et al., 2022). These genetic and biochemical distinctions highlight the complexity of PPO-mediated oxidation within the intact leaf environment.

PPO activity increases markedly during withering (up to approximately 2.9-fold due to moisture loss and tissue softening) and peaks during rolling as cell damage maximizes substrate–enzyme–oxygen interactions. In fermentation, PPOs initiate TF formation, but their activity declines as oxidation advances, influenced by oxygen availability (often rate-limiting), temperature, humidity, and duration. Low fermentation temperatures favor TF and TR accumulation, whereas excessive heat or prolonged exposure inactivates PPOs (Verloop et al., 2016). This dynamic activity profile underscores the sensitivity of PPOs to processing conditions and the difficulty of achieving consistent oxidation outcomes.

2.4.2 Biochemical and environmental limitations

Despite their significant role, endogenous PPOs exhibit inherent constraints. They are highly temperature-sensitive: activity typically peaks around 30 °C, declines progressively above this as partial denaturation sets in, with only around 45% of maximum activity remaining by 60 °C (Altunkaya, 2014), while temperatures below approximately 20 °C slow reaction rates and risk incomplete oxidation (Jayasinghe et al., 2020). Oxygen diffusion through rolled leaf masses is often uneven, producing spatially variable oxidation patterns (Liu et al., 2022a). Substrate specificity limits versatility, with PPOs preferentially oxidizing catechins over pyrogallol-type or galloylated forms, restricting pathway diversity (Abudureheman et al., 2022; Zou et al., 2024).

Accumulated o-quinones can inhibit PPOs or trigger uncontrolled polymerization, diverting reactions from desirable TFs toward excessive TRs or insoluble polymers (Du et al., 2025). These biochemical constraints collectively narrow the operational window in which PPOs can function effectively. PPO levels and performance are further modulated by agronomic factors (cultivar, leaf maturity, plucking standard) and seasonal conditions (e.g., rainy/cloudy weather reduces activity and catechin content, lowering liquor brightness) (Liu et al., 2022b). Mechanical inconsistencies during rolling cause uneven cell rupture and variable enzyme–substrate contact. The short oxidation window (1–3 hours) ends abruptly upon drying, halting transformations despite remaining substrates and contributing to batch-to-batch inconsistency in pigment ratios, color, aroma, and sensory attributes (Jayasinghe et al., 2020). These interacting variables illustrate why endogenous PPOs are difficult to control and why black tea quality is inherently variable.

2.4.3 Implications and opportunities for innovation

Limitations, such as environmental sensitivity, substrate bias, oxygen dependence, and temporal/process variability, hinder consistent oxidation outcomes and TF/TR balance, leading to quality fluctuations. This has spurred interest in supplementary systems. Exogenous tyrosinases (cresolase/catecholase) from *Agaricus bisporus* or pear approximately doubled TF yields in green tea extracts, yielding stable, high-TF profiles with improved color, while laccases promote over-oxidation and insoluble complexes (Faustina et al., 2022; Verloop et al., 2016). MPLOs and related oxidases offer greater stability, tolerance of broader reaction conditions, and more controlled application than endogenous plant PPO (Gupta et al., 2013; Kumar et al., 2024b; Nikolaivits et al., 2018). Because microbial oxidoreductases differ in substrate specificity, they may also generate theaflavin-type or other oxidative-coupling pigments with substitution patterns distinct from those produced by plant PPO. Such pigments would be expected to contribute to color development and, by analogy with theaflavins and thearubigins, may also carry antioxidant activity, although this remains to be directly characterized. Together, these features could improve the functional properties and reproducibility of black tea-like products. These contrasts are summarized in Table 2.2.

Taken together, Section 2.4 demonstrates that while plant PPOs have been characterized in considerable biochemical detail, their behavior within tea processing remains strongly constrained

by the complexity and variability of the leaf matrix. Here, "leaf matrix" refers to the intact plant tissue's physical and cellular architecture, in which PPO and its catechin substrates are normally compartmentalized separately (chloroplast-bound enzyme versus vacuole-stored substrate) prior to disruption, and in which cell-wall thickness, moisture content, and oxygen access vary unevenly across the leaf and between individual leaves, plants, and harvests. This structural heterogeneity means that the same nominal processing conditions can produce inconsistent, difficult-to-predict PPO activity from one batch to the next, in contrast to a defined enzyme preparation acting on a homogeneous liquid substrate. The growing interest in exogenous oxidoreductases highlights a broader shift from descriptive studies of endogenous enzymes toward the exploration of alternative catalytic systems. This transition provides the conceptual basis for examining microbial contributions to tea polyphenol transformation, which are discussed in the following section.

Table 2.2: Conceptual comparison of endogenous PPOs and microbial oxidoreductases (synthesized from literature discussed in Sections 2.3 and 2.4).

Feature	Endogenous PPO (tea leaf)	Microbial oxidoreductases
Optimal conditions	Narrow (pH 4.5–5.5; moderate temperature)	Broad pH and temperature tolerance
Oxygen dependence	High; diffusion-limited in leaf tissue	Aeration can be externally controlled
Substrate scope	Catechol-type favored	Broader substrate range, including gallated catechins
Stability	Easily denatured by heat or moisture	High thermal and operational stability
Reaction control	Limited by leaf matrix heterogeneity	Tunable through enzyme dosage, immobilization, and media composition
Product distribution	TF/TR ratio highly variable	More reproducible pigment profiles

2.5 Microbial contributions to tea processing and quality

2.5.1 Microbial presence during black tea manufacturing

Although black tea manufacturing is primarily driven by endogenous enzymatic oxidation, increasing evidence indicates that microorganisms are increasingly associated with biochemical

changes during withering, rolling, and especially the oxidation stage (Jia et al., 2022; Shiquan et al., 2023; Tong et al., 2021). Fresh tea leaves naturally harbor diverse epiphytic bacteria and fungi, and additional microbes originate from processing equipment and the surrounding environment. Compared with post-fermented teas, the relatively short and aerobic oxidation phase of orthodox black tea processing limits extensive microbial proliferation. Nevertheless, metabolically active surface-associated microbial communities may influence oxidation chemistry through the secretion of extracellular enzymes and secondary metabolites. These contributions may lead to subtle yet meaningful changes in catechin transformation, pigment formation, and aroma development (Jia et al., 2022; Shiquan et al., 2023).

Current evidence for microbial involvement is derived largely from correlations between microbial community dynamics and metabolite profiles obtained through culture-dependent and omics-based studies. Direct causal attribution remains limited because many studies rely on non-specific activity assays and incompletely capture unculturable populations. Despite these limitations, microbial oxidoreductases are of considerable interest. Unlike endogenous leaf enzymes, their dosage, exposure time, and reaction conditions can be externally controlled. This distinction provides a strong rationale for investigating microbial enzyme systems as complementary and potentially more tunable catalysts for tea catechin oxidation, while acknowledging that food safety and regulatory considerations remain essential for future industrial application

2.5.2 Microbial succession and enzymatic activity in black tea

High-throughput sequencing analyses (e.g., 16S rRNA, ITS) reveal dynamic microbial succession across black tea processing stages. Dominant bacterial genera often include *Chryseobacterium*, *Sphingomonas*, *Acidovorax*, *Microbacterium*, and *Rhizobium*, while fungal groups such as Pleosporales also appear, with abundances increasing after withering and rolling and peaking during oxidation (Shiquan et al., 2023). These microorganisms may secrete extracellular oxidoreductase-associated activities, including PPO-like, POD-associated, and other phenol-oxidizing systems, which supplement endogenous plant enzymes. Their activity contributes to catechin oxidation, pigment formation, and the development of aroma-active compounds (Liu et al., 2023c). Correlations between microbial abundance and quality-related metabolites, such as TFs, TRs, and soluble sugars, suggest that microbial activity may enhance brightness, aroma

complexity, and taste uniformity in black tea (Jia et al., 2022; Liu et al., 2023a; Zhang et al., 2023b). These findings indicate that even modest microbial activity during black tea manufacture may subtly modify oxidation trajectories and sensory outcomes.

2.5.3 Microbial fermentation in dark and post-fermented teas

In contrast to black tea, dark and post-fermented teas including Pu-erh, Fu-brick, Qingzhuan, and Liupao, rely heavily on microbial fermentation during post-processing. These teas undergo extended wet-piling or deliberate inoculation, enabling fungi such as *Aspergillus* spp. and *Eurotium cristatum* ("golden flower" fungus), along with diverse bacteria, to dominate the fermentation ecosystem (Jiang et al., 2022; Zheng et al., 2024). These microbes produce a broad suite of extracellular enzymes and oxidoreductase-associated activities, including laccase-like, tyrosinase-like, and catechol oxidase-like systems, together with cellulases and proteases, which contribute to catechin transformation, formation of phenolic acids, γ-aminobutyric acid (GABA), and theabrownins (TBs), as well as the development of the characteristic earthy and mellow flavor profiles that intensify during aging (Zhang & Zhang, 2024). Unlike black tea's rapid, plant-PPO-initiated oxidation, which typically completes within hours, these post-fermented systems undergo prolonged microbial fermentation over weeks to years, enabling structural transformations beyond simple catechin oxidation to theaflavins and thearubigins. These include further oxidative polymerization into the larger, more heterogeneous theabrownin structures characteristic of aged dark teas, microbial cleavage of glycosidic bonds releasing bound aglycones, and incorporation of microbial metabolites and amino acid-derived compounds into the polymer matrix via Maillard-type condensation reactions. This extended timescale and broader enzymatic repertoire produce chemical profiles unattainable through endogenous leaf enzymes alone (Zheng et al., 2024).

2.5.4 MPLOs as biotechnological tools

In this thesis, microbial polyphenol-oxidizing-like oxidoreductases (MPLOs) refer to microbial extracellular phenol-oxidizing systems, including laccase-like, tyrosinase-like, catechol oxidase-like, and peroxidase-associated activities, that are capable of catalyzing phenolic oxidation reactions of tea polyphenols through mechanisms functionally analogous to those of plant PPOs. Unlike endogenous plant PPOs, microbial oxidoreductase systems may be secreted extracellularly

and can exhibit greater operational stability across pH and temperature ranges, making them attractive candidates for controlled biotechnological applications (Nikolaivits et al., 2018; Singh et al., 2016).

In tea systems, microbial enzymes can supplement or mimic endogenous oxidation, thereby generating novel metabolites with potential health benefits, including antioxidant and anti-obesity activities (Zhang et al., 2024). Experimental studies demonstrate this potential, where Wang et al. (2023c) and Xiao et al. (2021) showed that fermenting black and green tea with *E. cristatum* produces new metabolites and alters catechin profiles in ways not achievable through endogenous plant enzymes alone. These findings highlight MPLOs as promising tools for enhancing or diversifying black tea quality.

MPLOs offer several advantages over plant-derived enzymes. They are produced extracellularly, enabling direct interaction with tea substrates without requiring cell disruption. They also exhibit broader operational ranges, including tolerance to wider pH and temperature conditions, and can be produced at scale through fermentation or recombinant expression (Espina et al., 2021; Vivekanandhan et al., 2024). These properties make MPLOs attractive for controlled oxidation processes where endogenous PPOs are insufficient or inconsistent.

Similar oxidoreductases from fungi, particularly laccases, have been widely studied for their ability to oxidize diverse phenolic substrates and generate complex polymeric pigments. Their activity aligns well with traditional fermentation environments, although their moderate thermal stability can limit industrial applications (Hasan et al., 2023; Janusz et al., 2020). MPLOs of bacterial origin, by contrast, often display superior thermal stability, broader pH tolerance, and higher catalytic efficiency under processing-relevant conditions. These characteristics position them as promising candidates for the precision oxidation of tea catechins and controlled pigment formation.

2.5.5 Bacterial extracellular enzymes as biocatalysts

Enzymes capable of oxidizing polyphenols occur in plants, fungi, and bacteria, but their functional characteristics differ markedly by biological origin. Plant PPOs, such as those in *C. sinensis*, are intracellular and activated only after mechanical disruption. In contrast, microbial polyphenol-oxidizing-like oxidoreductases (MPLOs) are typically secreted extracellularly. Fungal MPLOs

(primarily laccases and tyrosinases) are typically secreted extracellularly and contribute to pigment formation in post-fermented teas. Bacterial MPLOs represent a third major source and have gained increasing attention due to their reproducibility, extracellular secretion, and suitability for controlled biocatalysis (Nikolaivits et al., 2018; Yang et al., 2023). Unlike the microbial communities involved in natural tea fermentation, bacterial MPLOs can be applied as purified or engineered enzymes, offering precision and reproducibility in tea biotransformation.

Bacterial MPLOs include several enzyme classes with distinct catalytic properties. Laccases, produced by genera such as *Bacillus*, *Streptomyces*, and *Pseudomonas*, are multicopper oxidases capable of oxidizing a broad range of phenolic substrates. They typically exhibit frequently reported high thermostability (often up to 60–70 °C) and broad pH tolerance (3–8), making them suitable for industrial applications where processing conditions fluctuate (Kumar et al., 2024b; Sodhi et al., 2024). Tyrosinases, another major MPLO type, catalyze both monophenol hydroxylation and o-diphenol oxidation. Their dual activity enables selective modification of catechins and controlled formation of quinone intermediates, which can be directed toward specific pigment or flavor outcomes (Vivekanandhan et al., 2024). Catechol oxidases, which exclusively oxidize o-diphenols, offer narrower substrate specificity and are valuable when selective oxidation is required without monophenolase activity.

A defining advantage of bacterial MPLOs is their extracellular secretion, which eliminates the need for cell lysis and allows direct interaction with tea substrates in liquid or solid-state systems. Their compatibility with recombinant expression platforms such as *Escherichia coli* further enhances scalability, enabling high-yield, low-cost production of tailored PPO variants (J. et al., 2025; Sharma et al., 2024). From a food-safety perspective, bacterial systems also avoid the mycotoxin risks associated with filamentous fungi and include many species with food-grade status, strengthening their suitability for beverage applications. These properties contrast with plant PPOs, which are rapidly inactivated during thermal processing, and fungal MPLOs, which often exhibit moderate thermal stability and narrower operational windows (Hasan et al., 2023; Janusz et al., 2020). As biocatalysts, bacterial extracellular MPLO systems may enable more precise modulation of catechin oxidation, pigment formation, and flavor development. Their stability and tunability make them promising tools for enhancing theaflavin yields, adjusting TR profiles, reducing bitterness and astringency, and generating novel bioactive compounds. Because

they can be applied independently of microbial growth, bacterial extracellular MPLOs offer a level of control not achievable through natural fermentation alone. This positions them as valuable biotechnological agents for modern tea innovation and targeted polyphenol transformation.

Overall, Section 2.5 clearly demonstrates that microorganisms contribute to the diversification of tea polyphenols and the development of distinctive sensory and functional properties during fermentation. However, current research largely emphasizes naturally occurring fermentation systems and complex microbial communities, with limited emphasis on translating these observations into controlled and reproducible laboratory-scale biotransformation strategies. The integration of microbial enzyme production, biochemical characterization, and targeted catechin conversion therefore remains an important yet insufficiently developed research direction, providing a logical transition to the analytical and experimental considerations discussed in the following sections.

2.6 Advances in production, purification, and application of MPLOs

Recent progress in microbial biotechnology has significantly expanded the strategies available for producing, optimizing, and applying MPLOs. These advances are particularly relevant for tea biotransformation, where externally regulated oxidation can enhance pigment formation, flavor development, and functional properties. This section synthesizes current developments in microbial screening, enzyme production, purification, and application, with emphasis on scalable approaches suitable for industrial deployment. Figure 2.10 summarizes the overall workflow used in this study, outlining the sequential stages of PPO-like enzyme screening, production, purification, and application that are detailed in Sections 2.6.1 to 2.6.6.

2.6.1 Screening and identification of PPO-producing microorganisms

Preliminary screening of PPO-producing bacteria is a critical first step in identifying promising strains from diverse ecological niches. Common sources include rhizosphere soils, industrial effluents, agro-industrial wastes, and tea-processing environments, ecosystems enriched in phenolic compounds that select for microorganisms capable of oxidoreductive metabolism (Hakim et al., 2021; Korenblum et al., 2022).

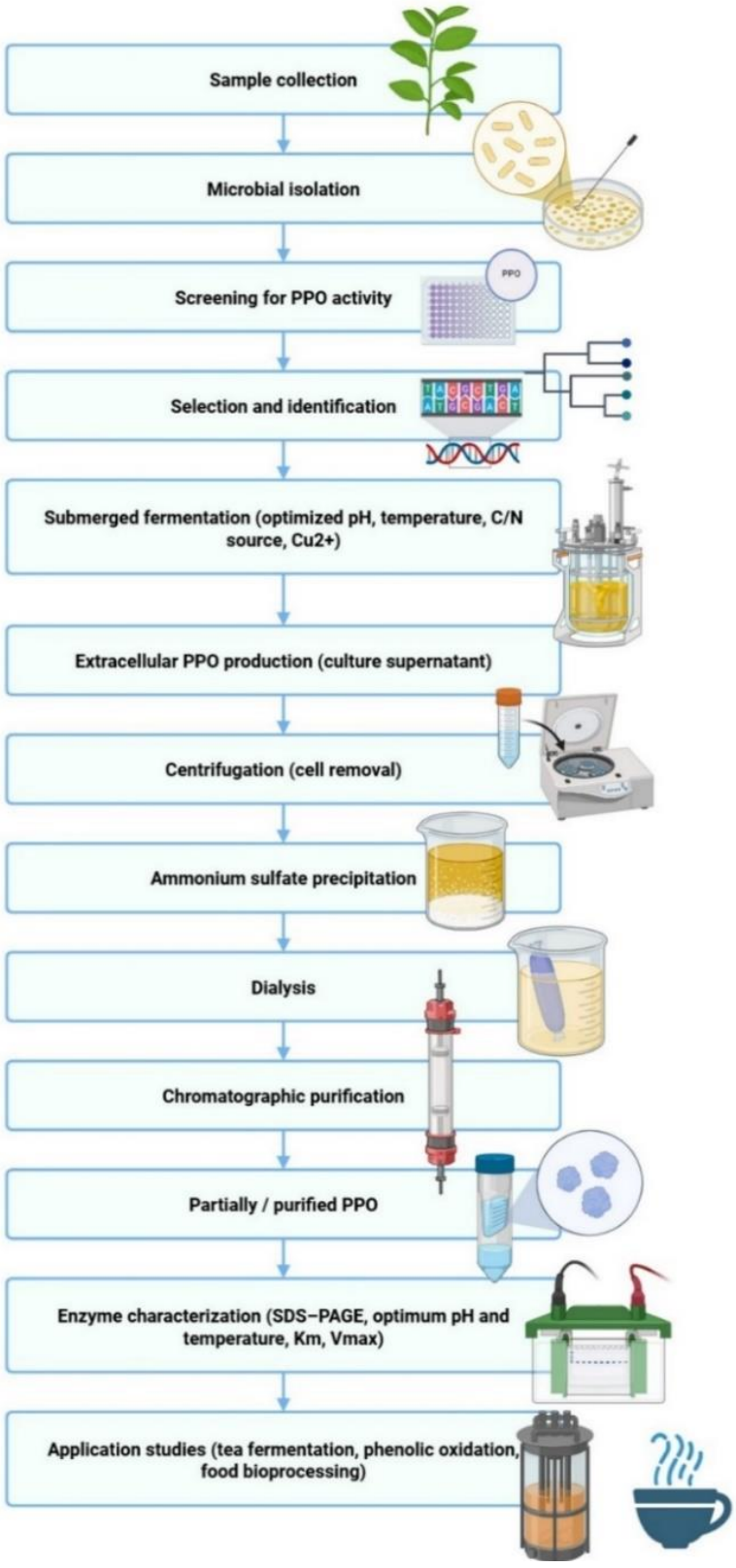

Figure 2.10: Flow chart of PPO-like enzyme production, purification and application pipeline.

Genera such as *Pseudomonas*, *Bacillus*, *Alcaligenes*, and *Burkholderia* frequently exhibit PPO activity due to ecological pressures favoring phenolic detoxification and nutrient cycling (Kumar et al., 2005; Morya et al., 2020; Ray & Pattnaik, 2024; Zeng et al., 2023b). These environments therefore provide a rich reservoir of microorganisms with potential for targeted polyphenol biotransformation.

Screening typically begins with enrichment in phenolic-supplemented media (e.g., catechol- or tannic acid-amended broths), followed by qualitative plate assays. On agar plates containing catechol (10–50 mM), PPO-positive colonies develop dark brown or black halos due to quinone formation. Negative controls such as heat-inactivated cultures or copper-chelating agents (e.g., ethylenediaminetetraacetic acid (EDTA) or diethyldithiocarbamate (DDC)) are recommended to confirm that color development is enzymatic and copper-dependent. Quantitative screening in broth cultures measures extracellular PPO activity spectrophotometrically by monitoring the increase in absorbance at 420 nm corresponding to catechol oxidation to o-benzoquinone (Jan et al., 2023; Kumar et al., 2005).

A range of substrates is used to differentiate PPO subtypes. Catechol remains the most widely used due to its rapid oxidation and strong chromogenic response, although it is non-specific and can report activity from multiple oxidoreductases, making it ideal for high-throughput screening but insufficient for mechanistic discrimination (Biswas & Radhakrishna, 2025; Kumar et al., 2005). Confirmatory assays using L-tyrosine (monophenolase) and L-DOPA (diphenolase) help distinguish tyrosinase activity from catechol oxidase-type MPLOs. Guaiacol and 4-tert-butylcatechol support broader oxidoreductase screening (Surwase & Jadhav, 2011). This tiered substrate approach enables both rapid detection and functional differentiation of PPO-like enzymes.

In the case of laccase screening, redox mediators such as HBT (1-hydroxybenzotriazole) or 2,2,6,6-tetramethylpiperidine-1-oxyl, a stable nitroxyl radical (TEMPO) can expand substrate range and enhance signal intensity (Bourbonnais & Paice, 1990; Kunamneni et al., 2008), although their use is generally avoided in food-related applications due to toxicity and regulatory concerns (Camarero et al., 2005; Widsten & Kandelbauer, 2008). Substrate choice therefore influences sensitivity, specificity and suitability for downstream food-grade biotransformation workflows.

2.6.2 Analytical methods for polyphenol oxidizing enzymatic activity measurement

Spectrophotometric assays remain the dominant method for PPO activity quantification due to their simplicity, rapidity, and compatibility with crude extracts. Quinone formation is typically monitored at 420–490 nm depending on the substrate (Mayer, 2006). Variants include cysteine-coupled assays, which improve linearity and sensitivity, and chromogenic coupling reactions that enhance detection specificity (Espín et al., 1997; García-Molina et al., 2005; Zou et al., 2025b).

More advanced analytical techniques provide higher precision. High-performance liquid chromatography (HPLC) quantifies substrate depletion or product formation, including catechin-derived pigments such as TFs (Tao et al., 2016). Electrochemical methods, such as amperometric detection of quinones or oxygen consumption, offer real-time monitoring with high sensitivity but require specialized equipment (Campuzano et al., 2020; Karyakin, 2001). Polarographic oxygen electrodes directly measure O_2 uptake but are less commonly used due to interference from non-enzymatic oxidation (Zawistowski et al., 1991).

Normalization of PPO activity is essential for comparing strains or purification steps. Volumetric activity (U/mL) is preferred during initial screening, while specific activity (U/mg protein) is used after purification. Because phenolic compounds can interfere with protein assays and artificially inflate specific activity values, cleanup steps such as dialysis or buffer exchange are often required to ensure accurate quantification (Espín et al., 1997; Mayer, 2006; Yoruk & Marshal, 2003). These considerations are particularly important when working with tea extracts, which contain abundant interfering phenolics.

2.6.3 Screening of related MPLO and associated oxidoreductases

Microbial strains exhibiting polyphenol-oxidizing activity often possess multiple extracellular oxidoreductase-associated activities, including catechol oxidase-like, laccase-like, tyrosinase-like, and peroxidase-associated systems, that collectively broaden their capacity for phenolic biotransformation. Because these oxidoreductases act on overlapping but distinct substrate groups, screening workflows commonly incorporate multiple substrate-based assays to identify strains with complementary oxidative capabilities. This multi-enzyme perspective is particularly relevant for complex polyphenol systems such as tea, where catechin oxidation involves diverse oxidative

and condensation reactions. Representative structures and reactions of MPLOs are shown in Figure 2.11.

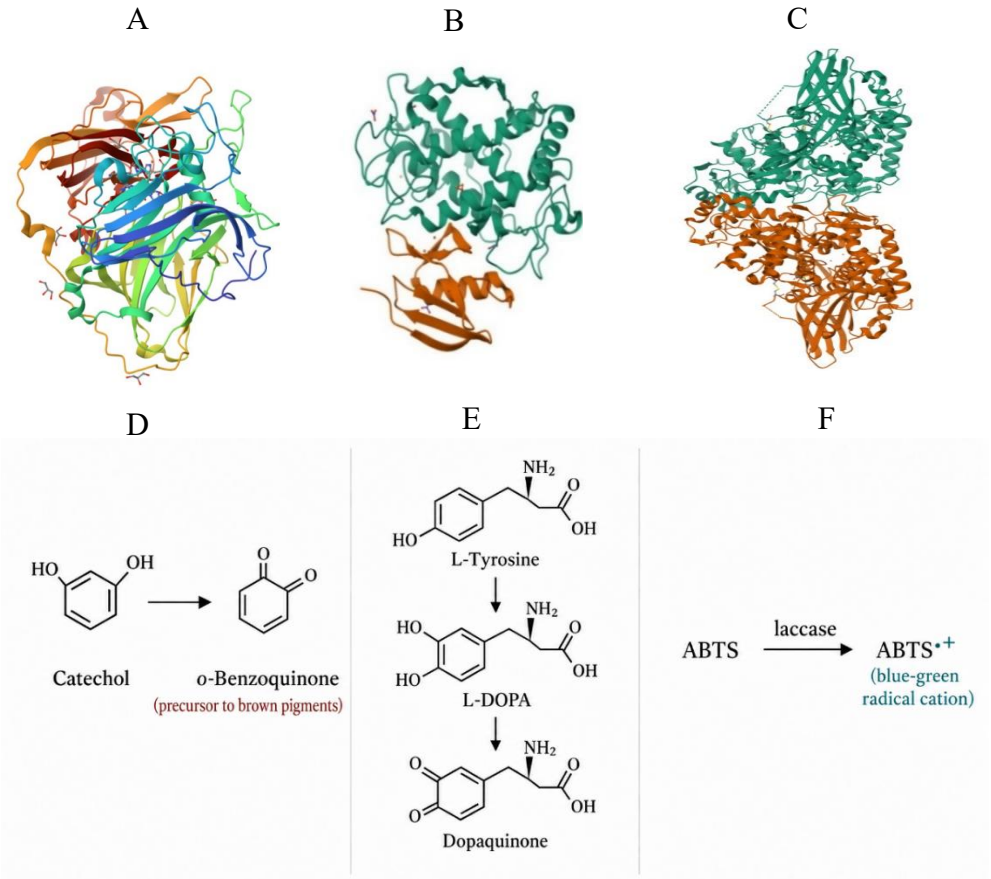

Figure 2.11: Representative tertiary structures and reactions of microbial polyphenol-oxidizing-like oxidoreductases (MPLOs). (A) CotA laccase from *Bacillus subtilis* (PDB ID: 1GSK): a thermostable multicopper oxidase containing the T1/T2/T3 copper cluster; functions as a model for bacterial laccases and related multicopper oxidases. (B) Tyrosinase from *Streptomyces castaneoglobisporus* in the oxy form (PDB ID: 1WX2): shown with its caddie protein; features the conserved CuA–CuB dinuclear center; catalyses monophenol hydroxylation and diphenol oxidation. (C) Catechol oxidase from *Aspergillus oryzae* (PDB ID: 4J3P): a polyphenol oxidase with the canonical dinuclear copper active site; represents catechol-oxidase-type diphenolases. (D) Catechol oxidase reaction: catechol is oxidized to o-quinone; produces brown pigments. (E) Tyrosinase pathway: L-tyrosine is converted to L-DOPA; L-DOPA is further oxidized to dopaquinone; forms melanin-like intermediates. (F) Laccase reaction: ABTS is oxidized to the green-blue radical cation $ABTS^{+}$; it serves as a chromogenic reporter for multicopper oxidase activity.

Catechol oxidases, a major subclass of polyphenol oxidizing enzymes, catalyze the oxidation of o-diphenols to o-quinones but lack the monophenolase activity characteristic of tyrosinases (Mayer, 2006). They are typically detected using catechol-based assays, where rapid quinone formation produces dark brown or black pigmentation. Catechol oxidase activity responds strongly

to catechol and L-DOPA but shows no activity toward L-tyrosine, enabling clear differentiation from tyrosinase (Espín et al., 1997; Yoruk & Marshal, 2003).

Laccase (EC 1.10.3.2) screening relies on chromogenic substrates such as 2,2′-azinobis(3-ethylbenzothiazoline-6-sulfonic acid) (ABTS), guaiacol, and syringaldazine, each producing distinct colored oxidation-associated metabolites (Baldrian, 2006; Coll et al., 1993). ABTS is widely preferred because its oxidation yields a stable green–blue radical cation with high sensitivity and minimal interference from peroxidases (Claus, 2004). Guaiacol and syringaldazine generate orange-brown and purple products, respectively, and are useful for distinguishing laccase from other oxidases, although they are more susceptible to auto-oxidation in plate assays.

Tyrosinase (EC 1.14.18.1) is screened using L-3,4-dihydroxyphenylalanine (L-DOPA) or L-tyrosine. L-DOPA oxidation produces dark melanin-like pigments, enabling rapid detection of diphenolase activity, while tyrosine oxidation proceeds more slowly and is used to confirm monophenolase activity (Agarwal et al., 2019). These assays are essential for distinguishing tyrosinase from catechol oxidase-type MPLOs, which lack monophenol hydroxylation capability (Belle, 2013). To improve clarity and highlight the complementary nature of these assays, Table 2.3 summarizes the major oxidoreductases screened alongside PPOs, their preferred substrates, assay formats, and supporting references.

Table 2.3: Common screening assays, substrates, and references for catechol oxidase, laccase and tyrosinase.

Enzyme	Primary Function	Common Screening Substrates	Assay Type / Observable Response	Key References
Catechol oxidase (diphenolase)	Oxidation of o-diphenols to o-quinones	Catechol, 4-methylcatechol, L-DOPA	Brown/black pigmentation on catechol agar; A_{420} increase in broth assays	Mayer (2006); Yoruk and Marshal (2003); Espín et al. (1997)
Tyrosinase (monophenolase + diphenolase)	Hydroxylation of monophenols; oxidation of diphenols	L-tyrosine, L-DOPA	Melanin-like dark pigments; monophenolase vs diphenolase differentiation	Solano et al. (2000); Hearing and Tsukamoto (1991); Espín et al. (1997)
Laccase (multicopper oxidase)	Oxidation of phenolics, aromatics, and amines	ABTS, guaiacol, syringaldazine	Green-blue (ABTS), orange-brown (guaiacol), purple (syringaldazine)	Coll et al. (1993); Baldrian (2006); Claus (2004)

Across these assays, several substrates serve as common indicators due to their strong chromogenic responses and broad compatibility with multiple oxidoreductases. Catechol, L-DOPA, tyrosine, guaiacol, and ABTS are the most widely used substrates across PPO, catechol oxidase, laccase, and tyrosinase screening workflows (Coll et al., 1993; Mayer, 2006). Their combined use provides a versatile and sensitive toolkit for identifying microbial strains with diverse phenol modifying capabilities, particularly relevant for tea polyphenol biotransformation, where multiple oxidative and hydrolytic pathways contribute to pigment formation, flavor development, and structural diversification (Nikolaivits et al., 2018).

2.6.4 Optimization of enzyme production

Optimizing culture conditions can significantly enhance PPO yields. Inducers such as tannic acid, catechol, or copper ions stimulate native enzyme expression in many bacterial isolates. Co-culture strategies have also been explored to activate silent metabolic pathways or enhance oxidative enzyme secretion. Alternatively, heterologous expression offers a route to scalable enzyme production that avoids the low native yields of many wild-type strains. *Escherichia coli* and *Pichia pastoris* are the most widely used hosts for recombinant protein production, with *P. pastoris* offering high-yield secretion of properly folded protein (Ergün et al., 2021). In tea, four *Camellia sinensis* PPO isozymes have been expressed in *E. coli*; although much of the recombinant protein formed inclusion bodies, three isozymes (CsPPO1–3) were active toward tea polyphenols and catalysed the synthesis of theaflavin-3,3′-digallate, whereas CsPPO4 was inactive (Liu et al., 2023b). Expression conditions strongly influence how much active plant PPO is obtained in bacterial hosts (Dirks-Hofmeister et al., 2013). Recombinant systems also enable protein engineering, affinity tag-based purification, and the generation of thermostable or otherwise tailored PPO variants suitable for industrial applications.

Heterologous expression has become the dominant strategy for scalable PPO production. Expressing PPO genes in *E. coli*, *Pichia pastoris* or other recombinant hosts overcomes the low native yields, strain heterogeneity and complex downstream purification associated with native sources (Ergün et al., 2021; Nikolaivits et al., 2018). Recombinant systems also allow PPO variants to be engineered for enhanced activity, stability or substrate specificity

In optimization studies employing statistical design frameworks such as Response Surface Methodology (RSM), PPO production is typically governed by a defined set of critical factors. These include copper concentration (commonly 0.05–1.0 mM Cu^{2+}), inducer type and concentration (catechol, tannic acid, phenolic analogues), carbon-to-nitrogen ratio (5:1–20:1), dissolved oxygen levels (controlled via agitation or aeration rate), and pH (typically explored between 5.5 and 8.0) (Myers et al., 2016; Saad et al., 2021). These variables form the core design space for factorial, Box–Behnken, or central composite designs aimed at maximizing oxidoreductase output.

For multi-enzyme systems, such as those producing laccases, tyrosinases, catechol oxidases, and peroxidases simultaneously, multi-response optimization is often required. In such cases, the Derringer desirability function provides an enhanced approach to balancing competing objectives by converting each oxidoreductase-associated activity into a desirability score (0–1) and combining them into an overall composite desirability index (D). This allows simultaneous optimization of multiple oxidoreductase activities under a single set of culture conditions, ensuring that no single enzyme is maximized at the expense of others (Derringer & Suich, 1980).

2.6.5 Purification strategies for MPLOs

Purification workflows for extracellular MPLOs typically begin with culture clarification through centrifugation or membrane filtration to remove cells and debris (Mayer, 2006). The clarified supernatant is then subjected to ammonium sulfate precipitation, commonly up to 80% saturation, to enrich MPLOs from the extracellular protein pool (Espín et al., 1997; Yoruk & Marshal, 2003). Three-phase partitioning (TPP), which combines ammonium sulfate and tert-butanol, provides an alternative rapid enrichment method that offers high recovery with minimal processing steps (Aguilar et al., 2007). Ultrafiltration using molecular weight cut-off membranes is often incorporated at this stage to concentrate the enzyme and perform buffer exchange before chromatographic separation (Baldrian, 2006).

Chromatographic methods provide further purification and resolution. Anion-exchange chromatography (e.g., Diethylaminoethyl (DEAE)-cellulose, HiTrap Q) is frequently employed to separate PPOs based on surface charge, while size-exclusion chromatography (e.g., Superdex G-100) is used to polish partially purified fractions according to molecular weight (Solano et al.,

2006). Affinity chromatography using tyrosine-like ligands, such as sepharose-L-tyrosine, has demonstrated high specificity for PPOs and has produced substantial purification folds in several microbial studies (Pretzler & Rompel, 2024).

In addition to purification, immobilization techniques, including covalent attachment to functionalized pumice, silica, or polymeric beads, have been shown to enhance PPO stability, broaden operational pH and temperature ranges, and enable enzyme reuse in continuous or semi-continuous processes (Claus, 2004; Claus, 2010). When immobilizing MPLOs for reactions involving high-molecular-weight phenolics, such as catechins and TF precursors, mass transfer becomes an important consideration. Bead size, pore diameter, and internal porosity influence substrate diffusion and can significantly affect the apparent activity of immobilized MPLOs.

2.6.6 Applications of MPLOs in tea biotransformation and beyond

MPLOs have become increasingly valuable biocatalysts in tea processing due to advances in enzyme production, purification, and immobilization technologies. In black tea manufacture, PPOs catalyze the oxidation of catechins to reactive o-quinones, which subsequently polymerize into key quality-defining pigments. Controlled enzymatic oxidation using purified or immobilized PPOs can enhance TF formation, improving brightness, briskness, and antioxidant capacity (Li et al., 2022a; Tao et al., 2016; Teng et al., 2021).

PPOs also contribute to modulating TR profiles, influencing body, color density, and mouthfeel in black tea infusions (Nguyen Ngoc et al., 2015; Zheng, 2025). Selective oxidation of gallated catechins can reduce bitterness and astringency, improving sensory smoothness and consumer acceptability (Obanda et al., 1997). Beyond conventional pigments, MPLO-mediated oxidation can generate potentially bioactive oxidation-associated metabolites, including catechin dimers, quinone adducts, and polymeric phenolics with enhanced antioxidant or metabolic benefits (Nikolaivits et al., 2018). Outside the tea sector, MPLOs have emerged as versatile industrial biocatalysts. Their broad substrate range and strong oxidizing capacity underpin applications in dye decolorization (Claus, 2004), bioremediation of phenolic pollutants (Baldrian, 2006), biosensor development for phenolics and environmental monitoring (Campuzano et al., 2020), and phenolic waste valorization in agro-industrial systems (Aguilar et al., 2007). While these applications demonstrate the adaptability of MPLOs across food, environmental, and

biotechnological domains, only a subset of these processes are compatible with food-grade constraints and beverage processing requirements.

In the context of tea biotransformation, the most relevant applications include controlled catechin oxidation to enhance TF formation, modulation of TR composition to improve body and color density, selective oxidation of gallated catechins to reduce bitterness and astringency, and the generation of catechin-derived bioactives with potential health benefits. Immobilized MPLOs on food-safe supports also offer opportunities for repeated batch or continuous tea oxidation, provided that materials and process conditions meet beverage-grade standards. In contrast, applications such as dye decolorization, pollutant remediation, and industrial biosensing are not directly transferable to tea processing due to solvent, material, or regulatory limitations. To provide a consolidated overview, Table 2.4 summarizes the major applications of PPOs, their functional roles, and representative references.

Table 2.4: Applications of PPOs in tea biotransformation and other industries

Application Area	Functional Role of PPO	Representative Outcomes	Key References
Black tea processing	Controlled catechin oxidation	Enhanced theaflavin formation; improved brightness and briskness	Tao et al. (2016); Sang et al. (2020)
Thearubigin modulation	Oxidation of polymeric phenolics	Improved body, color density, and mouthfeel	Obanda et al. (1997)
Bitterness/astringency reduction	Selective oxidation of gallated catechins	Smoother sensory profile	Liang et al. (2003)
Generation of novel bioactives	Formation of catechin dimers and quinone adducts	Increased antioxidant or metabolic activity	Nikolaivits et al. (2018)
Controlled fermentation in specialty teas	Reproducible enzymatic oxidation	Consistent flavor and functional profiles	Singh & Gupta (2020)
Dye decolorization	Oxidation of synthetic dyes	Removal of textile dye pollutants	Claus (2004)
Bioremediation	Oxidation of phenolic pollutants	Detoxification of industrial effluents	Baldrian (2006)
Biosensor development	Quinone-based electrochemical detection	High-sensitivity phenolic biosensors	Campuzano et al. (2020)
Phenolic waste valorization	Conversion of phenolics into value-added products	Biotransformation of agro-industrial wastes	Aguilar et al. (2007)

2.7 Analytical approaches for tea chemical and functional evaluation

Accurate and reproducible analytical methods are essential for monitoring catechin oxidation, quantifying pigments, detecting secondary metabolites, and assessing functional changes during both conventional black tea processing and novel biocatalytic interventions. These methods collectively enable mechanistic interpretation of oxidation systems and provide the comparative framework required to evaluate microbial PPO-driven transformations. A rigorous analytical strategy is therefore fundamental to determining whether microbial systems reproduce, enhance, or diverge from orthodox black tea chemistry.

2.7.1 Sample preparation and extraction techniques

Robust sample preparation is pivotal for accurate analysis. Ultrasound-assisted extraction (UAE) optimizes yields (>90%) in 15–30 minutes, using solvents like 70% methanol or boiling water, with advantages in efficiency and reduced solvent usage but potential degradation of thermolabile compounds (Huang et al., 2025; Myo et al., 2023). Microwave-assisted extraction (MAE) applies microwave energy for faster penetration, applied to green tea for polyphenols and catechins (Rehder et al., 2021). Pressurized fluid extraction (PFE) uses elevated pressure/temperature for selectivity, extracting gallic acid and flavonols from black tea (Souza et al., 2019).

Microextraction techniques include microextraction by packed sorbent (MEPS), minimizing matrix effects for pesticides/minerals in tea (Martins et al., 2025), and dispersive liquid-liquid microextraction (DLLME) for polycyclic aromatic hydrocarbons, offering preconcentration but limited capacity (Timofeeva et al., 2021). Green solvents, such as butylene glycol or deep eutectic solvents, reduce environmental impact while maintaining efficiency (Myo et al., 2023). Collectively, these developments reflect a broader shift toward sustainable, high-efficiency extraction workflows aligned with green chemistry principles.

For biotransformed teas, preparation must address both original tea compounds and microbial-derived metabolites. Effective analysis of tea pigments begins with the proper preparation and extraction of the tea matrix. Conventional methods often involve solvent extraction using hot water or organic solvents like ethanol or methanol (Wang et al., 2018; Yang et al., 2025a). These traditional methods are straightforward but can be time-consuming and may use toxic solvents

(Yang et al., 2025a). Together, these innovations improve extract quality and reproducibility, particularly important when analyzing complex biotransformed matrices. For consistency across this thesis, a single solvent extraction protocol with ultrasound assistance under controlled temperature and time conditions was used for all sample types. Greener solvents and emerging extraction technologies are discussed for contextual relevance but were not experimentally applied in this study. Table 2.5 summarizes the principal extraction techniques, mechanisms, advantages, limitations, and representative operating parameters.

Table 2.5: Summary of extraction techniques used for tea and biotransformed tea metabolites, including mechanisms, advantages, limitations, and typical operating parameters.

Technique	Mechanism	Advantages	Limitations	Typical Parameters	Citation
Ultrasound-Assisted Extraction (UAE)	Uses ultrasonic waves to disrupt cell walls and enhance solvent penetration	High yield (>90%), reduced solvent use, short time (15–30 min)	Potential degradation of thermolabile compounds, equipment cost	Solvent type (e.g., 70% methanol), temperature (50–70°C), time (15–30 min)	Myo et al. (2023); (Huang et al., 2025)
Microwave-Assisted Extraction (MAE)	Employs microwave energy for rapid heating and solvent penetration	Faster extraction, better compound preservation, reduced solvent use	Risk of thermal degradation, higher initial cost	Microwave power (300–600 W), solvent ratio (1:20), time (5–15 min)	Rehder et al. (2021)
Pressurized Fluid Extraction (PFE)	Utilizes elevated pressure/temperature to enhance solubility	High selectivity, short extraction time, reduced solvent use	Thermal degradation risk, expensive equipment	Pressure (100-200 bar), temperature (100–150°C), time (10–20 min)	Souza et al. (2019)
Microextraction by Packed Sorbent (MEPS)	Partitions compounds between solid sorbent and sample	Minimizes matrix effects, preconcentration effect, low solvent use	Limited capacity, potential competitive effects	Sorbent type (C18), volume (50–200 µL), temperature (25–40°C)	Martins et al. (2025)
Dispersive Liquid-Liquid Microextraction (DLLME)	Partitions compounds between liquid phases with disperser solvent	Preconcentration effect, reduced solvent use, high selectivity	Limited solvent options, low capacity	Disperser solvent (acetone), extractant (chloroform), volume (50–100 µL)	Timofeeva et al. (2021)
Pressurized Liquid Extraction (PLE)	Uses high pressure and temperature to extract with liquid solvents	High efficiency, shorter extraction time, higher yields	High equipment cost, potential analyte degradation	Pressure (100–150 bar), temperature (80–120°C), solvent (ethanol)	Raghunath et al. (2023)
Soxhlet Extraction (Traditional)	Continuous solvent reflux to extract compounds	Simple, well-established, thorough extraction	Long extraction time, high solvent use	Solvent (e.g., methanol), time (6–12 hours), temperature (60–80°C)	Raghunath et al. (2023)

2.7.2 Traditional analytical methods

Traditional wet-chemistry methods remain essential for rapid and cost-effective assessments in industrial settings (Pérez et al., 2023). The Folin-Ciocalteu assay, standardized under ISO 14502-1:2005 and AOAC 2017.13 (AOAC, 2023; ISO, 2005), measures total polyphenols as gallic acid equivalents (GAE) at 765 nm (Abdallah et al., 2024). While achieving 99.9–101.1% recovery, it is prone to interference from non-phenolic reductants like sugars or microbial metabolites in biotransformed teas (Bastola et al., 2017; Ge et al., 2019). These interferences can lead to substantial overestimation, particularly in fermented teas rich in phenolic acids. Modified approaches, such as the 18 MPC method, improve selectivity in complex matrices (Al-Shwaiyat et al., 2018).

Given these matrix-dependent interferences, Table 2.6 presents a comparative summary of traditional analytical methods, highlighting their strengths, limitations, and the specific issues encountered when analyzing biotransformed teas. Titration methods, for example, potassium permanganate oxidation, offer high precision but are limited by subjective endpoints and lack specificity for individual phenolic subclasses. Ultraviolet (UV) visible spectrophotometry provides rapid screening of catechins, caffeine, and TFs, although overlapping absorptions reduce accuracy (Engelhardt, 2023). Colorimetric assays targeting flavonoids, proanthocyanidins, or tannins provide class-specific data but are pH-sensitive and less reproducible across different tea types (Zeb, 2021).

In biotransformed teas, these challenges are amplified. Microbial activity reduces catechins while increasing phenolic acids, which elevates Folin Ciocalteu readings (Ge et al., 2019). TFs and polymeric pigments also interfere with catechin absorbance in black tea, complicating UV-based quantification (Zhang et al., 2020). Recent advances, such as microfluidic paper-based devices (LOD 5×10^{-7} mol/L), offer portable, matrix-tolerant analysis (Hidayat et al., 2016).

Despite low cost and rapidity, traditional methods lack specificity for individual compounds, limiting their utility in authenticating complex biotransformed teas (Huang et al., 2022; Xu et al., 2022). They remain valuable for preliminary screening but benefit from integration with chromatographic or mass spectrometric techniques. To complement these assays, chromatographic quantification of catechins and caffeine using HPLC is standardized under ISO 14502-2, which provides validated conditions for accurate profiling of green and black tea catechins. In this thesis,

HPLC catechin analysis followed ISO 14502-2 with predefined quality control criteria ($R^2 > 0.999$; RSD < 5%; recovery 95–105%). These criteria ensure analytical comparability across all tea and biotransformed tea samples.

Table 2.6: Overview of traditional analytical methods, including their strengths, limitations, and challenges in analyzing biotransformed teas.

Method	Principle/Mechanism	Key applications in tea	Advantages	Limitations	Examples of biotransformed teas
Folin-Ciocalteu Assay	Redox reaction with phosphomolybdic-phosphotungstic acid; absorbance at 765 nm	Total polyphenol quantification (as GAE)	Cost-effective, simple, high recovery (99.9–101.1%)	Interferences from non-phenolics (e.g., sugars, acids); overestimation in Pu-erh	Overestimation due to microbial metabolites like phenolic acids
Titration (e.g., KMnO4)	Oxidation-reduction titration	Polyphenol content estimation	High precision	Subjective endpoint; not for individual compounds	Limited use in black tea due to theaflavin interference
UV-Vis Spectrophotometry	Absorbance at specific wavelengths (e.g., 280 nm for catechins)	Screening catechins, caffeine, theaflavins	Quick, non-destructive	Overlapping absorptions; low specificity	Challenges in oolong/Pu-erh with diverse pigments
Colorimetric Assays (e.g., AlCl3 for flavonoids)	Complex formation with reagents	Class-specific (flavonoids, tannins)	Targeted, inexpensive	pH-sensitive; poor reproducibility	Interference from phenolic acids in fermented teas

2.7.3 High-performance liquid chromatography with diode array detection (HPLC–DAD) for targeted polyphenol quantification

Reversed-phase HPLC-DAD remains the most widely applied and optimized method for quantifying major tea polyphenols, particularly flavan-3-ols and theaflavins that dominate green tea substrates and early-to-mid oxidation-associated metabolites. Using C18 stationary phases and acidified aqueous–acetonitrile or methanol gradients, HPLC-DAD routinely separates EGCG, EGC, ECG, EC, and the four principal TFs (TF, TF-3-G, TF-3'-G, TF-3,3'-diG) with limits of detection of 0.1–1 μg mL^{-1} and relative standard deviations of 1–5% (Custodio-Mendoza et al., 2024; Rha et al., 2021). The method provides excellent linearity ($R^2 > 0.99$) across concentrations relevant to tea infusions and enzymatic oxidation studies, while UV spectra enable reliable peak

confirmation in moderately complex matrices (Cordero et al., 2009; Romers et al., 2023). Although HPLC-DAD is ideal for monitoring catechin depletion and TF accumulation, it cannot resolve structurally similar oligomers or transient intermediates.

In this thesis, HPLC-DAD served as the primary analytical platform for the comparative quantification of catechins, caffeine, and selected oxidation-associated metabolites in green tea, black tea, and microbial enzyme-treated samples.

2.7.4 LC-MS/MS and LC-HRMS for structural confirmation and intermediate detection

Liquid chromatography coupled with tandem mass spectrometry (LC-MS/MS) and high-resolution mass spectrometry (LC-HRMS) extend analytical scope by providing structural confirmation, higher sensitivity, and detection of low-abundance intermediates and degradation products. Operating in negative electrospray ionization mode, LC-MS/MS achieves limits of quantification of 0.01–0.5 μg mL^{-1} and enables targeted monitoring of precursor-to-product ion transitions for catechins, galloylated derivatives, gallic acid, and TFs (Ge et al., 2019; Kikkawa et al., 2022). These capabilities are particularly valuable in biotransformed teas where enzymatic or microbial activity generates diverse phenolic acids and quinone-derived species not easily resolved by UV detection (Qiu et al., 2025; Wang et al., 2022c). LC-MS/MS has been used to track transient o-quinone intermediates and small-molecule breakdown products, clarifying oxidation systems beyond primary pigments (Frańska & Frański, 2024). However, matrix effects and the need for isotopically labeled internal standards or matrix-matched calibration remain important limitations. In the context of this study, LC-MS/MS is essential for verifying whether microbial PPOs generate oxidation intermediates comparable to those in orthodox black tea.

In this thesis, LC-MS/MS was used primarily for comparative profiling of polyphenols and for structural confirmation of selected oxidation-associated metabolites. Advanced LC-HRMS and ion-mobility methods discussed here are included for contextual comparison but were not applied experimentally.

2.7.5 Gas chromatography–mass spectrometry (GC–MS) for volatile and semi-volatile profiling

GC-MS, typically following derivatization of polar hydroxyl groups, is the method of choice for profiling volatile and semi-volatile compounds generated or modified during tea oxidation and microbial processing. With limits of detection of 0.05–0.5 ng mL^{-1} and precision of 2–7%, GC-MS identifies aroma-active aldehydes, alcohols, ketones, terpenoids, and furanones arising from lipid oxidation, Maillard-type reactions, or side activities of PPOs and associated enzymes (Liang et al., 2024; Rong et al., 2023).

Although catechins and theaflavins are non-volatile and not directly amenable to GC-MS, the technique provides complementary information on aroma changes accompanying polyphenol transformations, especially when evaluating sensory impacts of controlled enzymatic oxidation relative to conventional black tea (Guo et al., 2025; Shi et al., 2019). For this study, GC-MS is critical for determining whether microbial PPO-treated teas develop aroma profiles consistent with black tea or diverge due to altered oxidation dynamics.

GC-MS-based volatile profiling is discussed here as an important complementary analytical approach relevant to tea oxidation studies; however, it was not applied experimentally in this thesis.

2.7.6 Analytical challenges in thearubigin characterization

TRs, the dominant high-molecular-weight oxidation-associated metabolites in black tea (commonly reported at about 10–20% of dry weight, depending on the fractionation method used), remain analytically challenging due to polydispersity, structural heterogeneity, molecular weights often exceeding 1000 Da, and the absence of authentic reference standards (De et al., 2024; Wang et al., 2018). Direct chromatographic resolution is not feasible with current reversed-phase or size-exclusion systems because of poor peak shape, insolubility, and co-elution with other polymers. Consequently, indirect estimation, absorbance at 380–460 nm after ethyl acetate partitioning or total phenolic content corrected for quantified monomers, remains standard (Engelhardt, 2023). These approaches allow relative comparisons but cannot distinguish substructures or galloylation patterns.

Advanced ultra-high-performance liquid chromatography–high-resolution mass spectrometry (UHPLC–HRMS) and ion-mobility quadrupole time-of-flight mass spectrometry (IM–QTOF–MS) improve characterization of molecular weight distributions and isobaric species, though quantification remains semi-quantitative (Chen et al., 2018; Yue & Cao, 2022). Beyond mass spectrometry, several emerging distribution-based techniques offer complementary insights into TR size and aggregation behavior. Asymmetric flow field flow fractionation coupled with multi angle light scattering (AF4 MALS) provides high resolution separation of colloidal and polymeric phenolics without stationary phase interactions (Gigault et al., 2017). Gel permeation chromatography–multi-angle light scattering (GPC MALS) enables absolute molecular weight determination independent of calibration standards and has been applied to complex plant polyphenols and lignin-derived polymers (Kleks et al., 2021). Diffusion-ordered spectroscopy nuclear magnetic resonance (DOSY NMR) offers non-chromatographic separation based on diffusion coefficients, allowing estimation of hydrodynamic radii and aggregation states in heterogeneous mixtures (Harvey et al., 2023; Kleks et al., 2021). Although these techniques are not applied in this thesis, they represent the current frontier for resolving TR heterogeneity and highlight the methodological limitations that still constrain structural interpretation.

2.7.7 Antioxidant capacity assays for functional evaluation

The functional consequences of catechin oxidation and biotransformation are commonly assessed using antioxidant assays, including 2,2-diphenyl-1-picrylhydrazyl (DPPH), 2,2′-azino-bis(3-ethylbenzothiazoline-6-sulfonic acid) (ABTS), and Ferric reducing antioxidant power (FRAP). These rapid, inexpensive assays require minimal preparation and generate Trolox-equivalent values reflecting net radical-scavenging or reducing power (Sun et al., 2022b). DPPH (517 nm) and ABTS (734 nm) capture the high activity of monomeric catechins and the variable activity of theaflavins and thearubigins, while FRAP (593 nm) highlights contributions from iron-chelating galloyl groups (Pérez et al., 2023). Combined use provides complementary mechanistic insight, distinguishing hydrogen-atom-transfer from single-electron-transfer behavior and supports accurate comparative evaluation across treatments.

Additional assays extend this functional coverage. The Cupric ion reducing antioxidant capacity (CUPRAC) assay quantifies cupric-reducing antioxidant capacity under near-neutral pH, offering

improved compatibility with polymeric phenolics and TR-rich matrices (Apak et al., 2016). ORAC measures peroxyl radical scavenging based on fluorescence decay kinetics and is particularly sensitive to gallated catechins and early-stage oxidation-associated metabolites (Zeb, 2021). Together, these assays provide a broader functional profile of antioxidant behavior across the stages of biotransformation. In this thesis, antioxidant assays were used as comparative functional indicators rather than definitive measures of *in vivo* biological activity.

2.7.8 Integrated multi-method frameworks for comprehensive evaluation

Integrating targeted chromatographic profiling (HPLC-DAD and LC-MS/MS for catechins, TFs, and phenolic markers) with volatile fingerprinting (GC-MS) and functional assays (DPPH, ABTS, FRAP) provides a powerful multi-method framework for oxidation studies. This combined strategy overcomes individual limitations, lack of structural detail in bulk assays, inability to quantify polymers chromatographically, and absence of functional context in pure profiling, while enabling comprehensive evaluation of substrate conversion, pigment formation, aroma evolution, and retained bioactivity. Such integration is particularly suited to assessing novel biocatalytic interventions, where both chemical fidelity to orthodox black tea and preservation or enhancement of functional properties must be demonstrated (Huang et al., 2025; Romers et al., 2024).

In biotransformed teas, where microbial metabolites introduce variability, combined GC-MS VOC fingerprinting and LC-MS polyphenolic mapping support authentication and quality control (Huang et al., 2025; Romers et al., 2024). Emerging non-destructive techniques such as Near-infrared spectroscopy (NIRS) and Fourier transform infrared spectroscopy (FTIR) further enhance this framework, enabling rapid screening (R^2 0.90–0.98) (Arifah et al., 2022; Chen et al., 2025a) without extensive preparation and supporting process optimization and innovation in the tea industry. For this study, such a multi-method approach is essential to rigorously compare microbial PPO-generated products with conventional black tea and to validate the biochemical fidelity of the biocatalytic system.

Within the analytical pipeline, each method contributes a specific decision point: HPLC-DAD quantifies catechin depletion and theaflavin formation as primary conversion indicators; LC-MS/MS verifies key intermediates such as benzotropolone-containing species and tracks low-abundance oxidation-associated metabolites; GC-MS determines whether volatile profiles

converge with or diverge from orthodox black tea aroma; and antioxidant assays confirm whether functional activity is preserved or enhanced following microbial PPO-driven oxidation. Together, these complementary approaches provided the comparative analytical framework necessary to evaluate whether microbial oxidation systems reproduce, modify, or diverge from conventional black tea chemistry.

2.8 Synthesis of literature and identification of research gaps

The preceding sections demonstrate that tea polyphenol oxidation is governed by complex interactions among catechin composition, enzymatic activity, oxygen availability, and processing conditions. Although substantial progress has been made in characterizing major oxidation-associated metabolites such as theaflavins and thearubigins, many downstream oxidation pathways remain only partially resolved because of the structural heterogeneity and analytical complexity of polymeric tea pigments. Consequently, direct relationships between oxidation conditions, reaction pathways, and final product quality remain difficult to establish.

Conventional black tea processing relies primarily on endogenous PPOs and PODs to initiate catechin oxidation following cellular disruption. While these enzymes are essential for pigment formation, their activities are strongly influenced by cultivar, leaf maturity, environmental conditions, and processing variables. As a result, oxidation dynamics remain difficult to regulate reproducibly within heterogeneous leaf matrices, contributing to variability in pigment composition and sensory quality.

At the same time, increasing evidence suggests that microorganisms and their extracellular oxidoreductases may also contribute to tea-associated oxidation processes. Microbial enzymes such as tyrosinases, laccases, and related oxidoreductases exhibit catalytic properties distinct from those of endogenous plant PPOs, including extracellular activity, broader operational stability, and greater substrate tolerance. These characteristics suggest potential utility as alternative or complementary systems for controlled catechin biotransformation. However, the current understanding of microbial contributions to tea oxidation remains limited, largely based on correlation-based observations or studies of post-fermented teas rather than on controlled black-tea-like oxidation systems.

Despite advances in microbial enzyme screening and characterization, several important research gaps remain. First, the mechanistic understanding of microbial enzyme-mediated catechin oxidation remains limited, particularly in comparison with endogenous PPO-driven pathways. Second, direct comparative evaluations of microbial and plant enzyme-mediated oxidation under controlled conditions are scarce. Third, systematic studies linking microbial enzyme properties, reaction conditions, and reproducible oxidation outcomes in tea matrices remain limited. Together, these gaps constrain the development of controlled biocatalytic approaches for directing tea polyphenol oxidation.

Analytical limitations further complicate this field. Although chromatographic and mass spectrometric methods have substantially improved targeted catechin and metabolite profiling, many higher-order oxidation-associated metabolites, particularly thearubigins, remain only partially characterized. Consequently, mechanistic interpretation of downstream polymerization pathways continues to rely heavily on operationally defined fractions and comparative profiling approaches rather than definitive structural resolution. Within the analytical framework of this thesis, HPLC-DAD, LC-MS/MS, spectrophotometric pigment analysis, and antioxidant assays constitute the primary experimental methods used to evaluate catechin transformation and functional changes. Additional advanced analytical approaches discussed in this chapter are included for contextual comparison but were not applied experimentally in this study.

Collectively, the literature indicates that although the general biochemical basis of tea oxidation is well established, an integrated understanding at the interface of enzymology, oxidation control, and process reproducibility remains incomplete. In particular, the deliberate application of microbial extracellular oxidoreductases as controllable catalytic systems for tea catechin oxidation has not been systematically investigated.

Accordingly, the present study evaluates whether a bacterial extracellular polyphenol-oxidizing-like oxidoreductase system can function as a controllable platform for catechin biotransformation under defined experimental conditions. Rather than attempting to replicate conventional black tea manufacture directly, this work investigates whether MPLO-mediated oxidation can provide mechanistic insights into catechin transformation pathways and enable improved experimental control over oxidation outcomes. Figure 2.12 summarizes the literature synthesis and principal research gaps that motivate the experimental framework of this thesis.

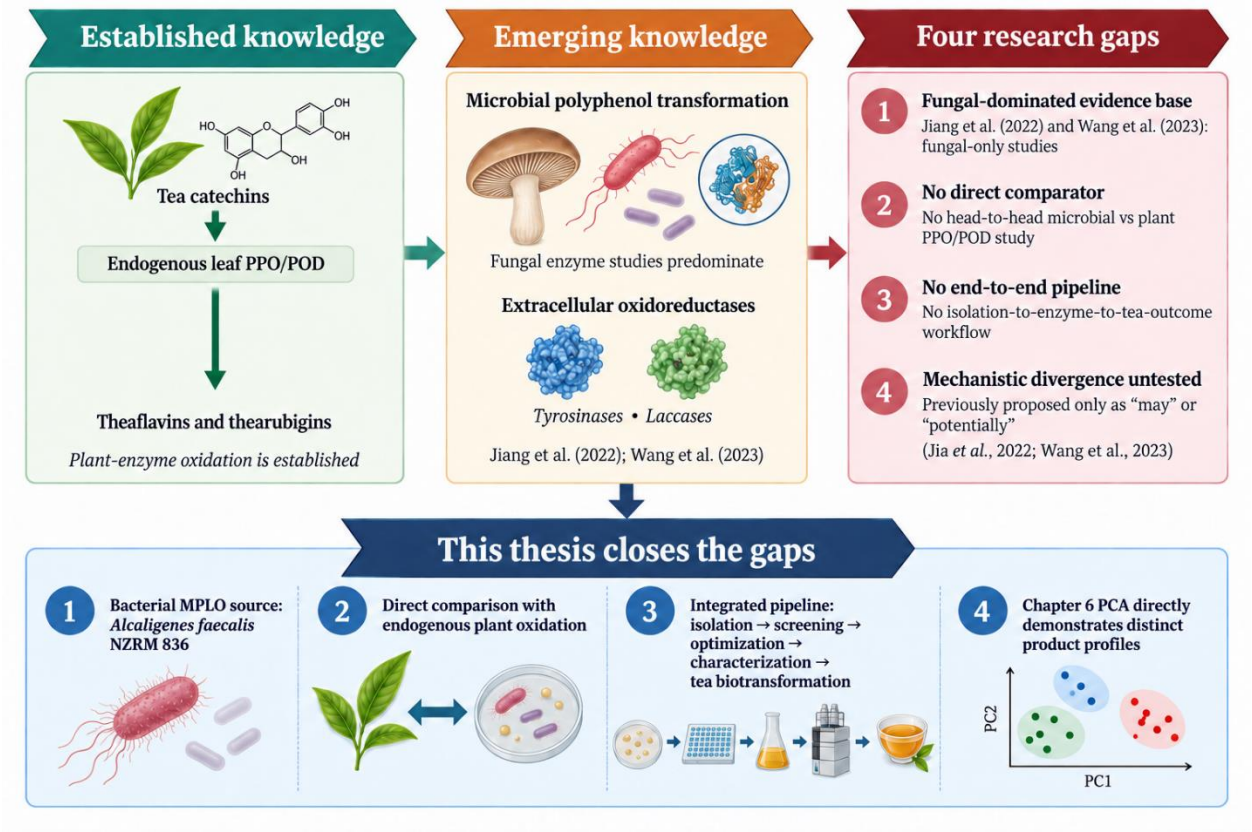

Figure 2.12: Conceptual overview of literature synthesis and research gaps in microbial enzyme-mediated tea biotransformation.

Chapter 3

Analytical determination of key non-volatile metabolites and their transformation during black tea manufacture

Preface

This chapter describes the development and validation of chromatographic methods for profiling catechins, theaflavins, alkaloids, and related tea metabolites. It also evaluates extraction strategies and establishes a reproducible analytical framework for monitoring polyphenol transformations during microbial and conventional tea oxidation processes.

Abstract

Tea (*Camellia sinensis*) is valued for its polyphenolic compounds, which substantially influence its sensory and functional properties. However, accurately quantifying these compounds across processing stages remains challenging. These challenges arise from extraction variability, matrix effects, and analytical limitations. This study developed and validated a rapid high-performance liquid chromatography with diode array detection (HPLC-DAD) method. The method allows for simultaneous analysis of 12 major tea constituents, including gallic acid, theobromine, caffeine, catechins (C, EC, EGC, EGCG, ECG), and theaflavins (TF, TF3G, TF3′G, TF3-3′G), in green and black tea matrices.

The method achieved high linearity ($r^2 \geq 0.9995$), adequate sensitivity (LOD: 0.01–0.56 µg/mL; LOQ: 0.03–1.68 µg/mL), acceptable precision (RSD < 4.68%), and high recovery across most analytes. The method also improved separation of previously co-eluting compounds within a 40 min runtime. Recovery of gallated theaflavins was lower in black tea matrices, suggesting that matrix components may interfere with analyte measurement and reduce the accuracy of absolute quantification. Extraction optimization showed that UAE with 70% methanol yielded higher recovery than hot-water and ISO-standard methods under the study conditions.

Applying the method across black tea processing stages revealed several changes, including a 95.6% reduction in total catechin content (FTL to FBT), as well as transient increases in theaflavins after rolling. In addition, gallic acid, caffeine, and theobromine concentrations showed dynamic fluctuations. Collectively, these observations were consistent with processing-associated oxidation, substrate transformation, and extraction-related variability during black tea manufacture.

The validated HPLC-DAD workflow was suitable for comparative profiling of major tea polyphenols across processing stages. It provided a targeted analytical framework for investigating processing-induced chemical transformations. This method may also support applications in tea quality evaluation, nutritional analysis, and functional food research involving polyphenol-rich systems.

Keywords: *Camellia sinensis*, polyphenols, catechins, theaflavins, HPLC-DAD, black tea processing.

3.1 Introduction

Tea (*Camellia sinensis*) is a globally consumed beverage valued for its sensory properties, cultural significance, and health-promoting potential. These attributes are largely associated with a diverse range of polyphenolic compounds and alkaloids, including catechins, theaflavins, gallic acid, caffeine, and theobromine (Chaudhary et al., 2023; Wang et al., 2023b). Green tea is characterized by high concentrations of catechins, including epigallocatechin gallate (EGCG) and epicatechin gallate (ECG), which contribute substantially to its antioxidant activity. In contrast, black tea undergoes enzymatic oxidation during processing, leading to catechin oxidation, condensation, and polymerization reactions that generate theaflavins and related oxidation-associated metabolites responsible for the characteristic color, briskness, and astringency (Deka et al., 2021).

Black tea manufacture involves sequential stages, including plucking, withering, rolling, cutting, oxidation, and firing. During oxidation, endogenous polyphenol oxidases (PPOs) catalyze biochemical transformations that strongly influence tea composition, bioactivity, and sensory quality (Takeo, 2014; Tanaka & Matsuo, 2020). However, variation among cultivars, terroirs, and processing conditions contributes to substantial differences in polyphenol composition and oxidation dynamics, emphasizing the need for comprehensive analytical methods capable of monitoring chemical changes across diverse tea matrices (Li et al., 2021).

The precise quantification of tea constituents is important for quality evaluation, nutritional labeling, and functional food development, as tea polyphenols are associated with anti-inflammatory, cardioprotective, and antioxidant activities (Sun et al., 2022a). Although high-performance liquid chromatography with diode array detection (HPLC-DAD) is a well-known analytical technique for quantifying polyphenols because of its sensitivity and specificity, current methods have limitations. These limitations include the co-elution of structurally similar compounds, like catechins and theaflavins, which complicates separation. Additionally, method optimization is needed for specific tea types, reducing method versatility. Traditional C_{18} columns, commonly used in HPLC-DAD, often result in long run times, reducing sample throughput (Dimcheva et al., 2019; Rha et al., 2021). Ultra-high-performance liquid chromatography can improve analytical speed and separation efficiency but often requires specialized instrumentation, thereby increasing operational costs (Wang et al., 2022b). Consequently, development of a

validated and comparatively rapid HPLC-DAD workflow suitable for simultaneous profiling of major tea metabolites remains analytically relevant.

Extraction efficiency is another pivotal factor, as the chemically complex tea matrix, comprising cellulosic structures and diverse metabolites, challenges consistent recovery. Traditional techniques, such as hot-water extraction or ISO-standard infusions, often fail to solubilize all bioactives, particularly less polar compounds like theaflavins (Shaukat et al., 2023). Ultrasonication, combined with solvents like methanol or ethanol, enhances extraction through cavitation, improving solvent penetration and yield (Demesa et al., 2024). However, optimal solvent polarity, temperature, and extraction duration vary by tea type and compound, necessitating systematic optimization to ensure reproducibility across green and black tea matrices (Alshammari et al., 2021; Shaukat et al., 2023).

To address these challenges, this study developed and validated an HPLC-DAD method for simultaneous quantification of 12 major tea constituents in green and black tea, including gallic acid, theobromine, caffeine, catechins (C, EC, EGC, EGCG, ECG), and theaflavins (TF, TF3G, TF3′G, TF3-3′G). The study also evaluated extraction efficiency by comparing hot-water extraction, ISO-standard, and ultrasound-assisted extraction (UAE) methods using graded methanol and ethanol solutions. In addition, changes in major polyphenols during black tea processing were investigated to establish a comparative baseline profile of conventional plant enzyme-mediated oxidation. By integrating method validation, extraction optimization, and comparative profiling across processing stages, this study provides a targeted analytical framework for investigating processing-induced polyphenol transformations in tea systems.

3.2 Materials and methods

3.2.1 Chemicals and instrumentation

High-purity reagents were used for accurate quantification of tea polyphenols and alkaloids. Reference standards, including (+)-catechin, (-)-epicatechin (EC), (-)-epicatechin gallate (ECG), (-)-epigallocatechin (EGC), (-)-epigallocatechin gallate (EGCG), caffeine, theobromine, gallic acid, theaflavin (TF), theaflavin-3-gallate (TF3G), theaflavin-3′-gallate (TF3′G), and theaflavin-3,3′-digallate (TF3-3′G), were obtained from Sigma-Aldrich (St. Louis, MO, USA) and Phytolab

(Vestenbergsgreuth, Germany), all with ≥98% purity and suitable for HPLC analysis. HPLC-grade solvents, methanol, ethanol, and acetonitrile, as well as orthophosphoric acid (≥85%) for mobile phase preparation, were sourced from Fisher Scientific (Fair Lawn, NJ, USA). Ultrapure water was produced using a Milli-Q system (Millipore, Billerica, MA, USA). Polypropylene 50 mL volumetric flasks and 0.22 µm Stericup filter units (Millipore, Billerica, MA, USA) were employed for solution preparation and filtration. Ceylon green and black tea powders purchased from local supermarkets, finely ground with a coffee grinder (Breville, New Zealand), were stored in sealed, desiccated containers until analysis. A Fisherbrand ultrasonic water bath (Model 1123, Fisher Scientific, Hampton, USA) was used for ultrasound-assisted extractions.

Chromatographic analyses were conducted using a Vanquish HPLC system (Thermo Fisher Scientific, Waltham, MA, USA), equipped with a binary solvent pump, autosampler, column oven, and diode array detector (DAD). Separation was performed on a Kinetex XB-C_{18} column (100 × 4.6 mm, 2.6 µm particle size, 100 Å pore size; Phenomenex, Torrance, CA, USA), selected for its high efficiency and ability to provide adequate resolution of structurally similar polyphenols (Lee et al., 2018). UV absorbance was monitored simultaneously at 210 nm and 280 nm to monitor phenolic acid and flavonoid absorbance profiles, respectively (Lee et al., 2018; Wang et al., 2003).

3.2.2 Preparation of standard solutions

Standard solutions were prepared for HPLC calibration following a modified method based on ISO (2021), with stabilizing agents to prevent oxidation of polyphenols. Accurately weighed amounts (3.000 ± 0.001 mg) of each reference compound—gallic acid, theobromine, epigallocatechin (EGC), caffeine, catechin, epicatechin (EC), epigallocatechin gallate (EGCG), epicatechin gallate (ECG), theaflavin (TF), theaflavin-3-gallate (TF3G), theaflavin-3′-gallate (TF3′G), and theaflavin-3,3′-digallate (TF3-3′G) were dissolved in 2 mL acetonitrile with 1 min of ultrasonication. A stabilization solution consisting of 12.5% (w/v) EDTA and 12.5% (w/v) ascorbic acid was freshly prepared and added at 10% (v/v) to all stock standard solutions to prevent oxidative degradation of polyphenols (ISO, 2021). Each was subsequently diluted to 10 mL with HPLC-grade water, yielding individual stock solutions at 300 µg/mL.

Six levels of mixed calibration standards were prepared by combining appropriate volumes of the individual stock solutions (300 µg/mL) to achieve target concentrations ranging from 0.9375 to

150 µg/mL, as listed in Table S3.1 (Appendix B). This concentration range was selected to encompass the expected analyte levels in tea extracts. Calibration curves were constructed by plotting concentration against peak area using least-squares regression. The preparation of six-level calibration standards is detailed in Table S3.2 (Appendix B).

3.2.3 HPLC analysis

The HPLC method was designed to simultaneously separate 12 tea constituents in 40 min. The mobile phase consisted of solvent A (0.1% v/v orthophosphoric acid in ultrapure water) and solvent B (0.1% v/v orthophosphoric acid in acetonitrile). The HPLC elution gradient was programmed as follows: starting at 10% solvent B, increasing to 11% B over 5 min, then rising to 20% B over the next 5 min. This was followed by a 6-minute hold at 20% B, an increase to 30% B over 8 min, and a further rise to 45% B over 8 minutes. The gradient then increased to 90% B over 2 min, held at 90% B for 2 min, and concluded with a 4-min re-equilibration to the initial 10% B condition.

The flow rate was maintained at 0.4 mL/min with a column temperature of 25 °C and an injection volume of 10 µL. Analytes were identified by comparing retention times and UV absorption spectra with those of authenticated reference standards. Peak purity was additionally evaluated using DAD spectral analysis to assess potential co-elution.

3.2.4 Calibration and validation

The HPLC method was validated to assess analytical reliability and reproducibility. Calibration curves were generated using least-squares regression for each analyte (Table 3.1). Limits of detection (LOD) and quantification (LOQ) were determined using serial dilutions of standards based on signal-to-noise ratios of 3:1 and 10:1, respectively (Saadati et al., 2013). Precision was evaluated using six replicate injections of a 150 µg/mL mixed standard solution within a single day (intra-day precision) and across three consecutive days (inter-day precision).

Recovery experiments were performed by spiking ultrapure water and black tea extract matrices with known concentrations of analytes, followed by identical extraction and analytical procedures to evaluate matrix-associated effects (Xu, 2012). Because recovery for TF3-3′G (and to a lesser

extent some other theaflavins) was lower in the black tea extract matrix (approximately 83.86%), comparisons of TF3-3′G and total theaflavins between green tea and black tea matrices, as well as across different extraction methods and processing stages, are interpreted primarily in terms of directional trends rather than precise absolute concentration differences. These validation steps were performed to ensure accuracy and reproducibility across different sample matrices.

3.2.5 Extraction procedure and optimization

Green and black tea samples used for extraction method development and optimization were purchased locally from commercial retail sources, distinct from the Somerset Tea Estate leaf material used for the processing-stage sampling described in the following section. The dry matter content of green and black tea samples was determined by measuring mass loss at 103 °C following the ISO 1573 method (ISO, 1980). Extraction procedures were optimized to maximize recovery of tea polyphenols across both tea types. For UAE, a solid-to-solvent ratio of 1:20 was used. Specifically, 2.5 g of freeze-dried, finely powdered tea was mixed with 20 mL of solvent consisting of water or aqueous ethanol/methanol at 20%, 50%, 70%, or 90% (v/v). Samples were extracted using an ultrasonic water bath operating at 20 kHz and 60 W for 30 min. These conditions were selected to improve extraction efficiency while minimizing degradation of polyphenolic compounds (Athirojthanakij & Rashidinejad, 2024).

Extracts were centrifuged at 3500 rpm for 10 min, and the supernatant was collected. Residual solids were re-extracted using an additional 25 mL of the same solvent under identical conditions. Combined supernatants were filtered through a 0.22 µm membrane filter and adjusted to volume in a 50 mL volumetric flask. A 1 mL aliquot of each extract was subsequently analyzed by HPLC.

For comparative evaluation, polyphenols were also extracted using the ISO 14502-1:2005 standard method and conventional hot extraction (80 °C for 20 min). All extractions were performed in triplicate with two independent repeats (n = 6) (Athirojthanakij & Rashidinejad, 2024; ISO, 2005).

3.2.6 Dynamics of the major tea polyphenols during black tea processing

Tea leaves (*C. sinensis* (L.) Kuntze) were collected from Somerset Tea Estate, Talawakelle Tea Estates, Sri Lanka (6.92403° N, 80.68446° E). Leaves were plucked by trained workers wearing

gloves and facemasks at the “two leaves and a bud” stage, following the Tea Research Institute, Sri Lanka's guidelines for orthodox black tea manufacture (Wijeratne, 2003). Fresh leaves were transported in aerated nylon bags to the processing facility and manufactured into black tea using a modified orthodox processing sequence consisting of withering, rolling, rotovane cutting, oxidation, and firing (Figure 3.1). Oxidized tea samples were collected at three time points, 45 min apart. To minimize contamination risk, gloves and facemasks were worn throughout processing.

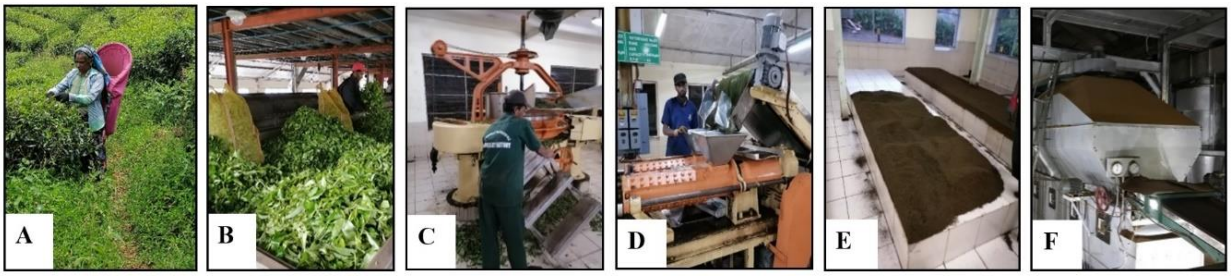

Figure 3.1: Black tea processing stages, including plucking (A), withering (B), Rolling (C), Rotovane cutting (D), Oxidation (E), and Firing (F).

Samples were collected from three independent production batches at 2-month intervals from January to August 2022. Each sample was wrapped in aluminum foil, sealed in sterile polyethylene bags, transported on dry ice, and stored at −80 °C for 24 h prior to freeze-drying. Samples were subsequently ground and stored at −20 °C until analysis (Punyasiri et al., 2015). Each batch included duplicate samples collected at each processing stage, yielding 18 analytical observations per stage across three independent processing experiments across three independent experiments. This sampling design was implemented to capture variability among processing batches.

Dry matter content was determined by measuring mass loss at 103 °C according to ISO 1573 (ISO, 1980) method. Polyphenol extraction was performed using 70% methanol under ultrasonication (20 kHz, 60 W, 30 min), yielding the highest recovery of targeted analytes during extraction optimization (Section 3.2.5). Total phenolic content (TPC) was determined using the Folin-Ciocalteu method (ISO, 2005), with spectrophotometric detection at 765 nm. Gallic acid calibration standards were prepared at concentrations ranging from 10 to 50 µg/mL.

3.2.7 Statistical and data analysis

Bioactive compound concentrations were quantified using the validated HPLC-DAD method and expressed as mean ± standard deviation (mg/g DW, n = 18). Data were standardized to z-scores prior to multivariate analysis. Principal component analysis (PCA) was performed to reduce data dimensionality and identify major sources of variation among samples.

Clustered heatmaps were generated using hierarchical clustering with Ward's linkage, and Pearson correlation coefficients were calculated to evaluate relationships among analytes. One-way ANOVA followed by Tukey's HSD test was used to determine significant differences at $p < 0.05$.

Values below the limit of detection (LOD) were treated as non-detected for descriptive reporting and assigned a value of zero only for multivariate statistical analyses in which absence of detection was considered analytically meaningful, particularly for compounds not expected during specific processing stages (e.g., theaflavins in fresh tea leaves) (Li et al., 2012). Because the frequency of non-detected values was low and primarily restricted to early processing stages, this approach was considered unlikely to substantially influence overall clustering or PCA outcomes. Interpretation of low-abundance compounds near detection limits was therefore performed conservatively.

3.3 Results and discussion

3.3.1 Separation of tea compounds

The developed high-performance liquid chromatography (HPLC) method effectively separated and quantified 12 key compounds in *C. sinensis* leaves across black tea processing stages at Somerset Tea Factory. These compounds included gallic acid, theobromine, epigallocatechin (EGC), caffeine, catechin, epicatechin (EC), epigallocatechin gallate (EGCG), epicatechin gallate (ECG), theaflavin (TF), theaflavin-3-gallate (TF3G), theaflavin-3'-gallate (TF3'G), and theaflavin-3,3'-digallate (TF3-3'G). Figure 3.2 presents a representative chromatogram of a mixed standard, green tea extract, and black tea extract at 210 nm, showing well-resolved peaks for all analytes, with retention times ranging from 3.75 min (gallic acid) to 32.50 min (TF3-3'G) (Table 3.1). These results indicate adequate chromatographic resolution for the simultaneous quantification of structurally related catechins, alkaloids, and theaflavins.

3.3.1.1 Method validation and performance

Validation results demonstrated the method's effectiveness for routine tea analysis. Calibration curves showed excellent linearity ($r^2 \geq 0.9995$) for all analytes over compound-specific ranges spanning 0.9375–150 µg/mL overall (0.9375–30 µg/mL for EGC, catechin, EC, ECG and theobromine; 1.875–60 µg/mL for gallic acid; 2.8125–90 µg/mL for the theaflavins; and 4.6875–150 µg/mL for caffeine and EGCG; Table 3.1). Figure S3.1 (Appendix B) illustrates the calibration curves for all tea compounds, supporting the reliability of quantification across the tested range. Limit of detection (LOD) and limit of quantification (LOQ) values ranged from 0.01–0.56 µg/mL and 0.03–1.68 µg/mL, respectively, comparable to or lower than those reported by Lee et al. (2018), particularly for EC (LOD: 0.01 µg/mL; LOQ: 0.03 µg/mL) and catechin (LOD: 0.01 µg/mL; LOQ: 0.04 µg/mL).

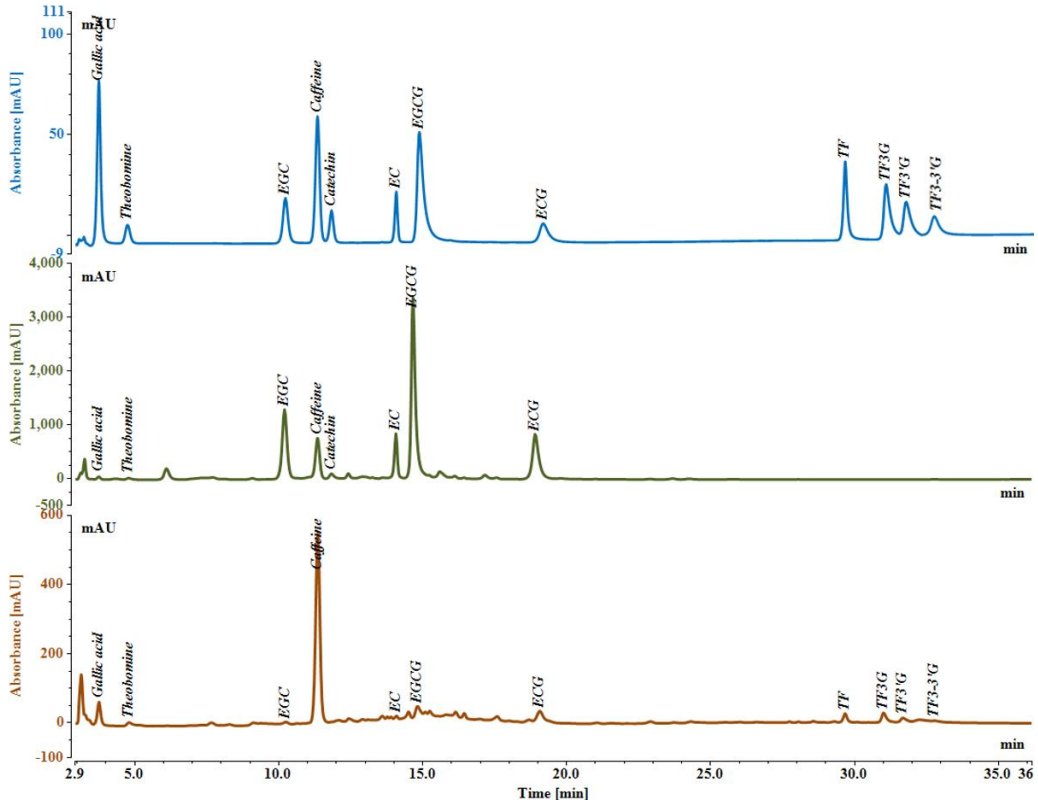

Figure 3.2: HPLC-DAD chromatograms of a mixed standard of 12 compounds (A), Green tea extract using 70% methanol by ultrasonication (B), and Black tea extract using 70% methanol by ultrasonication (C) at 210 nm. Peaks shown are gallic acid (3.75 min), theobromine (4.75 min), EGC (10.22 min), caffeine (11.35 min), catechin (11.83 min), EC (14.08 min), EGCG (14.86 min), ECG (19.12 min), TF (29.69 min), TF3G (31.05 min), TF3'G (31.72 min), and TF3-3'G (32.50 min).

Table 3.1: Calibration parameters for standard compounds analyzed by HPLC, including retention times, linearity ranges, regression equations, correlation coefficients (r^2), limits of detection (LOD), and limits of quantification (LOQ).

Compound	Retention Time (min)	Range (µg/mL)	Regression Equation	Correlation Coefficient (r^2)	LOD (µg/mL)	LOQ (µg/mL)
Gallic acid	3.75	1.875-60	y = 1.593x + 0.353	0.9997	0.07	0.21
Theobromine	4.75	0.9375–30	y = 0.493x + 0.030	0.9998	0.04	0.12
EGC	10.22	0.9375–30	y = 1.279x - 0.160	0.9997	0.15	0.46
Caffeine	11.35	4.6875–150	y = 0.576x + 0.129	1.0000	0.56	1.68
Catechin	11.83	0.9375–30	y = 0.673x + 0.085	0.9997	0.01	0.04
EC	14.08	0.9375–30	y = 0.744x + 0.144	0.9997	0.01	0.03
EGCG	14.86	4.6875–150	y = 0.840x - 0.668	0.9999	0.02	0.07
ECG	19.12	0.9375–30	y = 1.005x - 0.006	0.9999	0.02	0.05
Theaflavin	29.69	2.8125–90	y = 0.584x - 0.305	0.9995	0.28	0.85
TF3G	31.05	2.8125–90	y = 0.642x - 0.542	0.9998	0.03	0.10
TF3'G	31.72	2.8125–90	y = 0.412x - 0.159	0.9996	0.55	1.67
TF3-3'G	32.50	2.8125–90	y = 0.398x - 0.612	0.9998	0.30	0.89

Precision analysis demonstrated good analytical reproducibility (Table 3.2), as reflected in the low relative standard deviation (RSD) values observed. Specifically, RSD values for peak areas were below 3.59% for intra-day precision and 4.68% for inter-day precision, while retention time RSD values were below 0.51% for intra-day and 0.86% for inter-day measurements. Collectively, these values were within ranges commonly reported for validated HPLC-DAD tea analyses (Lee et al., 2018).

Recovery experiments (Table 3.3) demonstrated acceptable accuracy, with values ranging from 89.10–100% in ultrapure water and 83.86–99.16% in black tea extract. EGCG recovery remained high in both matrices (91.08% and 98.00%, respectively), despite being a galloylated catechin, reflecting its relatively small, well-characterized monomeric structure and established chromatographic behavior. Recoveries in black tea extract were generally within acceptable

ranges; however, TF3-3′G showed comparatively lower recovery (83.86%), indicating potential matrix-related underestimation. This contrast suggests that recovery is influenced less by the presence of a galloyl group per se than by overall molecular size and structural complexity: TF3-3′G is a larger, di-galloylated theaflavin formed by oxidative coupling of two catechin-derived units, structurally more similar to the abundant polymeric thearubigin pigments already present in black tea extract, and may therefore be more susceptible to co-precipitation or non-specific binding within this complex matrix than the smaller, monomeric EGCG. Accordingly, absolute concentrations of TF3-3′G (and to a lesser extent other gallated theaflavins) in complex tea matrices should be interpreted conservatively. Emphasis is therefore placed on relative trends and between-treatment comparisons rather than precise absolute quantification (Peng et al., 2008).

Table 3.2: Intra-day and inter-day precision expressed as relative standard deviations (RSD) of the HPLC method in terms of the retention time and peak areas of the 12 standards; n = 6 per day, 3 days.

Standard	Peak area precision (%RSD) inter-day	Peak area precision (%RSD) intra-day	Retention time precision (%RSD) inter-day	Retention time precision (%RSD) intra-day
Gallic acid	2.75	1.70	0.21	0.12
Theobromine	0.57	1.94	0.10	0.14
EGC	1.37	1.97	0.31	0.05
Caffeine	2.45	1.84	0.32	0.02
Catechin	2.71	1.14	0.24	0.04
EC	2.00	1.84	0.08	0.02
EGCG	2.81	1.16	0.38	0.26
ECG	2.27	1.96	0.15	0.15
Theaflavin	2.51	3.59	0.22	0.08
TF3G	2.86	2.94	0.52	0.10
TF3′G	3.68	3.33	0.75	0.12
TF3-3′G	4.20	1.70	0.86	0.51

Table 3.3: Recovery analysis of key analytes of tea using blank (ultrapure water) and black tea extract (n=3).

	Ultrapure water				Black tea extract		
Standards	Spiked amount (µg/mL)	Found amount	Recovery %	Content in the sample	Spiked amount	Found amount	Recovery %
Gallic acid	50	50.00	100	4.77	50	52.32	95.10
Theobromine	50	50.00	100	3.02	50	50.18	94.32
EGC	50	49.22	98.44	0.46	50	50.04	99.16
Caffeine	50	47.78	95.56	74.85	50	120.95	92.20
Catechin	50	48.80	97.6	1.34	50	50.07	97.46
EC	50	49.92	99.84	3.01	50	51.23	96.44
EGCG	50	45.54	91.08	3.22	50	52.22	98.00
ECG	50	50.00	100	6.01	50	54.32	96.62
Theaflavin	50	44.55	95.10	2.66	50	49.44	93.56
TF3G	50	47.77	95.54	3.49	50	51.67	96.36
TF3'G	50	48.90	97.8	2.32	50	48.76	92.88
TF3-3'G	50	46.32	92.64	2.37	50	44.30	83.86

3.3.1.2 Method comparison with published methods

Comparison of previously published HPLC methods showed that the present workflow achieved a short runtime. It also maintained acceptable sensitivity, precision, and chromatographic resolution for the targeted analyte panel (Table 3.4). This performance was likely due to the use of the Kinetex XB-C18 column (2.6 µm). This column improves chromatographic efficiency by reducing band broadening and enhancing mass transfer. The eXtra Base (XB) deactivation chemistry also minimizes peak tailing for structurally diverse tea polyphenols and alkaloids.

Wang et al. (2010) analyzed a greater number of compounds (18) but required a longer runtime (86 min), reflecting a trade-off between compound coverage and throughput. The LODs of the present method (0.01–0.56 µg/mL) were comparable to or lower than those reported by Peng et al. (2008; 0.2–2.8 µg/mL), Wang et al. (2010; 0.2–3.21 µg/mL) and Ai et al. (2024; 0.19–5.14 µg/mL), although these ranges are not strictly comparable because the studies quantified different

analyte panels. Ai et al. (2024) reported higher recovery values but comparatively higher detection limits.

Table 3.4: Comparison of analytical performance parameters between the present HPLC method and previously reported methods.

Parameter	Present Study	Ai et al. (2024)	Peng et al. (2008)	Wang et al. (2010)
No. of compounds	12	14	14	18
Run time (min)	40	55	45	86
Limit of Detection (LOD)	0.01–0.56 (0.285*) (µg/mL)	0.19–5.14 (2.665*) (µg/mL)	0.2–2.8 (1.5*) ng/µL	0.2–3.21(1.705*) ng/µL
Relative Standard Deviation (RSD Inter-day, %)	≤ 3.68	≤ 3.48	< 2.81	0.09–4.03
Linearity (r^2)	> 0.9995	> 0.9993	> 0.9994	> 0.9991
Recovery (%)	83.86–100 (91.93)	98.02–102.57 (100.295)	85.56–103.86 (94.71)	85.67–103.47 (94.57)
Column used	Kinetex XB-C18, 100 × 4.6 mm, 2.6 µm	Agilent SB-C18, 250 × 4.6 mm, 5 µm	RP-Amide C16, 150 × 4.6 mm, 5 µm	RP-Amide C16, 250 × 4.6 mm, 5 µm
Detection wavelength	210 & 280 nm	280 nm	210 nm and 280nm	210 nm

*Mid-point in parentheses.

All studies exhibited high linearity (>0.999), with the present study showing slightly higher correlation coefficients (>0.9995), supporting reliable quantification across a broad concentration range. However, recovery values in the present study were slightly lower, suggesting possible matrix-related limitations under complex sample conditions.

The radar chart (Figure 3.3) illustrates these trade-offs, indicating that the present method performs favorably in terms of run time, sensitivity, linearity, and precision, while other methods may offer advantages in compound coverage or recovery. These results highlight that method selection depends on the intended analytical application, whether for rapid screening or trace-level quantification.

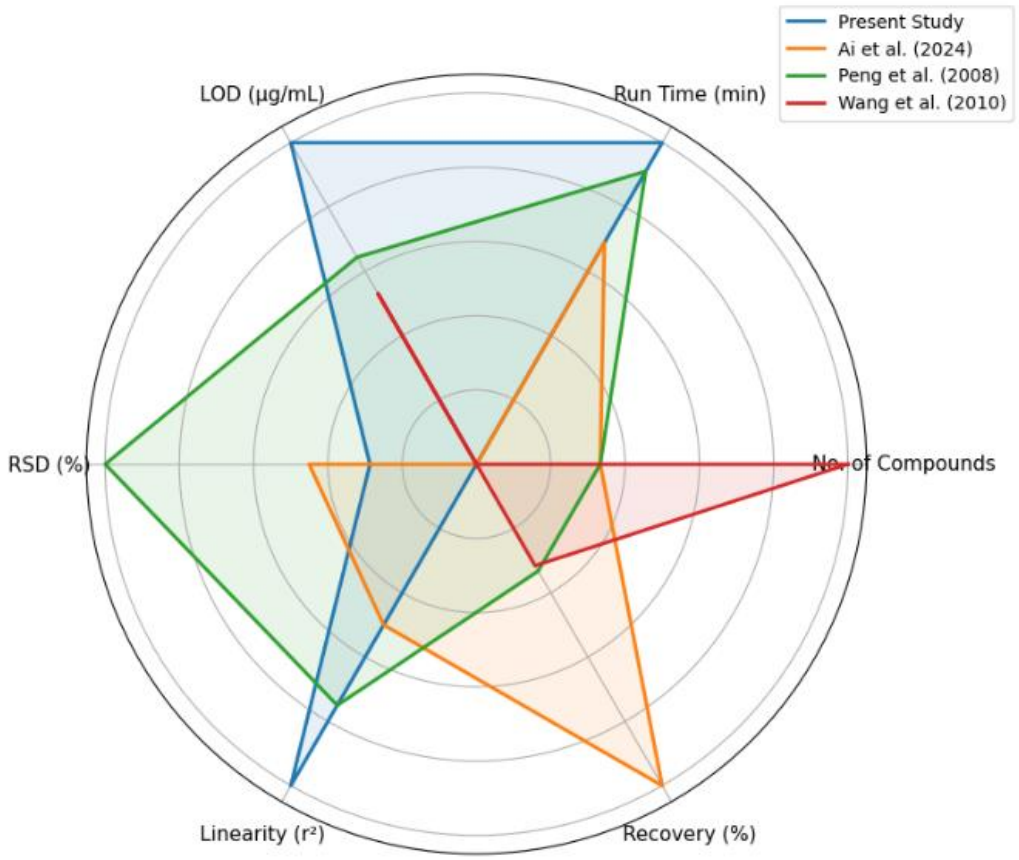

Figure 3.3: Radar plot comparing the normalized analytical performance of the present HPLC method with previously reported methods.

3.3.2 Optimization of extraction methods

The standardized dataset included concentrations of 12 bioactive compounds. These were gallic acid, theobromine, EGC, caffeine, catechin, EC, EGCG, ECG, TF, TF3G, TF3′G, and TF3-3′G. These were evaluated across 22 extraction conditions applied to green tea (GT) and black tea (BT). Extraction approaches included hot-water extraction (HW), ultrasonication with water (U_W), ethanol (U_E20–U_E90), methanol (U_M20–U_M90), and the ISO method (ISO, 2005). Table 3.5 summarizes yields of gallic acid, caffeine, total catechin, and total theaflavin under different extraction conditions. Figure 3.4 shows a clustered heatmap (Figure 3.4A), PCA biplot (Figure 3.4B), and scree plot (Figure 3.4C) to visualize extraction trends.

The heatmap (Figure 3.4A) revealed distinct extraction patterns between green and black tea matrices. Green tea extraction methods generally produced high catechin concentrations. Methanol-based ultrasonication methods, such as GT_U_M70, yielded elevated EGCG and ECG

concentrations. These findings are consistent with previous reports showing that aqueous organic solvents improve the extraction efficiency of catechin-rich tea matrices (Wang et al., 2000). Theaflavins were negligible in most green tea extracts. This reflects the limited oxidative conversion in unfermented tea processing (Harbowy et al., 2010).

Black tea extracts had much higher theaflavin concentrations, especially under methanol ultrasonication (U_M50–U_M70). This is consistent with oxidation-associated catechin conversion during black tea manufacture (Liang et al., 2003a). Extraction with 90% ethanol generally produced lower analyte recovery in both tea types. This suggests reduced extraction efficiency under high-organic-solvent conditions.

The PCA biplot (Figure 3.4B) clearly distinguished green tea and black tea extraction profiles. Green tea methods clustered by catechin-related variables, such as EGCG and EGC. Black tea methods were influenced mainly by theaflavins and caffeine. Black tea extracts showed greater dispersion, suggesting greater compositional variability resulting from oxidative processing. Green tea extracts formed tighter clusters, reflecting consistent catechin-rich profiles.

The scree plot (Figure 3.4C) demonstrated that the first two principal components explained most of the dataset variance, supporting the suitability of the two-dimensional PCA representation for interpretation of extraction-associated differences.

Table 3.5: The comparison of different extraction methods and the yield of gallic acid, caffeine, total catechins, and total theaflavins (values denote mean ± SD, 6 replicates of each).

Tea Type	Extraction Method	Solvent	Conc. (%)	Abbrev.	Gallic Acid (mg/g)	Caffeine (mg/g)	Total Catechins (mg/g)	Total TF (mg/g)
Green tea	Hot Water	Water	100	GT_HW	0.64 ± 0.03a	34.35 ± 1.20^{a}	159.52 ± 5.44^{c}	0.08 ± 0.00^{d}
	Ultra sonication-assisted	Water	100	GT_U_W	0.65 ± 0.14^{a}	34.67 ± 0.85^{a}	161.52 ± 5.21^{c}	0.12 ± 0.00^{d}
		Ethanol	20	GT_U_E20	0.53 ± 0.01^{b}	34.42 ± 0.18^{a}	177.63 ± 0.24^{b}	0.21 ± 0.20^{c}
		Ethanol	50	GT_U_E50	0.33 ± 0.05^{c}	28.05 ± 2.67^{b}	138.14 ± 17.63^{d}	0.19 ± 0.23^{c}
		Ethanol	70	GT_U_E70	0.23 ± 0.08^{d}	23.87 ± 2.34^{c}	115.33 ± 12.60^{e}	0.03 ± 0.03^{d}
		Ethanol	90	GT_U_E90	0.09 ± 0.04^{e}	15.59 ± 1.72^{d}	40.38 ± 3.87^{f}	ND
		Methanol	20	GT_U_M20	0.00 ± 0.00^{f}	2.17 ± 0.26^{e}	170.98 ± 8.51^{b}	0.07 ± 0.00^{d}
		Methanol	50	GT_U_M50	0.48 ± 0.01^{b}	35.52 ± 1.51^{a}	191.18 ± 10.28^{a}	0.10 ± 0.01^{d}
		Methanol	70	GT_U_M70	0.52 ± 0.04^{b}	37.72 ± 2.23^{a}	214.30 ± 12.86^{a}	0.52 ± 0.02^{a}
		Methanol	90	GT_U_M90	0.44 ± 0.01^{c}	34.10 ± 2.18^{a}	189.72 ± 10.80^{a}	0.36 ± 0.09^{b}
	ISO 14502-1:2005	Methanol	70	GT_ISO	0.33 ± 0.05^{c}	34.42 ± 0.18^{a}	165.60 ± 6.36^{b}	0.07 ± 0.00^{d}
Black tea	Hot Water	Water	100	BT_HW	1.49 ± 0.02^{b}	21.79 ± 0.88^{c}	10.91 ± 0.93^{c}	2.12 ± 0.01^{c}
	Ultra sonication-assisted	Water	100	BT_U_W	0.33 ± 0.05^{d}	35.18 ± 0.55^{b}	16.48 ± 0.91^{d}	4.09 ± 0.33^{d}
		Ethanol	20	BT_U_E20	1.75 ± 0.13^{b}	41.31 ± 2.76^{a}	27.32 ± 1.52^{a}	9.21 ± 0.30^{c}
		Ethanol	50	BT_U_E50	0.90 ± 0.22^{c}	28.41 ± 2.51^{b}	16.96 ± 1.33^{d}	7.89 ± 2.11^{c}
		Ethanol	70	BT_U_E70	1.09 ± 0.17^{c}	31.17 ± 3.18^{b}	17.96 ± 3.25^{d}	8.84 ± 1.84^{c}
		Ethanol	90	BT_U_E90	0.08 ± 0.03^{e}	7.17 ± 0.29^{d}	3.11 ± 0.36^{f}	1.03 ± 0.30^{e}
		Methanol	20	BT_U_M20	1.50 ± 0.12^{b}	44.21 ± 4.46^{a}	18.01 ± 1.14^{d}	11.30 ± 0.24^{b}
		Methanol	50	BT_U_M50	1.89 ± 0.09^{b}	46.90 ± 0.35^{a}	25.75 ± 2.80^{b}	15.08 ± 1.15^{b}
		Methanol	70	BT_U_M70	2.35 ± 0.29^{a}	48.62 ± 0.90^{a}	23.97 ± 1.58^{b}	19.73 ± 1.33^{a}
		Methanol	90	BT_U_M90	1.77 ± 0.07^{b}	47.08 ± 2.57^{a}	24.97 ± 1.37^{b}	15.11 ± 1.88^{b}
	ISO 14502-1:2005	Methanol	70	BT_ISO	0.90 ± 0.22^{c}	41.31 ± 2.76^{a}	17.46 ± 1.16^{d}	15.07 ± 1.25^{b}

Values are expressed as mean ± standard deviation (n = 6; Table 5.4; triplicate extractions × two independent repeats). Within each column, values followed by different superscript letters (a–f) are significantly different at $p < 0.05$ based on one-way ANOVA followed by Tukey's post hoc test. ND: Not Detected.

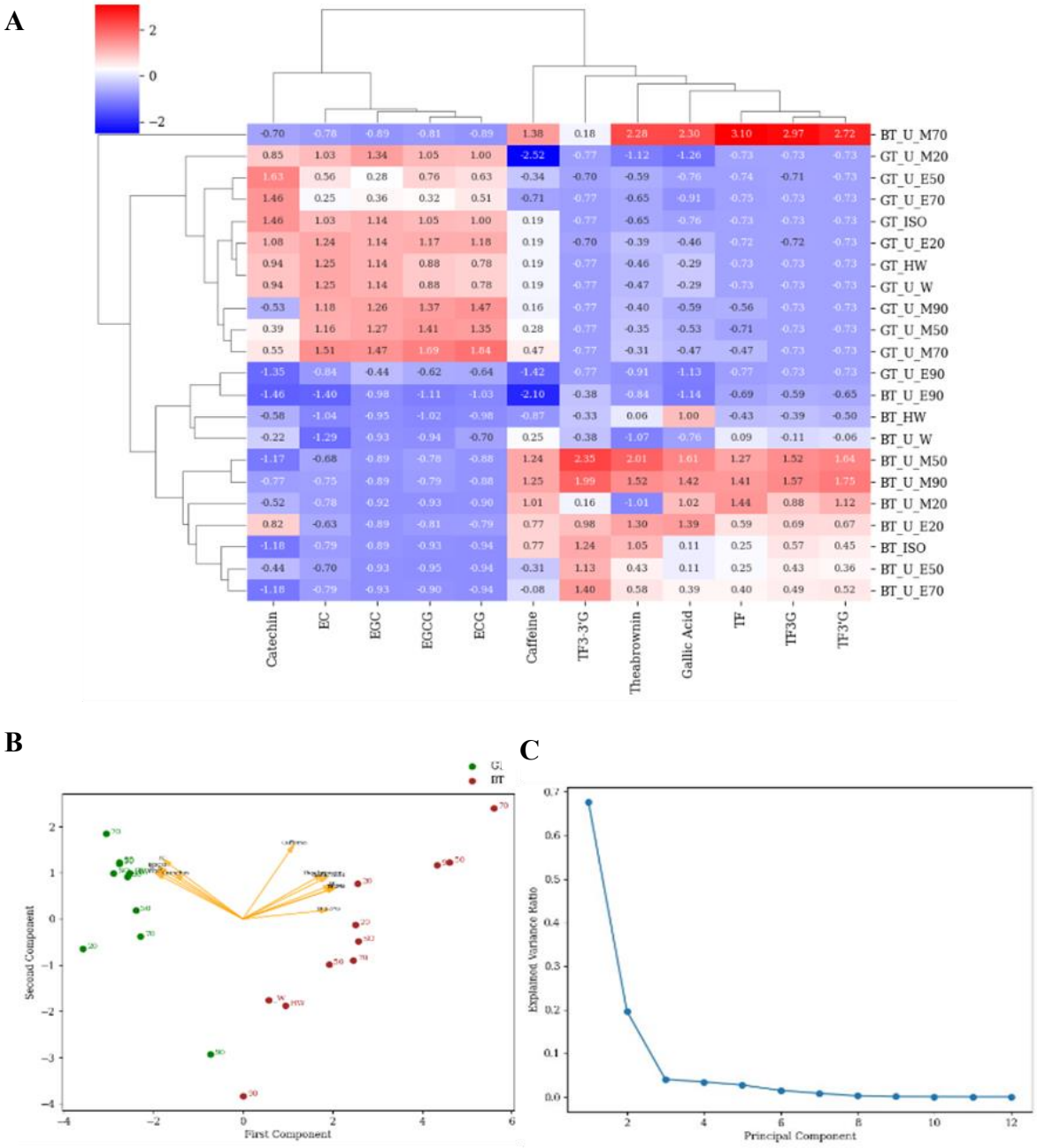

Figure 3.4: Analytical visualization of bioactive compound profiles in green tea (GT) and black tea (BT) across 22 extraction methods. (A) Clustered heatmap of standardized concentrations (z-scores) for catechins, alkaloids, phenolic acids, and theaflavins across hot-water, ultrasonication-assisted solvent extractions, and ISO methods. Blue indicates below-average and red indicates above-average concentrations. (B) Principal component analysis (PCA) biplot showing sample clustering and compound loadings based on standardized concentrations. (C) Scree plot showing the proportion of variance explained by principal components.

3.3.3 Dynamics of the major tea polyphenols during black tea processing

Black tea processing transforms *C. sinensis* leaves through enzymatic and oxidative reactions, reshaping polyphenol profiles critical to sensory and health attributes (Tanaka & Matsuo, 2020). This section evaluates changes in catechins (C, EC, EGC, EGCG, ECG), theaflavins (TF, TF3′G, TF3G, TF3-3′G), gallic acid, theobromine, caffeine, and total phenolic content across processing stages. The stages include fresh tea leaves (FTL), withered tea leaves (WTL), rolled leaves (ROL), rotovaned leaves (RTL), orthodox tea leaves during oxidation (OTL 1–3), and fired black tea (FBT). Data from the validated HPLC-DAD workflow showed substantial compositional changes resulting from enzymatic oxidation during black tea manufacture (Table 3.6; Figures 3.5–3.7).

3.3.3.1 Polyphenol dynamics

Total catechin declined 95.6% from 328.36 mg/g in FTL to 14.33 mg/g in FBT (one-way ANOVA, $p < 0.05$), with EGCG exhibiting the steepest drop (98.2%, 186.66 to 3.29 mg/g; Tukey's HSD, $p < 0.01$), suggesting PPO-associated catechin oxidation into theaflavins and thearubigins during rolling and oxidation (Deka et al., 2021). Withering reduced catechins by 44.6% to 190.95 mg/g, driven by cell disruption and moisture loss, enhancing PPO activity, while rolling further decreased them by 27.8% to 180.26 mg/g (Pou et al., 2019).

Theaflavins were not detected in fresh tea leaves and first appeared during withering (12.40 mg/g total theaflavins). Concentrations increased following rolling, reaching peak levels after cellular disruption promoted catechin oxidation and condensation reactions. During extended oxidation, total theaflavins decreased by approximately 24.2%, likely indicating continued oxidative polymerization and conversion into higher-order pigments such as thearubigins (Pou et al., 2019). Firing stabilized remaining theaflavins through thermal inactivation of PPO activity.

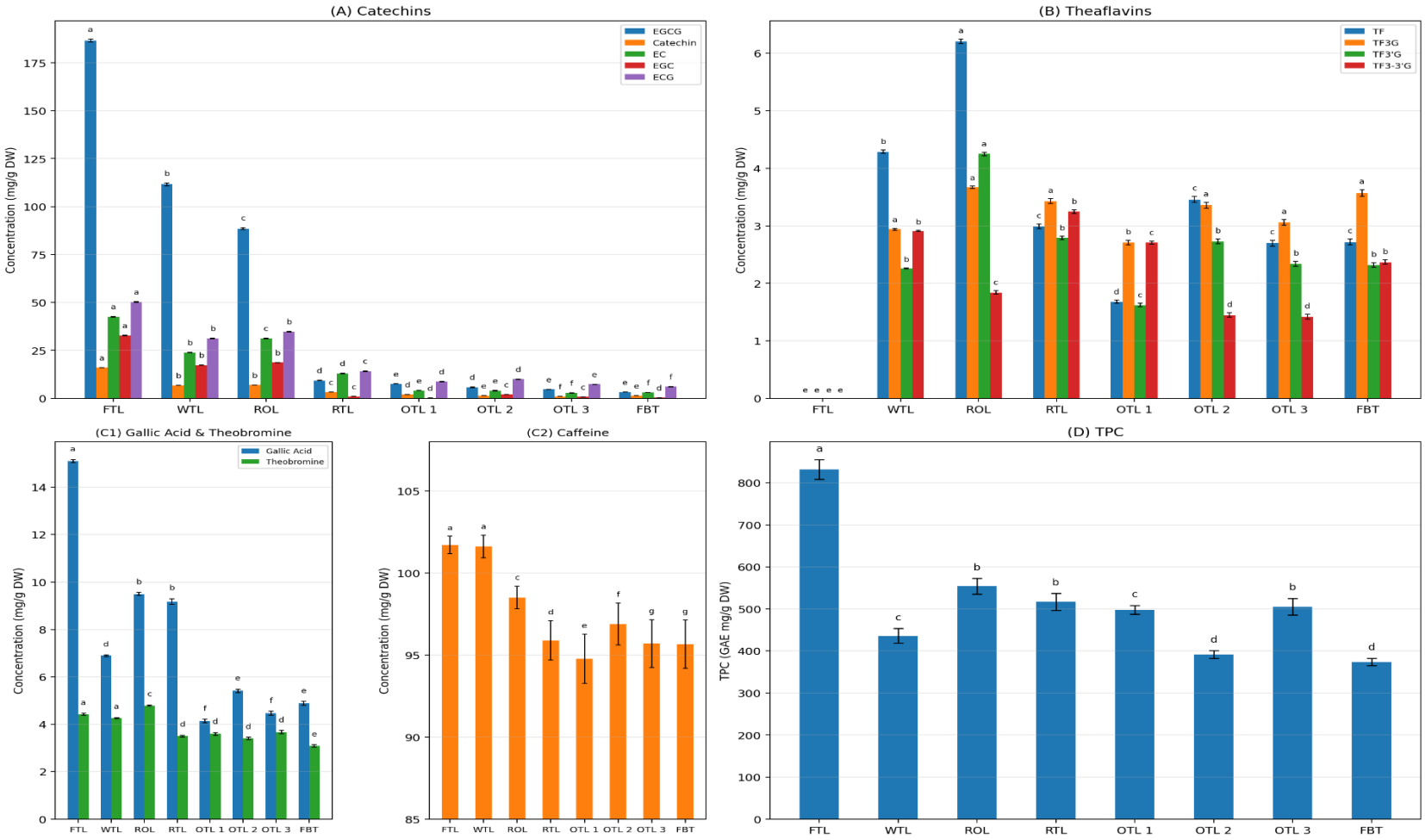

Figure 3.5: Major catechins (A), theaflavins (B), gallic acid and theobromine (C1), caffeine (C2), and TPC (D) across eight black tea processing stages (FTL–FBT). Values represent SD (n = 18); different superscript letters indicate significant differences between stages (Tukey's HSD, $p < 0.05$).

Table 3.6: Major polyphenolic content during black tea processing (mg/g DW ± SD, n=18).

Processing Stage	FTL	WTL	ROL	RTL	OTL 1	OTL 2	OTL 3	FBT
Gallic acid	15.10 ± 0.06^{a}	6.89 ± 0.04^{d}	9.50 ± 0.06^{b}	9.18 ± 0.12^{b}	4.14 ± 0.07^{f}	5.41 ± 0.08^{e}	4.47 ± 0.08^{f}	4.88 ± 0.08^{e}
Theobromine	4.42 ± 0.04^{a}	4.26 ± 0.03^{a}	4.79 ± 0.03^{c}	3.50 ± 0.04^{d}	3.60 ± 0.06^{d}	3.40 ± 0.05^{d}	3.67 ± 0.06^{d}	3.08 ± 0.05^{e}
EGC	32.77 ± 0.14^{a}	17.33 ± 0.11^{b}	18.66 ± 0.12^{b}	1.07 ± 0.01^{c}	0.27 ± 0.00^{d}	2.00 ± 0.03^{c}	0.90 ± 0.02^{c}	0.47 ± 0.01^{d}
Caffeine	101.70 ± 0.54^{a}	101.62 ± 0.69^{a}	98.51 ± 0.68^{c}	95.89 ± 1.20^{d}	94.77 ± 1.49^{e}	96.89 ± 1.28^{f}	95.70 ± 1.45^{g}	95.67 ± 1.47^{g}
Catechin	16.02 ± 0.07^{a}	6.77 ± 0.04^{b}	6.99 ± 0.04^{b}	3.26 ± 0.04^{c}	2.03 ± 0.03^{d}	1.37 ± 0.02^{e}	1.01 ± 0.02^{f}	1.37 ± 0.02^{e}
EC	42.65 ± 0.18^{a}	23.92 ± 0.14^{b}	31.34 ± 0.20^{c}	13.00 ± 0.16^{d}	4.12 ± 0.07^{e}	4.00 ± 0.06^{e}	2.80 ± 0.05^{f}	3.07 ± 0.05^{f}
EGCG	186.66 ± 0.79^{a}	111.68 ± 0.69^{b}	88.57 ± 0.57^{c}	9.31 ± 0.12^{d}	7.65 ± 0.03^{e}	5.80 ± 0.20^{d}	4.70 ± 0.04^{e}	3.29 ± 0.06^{e}
ECG	50.26 ± 0.21^{a}	31.25 ± 0.19^{b}	34.70 ± 0.22^{b}	14.25 ± 0.18^{c}	8.80 ± 0.14^{d}	9.99 ± 0.15^{d}	7.35 ± 0.13^{e}	6.13 ± 0.10^{f}
Theaflavin	ND^{e}	4.29 ± 0.03^{b}	6.21 ± 0.04^{a}	2.99 ± 0.04^{c}	1.68 ± 0.03^{d}	3.46 ± 0.05^{c}	2.70 ± 0.05^{c}	2.72 ± 0.05^{c}
TF3G	ND^{e}	2.94 ± 0.02^{a}	3.67 ± 0.02^{a}	3.43 ± 0.04^{a}	2.71 ± 0.04^{b}	3.36 ± 0.05^{a}	3.06 ± 0.05^{a}	3.57 ± 0.06^{a}
TF3'G	ND^{e}	2.26 ± 0.01^{b}	4.25 ± 0.03^{a}	2.79 ± 0.03^{b}	1.62 ± 0.03^{c}	2.73 ± 0.04^{b}	2.34 ± 0.04^{b}	2.32 ± 0.04^{b}
TF3-3G	ND^{e}	2.91 ± 0.01^{b}	1.84 ± 0.03^{c}	3.25 ± 0.03^{b}	2.71 ± 0.03^{c}	1.45 ± 0.04^{d}	1.42 ± 0.04^{d}	2.37 ± 0.04^{b}
TPC (GAE mg/g DW)	831.73± 23.32^{a}	436.22± 17.54^{c}	554.08± 18.65^{b}	517.25± 20.05^{b}	497.96± 10.61^{c}	391.74± 9.37^{d}	505.61± 19.77^{b}	374.18± 8.44^{d}

Data show concentrations (mg/g DW ± SD, n=18). ND = Not Detected (below LOD, treated as 0 mg/g for ANOVA and Tukey's HSD). Superscripts ($^{a–g}$) denote significant differences within rows ($p < 0.05$). LODs for theaflavins range from 0.03–1.68 µg/mL.

Gallic acid concentration declined 67.7% over processing, though it temporarily increased during rolling. This may result from esterase-mediated hydrolysis of gallated catechins (Karas et al., 2017). Theobromine concentration decreased by 30.3%. Caffeine showed only minor reductions (5.93%) throughout processing. These small changes in caffeine align with the chemical stability of methylxanthines during manufacturing. They may also reflect moisture effects, extraction variability, and physical losses during processing (Lee et al., 2016; Sanaeifar et al., 2020).

Total phenolic content (TPC) declined by approximately 55.0% during processing, broadly mirroring catechin depletion patterns. A transient increase during OTL 3 may reflect variation in oxidation kinetics, extraction efficiency, or secondary oxidation reactions occurring during processing (Leonard et al., 2021). One-way ANOVA confirmed significant differences among processing stages for catechins and theaflavins ($p < 0.001$), with rolling and oxidation representing the major transition points in polyphenol transformation.

3.3.3.2 Correlation and clustering analysis

Pearson correlation analysis (Figure 3.6) revealed strong positive correlations within catechin groups (0.81–0.98) and within theaflavin groups (0.58–0.89). Positive correlations were also observed among catechins, gallic acid, caffeine, and theobromine, whereas catechins generally showed negative correlations with theaflavins, consistent with oxidative conversion pathways during black tea processing (Ito & Yanase, 2022).

Theaflavins showed comparatively weak correlations with caffeine and methylxanthines, corresponding to differences in biosynthetic origin and oxidation behavior. These relationships indicate that catechin depletion and theaflavin formation may serve as useful indicators of oxidation progression and processing-associated metabolic changes (Lee et al., 2016).

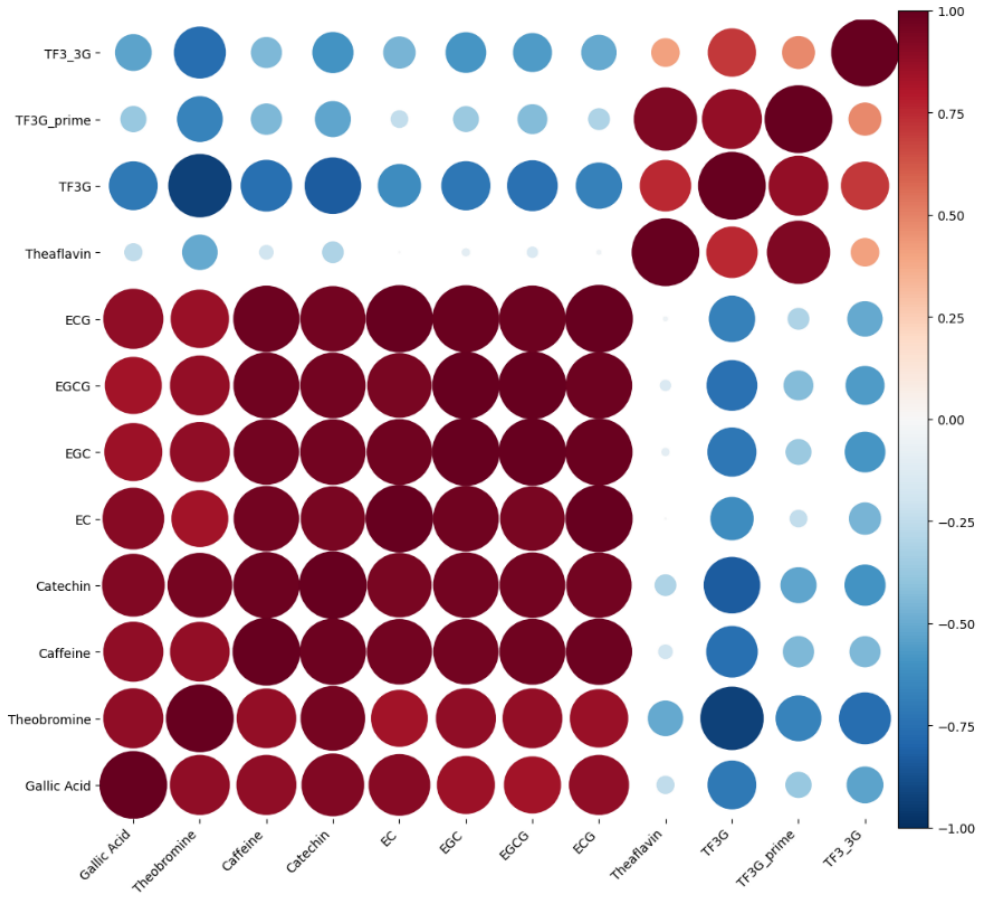

Figure 3.6: Correlogram of Pearson correlation coefficients among bioactive compounds during black tea processing. Compounds include catechins (Catechin, EC, EGC, EGCG, ECG), theaflavins (Theaflavin, TF3G, TF3'G, TF3-3'G), and others (Gallic acid, Theobromine, Caffeine), assessed across processing stages: FTL, WTL, ROL, RTL, OTL 1, OTL 2, OTL 3, and FBT. Circle size represents the absolute value of the correlation coefficient. Color scale: blue = positive correlation, red = negative correlation, ranging from -1 to 1**.**

Hierarchical cluster analysis (Figure 3.7) identified two major metabolite groups. The first cluster, comprising EGCG, EGC, EC, catechin, ECG, gallic acid, and theobromine, predominated in early processing stages and progressively declined during oxidation and firing. This pattern was consistent with established PPO- and POD-mediated catechin oxidation systems (Lee et al., 2016; Liang et al., 2003a).

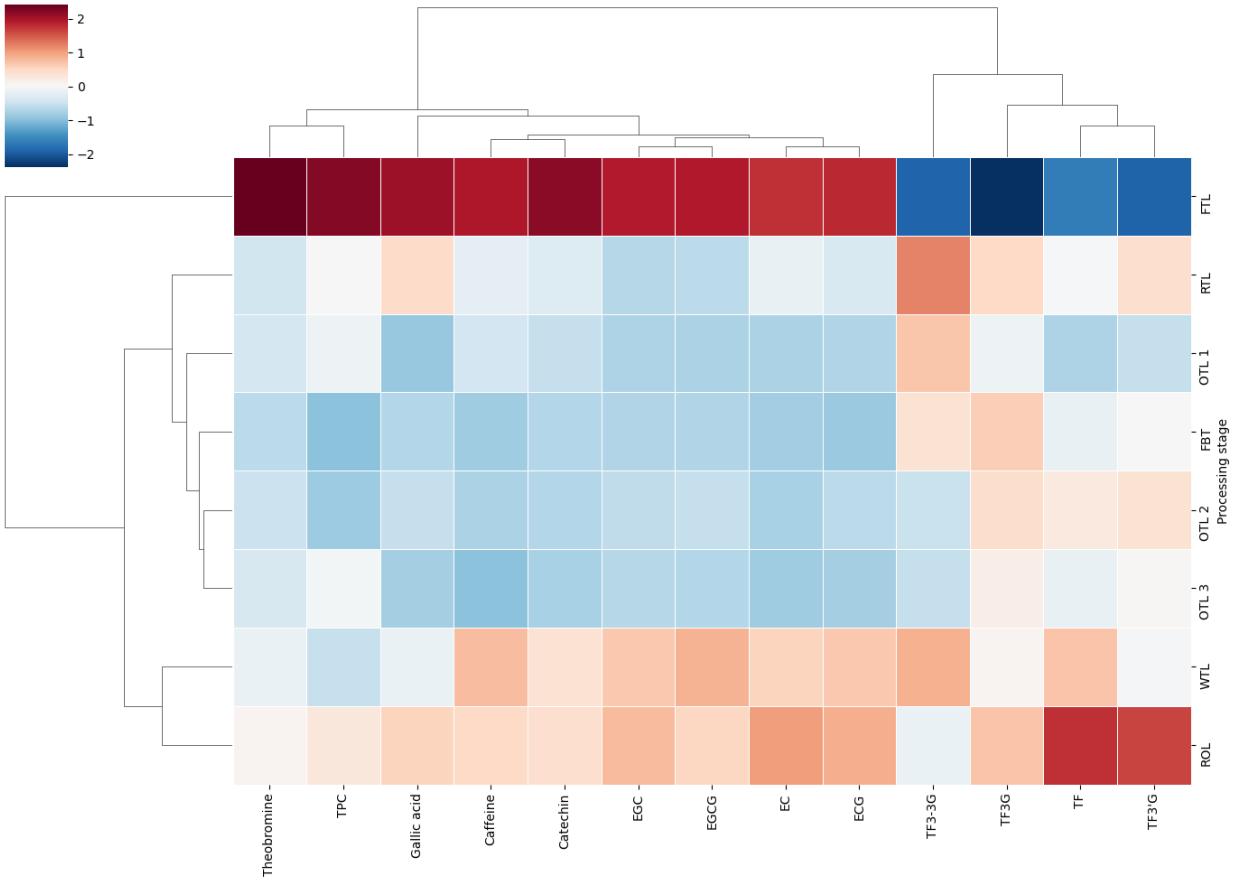

Figure 3.7: Clustered heatmap of normalized z-scores for 12 bioactive compounds across black tea processing stages. Compounds are grouped into catechins, theaflavins, and others. Processing stages include FTL, WTL, ROL, RTL, OTL 1, OTL 2, OTL 3, and FBT. Z-scores are normalized per compound to highlight relative concentration trends. Color scale: blue = low z-scores (low concentrations), red = high z-scores (high concentrations). Dashed lines separate compound categories.

The second cluster, dominated by theaflavins (TF, TF3G, TF3′G, TF3-3′G), emerged following rolling and increased during oxidation stages, reflecting oxidative catechin condensation reactions associated with black tea formation (Roberts & Smith, 1961; Samanta et al., 2015). TPC broadly mirrored catechin-associated patterns, declining during later oxidation stages as monomeric phenolics underwent oxidation and polymerization.

Hierarchical clustering separated fresh tea leaves (FTL) as a distinct outgroup, reflecting its unoxidized catechin-rich, theaflavin-absent profile. The remaining stages formed two clusters: withered and rolled leaves (WTL, ROL), representing early-stage transformation with substantial catechin retention, and rotovaned leaves through fired black tea (RTL–FBT), reflecting the major catechin depletion that occurs specifically at the rotovane-cutting step and persists through the

remainder of processing. These clustering patterns support previously reported biochemical trends in black tea oxidation and provide a comparative framework for monitoring processing-related changes in tea metabolite composition (Chandini et al., 2011; Liang et al., 2003a).

3.4 Conclusions

This study successfully developed and validated an HPLC-DAD method for the simultaneous quantification of 12 key polyphenolic compounds in *C. sinensis*, including catechins, theaflavins, gallic acid, caffeine, and theobromine. Utilizing a Kinetex XB-C18 column and dual-wavelength detection (210 and 280 nm), the method demonstrated excellent performance: linearity ($r^2 \geq 0.9995$), sensitivity (LOD: 0.01–0.56 μg/mL; LOQ: 0.03–1.68 μg/mL), precision (RSD < 4.68%), and recovery (83.86–99.16%). It also provided comparatively shorter run times while maintaining acceptable analytical performance in terms of run time (40 min) and robustness.

Building upon the analytical method described above, UAE with 70% methanol yielded the highest recovery of the targeted polyphenols. Notably, green tea extracts delivered the highest catechin concentrations (214.30 ± 12.86 mg/g), while black tea extracts featured elevated theaflavin concentrations (19.73 ± 1.33 mg/g). Both results surpassed those obtained with hot-water extraction and ISO-standard extraction methods under the specific conditions evaluated in this study. The black tea processing stages demonstrated substantial polyphenol transformations during orthodox manufacture ($p < 0.001$, ANOVA). Total catechin concentration decreased by approximately 95.6% (from 328.36 to 14.33 mg/g DW) because of oxidation-associated conversion reactions, whereas theaflavins increased following rolling before declining during extended oxidation, likely corresponding to continued polymerization into higher-order pigments. Gallic acid and theobromine concentrations decreased progressively during processing, while caffeine remained comparatively stable.

This analytical workflow enabled comparative profiling of major tea metabolites across green tea, black tea, and black tea processing stages. This baseline metabolite profile lays a strong foundation for the chapters ahead, which will explore the subsequent investigation of microbial enzyme-mediated catechin biotransformation systems in catechin oxidation and tea biotransformation systems. Despite these strengths, several limitations should be acknowledged. While the recovery

of TF3-3′G and selected gallated theaflavins was comparatively lower in black tea matrices, this suggests potential matrix effects that may influence absolute quantification. The targeted analytical panel, which focused primarily on major catechins, alkaloids, and theaflavins, did not comprehensively resolve higher-order oxidation-associated metabolites such as thearubigins. As a result, the interpretation of downstream polymerization products remains limited.

In light of these limitations, future studies should explore additional tea types, such as oolong and white tea, to reveal the broader applicability of the analytical workflow across partially oxidized tea systems. Future studies incorporating techniques such as solid-phase extraction, enzyme-assisted extraction, or LC-MS-based metabolomics could deepen the characterization of minor and higher-molecular-weight oxidation-associated metabolites. Expanding these analytical approaches will enable more insightful investigation of microbial enzyme-mediated oxidation systems and comparative evaluation of controlled tea biotransformation systems described in subsequent chapters of this thesis.

Chapter 4

Biotransformation potential of tea-associated microbes

Preface

This chapter investigates culturable bacteria and fungi associated with orthodox black tea processing environments. Isolates were screened for extracellular MPLO-associated activities, molecularly identified, and phylogenetically analyzed to identify high-activity strains capable of contributing to catechin oxidation and tea pigment formation.

Abstract

Black tea fermentation depends on the oxidation of catechins into theaflavins, thearubigins, and other pigments that shape color, flavor, and antioxidant properties. While plant polyphenol oxidases (PPOs) are traditionally viewed as the main catalysts, the contribution of tea-associated microbes remains insufficiently understood. This study investigated culturable bacteria and fungi associated with Sri Lankan orthodox black tea manufacture to identify extracellular microbial polyphenol-oxidizing-like oxidoreductase (MPLO) activities relevant to tea catechin biotransformation.

Among 43 bacterial and 40 fungal isolates, several exhibited measurable MPLO activities. *Alcaligenes faecalis* showed the highest bacterial MPLO activity (132.57 U/mL), whereas *Aspergillus fumigatus*, isolated as an endophyte of tea leaves, displayed the strongest fungal MPLO activity (119.03 U/mL). Molecular identification using 16S ribosomal RNA (rRNA) and Internal Transcribed Spacer (ITS) region sequencing (≥95% similarity thresholds) confirmed taxonomic assignments, and phylogenetic analysis supported clustering patterns consistent with MPLO activity. One-way ANOVA revealed significant interspecific variation among isolates ($F(25,52) = 9.20$, $p < 0.001$), with Tukey's HSD identifying *A. faecalis* as significantly more active than most other bacterial taxa. Due to biosafety and scalability considerations, *A. faecalis* NZRM 836 was selected as the representative high-MPLO-activity strain for further characterization. Substrate-based enzyme profiling of crude extracellular preparations showed peak laccase-like and catechol oxidase-like activities at 36 h (12.6 and 3.6 U/mL) and peroxidase-associated activity at 24 h (4.2 U/mL). Crude 36-h enzyme filtrates oxidized epigallocatechin gallate (EGCG) in a concentration-dependent manner, reducing EGCG from 816.24 to 333.33 mg/L and generating gallic acid (up to 29.81 mg/L), epigallocatechin, gallocatechin gallate, and low levels of theaflavin derivatives. Overall, the findings demonstrate that tea-associated bacterial and fungal communities possess functionally relevant extracellular MPLO activities capable of mediating tea catechin biotransformation. The results further establish *A. faecalis* as a promising microbial source of controllable extracellular oxidoreductase activities for oxidation-based tea bioprocessing applications.

Keywords: Black tea fermentation, Polyphenol oxidase, Polyphenol-oxidizing-like oxidoreductases, *Alcaligenes faecalis*, Epigallocatechin gallate (EGCG) oxidation, Tea pigments,

4.1 Introduction

Tea, produced from the young leaves and buds of *Camellia sinensis*, is one of the most widely consumed beverages globally (Abudureheman et al., 2022; Casanova et al., 2019; Govindarajan et al., 2021). Based on processing methods, teas are broadly categorized into unfermented (green), semi-fermented (oolong), fully-fermented (black), and post-fermented (dark) teas (Abudureheman et al., 2022; Theuma & Attard, 2020). Black tea manufacture relies on enzymatic oxidation, during which catechins are transformed into theaflavins (TFs), thearubigins (TRs), and theabrownins (TBs), compounds responsible for its characteristic color, briskness, aroma, and antioxidant properties (Aaqil et al., 2024; Chen et al., 2023a).

Traditionally, tea oxidation has been attributed to endogenous plant polyphenol oxidases (PPOs) and peroxidases (PODs) (Li et al., 2013). However, polyphenol oxidation is also mediated by diverse microbial oxidoreductase systems capable of generating reactive quinone intermediates from phenolic substrates. In this chapter, the term microbial polyphenol-oxidizing-like oxidoreductases (MPLOs) is used as a functional umbrella descriptor for microbial phenol-oxidizing systems exhibiting laccase-like, catechol oxidase-like, tyrosinase-like, and peroxidase-associated activities relevant to tea catechin oxidation (Claus, 2004; Claus & Decker, 2006). These activities are interpreted operationally based on substrate-dependent oxidation assays rather than structurally confirmed enzyme identities. Plant PPO activities vary with cultivar, leaf maturity, and processing conditions, often contributing to inconsistency in catechin oxidation and black tea quality (Chen et al., 2022a; Zou et al., 2024). These limitations have increased interest in alternative or complementary microbial biocatalytic systems that can provide more controlled and reproducible oxidation (Fang et al., 2019; Govindarajan et al., 2021).

Recent research has revealed that microbial communities naturally present on tea leaves and processing equipment can influence black tea chemistry. Bacteria such as *Pantoea*, *Pseudomonas*, and *Sphingomonas* have been shown to enhance PPO and POD activity, acting synergistically with plant enzymes under oxygen-rich processing conditions (Tong et al., 2021; Wang et al., 2023a). Fungal genera, including *Aspergillus, Talaromyces,* and *Colletotrichum,* are also frequently associated with tea environments and are known producers of extracellular oxidoreductases that can modify polyphenols (Lin et al., 2022; Liu et al., 2023c). Although fungal oxidoreductase systems are relatively well studied in post-fermented dark teas, their contribution to orthodox black

tea processing remains unclear. Even less is known about extracellular bacterial MPLO systems, despite advantages including rapid growth, ease of cultivation, and industrial scalability (Muniraj et al., 2021).

Culture-independent approaches such as metabarcoding and metagenomics have revealed substantial microbial diversity during tea processing (Assad et al., 2023; Shiquan et al., 2023), but these methods cannot distinguish viable, functionally active strains. As a result, the functional role of culturable, MPLO-producing microbes in orthodox black tea manufacture remains poorly understood. To date, few studies have systematically screened culturable bacteria and fungi from orthodox black tea processing environments for extracellular MPLO activity or evaluated the catechin-oxidizing capacity of high-activity bacterial isolates.

Culture-dependent studies are therefore essential for isolating functionally relevant microbes that are not only present but also capable of secreting active extracellular MPLOs under processing-relevant conditions (Tibpromma et al., 2022). To address these gaps, this study isolated and genetically identified culturable bacteria and fungi associated with Sri Lankan orthodox black tea processing and screened them for extracellular MPLO activity. Epigallocatechin gallate (EGCG), the most abundant and chemically reactive tea catechin, was selected as the model substrate for functional oxidation assays. The chapter therefore progresses through three stages: (i) screening tea-associated microorganisms for extracellular MPLO activity, (ii) selecting and identifying high-MPLO-activity isolates, and (iii) demonstrating catechin oxidation using crude extracellular bacterial enzyme preparations.

4.2 Materials and methods

4.2.1 Chemicals, media, and instruments

All chemicals were of analytical grade. Nutrient Agar (NA), Tryptic Soy Agar (TSA), Nutrient Broth (NB), Malt Extract Agar (MEA), Potato Dextrose Agar (PDA), and Potato Dextrose Broth (PDB) were obtained from HiMedia Laboratories Pvt. Ltd. (Mumbai, India). High-purity catechin standards, (+)-catechin (C), (−)-epicatechin (EC), (+)-gallocatechin (GC), (−)-epigallocatechin (EGC), (+)-catechin gallate (CG), (−)-epicatechin gallate (ECG), (+)-gallocatechin gallate (GCG), (−)-epigallocatechin gallate (EGCG), and gallic acid (GA), were purchased from Sigma-Aldrich

(St. Louis, USA). Theaflavin (TF), TF3G, TF3'G, and TF3-3'G standards were obtained from PhytoLab GmbH (Germany). Syringaldazine, catechol, EDTA, L-ascorbic acid, and hydrogen peroxide (30% w/w) were sourced from Sigma-Aldrich. Solvents, including formic acid (LC-MS grade), acetonitrile (HPLC/LC-MS grade), ethyl acetate, and n-butyl alcohol were purchased from Thermo Fisher Scientific (USA). Milli-Q water (18.2 MΩ·cm) was used for all preparations.

Key instruments included a Microplate Spectrophotometer (Multiskan SkyHigh), UV-Visible spectrophotometer (Shimadzu UV-2450), HPLC-DAD system (Vanquish, Thermo Fisher Scientific), centrifuge (Sorvall ST1 Plus), and orbital shaker incubator (Solaris). Statistical analyses were performed using Minitab (v21). Chemical structures were drawn using the RCSB chemical sketch tool.

4.2.2 Sample collection

Tea leaves (*C. sinensis* (L.) Kuntze) were collected from Somerset and Radella Tea Estates, Sri Lanka, following Tea Research Institute guidelines (Wijeratne, 2003) for plucking "two leaves and a bud." Workers wore gloves and face masks to minimize contamination. Leaves were transported in aerated nylon bags and processed into black tea using a modified orthodox method (Figure 4.1): withering, rolling, rotovane cutting, oxidation, and firing. Sampling from each processing stage was conducted in three independent batches, collected between January and August 2022. Within each batch, three spatially separated subsamples were collected per stage to ensure independence and reduce localized bias. Samples were transported at 4 °C and stored overnight before analysis.

4.2.3 Isolation of bacteria and fungi from tea and processing environments

This section describes the isolation of tea-associated microorganisms from fresh leaves, withered leaves, rolled leaves, oxidized leaves, fermentation beds, and equipment surfaces (rollers, withering trays, etc.). Both bacterial and fungal isolates were obtained using selective media to capture a broad diversity of epiphytic and endophytic communities. These isolates formed the basis for the subsequent screening of extracellular MPLO activity and selection of the candidate strains for further investigation.

This study employed a culture-dependent approach; therefore, the isolates recovered represent only the fraction of the microbiota capable of growth under the selected media and incubation conditions. Non-culturable, slow-growing, or fastidious taxa may be under-represented, and the recovered taxonomic distribution should not be interpreted as a complete microbiome profile of the tea processing environment.



Figure 4.1: Black tea manufacturing process: Plucking of tea leaves (A); spreading of leaves on withering trays (B); withering of tea leaves (C); feeding withered leaves into rollers (D); rolling (E); cutting rolled leaves using a rotovane (F); oxidation (fermentation) of leaves on fermentation beds (G); drying and sorting of leaves for packing (H).

4.2.3.1 Bacterial isolation

Epiphytic bacteria were isolated by swabbing leaf surfaces with sterile cotton swabs moistened in 0.85% NaCl, vortexing in 10 mL saline, serial dilution (10^{-1}–10^{-6}), and plating on NA and TSA. Endophytic bacteria were isolated after surface sterilization with 75% ethanol (1 min) and 4% sodium hypochlorite (3 min), followed by sterile water rinses and leaf sectioning. Bacteria from processing stages (withered, rolled, oxidized, fired leaves) and equipment (withering trays, rollers,

oxidation beds) were isolated by swabbing and plating on NA/TSA. Plates were incubated at 37 °C for 24–48 h to maximize growth and enzyme secretion for screening, although tea-associated bacteria may also grow at lower temperatures.

4.2.3.2 Fungal isolation

Epiphytic fungi were isolated by swabbing leaf surfaces with sterile swabs moistened in 0.85% NaCl, followed by vortexing, dilution, and plating on PDA and MEA supplemented with ciprofloxacin (50 µg/mL). Endophytic fungi were isolated after surface sterilization with 70% ethanol and 2% sodium hypochlorite, followed by sterility checks via leaf imprinting. Fungi from processing equipment and environments were isolated similarly. Plates were incubated at 25–28 °C (room temperature range) for 5–7 days.

4.2.3.3 Preservation and morphological characterization

Bacterial and fungal isolates were stored short-term on agar slants at 4 °C under sterile mineral oil and long-term in 15% glycerol at –80 °C. Colony morphology, microscopic features, and Gram staining (for bacteria) were recorded.

4.2.4 Screening for extracellular MPLO activity

A pure bacterial colony was grown for 18 h and adjusted to an OD_{600} of 0.6. A 2% (v/v) inoculum was then transferred into 50 mL of TSB, grown to an OD_{600} of 0.2, and subsequently incubated at 37 °C and 100 rpm (Solaris, Thermo Fisher Scientific, USA) for 48 h for extracellular enzyme production. Fungal isolates (5 × 5 mm agar plugs) were inoculated into 100 mL PDB and incubated at 150 rpm (Solaris, Thermo Fisher Scientific, USA) for 5 days. Culture filtrates were obtained by centrifugation (10,000 × g, 10 min, 4 °C).

MPLO activity was quantified using catechol in citric acid–sodium citrate buffer (pH 5.5), measuring absorbance at 410 nm. One MPLO activity unit was defined as a 0.001 absorbance change per min. Because this stage served as a preliminary screen, activities were expressed per milliliter of culture supernatant without protein normalization. The purpose was to compare

relative extracellular MPLO production among isolates, while normalization and kinetic analyses are addressed in later chapters.

Catechol was chosen as the substrate for initial MPLO screening because it captures broad-spectrum catechol-oxidizing activity, indicating the combined contributions of catechol oxidase-like, tyrosinase-like, laccase-like, and other diphenol-oxidizing systems (Claus & Decker, 2006; Eicken et al., 1998). Peroxidase activity was intentionally excluded because hydrogen peroxide was not added as a co-substrate in the screening assays.

4.2.5 Molecular identification of MPLO-positive isolates

High-MPLO-activity bacterial isolates were identified by 16S ribosomal RNA (rRNA) gene sequencing using primers 27F and 1492R (Weisburg et al., 1991). High-MPLO-activity fungal isolates were identified by Internal Transcribed Spacer (ITS) region (ITS1–ITS4) sequencing (White et al., 1990). Macrogen (Seoul, South Korea) performed sequencing, with Genetech Molecular Diagnostics providing additional PCR support for fungi and bacteria. Sequence alignment and phylogenetic analysis were performed by the candidate at Massey University, New Zealand, using multiple sequence alignment in MEGA12. Phylogenetic trees for the bacterial (16S rRNA) and fungal (ITS) isolates were constructed by the Maximum Likelihood (ML) method, which is model-based, accommodates variation in nucleotide substitution rates, and is suitable for resolving closely related taxa such as *A. faecalis* strains and filamentous fungi, with bootstrap support from 1,000 replicates.

We selected the isolate with the highest extracellular MPLO activity, identified as Alcaligenes faecalis, for further analysis. Due to import restrictions, *A. faecalis* NZRM 836 (a New Zealand reference strain) was used in subsequent experiments. The identity of *A. faecalis* NZRM 836 was confirmed by morphological, biochemical (Gram staining, oxidase, catalase, motility, indole, gelatin hydrolysis, growth at 7.5% salt, and TSI), and molecular methods (MALDI-TOF and 16S rRNA gene sequencing using primers 27F and 1492R).

4.2.6 Enzyme activity profiling of *A. faecalis*

The bacterium *A. faecalis* NZRM 836 was cultured in NB at 37 °C and 150 rpm using an orbital shaker (Solaris, Thermo Fisher Scientific, USA) as per Kumar and Azmi (2016). Growth was monitored every 12 h for 72 h by measuring its OD_{600} value using a UV spectrophotometer. At each interval, 20 mL of culture was centrifuged at 10,000 × g for 10 min at 4 °C, and the resulting supernatant was filtered through a 0.22 µm membrane to obtain a cell-free crude extracellular enzyme preparation; cell-free status was confirmed by plating an aliquot of the filtrate on nutrient agar (NA) and verifying the absence of colony growth. The 36-h timepoint, identified as the peak activity interval (Section 4.3.6), was used to generate the crude enzyme filtrate applied throughout the subsequent EGCG oxidation experiments; heat-inactivated controls were prepared by autoclaving an aliquot of this same 36-h filtrate prior to use. All enzyme assays were performed using triplicate biological replicates, each measured in technical triplicate, to ensure adequate replication and statistical power.

4.2.6.1 Catechol-like oxidase activity

Catechol oxidase-like activity was determined spectrophotometrically by monitoring the formation of benzoquinone at 410 nm, following the method of Eicken et al. (1998) with slight modifications. The reaction mixture (1.0 mL total volume) contained 950 µL of 50 mM phosphate buffer (pH 6.5), 20 µL of 100 mM catechol (final 2 mM), and 30 µL of enzyme extract. The reaction was initiated by enzyme addition, and the increase in absorbance was recorded for 2 min at 25 °C. One unit (U) of catechol oxidase-like activity was defined as the amount required to produce 1 µmol of benzoquinone per min.

4.2.6.2 Laccase-like activity

Laccase-like activity was determined spectrophotometrically by monitoring the oxidation of syringaldazine at 530 nm (Holm et al., 1998). The reaction mixture (1.0 mL total volume) contained 700 µL of 100 mM phosphate buffer (pH 6.5), 100 µL of 10 mM syringaldazine (final 1.0 mM), and 200 µL of enzyme extract. The reaction was initiated by enzyme addition, and the

increase in absorbance was recorded for 3 min at 30 °C. One unit (U) of laccase-like activity was defined as the amount of enzyme required to oxidize 1 µmol of syringaldazine per min.

4.2.6.3 Peroxidase-associated activity

Peroxidase-associated activity was determined spectrophotometrically by monitoring guaiacol oxidation at 470 nm, following Tonami et al. (2004) with minor modifications. The reaction mixture (1.0 mL total volume) contained 850 µL of 50 mM phosphate buffer (pH 6.5), 50 µL of 400 mM guaiacol (final 20 mM), 50 µL of 240 mM H_2O_2 (final 12 mM), and 50 µL enzyme extract. The reaction was initiated by enzyme addition, and the linear absorbance change was recorded for 1 min at 25 °C. One unit (U) of peroxidase-associated activity was defined as the amount producing 1 µmol of tetraguaiacol per min under these conditions.

4.2.7 EGCG oxidation by *A. faecalis* crude enzymes

EGCG was used as the model substrate for oxidation. A substrate mixture was prepared by adding 1 mL of 20 mM EGCG stock solution and varying volumes of 36-h enzyme filtrate, adjusted to a final volume of 10 mL with phosphate buffer, yielding a final EGCG concentration of 2 mM (916.74 mg/L; Table 4.2). Controls used autoclaved enzyme. Reactions were incubated at 60 °C for 2 h, stopped in an ice bath, and filtered. The use of 60 °C was based on evidence that extracellular MPLO preparation retained measurable substrate-oxidizing activity at elevated temperatures and that similar temperatures have been used in catechin oxidation protocols; detailed justification is provided in the discussion. Aliquots were stored for HPLC analysis and pigment quantification.

4.2.7.1 HPLC analysis of EGCG oxidation-associated metabolites

Oxidation-associated metabolites were analyzed using an HPLC-DAD system (Thermo Fisher Scientific, Waltham, Massachusetts, USA) equipped with a Hypersil GOLD 2.6 µm C18 column (150 × 2.1 mm, Thermo Scientific, Waltham, MA, USA) and a diode-array detector (DAD) set at 210 nm and 280 nm. The mobile phase consisted of solvent A (0.1% v/v formic acid in Milli-Q water) and solvent B (100% acetonitrile). The column was maintained at 25 °C with a 10 µL

injection volume and a flow rate of 0.3 mL/min. The gradient elution program was as follows: 8–11% B (0–5 min), 11–20% B (5–10 min), 20% B (10–16 min), 20–28% B (16–25 min), 28–30% B (25–30 min), 30–35% B (30–34 min), 35–90% B (34–36 min), 90% B (36–39 min), followed by 6 min of re-equilibration at initial conditions.

4.2.7.2 Quantification of tea pigments (TFs, TRs, and TBs)

Tea pigments (TFs, TRs, and TBs) were quantified using a method modified from Wang et al. (2011) adapted for EGCG oxidation-associated metabolites. A 5 mL reaction mixture was processed via sequential solvent partitioning to prepare four solutions (A–D) that are explained below:

Solution A: A 2 mL sample was extracted with 2 mL ethyl acetate (Thermo Fisher Scientific), shaken for 5 min, and the organic layer was separated. A 0.2 mL aliquot was diluted to 1 mL with 95 % ethanol.

Solution B: 1 mL of the ethyl acetate layer (from Solution A) was extracted with 1 mL 2.5 % (w/v) sodium bicarbonate (Sigma-Aldrich) for 30 s; the 0.2 mL organic layer was diluted to 1 mL with 95 % ethanol.

Solution C: 1 mL of the original sample was mixed with 1 mL n-butyl alcohol (Thermo Fisher Scientific); 0.2 mL aqueous layer was combined with 0.2 mL saturated oxalic acid (Sigma-Aldrich), 0.6 mL Milli-Q water, and 1 mL 95 % ethanol.

Solution D: 1 mL of the aqueous layer (from ethyl acetate extraction) was mixed with 0.2 mL saturated oxalic acid, 0.6 mL Milli-Q water, and 1 mL 95 % ethanol.

Absorbance of solutions A–D (E_A, E_B, E_C, and E_D) was measured at 380 nm using a spectrophotometer set to a 1-cm path length. Total concentrations of TFs (%), TRs (%), and TBs (%) were calculated using equations (4.1), (4.2), (4.3) (Wang et al. 2011), normalized to EGCG dry weight equivalent. All analyses were performed in triplicate.

$$TFs(\%) = \frac{E_C \times 2.25}{\text{Weight of EGCG}(\%)} \times 100 \qquad \textit{(4.1)}$$

$$TRs(\%) -= \frac{7.06 \times (2E_A + 2E_D - E_C - 2\,E_B)}{\text{Weight of EGCG}(\%)} \times 100 \qquad \textit{(4.2)}$$

$$TBs(\%) = \frac{2E_B \times 7.06}{\text{Weight of EGCG}(\%)} \times 100 \quad \textit{(4.3)}$$

where:

$\boldsymbol{E_A}$ = absorbance of solution A at 380 nm; $\boldsymbol{E_B}$ = absorbance of solution B at 380 nm ; $\boldsymbol{E_C}$ = absorbance of solution C at 380 nm; $\boldsymbol{E_D}$ = absorbance of solution D at 380 nm; TFs (%) = percentage of total theaflavins; TRs (%) = percentage of total thearubigins; TBs (%) = percentage of total theabrownins; Weight of EGCG (%) = dry weight equivalent concentration of EGCG used as the reference basis for normalization 2.25 and 7.06 = empirical conversion factors derived from the spectrophotometric method described by Wang et al. (2011).

4.2.8 Statistical analysis

All experiments were performed in triplicate, and results were presented as mean ± standard deviation (SD). One-way analysis of variance (ANOVA) was used to compare extracellular PPO activities among bacterial and fungal isolates, and among EGCG oxidation treatments with different enzyme volumes. Although formal normality tests were not performed due to small sample sizes, residual plots and variance patterns were inspected visually to confirm that ANOVA assumptions were reasonably met. Significant pairwise differences were identified using Tukey's Honestly Significant Difference (HSD) post-hoc test. ANOVA, linear regression, and Pearson correlation analyses were conducted using Minitab 21.0 (Minitab LLC, State College, PA, USA).

Hierarchical clustering of MPLO activity was performed in Python using Ward's minimum variance method and Euclidean distance. Thresholds of 50 U/mL for fungal isolates and 40 U/mL for bacterial isolates were selected based on biological interpretability and sensitivity analysis, which showed that these values reliably separated high-activity isolates from the low-to-moderate activity majority while maintaining consistency with phylogenetic groupings. Statistical significance was set at $p < 0.05$.

4.3 Results and discussion

4.3.1 Microbial diversity across tea processing stages

Isolation and preliminary screening were performed by the candidate at Somerset Tea Estate, Talawakelle Tea Estates, Sri Lanka, across the black tea processing sequence (fresh leaf through fired black tea), targeting all morphologically distinct colonies recoverable under the cultivation

conditions used, rather than a further-narrowed subset. A total of 83 culturable microbial isolates were recovered from the Sri Lankan orthodox black tea manufacturing environment, comprising 43 bacterial and 40 fungal strains, representing the complete set of morphologically distinct isolates successfully purified from this sampling effort. Because this study used a culture-dependent approach, the taxonomic distributions and relative abundance patterns reported here refer only to the isolates recovered under the selected cultivation conditions and may not reflect the true community composition *in situ*.

Rather than detailing each processing stage individually, overall distribution patterns are summarized here. Bacterial isolates were most frequently recovered from rolled and oxidized leaves, stages characterized by mechanical disruption and elevated oxygen exposure, conditions known to favor aerobic and phenolic-tolerant bacteria (Tong et al., 2021; Zhao et al., 2022). In contrast, fungal isolates were predominantly associated with endophytic communities in fresh leaves, consistent with reports that filamentous fungi such as *Aspergillus* and *Penicillium* are well adapted to phenolic-rich plant tissues (Lin et al., 2022; Xie et al., 2020). These patterns indicate that bacteria tend to proliferate during processing, whereas fungi are more deeply embedded within leaf tissues prior to manufacture.

Because these observations are based on culture-dependent recovery, terms such as ‘abundance’ and ‘distribution’ refer to the number of isolates successfully cultured under the applied conditions and should not be interpreted as true ecological prevalence in the tea processing environment. Functionally, these distribution patterns suggest that stages involving cell rupture and early oxidation selectively enrich for taxa capable of tolerating phenolic stress and producing extracellular MPLO-associated activities. Mechanical disruption releases catechins and increases oxygen availability, creating microenvironments that favor oxidative phenolic metabolism (Wang et al., 2020). Similarly, the elevated MPLO activity observed among endophytic fungi reflects their long-term adaptation to host-derived phenolics and their established roles in polyphenol transformation (Liu et al., 2023c). These ecological trends guided the screening strategy by prioritizing isolates from rolled and oxidized stages for bacterial MPLO activity and endophytic isolates for fungal MPLO activity. The relative frequency of isolates showing detectable extracellular MPLO-associated activity at each isolation source is shown in Figure 4.2, and the source of each isolate is given in Tables S4.1 and S4.2 (Appendices C).

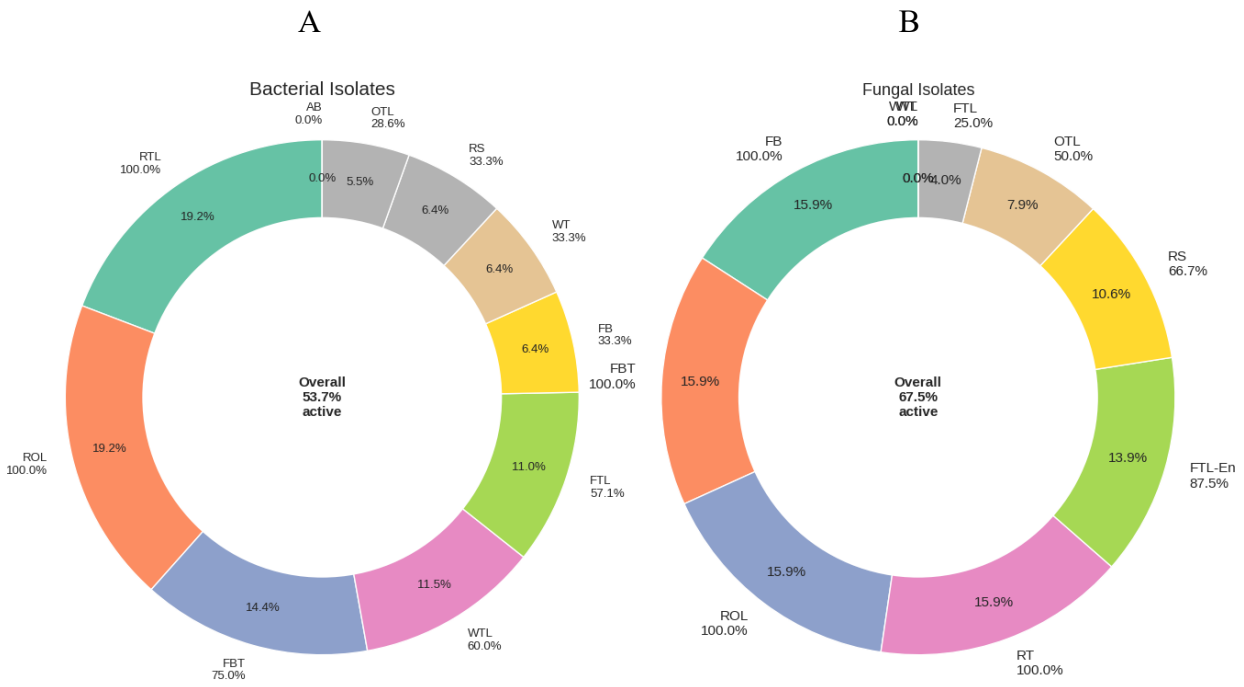

Figure 4.2: Relative frequency of isolates with detectable extracellular MPLO-associated activity (>0 U/mL) by isolation source in bacterial (A) and fungal (B) communities from tea processing. Abbreviations: FTL = fresh tea leaves; FTL-En = endophytes from fresh tea leaves; FTL-Ep = epiphytes from fresh tea leaves; WTL = withered leaves; RS = roller surfaces; RE = rolling equipment; RTL= rotovaned leaves; OTL = oxidized leaves; FB = fermentation beds; FBT = fired black tea; WT = withering trays; RT = Rotovane surfaces; AB = airborne/environmental.

4.3.2 Molecular identification and taxonomic composition of MPLO-positive isolates

Molecular identification was performed on high-MPLO-activity bacterial and fungal isolates to confirm their taxonomic placement and to evaluate patterns associated with extracellular MPLO activity. Bacterial isolates were identified through 16S rRNA gene sequencing using primers 27F and 1492R, and fungal isolates were identified using ITS1–ITS4 primers targeting the ITS region. BLAST searches with a similarity threshold of 95% verified the identities of all high-MPLO-activity isolates (Tables S4.1 and S4.2 of Appendix C). The taxonomic patterns reported here describe the subset of MPLO-positive isolates recovered under the culture conditions used and should not be interpreted as a complete profile of the tea-processing microbiota. Among the MPLO-positive bacterial isolates, members of the phylum Pseudomonadota were most frequently recovered, followed by Bacillota and Actinomycetota (Figure 4.3A). At the genus level, *Alcaligenes* was the most commonly recovered bacterial genus, reflecting its repeated isolation

across multiple processing stages and its strong association with high extracellular MPLO activity (Figure 4.3B). Among the MPLO-positive fungal isolates recovered, *Aspergillus* was the most frequently identified genus, consistent with the high MPLO activities observed in *A. fumigatus*, *A. sydowii*, and *A. versicolor* (Figure 4.3C and 4.3D).

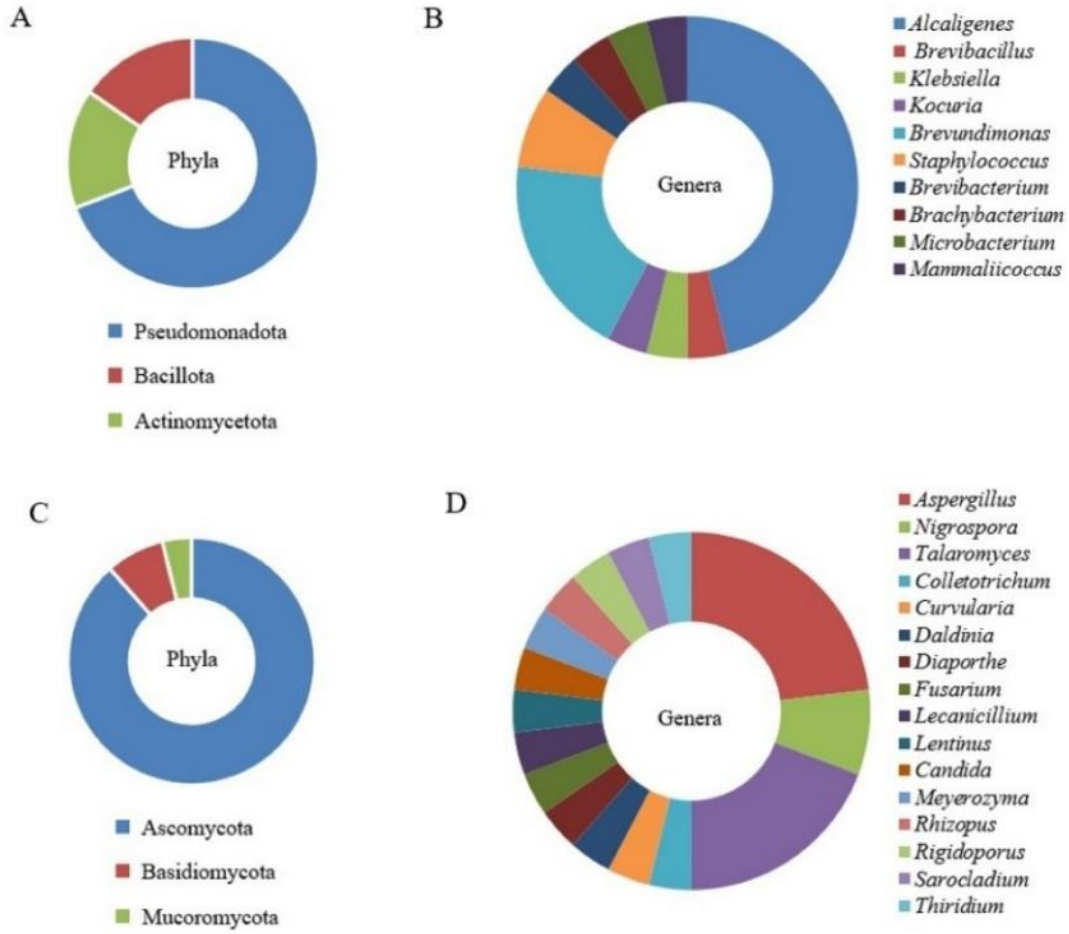

Figure 4.3: Taxonomic compositions of microbial isolates with extracellular MPLO activity, displaying bacteria at the phylum (A) and genus (B) levels, and fungi at the phylum (C) and genus (D) levels.

These lineage-level patterns suggest that elevated oxidative capacity appears concentrated within specific microbial groups adapted to phenolic-rich tea environments. This taxonomic trend informed the selection of *A. faecalis* for downstream characterization, as it combined high extracellular MPLO activity, repeated recovery across processing stages, and favorable laboratory handling characteristics, in contrast to several high-activity *Aspergillus* species that present greater biosafety concerns.

4.3.3 MPLO activity of the identified bacterial and fungal isolates

4.3.3.1 MPLO-positive bacterial isolates

Extracellular MPLO activity varied widely among the 43 bacterial isolates recovered from different stages of black tea processing. Activities ranged from 0.07 to 132.57 U/mL (Table S4.1-Appendix C). *A. faecalis* isolate B12 showed the highest activity (132.57 ± 0.65 U/mL), followed by isolate B23 (87.50 ± 0.50 U/mL). Several additional *A. faecalis* isolates exhibited moderate activity, while non-*Alcaligenes* taxa such as *Brevundimonas diminuta*, *Brevibacillus parabrevis*, and *Microbacterium testaceum* showed comparatively lower activities.

A one-way analysis of variance (ANOVA) demonstrated significant differences in MPLO activity among the 26 bacterial taxa represented in the dataset, $F(25, 52) = 9.20$, $p < 0.001$. Tukey's Honestly Significant Difference (HSD) test indicated that *A. faecalis* isolate B12 had significantly higher MPLO activity than most other isolates ($p < 0.05$). The distribution of activities was strongly right-skewed, with a small subset of high-producing isolates emerging from a majority of low-to-moderate producers. This skewed distribution supports the hierarchical clustering analysis it establishes the biological basis for the hierarchical clustering performed later and highlights *A. faecalis* as the representative high-MPLO-activity lineage.

The high MPLO activity observed in *A. faecalis* agrees with previous reports describing its ability to secrete oxidoreductases involved in phenolic transformation (Abdelgalil et al., 2020; Mehandia et al., 2020). However, its repeated recovery across multiple processing stages may also reflect greater cultivability under the media and incubation conditions used in this study; therefore, inferences regarding its ecological prevalence are limited to the culturable fraction sampled. Together, its high extracellular activity, frequent recovery, and suitability for safe laboratory handling made *A. faecalis* the most logical choice for downstream biochemical characterization and the development of an enzyme preparation in subsequent chapters.

4.3.3.2 MPLO-positive fungal isolates

Extracellular MPLO activity among the 40 fungal isolates ranged from 0.67 to 119.03 U/mL (Table S4.2). The highest activity was recorded in *A. fumigatus* (EP09, 119.03 ± 0.58 U/mL; EP06, 77.67 ± 0.33 U/mL), followed by *Talaromyces pinophilus* EP07 (55.00 ± 0.58 U/mL), *Lentinus*

sajor-caju PR03 (54.00 ± 1.00 U/mL) and *A. sydowii* EP15 (34.00 ± 0.58 U/mL); other *Aspergillus* isolates, including *A. versicolor*, showed low activity (11.00–11.67 U/mL). The fungal activity distribution was strongly right-skewed, with a small subset of high-producing isolates emerging from most low-to-moderate producers. This skewed pattern reinforces the presence of a distinct high-activity tier within the fungal community. The macroscopic and microscopic morphology of the highest-producing endophytic isolate, *A. fumigatus* EP09, is shown in Figure 4.4.

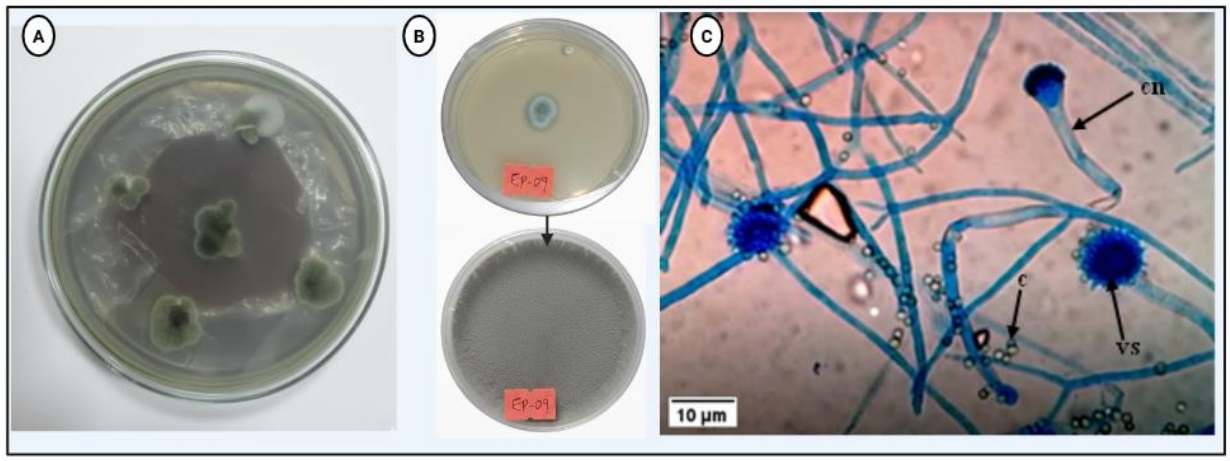

Figure 4.4: Macroscopic and microscopic morphology (scale bars = 10 µm) of the fungal isolate *Aspergillus fumigatus* EP09 grown on potato dextrose agar (PDA) medium for 168 h. Colonies arising from surface-sterilized leaf blocks (A). Colonies exhibit rapid growth, initially white, turning blue-green to grey-green with a powdery texture due to conidia development (B). Microscopic morphology shows conidia (c), conidiophores (cn), and vesicles (vs) (C). Conidiophores are uniseriate with a smooth stipe widening into a globular vesicle (20–30 µm) bearing phialides over the upper two-thirds. Conidia are globose to subglobose (2.5–3 µm), green, and arranged in chains. Hyphae are septate, hyaline, branched, and 2–4 µm in diameter.

A one-way ANOVA confirmed significant differences in MPLO activity among the 22 fungal taxa represented, $F(21, 42) = 11.34$, $p < 0.001$. Tukey's HSD test showed that the *A. fumigatus* EP09 and EP06 formed a statistically distinct high-activity group ($p < 0.05$). These results align with the well-documented ability of *Aspergillus* species to secrete potent oxidoreductases capable of modifying plant polyphenols, particularly under phenolic-rich conditions such as those found in tea leaves.

4.3.4 Phylogenetic relationships and association with MPLO activity

Phylogenetic analysis provided insights into the evolutionary relationships among MPLO-positive isolates and clarified how oxidative capacity is distributed across tea-associated microbial lineages. Among bacteria, *A. faecalis* was the most frequently recovered species and consistently exhibited the highest MPLO activity.

Isolates obtained from withered, rolled, and oxidized tea leaves showed 98–100% sequence identity to reference *A. faecalis* strains. ML phylogenetic analysis of 16S rRNA gene sequences placed these isolates within a well-supported monophyletic clade (Figure 4.5A, bootstrap values greater than or equal to 95%), indicating close genetic relatedness among high-MPLO-activity strains. This clustering pattern suggests that elevated oxidative capacity is conserved within this lineage, consistent with reports of *A. faecalis* adaptation to phenolic-rich environments (Zhang et al., 2023a).

Fungal isolates with high MPLO activity were predominantly members of the genus *Aspergillus*. ML analysis of ITS sequences placed *A. fumigatus* isolates EP06 and EP09 within a strongly supported clade (Figure 4.5B, bootstrap support 98–100%). These isolates were closely related to reference environmental and clinical strains. The recovery of *A. fumigatus* from fresh tea leaves suggests that it may function as an early colonizer or latent endophyte, although confirmation of endophytic status would require histological or in-plant evidence (Khan et al., 2015; Suryanarayanan, 2013). Endophytic fungi are known to produce oxidoreductase enzymes that interact with host phenolics (Liu et al., 2023c), and the high MPLO activity observed in EP06 and EP09 aligns with this functional role.

Activity-based hierarchical clustering supported phylogenetic patterns and demonstrated a clear association between evolutionary relatedness and oxidative capacity. MPLO activity displayed a strongly right-skewed distribution in both bacterial and fungal groups, with a small subset of high-producing isolates emerging from a larger pool of low-to-moderate producers.

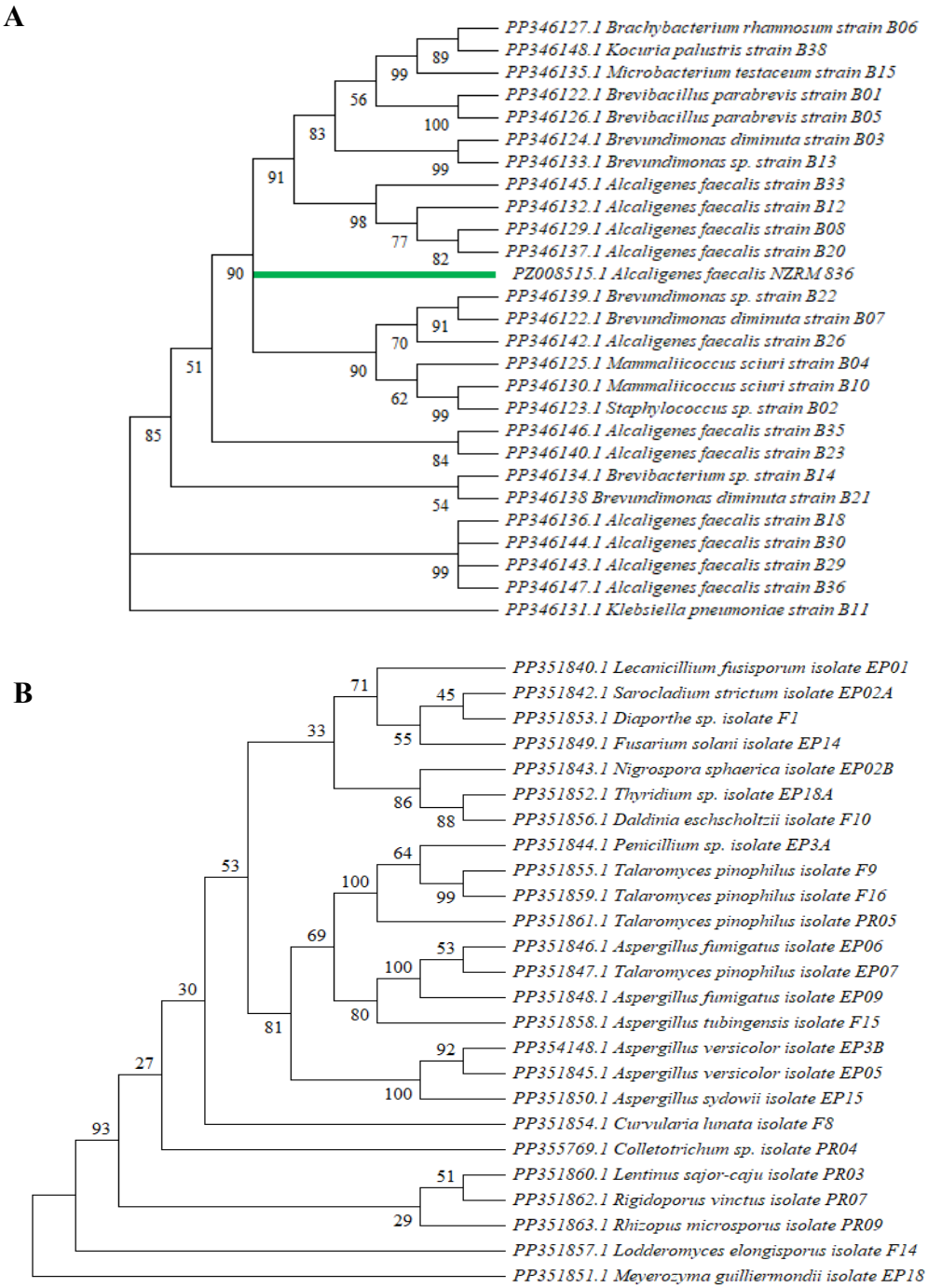

Figure 4.5: Maximum Likelihood phylogenetic analysis of bacterial (A) and fungal (B) isolates recovered from orthodox black tea fermentation. Trees were inferred using the Maximum Likelihood method with 1,000 bootstrap replicates, and branches supported by <50% bootstrap values were collapsed. Bootstrap percentages (>50%) are shown below the corresponding nodes. Initial heuristic trees were generated using the Neighbor-Joining method with p-distance estimates. The final bacterial dataset included 27 nucleotide sequences with 970 aligned positions. All evolutionary analyses were performed in MEGA12 using parallel computing.

Among fungi, isolates exceeding 50 U/mL formed a distinct high-activity cluster comprising *A. fumigatus* EP09 and EP06, *T. pinophilus* EP07 and *L. sajor-caju* PR03. Three of the four were recovered from fresh tea leaves.

Among bacteria, isolates exceeding 40 U/mL were dominated by *A. faecalis* strains such as B12 (132.6 U/mL) and B23 (87.5 U/mL), most of which originated from oxidized tea leaves. These relationships were reflected in the bacterial dendrogram and activity bar plots (Figure 4.6 A–B). The close correspondence between phylogenetic clades and activity-based clusters indicates that oxidative capacity is linked to specific evolutionary lineages within tea-associated microbial communities. This lineage-level signal also provided a biological rationale for selecting representative taxa for downstream characterization.

Although *Aspergillus* isolates exhibited the highest extracellular MPLO activities among fungal isolates, none of the recovered species (*A. fumigatus*, *A. sydowii*, *A. versicolor*) holds GRAS/QPS or food-grade status for use in food applications. Furthermore, several of these species are recognized as opportunistic human pathogens or producers of mycotoxins (Pitt & Hocking, 2009; Sewalt et al., 2016). For these biosafety reasons, they were not chosen for further biochemical characterization despite their superior MPLO activity.

In contrast, *A. faecalis* NZRM 836 was selected as the representative high-MPLO-activity lineage because it combined high extracellular MPLO activity with more practical laboratory handling and lower biosafety concerns than the high-activity fungal isolates (Centers for Disease Control and Prevention, 2020).

Although *A. faecalis* can act as an opportunistic pathogen in clinical settings, its cell-free extracellular enzyme preparations generally pose lower biosafety risk than live-cell applications in biochemical applications. Its placement within the *A. faecalis* clade in the 16S rRNA phylogeny (Figure 4.5A) indicates close taxonomic relatedness to the high-activity tea isolates and supports its use as a practical, regulatory-compliant model for downstream characterization.

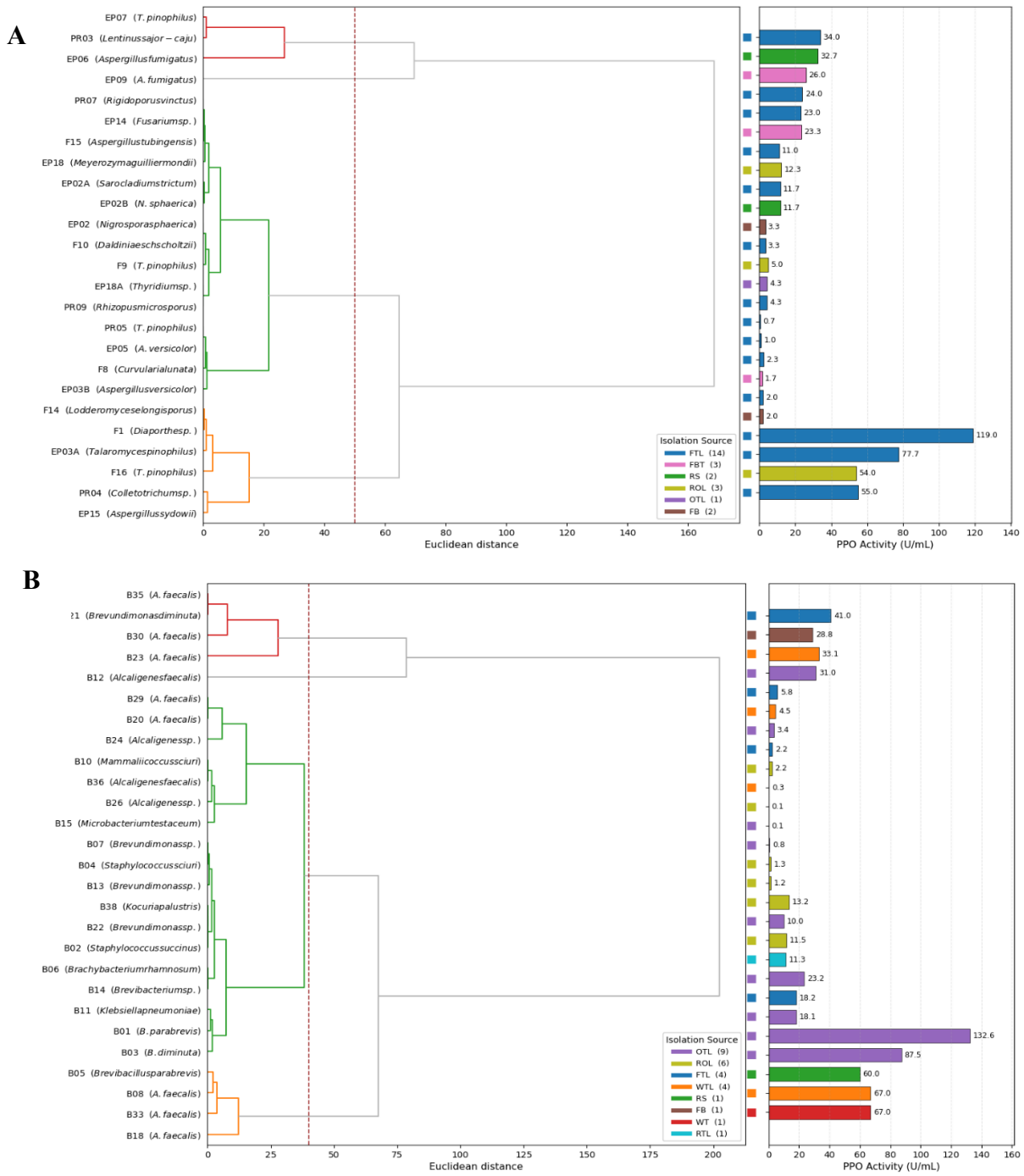

Figure 4.6: Comparative hierarchical clustering (Ward's method, Euclidean distance) of extracellular MPLO-associated activity in fungal and bacterial isolates from tea processing stages. (A, B) Fungal isolates: dendrogram with black leaf labels (A) and aligned MPLO activity bars colored by isolation source (B); clustering threshold 50 U/mL. (C, D) Bacterial isolates: dendrogram with black leaf labels (C) and aligned MPLO activity bars colored by isolation source (D); clustering threshold 40 U/mL. Isolation source color key: FTL (blue), FBT (pink), RS (green), RE (olive), OTL (purple), FB (brown), WTL (orange), WT (red), RTL (cyan).

4.3.5 Biochemical and molecular characterization of *Alcaligenes faecalis* NZRM 836

The reference strain *A. faecalis* NZRM 836 (Figure 4.7) displayed characteristics consistent with a strong extracellular oxidoreductase producer, including Gram-negative rod morphology, motility, catalase and oxidase positivity, and the ability to utilize citrate, traits associated with aerobic metabolism and oxidative enzyme secretion. Importantly, *A. faecalis* NZRM 836 presented more practical laboratory handling characteristics and lower biosafety concerns than the high-activity *Aspergillus* isolates, supporting its suitability for cell-free extracellular enzyme preparation.

The strain NZRM 836 was chosen as the substitute for isolate B12 due to New Zealand biosecurity restrictions preventing the transfer of unregistered environmental isolates. Because NZRM 836 grouped with the high-MPLO-activity *A. faecalis* isolates in the 16S rRNA phylogeny and showed biochemical traits consistent with the species description (Table 4.1), it was used as a traceable, regulatory-compliant model organism for the *A. faecalis* lineage. The extracellular MPLO profile of NZRM 836 was not compared directly with that of the original isolate B12, so strain-specific differences cannot be excluded (see Section 7.3). A concise summary of relevant biochemical traits for *A. faecalis* NZRM 836 is presented in Table 4.1.

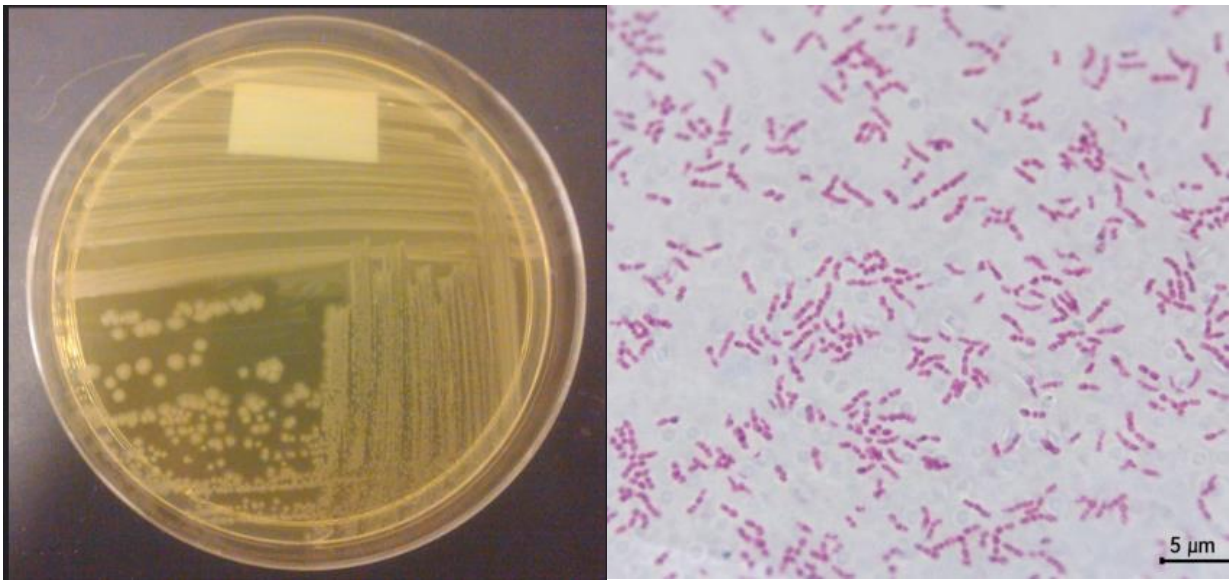

Figure 4.7: *Alcaligenes faecalis* NZRM 836: Colony morphology on nutrient agar (left) and Gram-stained rods (right; Gram-negative bacilli, scale bar = 5 µm).

Table 4.1: Morphological, biochemical, and growth characteristics of *Alcaligenes faecalis* NZRM 836.

Characteristic	Result	Inferences
Morphology & Cell Structure		
Shape	Rods or coccobacilli	Typical *Alcaligenes* morphology
Gram Staining	Gram-negative	
Motility	Positive	Flagella present
Flagella	Positive	Confirms motility
Enzymatic & Chemical Tests		
Catalase	Positive	Can detoxify H_2O_2
Oxidase	Positive	Cytochrome c oxidase present
Citrate Utilization	Positive	Uses citrate as carbon source
Gelatin Hydrolysis	Negative	Cannot hydrolyze gelatin
Indole	Negative	Cannot produce indole
Growth & Tolerance		
Growth in 7.5% NaCl	Negative	Not halotolerant
TSI (Triple Sugar Iron)	Red/Red reaction	No fermentation of lactose, sucrose, or glucose

4.3.6 Profiling of *Alcaligenes faecalis* NZRM 836 crude enzyme preparations

The oxidative enzyme system of *A. faecalis* NZRM 836 was characterized to determine its capacity to transform phenolic substrates relevant to tea chemistry. The analysis focused on MPLO-associated activities, specifically catechol oxidase-like, laccase-like, and peroxidase-associated activities, which are known to catalyze oxidation of o-diphenols and related phenolic substrates in bacterial systems (Abdelgalil et al., 2020; Mehandia et al., 2020). A preliminary monophenolase check, using L-tyrosine as substrate, was performed during the initial screening of MPLO-positive isolates, using the crude enzyme extract, and returned a nil result; consequently, a full diphenolase-based tyrosinase assay was not pursued at this stage, consistent with *A. faecalis* not being generally characterized as a strong producer of classical type-3 copper tyrosinases. However, because some *A. faecalis* strains possess diverse oxidative enzymes capable of acting on phenolic substrates (Zhang et al., 2023a), tyrosinase-associated activity was re-evaluated following partial purification, using L-DOPA as substrate, as described in Chapter 5.

The enzymatic profile of *A. faecalis* was monitored across its growth in nutrient broth (Figure 4.8). Optical density (OD_{600}) followed a typical bacterial growth curve: lag phase (0–12 h), exponential phase (12–36 h), stationary phase (36–60 h), and decline (60–72 h). Extracellular MPLO activities peaked at distinct phases, suggesting metabolic regulation. This pattern aligns with previous reports describing extracellular oxidative enzyme production in *A. faecalis* and related bacterial taxa (He et al., 2023).

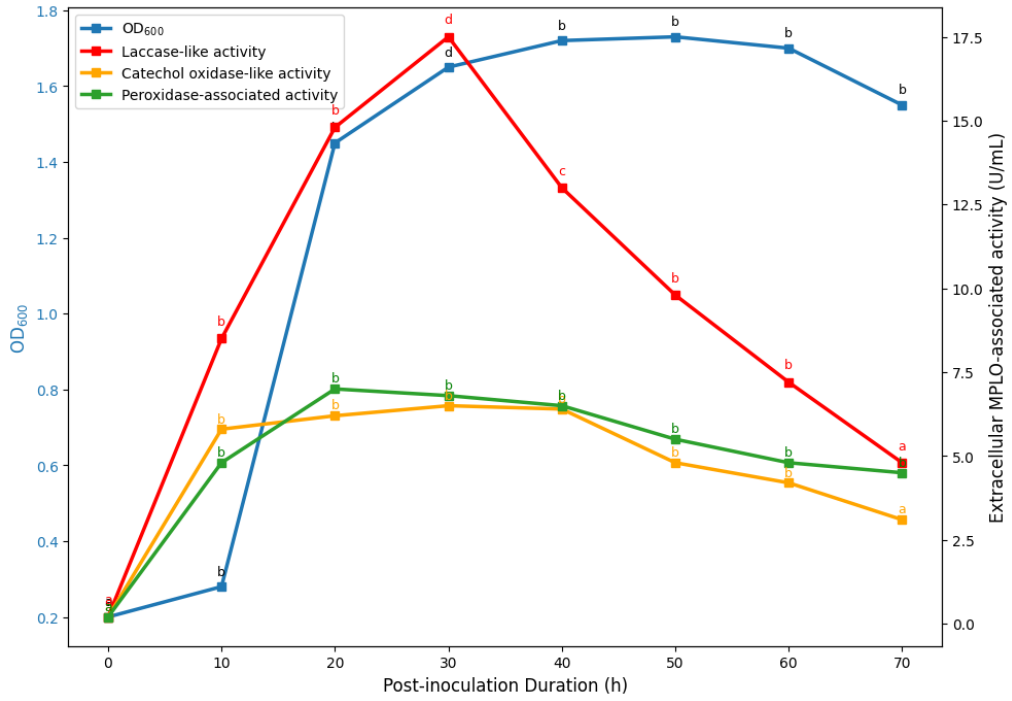

Figure 4.8: Trend of extracellular MPLO-associated activities during growth of *Alcaligenes faecalis* NZRM 836 in nutrient broth medium.

Laccase-like activity increased during the exponential phase, peaking at 12.6 ± 0.25 U/mL at 36 h ($p < 0.01$) before declining to 4.8 ± 0.10 U/mL by 72 h. Catechol oxidase-like activity followed a similar pattern, reaching 3.6 ± 0.07 U/mL at 36 h ($p < 0.01$) and decreasing to 1.1 ± 0.022 U/mL by 72 h. Peroxidase-associated activity peaked earlier, at 24 h (4.2 ± 0.08 U/mL, $p < 0.01$), and declined to 2.2 ± 0.04 U/mL by 72 h. Together, these temporal patterns indicate coordinated production of extracellular oxidoreductase-associated activities during late exponential growth, whereas the earlier peroxidase-like response may reflect oxidative stress adaptation during rapid biomass accumulation (El-Sayed et al., 2024). The 36-h time point in the nutrient broth medium

therefore represents the optimal operational stage for downstream assays, providing maximal oxidative capacity while avoiding stress-associated enzyme profiles. This choice directly informed the enzyme dose used in the EGCG oxidation experiments and guided the design of the response-surface optimization in Chapter 5. Specifically, the 36-h finding justified including duration as a factor worth optimizing rather than treating it as fixed; the response-surface design subsequently tested a broader 12–96 h range to capture potential interactions between duration and the other two factors, with 54 h emerging as the mathematical center-point of that range rather than a re-confirmation of the single-culture optimum identified here.

The interpretation of these activities is directly linked to the substrates and reaction chemistries described in Section 2.6. Laccase-like activity was measured using syringaldazine, a phenolic dimer that undergoes one-electron oxidation to form a stable quinone-type chromophore. This reaction reflects the broad phenoxy-radical-forming capability of multicopper oxidases. Catechol oxidase-like activity was quantified using catechol, an o-diphenol oxidized to o-benzoquinone via a two-electron diphenol oxidation typical of PPO-like enzymes. Peroxidase- associated activity was assayed using guaiacol, which is converted to tetraguacol in the presence of H_2O_2, representing a heme-dependent radical-coupling reaction characteristic of peroxidases. These substrate-specific assays therefore represent distinct modes of phenolic oxidation: laccase-like activity (one-electron phenoxy radical formation), catechol oxidase-like activity (o-quinone formation), and peroxidase-like activity (H_2O_2-dependent phenoxy radical polymerization).

Tyrosinase-associated activity was assessed using both L-tyrosine (monophenolase assay) and L-DOPA (diphenols assay). L-tyrosine requires ortho-hydroxylation to L-DOPA before oxidation, whereas L-DOPA is directly converted to dopaquinone (Cieńska et al., 2016). Neither substrate produced detectable activity in the crude extract, indicating the absence of an active type-3 copper tyrosinase under the tested conditions. Consequently, only catechol oxidase-like, laccase-like, and peroxidase-like activities were considered in subsequent interpretation.

The combined enzyme profile demonstrates that *A. faecalis* NZRM 836 produces a suite of MPLO-associated activities capable of acting on a broad range of phenolic substrates. The strong catechol-oxidizing activity observed in *A. faecalis* NZRM 836 is consistent with the high-activity phenotype of the *A. faecalis* lineage identified during screening. Because NZRM 836 and isolate B12 were not assayed side by side, functional equivalence is not established; NZRM 836 is therefore used

here as a representative, well-characterized, regulatory-compliant model of this lineage for investigating microbial catechin oxidation.

The activity patterns observed in *A. faecalis* NZRM 836 are consistent with previous reports describing the oxidative capabilities of *A. faecalis* and related taxa (Abdelgalil et al., 2020). The coordinated production of catechol oxidase-like, laccase-like, and peroxidase-like activities suggests that this species may contribute to oxidative catechin transformation during tea oxidation. These findings provide a mechanistic foundation for subsequent experiments examining the oxidation of epigallocatechin gallate (EGCG) and the formation of tea pigments, which are presented in Section 4.3.7.

4.3.7 Oxidation of EGCG by *A. faecalis* enzyme filtrate

Crude extracellular enzyme preparation from *A. faecalis* drove dose-dependent EGCG depletion (~58%) and formation of gallic acid (GA), epigallocatechin (EGC), gallocatechin gallate (GCG), and low-level theaflavins (TFs), indicating concurrent ester hydrolysis (degallation), epimerization, and early oxidative coupling. HPLC-DAD analysis (Figure 4.9) showed a progressive decline in EGCG concentration with increasing enzyme volume (31.25–500 µL), accompanied by the appearance of characteristic oxidation-associated metabolites.

EGCG decreased from 795.82 ± 55.71 mg/L (heat-inactivated control) to 333.33 ± 20.00 mg/L at 500 µL enzyme, representing a ~58% loss. In parallel, GA increased from 1.06 ± 0.02 mg/L (t = 0) to 29.81 ± 1.79 mg/L, and EGC rose from 1.14 ± 0.09 mg/L to 3.97 ± 0.24 mg/L. GCG accumulated substantially across all incubated samples, aligning with temperature-driven epimerization. Low but measurable amounts of theaflavin-3-gallate (TF3G) and theaflavin-3,3'-digallate (TF3,3'G) were detected at higher enzyme doses, indicating the onset of oxidative coupling. These changes are illustrated in the HPLC-DAD chromatograms (Figure 4.9) and quantified in Table 4.2.

Furthermore, Table 4.2 presents the concentrations of key oxidation-associated metabolites across enzyme volumes. The EGCG concentration at preincubation (t = 0) was 816.24 mg/L, which is approximately 10% below the theoretical value of 916.74 mg/L (from 1 mL of 20 mM EGCG diluted to 10 mL), likely due to impurities in the EGCG standard. After 2 h of incubation at 60 °C

without enzyme (control, 0 µL), the concentration decreased to 795.82 ± 55.71 mg/L, attributable to minimal thermal degradation (Xu et al., 2019).

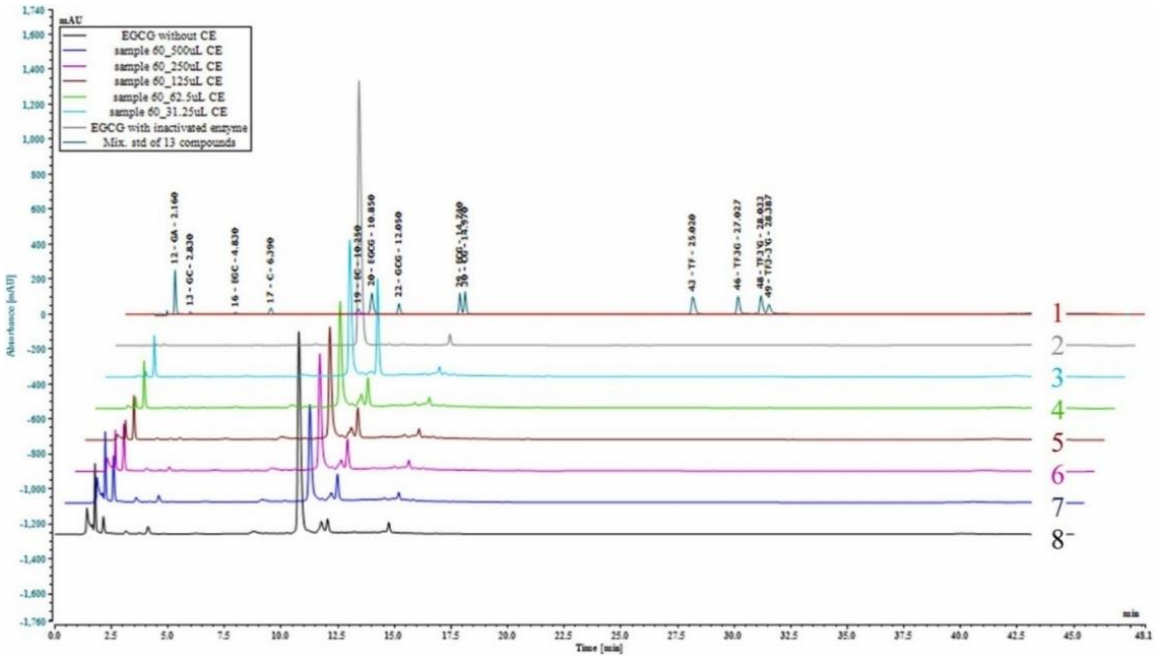

Figure 4.9: HPLC-DAD chromatograms showing the effect of different crude enzyme volumes on EGCG degradation, along with the appearance of oxidation-associated metabolites in the sample vials. Detection at 280 nm. (1) Mixed standard of 13 compounds; (2) Control (EGCG) before incubation; (3) 31.25 µL; (4) 62.5 µL; (5) 125 µL; (6) 250 µL; (7) 500 µL enzyme treatment; and (8) Control (EGCG) with inactivated enzyme preparation at the end of the reaction.

Significant epimerization of EGCG resulted in substantial GCG formation, ranging from 31.04 ± 2.17–42.14 ± 2.95 mg/L, also attributable to the incubation temperature (Xu et al., 2019). Despite the limited impact of temperature alone, the observed 58% reduction in EGCG highlights the pronounced effect of extracellular MPLO-associated activity (Figure 4.10A). Other catechins (Figure 4.10B), including catechin (C, 3.55 ± 0.25–5.11 ± 0.31 mg/L), gallocatechin (GC, 4.75 ± 0.29–9.19 ± 2.04 mg/L), and epigallocatechin gallate (ECG, 89.32 ± 6.25–30.79 ± 1.85 mg/L), were detected, with significant changes ($p < 0.05$) indicating minor degradation or oxidative contributions. Theaflavin-3-gallate (TF3G) increased to 0.14 ± 0.01 mg/L at 31.25 µL, while theaflavin-3,3′-digallate (TF3,3′-DG) reached 4.474 ± 0.148 mg/L at 500 µL. Other theaflavins (TF, TF3'G) remained undetectable (0.00 mg/L).

Table 4.2: Concentrations of oxidation-associated metabolites across enzyme volumes (mg/L, mean ± SD, n = 3) using HPLC quantification.

Enzyme vol. (µL)	GA	GC	EGC	C	EC	EGCG	GCG	ECG	CG	TF3G	TF3-3′G
0(i)	1.06 ± 0.02^{d}	7.12 ± 1.55^{b}	1.14 ± 0.09^{bc}	2.69 ± 0.25^{d}	20.67 ± 2.10^{bc}	816.24 ± 55.71^{a}	2.41 ± 0.06^{c}	79.32 ± 6.25^{a}	8.69 ± 2.71^{b}	0.00 ± 0.00^{b}	0.00 ± 0.00^{c}
0(ii)	15.33 ± 1.07^{d}	9.19 ± 2.04^{a}	1.29 ± 0.37^{bc}	3.55 ± 0.25^{bc}	43.36 ± 3.04^{b}	795.82 ± 55.71^{a}	31.04 ± 2.17^{b}	89.32 ± 6.25^{a}	18.69 ± 2.71^{b}	0.00 ± 0.00^{b}	0.08 ± 0.01^{c}
31.25	24.69 ± 1.48^{bc}	4.91 ± 1.49^{a}	1.44 ± 0.39^{a}	5.11 ± 0.31^{a}	74.00 ± 4.44^{a}	531.72 ± 31.90^{b}	40.92 ± 2.45^{a}	80.00 ± 4.80^{a}	19.83 ± 6.59^{a}	0.14 ± 0.01^{a}	1.07 ± 0.12^{ab}
62.5	24.43 ± 1.71^{bc}	5.64 ± 0.39^{bc}	2.33 ± 0.23^{d}	3.14 ± 0.22^{cd}	14.82 ± 1.04^{c}	380.45 ± 26.63^{c}	39.82 ± 2.79^{a}	43.93 ± 3.08^{b}	17.56 ± 1.23^{c}	0.06 ± 0.00^{ab}	2.15 ± 0.15^{a}
125	24.20 ± 1.45^{c}	4.75 ± 0.29^{c}	2.28 ± 0.20^{d}	3.15 ± 0.19^{cd}	4.19 ± 0.25^{d}	413.46 ± 24.81^{c}	41.79 ± 2.57^{a}	44.18 ± 2.65^{b}	21.02 ± 1.26^{c}	0.00 ± 0.00^{b}	2.06 ± 0.12^{ab}
250	25.81 ± 1.81^{b}	6.12 ± 0.43^{bc}	2.82 ± 0.20^{d}	2.76 ± 0.19^{d}	11.55 ± 0.81^{c}	405.58 ± 28.39^{c}	42.14 ± 2.95^{a}	48.14 ± 3.37^{b}	20.44 ± 1.43^{c}	0.00 ± 0.00^{b}	3.52 ± 0.11^{b}
500	29.81 ± 1.79^{a}	6.36 ± 0.38^{b}	3.97 ± 0.24^{c}	3.08 ± 0.19^{cd}	7.58 ± 0.46^{cd}	333.33 ± 20.00^{d}	41.58 ± 2.49^{a}	30.80 ± 1.85^{c}	17.79 ± 1.07^{c}	0.00 ± 0.00^{b}	4.47 ± 0.15^{a}

Means denoted by different letters (a–f) within each column are significantly different (Tukey's test, $p < 0.05$). (i) t = 0 pre-incubation control, and (ii) 0 µL heat-inactivated post-incubation control.

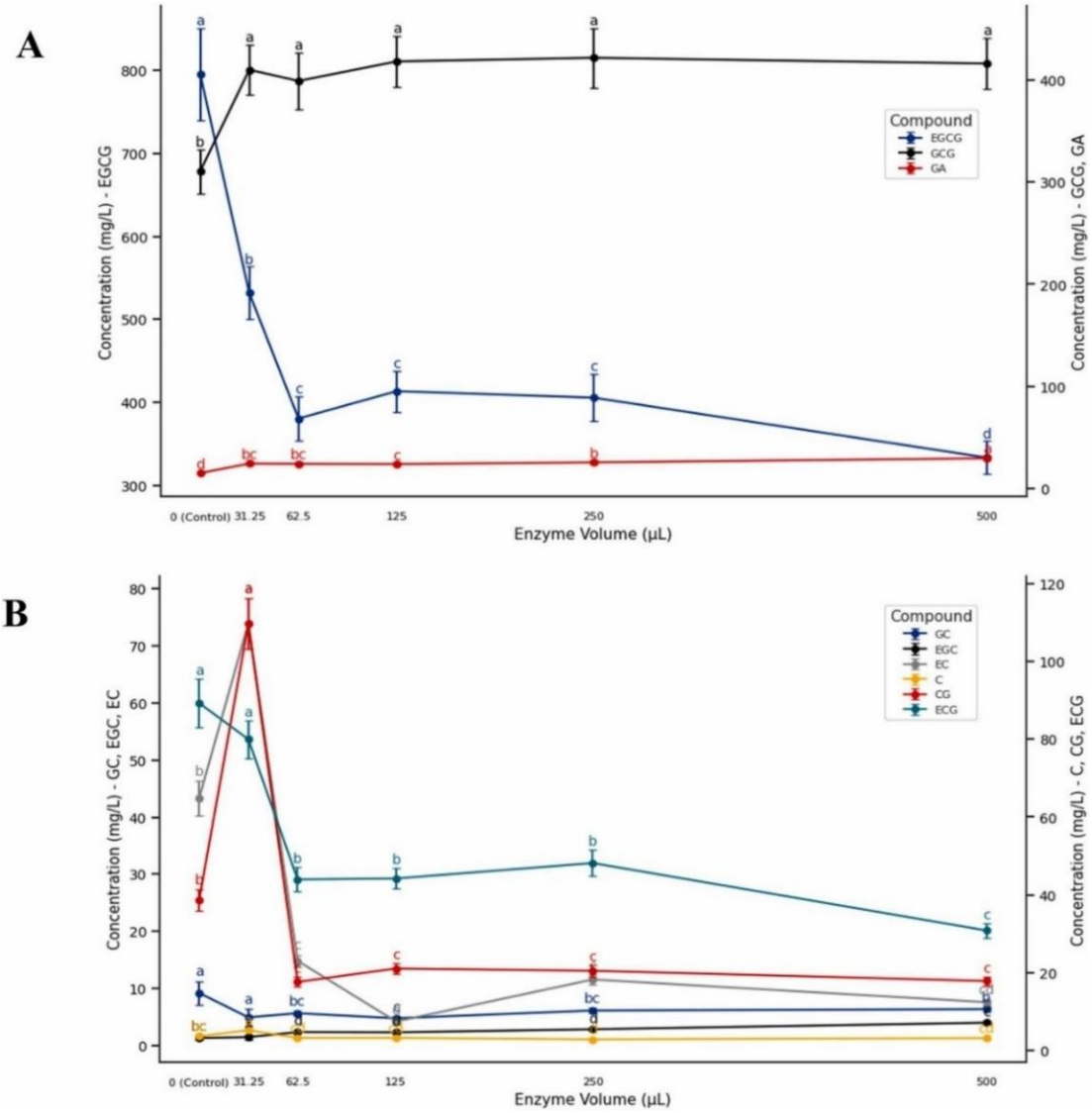

Figure 4.10: EGCG oxidation by *Alcaligenes faecalis* crude enzyme filtrate at 0, 31.25, 62.5, 125, 250, 500 µL, major products GA/GCG (A), and other catechins (GC, EGC, C, EC, ECG, CG) (B), SD error bars and letters denoting Tukey's HSD pairwise comparison results ($p < 0.05$).

The positive correlation between enzyme volume and oxidation-associated metabolites (Pearson's $r = 0.92$ for gallic acid, $p < 0.05$) suggests dose-dependent catalysis. The 60 °C incubation likely enhanced enzyme-substrate interactions, as *A. faecalis* extracellular MPLO preparations exhibited measurable oxidative activity under elevated temperatures in preliminary assays (and further characterized in Chapter 5), unlike typical plant PPOs (Li et al., 2013). The thermostability and pH stability of *A. faecalis* extracellular oxidoreductase systems make them well-suited for tea-processing conditions, which often involve elevated temperatures and varying pH levels. Notably,

the laccase from *A. faecalis* XF1 exhibits optimal activity at 80 °C and remarkable stability in the 70–90 °C range, while the NYSO strain laccase retains full activity up to 70 °C with a 7-h half-life at 60 °C, confirming its suitability for the incubation conditions employed here (Abdelgalil et al., 2020; Mehandia et al., 2020).

Additionally, the 60 °C incubation temperature is unlikely to affect polyphenol profiles significantly, as this temperature is commonly utilized in tea polyphenol extraction procedures without significant degradation of catechins or other phenolic compounds (Perva-Uzunalić et al., 2006; Vuong et al., 2011). However, oxidative agents, such as reactive oxygen species (ROS) or quinones generated during EGCG oxidation, may reduce enzyme activity by oxidizing critical amino acid residues or disrupting structural features like disulfide bridges, necessitating controlled conditions to maximize catalytic efficiency (Veetil et al., 2012). Therefore, controlled reaction conditions, including buffering, oxygen regulation, and temperature control, are important for maintaining catalytic efficiency during catechin oxidation and tea pigment formation.

These observations are consistent with the 60 °C incubation temperature and slightly acidic-to-neutral pH conditions not substantially impairing the extracellular MPLO system's activity or catechin stability under the fixed conditions tested in this chapter, based on the functional outcome observed (58% EGCG reduction) and supporting literature precedent from tea polyphenol extraction studies. This chapter did not include a systematic temperature or pH optimization; 60 °C and near-neutral pH were selected as fixed, literature-informed starting conditions rather than experimentally determined optima. The true temperature and pH optima for this enzyme system (70 °C; pH 3 for ABTS-oxidizing activity, pH 7 for L-DOPA-oxidizing activity) were subsequently established through the dedicated response-surface and stability experiments reported in Chapter 5.

In addition to theaflavins (TFs), other oxidative coupling products, such as thearubigins (TRs) and theabrownins (TBs), were identified, indicating the formation of complex tea pigments. Figure 4.11 demonstrates a significant increase in pigment accumulation, with total TFs rising from 1.11% in control to 4.16% at the highest enzyme concentration. TR and TB levels also exhibited substantial increases. However, controlled micro-scale experiments do not replicate these yields in large-scale production, where lower TF percentages are common (Friedman et al., 2005).To address this, the synergistic action of endogenous plant PPOs and PODs, which drive oxidative

coupling during leaf fermentation, could enhance yields. Recent studies suggest that co-incubating microbial enzymes with partially purified plant-derived oxidases can boost pigment formation and catechin turnover (Wang et al., 2024). Thus, combining *A. faecalis* enzymes could optimize TF production in future large-scale strategies.

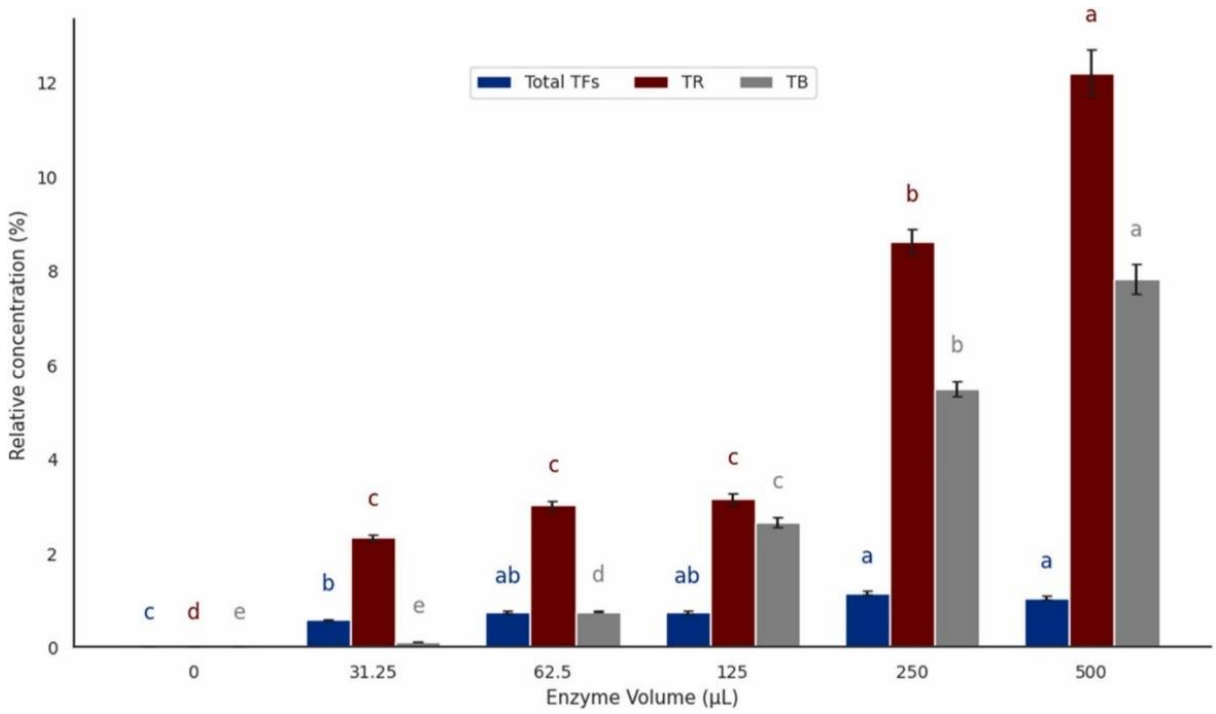

Figure 4.11: Relative concentrations (%) of total theaflavins, thearubigins, and theabrownins formed at different crude extracellular enzyme preparation volumes. Bars represent mean ± standard deviation (n = 3). Different letters above the bars indicate statistically significant differences ($p < 0.05$) according to Tukey's Honestly Significant Difference (HSD) test.

While *A. faecalis* enzymes show promise for microbial-assisted tea oxidation, safety considerations are critical due to the bacterium's classification as an opportunistic pathogen. This Gram-negative, aerobic bacterium, commonly found in soil, water, and the human intestinal tract as a saprophyte, is rarely isolated from healthy individuals (Batt, 2014). However, it has been linked to rare nosocomial infections, particularly in immunocompromised patients or those with indwelling medical devices, with concerns heightened by the emergence of multidrug-resistant strains (Huang, 2020). To mitigate risks, this study used crude enzyme filtrates (acellular extracts) harvested at 36 h, eliminating viable cells and minimizing contamination risks. This approach

aligns with biotechnological practices where *A. faecalis* cell-free extracts are safely used in processes like phenol degradation, biosurfactant production, and mycotoxin detoxification (Ray & Pattnaik, 2024). For large-scale tea flavor enhancement, prioritizing purified or immobilized enzyme preparations will ensure compliance with food safety standards while avoiding the use of live *A. faecalis* cells, thus maintaining consumer safety.

4.3.7.1 Proposed mechanism of EGCG oxidation

EGCG is the major catechin in green tea and contains a polyphenolic structure with multiple hydroxyl groups and a galloyl ester that confer high redox reactivity. These functional groups make EGCG susceptible to ester hydrolysis, C-ring transformations, and oxidative coupling during enzymatic or microbial processing. Crude enzyme filtrates from *A. faecalis* catalyzed EGCG oxidation through multiple concurrent pathways, producing gallic acid, EGC, GCG, and low-level theaflavins. These transformations are consistent with PPO- and POD-like activities reported in microbial polyphenol bioconversions (Teng et al., 2017). Heat-inactivated controls showed negligible EGCG loss, confirming that the reactions were enzyme-dependent.

Mechanistically, the EGCG oxidation likely proceeds through multiple pathways: ester hydrolysis, where the galloyl ester bond is cleaved to release gallic acid and epigallocatechin (EGC) , a reaction directly demonstrated for bacterial tannases acting on EGCG, including a tea-associated *Herbaspirillum camelliae* tannase shown to hydrolyze EGCG's ester bond and release gallic acid (Lei et al., 2021); and oxidative coupling, involving ortho-quinone intermediates that lead to the formation of dimeric compounds such as TFs (Nuraini et al., 2025).

These transformations align with previously described microbial or enzymatic polyphenol bioconversions and support the hypothesis that *A. faecalis*-associated extracellular oxidoreductases may contribute to catechin degradation and tea pigment biosynthesis. These key oxidative pathways, such as ester hydrolysis and dimer formation, are illustrated in Figure 4.12, which highlights the structural modifications resulting in GA, EGC, and TFs. However, crude enzyme extracts inherently contain a mixture of catalytic activities, including non-specific hydrolases and oxidases, which may contribute to EGCG breakdown independently of the intended PPO or laccase pathways. This enzymatic promiscuity complicates mechanistic attribution and underscores the need for purification to isolate specific activities (Westphal & van Berkel, 2021;

Zhuang et al., 2024). Without purification, it remains challenging to distinguish targeted biotransformation from background enzymatic noise, particularly in polyphenol-rich systems where EGCG is highly reactive.

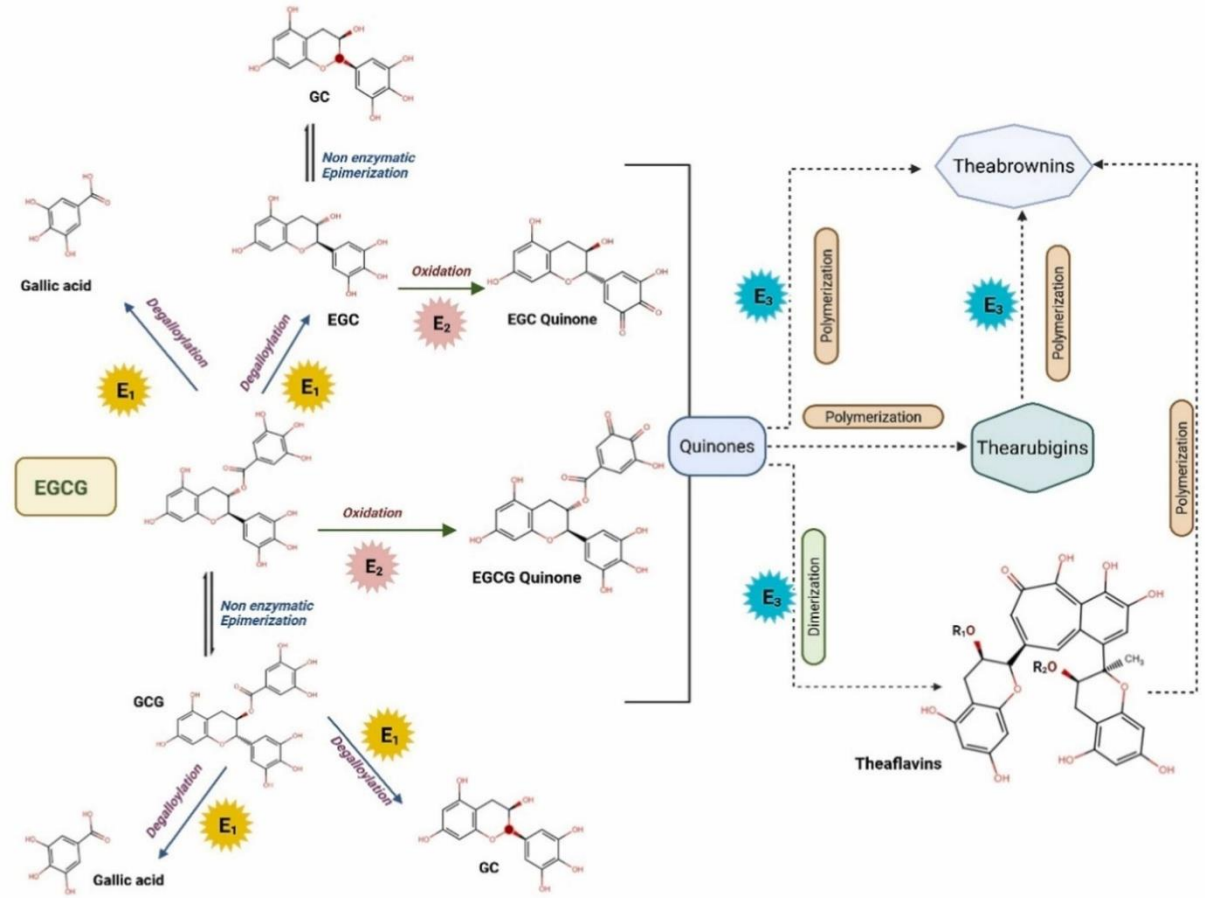

Figure 4.12: Pathway of epigallocatechin gallate biotransformation into oxidation-associated tea polyphenols, proposed by the authors as a modification of existing literature pathways (Lei et al., 2021) to reflect the extracellular oxidoreductase activities characterized in this study. E1 represents esterase-associated activity; E2 represents catechol oxidase-like, peroxidase-like, or laccase-like activity; and E3 represents peroxidase-like or laccase-like activity. Peroxide species generated during oxidation may include hydrogen peroxide.

Overall, the data strongly supports ester hydrolysis (increased GA and EGC formation) and epimerization (increased GCG formation), together with early oxidative coupling (low-level TF formation). However, the precise contribution of individual extracellular oxidoreductases and the identities of higher-order oxidation-associated metabolites remain putative and will require further

confirmation through enzyme-specific characterization and LC-MS/MS structural analysis in Chapters 5 and 6.

4.4 Conclusions

This study shows that culture-based screening can identify functionally active microbial polyphenol-oxidizing-like oxidoreductase (MPLO) systems associated with orthodox black tea, revealing both bacterial and fungal taxa capable of contributing to catechin turnover. Extracellular MPLO activity clustered strongly within specific bacterial (*Alcaligenes faecalis*) and fungal (*Aspergillus* spp.) lineages, suggesting that elevated oxidative capacity is conserved among tea-associated microorganisms adapted to phenolic-rich environments.

Crude extracellular preparations from *A. faecalis* catalyzed substantial EGCG depletion and generated gallic acid, epigallocatechin, gallocatechin gallate, low levels of theaflavin derivatives, and oxidation-associated pigments, supporting the role of microbial extracellular oxidoreductase systems in catechin biotransformation pathways traditionally attributed to endogenous plant PPO/POD systems. These findings establish *A. faecalis* as a promising model organism for controlled microbial catechin oxidation and provide a mechanistic basis for subsequent optimization, biochemical characterization, and metabolomic analyses presented in Chapters 5 and 6.

A major limitation of this study is that the crude extracellular preparations contained multiple overlapping oxidoreductase-associated activities, as directly demonstrated by the simultaneous detection of laccase-like, catechol oxidase-like, and peroxidase-associated activities from the same preparation (Section 4.2.6) and the broad substrate-oxidizing profile observed across six phenolic substrates following partial purification (Table 5.5), making definitive assignment of specific catalytic functions difficult. In addition, biosafety considerations associated with several high-activity fungal isolates limited their suitability for downstream application. Consequently, further purification, molecular characterization, and validation of individual oxidoreductase systems will be required before potential industrial implementation.

Chapter 5

Optimization and characterization of a bacterial polyphenol-oxidizing enzyme preparation for enhanced green tea functionality

Preface

This chapter focuses on the optimization, partial purification, and biochemical characterization of extracellular MPLO preparations from Alcaligenes faecalis NZRM 836. Substrate oxidation behavior, kinetic properties, and genome-informed oxidoreductase analysis were examined to evaluate the system's potential for controlled catechin biotransformation.

Abstract

A multifunctional polyphenol-oxidizing-like oxidoreductase (MPLO) preparation from *Alcaligenes faecalis* NZRM 836 was developed and optimized for the controlled biotransformation of green tea catechins. Media screening identified Tryptic Soy Broth (TSB) supplemented with (+)-catechin and $CuSO_4$ as optimal for biomass production and extracellular enzyme activity. Using a rotatable central composite design combined with Derringer's desirability function, process conditions were optimized to simultaneously maximize ABTS-, pyrogallol-, catechol-, and L-DOPA-oxidizing activities, achieving 79.2, 12.1, 23.8, and 23.5 U/mL, respectively.

Partial purification by ultrafiltration and dialysis yielded a concentrated enzyme preparation with 3.68–3.85-fold increases in specific activity and activity recoveries of 76.5–78.3%. The MPLO system exhibited temperature optima near 70 °C, substrate-dependent pH optima, and retained substantial stability under tea-relevant conditions. Apparent kinetic analysis with ABTS and L-DOPA demonstrated efficient substrate oxidation activity consistent with the multi-functional nature of the partially purified extracellular oxidoreductase system.

In a model EGCG system, the MPLO preparation depleted approximately 50% EGCG within 10 min and generated products consistent with degallation, epimerization, and oxidation reactions. In a green tea matrix, EGCG was reduced by 43.6% within 5 h, consistent with a deliberately controlled, intermediate degree of oxidation, accompanied by transient theaflavin accumulation and progressive color development. Genome mining of reference *A. faecalis* genomes identified multiple putative blue copper-containing laccase-like multicopper oxidase genes associated with the observed MPLO activities, suggesting the presence of functionally distinct oxidoreductase variants, whereas canonical tyrosinase homologs were not detected.

This study demonstrates a laboratory-scale proof of concept for a bacterial extracellular MPLO platform capable of facilitating controlled catechin biotransformation, with the potential to inform future enzyme-mediated tea processing applications, pending safety, regulatory, and pilot-scale validation.

Keywords: *Alcaligenes faecalis*; polyphenol-oxidizing-like oxidoreductases; response surface methodology; catechin biotransformation; enzymatic oxidation; green tea; theaflavins.

5.1 Introduction

Green tea, produced from the fresh, tender leaves of *Camellia sinensis*, is valued for its high content of bioactive catechins, particularly (−)-epigallocatechin gallate (EGCG), (−)-epigallocatechin (EGC), (−)-epicatechin gallate (ECG), and (−)-epicatechin (EC). These polyphenols substantially contribute to the characteristic astringency, bitterness, and fresh flavor of green tea while also underpinning many of its reported functional properties. However, these compounds also render green tea susceptible to enzymatic browning and quality deterioration during processing and storage (Cai et al., 2018; Yang, 1999). The high molecular weight and extensive galloylation of major catechins, especially EGCG, result in excessive astringency and limited solubility. These structural features also make EGCG prone to spontaneous auto-oxidation during storage, distinct from the deliberate, rate-controlled oxidation of black tea manufacture, leading to browning and off-flavors over shelf life. Partial transformation of EGCG into smaller, less-galloylated derivatives such as EGC would improve solubility and reduce astringency, since EGCG is the primary driver of green tea's sharp bitterness. This is a green-tea-specific concern, since black tea's catechins are already oxidized and no longer susceptible to this pathway (Abudureheman et al., 2022; Schantz et al., 2010).

Controlled enzymatic biotransformation offers a sustainable, enzyme-based approach to modulate the sensory and technological quality of green tea by generating smaller, more soluble phenolic metabolites through targeted degalloylation, epimerization, or mild oxidation (Gupta et al., 2013; Takemoto & Takemoto, 2018). Unlike traditional black tea fermentation, which involves extensive oxidation leading to polymeric pigments such as thearubigins, the objective of green tea modification is to selectively alter catechin structure while retaining desirable functional properties, specifically antioxidant capacity and enzyme-inhibitory bioactivity, rather than fully sacrificing these properties as occurs with extensive polymerization into thearubigins (Abudureheman et al., 2022; Verloop et al., 2016). Previous studies using fungal laccases, tyrosinases, and tannases demonstrated the feasibility of enzymatic catechin transformation and theaflavin production; however, single-enzyme systems often exhibit limited substrate range, incomplete conversion, or excessive formation of insoluble oxidation-associated metabolites (Subramanian et al., 1999; Zhang & Du, 2015).

Microbial systems capable of co-producing complementary oxidoreductase activities provide a potentially more versatile platform for controlled catechin transformations. In this study, the term microbial polyphenol-oxidizing-like oxidoreductases (MPLOs) is used operationally to describe the combined extracellular ABTS-, L-DOPA-, catechol-, and pyrogallol-oxidizing activities detected in *Alcaligenes faecalis* NZRM 836. This terminology is activity-based and reflects the collective substrate oxidation behavior of a heterogeneous extracellular oxidoreductase system rather than the presence of individually purified or genomically confirmed classical laccases, tyrosinases, catechol oxidases, or peroxidases. Such multifunctional behavior is consistent with the cooperative and overlapping substrate specificities commonly reported for bacterial multicopper oxidases and related oxidoreductase systems (Baldrian, 2006; Mayer, 2006).

Accordingly, this study aims to develop and evaluate a bacterial extracellular MPLO preparation for controlled oxidative modification of green tea catechins under conditions relevant to tea processing. Specifically, the objectives were: (1) to optimize cultivation conditions for simultaneous production of extracellular ABTS-, L-DOPA-, catechol-, and pyrogallol-oxidizing activities using response surface methodology; (2) to partially purify and characterize the resulting extracellular MPLO preparation with respect to pH and temperature optima, stability, substrate oxidation profiles, and apparent kinetic behavior; and (3) to evaluate its performance in model EGCG and green tea systems by monitoring catechin transformation, theaflavin formation, color development, pH changes, and residual oxidoreductase activities over time.

5.2 Materials and methods

5.2.1 Chemicals and reagents

All chemicals and reagents were of analytical or high-performance liquid chromatography (HPLC) grade. The HPLC standards (−)-epigallocatechin gallate (EGCG), (−)-epigallocatechin (EGC), (−)-epicatechin gallate (ECG), (−)-epicatechin (EC), (−)-gallocatechin gallate (GCG), (+)-catechin hydrate, gallic acid, caffeine, 2,2′-azinobis-(3-ethylbenzothiazoline-6-sulfonic acid) (ABTS), guaiacol, catechol, L-3,4-dihydroxyphenylalanine (L-DOPA), hydrogen peroxide (30% w/v), 2,2-diphenyl-1-picrylhydrazyl (DPPH), Trolox, β-mercaptoethanol, and Coomassie Brilliant Blue R-250 were purchased from Sigma-Aldrich (St. Louis, MO, USA).

$CuSO_4 \cdot 5H_2O$, $(NH_4)_2SO_4$, KH_2PO_4, Na_2HPO_4, $MgSO_4 \cdot 7H_2O$, $CaCl_2$, dextrose, tryptone, soytone, yeast extract, NaCl, K_2HPO_4, Tris base, citric acid, orthophosphoric acid, formic acid (HPLC grade), acetic acid, methanol, and HPLC-grade acetonitrile were obtained from Merck (Darmstadt, Germany) or local reputable suppliers. Pre-stained protein ladder (10–250 kDa) was purchased from Thermo Fisher Scientific (Waltham, MA, USA). Deionized water was prepared using a Milli-Q water purification system (Millipore, Billerica, MA, USA). Commercial green tea leaves (*C. sinensis*) were sourced locally. The commercial reference oxidoreductases, mushroom tyrosinase (≥1000 U/mg), *Aspergillus* laccase (≥0.5 U/mg), and horseradish peroxidase (≥250 U/mg), were obtained from Sigma-Aldrich (St. Louis, MO, USA) and used for comparative assays.

5.2.2 Culture media

Three culture media were evaluated for the production of polyphenol-oxidizing enzymes: Lysogeny broth (LB) (Difco™, BD) containing 10 g/L tryptone, 5 g/L yeast extract and 10 g/L NaCl (pH 7.0); tryptic soy broth (TSB) (Difco™, BD) containing 17 g/L tryptone, 3 g/L soytone, 2.5 g/L dextrose, 5 g/L NaCl and 2.5 g/L K_2HPO_4 (pH 7.0 ± 0.1); and a minimal broth containing 0.5 g/L $(NH_4)_2SO_4$, 0.5 g/L KH_2PO_4, 0.1 g/L $MgSO_4 \cdot 7H_2O$ and 0.01 g/L $CaCl_2$ (pH 7.0). Nutrient agar plates and nutrient broth (Difco™, BD) were used for routine culture maintenance. All media were prepared in Milli-Q water and autoclaved at 121 °C for 15 min. Because (+)-catechin and $CuSO_4 \cdot 5H_2O$ are heat-sensitive, these were not autoclaved; instead, 12.5 mM (+)-catechin and/or 25 mM $CuSO_4 \cdot 5H_2O$ were prepared separately, filter-sterilized through 0.22 μm membranes, and added aseptically to the cooled, autoclaved base media.

5.2.3 Instruments and analytical equipment

All analytical measurements were performed using calibrated laboratory instruments. UV–Vis absorbance measurements were conducted using a UV-3600 spectrophotometer (Shimadzu, Tokyo, Japan). Microplate-based assays were performed using a Varioskan™ LUX multimode microplate reader equipped with SkanIt™ PC software (Research Edition) (Thermo Scientific, Waltham, MA, USA). Protein quantification was conducted using a Qubit 4 Fluorometer with the Qubit Protein Assay Kit (Invitrogen, Thermo Fisher Scientific, Waltham, MA, USA).

Chromatographic analysis of non-volatile compounds was performed using a Vanquish HPLC system equipped with a binary solvent pump, autosampler, column oven, and diode array detector (DAD) (Thermo Fisher Scientific, Waltham, MA, USA). High-resolution metabolite profiling was conducted using an Accela 1250 UHPLC system coupled to a Q Exactive Orbitrap mass spectrometer equipped with a heated electrospray ionization (HESI) source (Thermo Scientific, Waltham, MA, USA).

Centrifugation procedures were performed using an X1 Pro benchtop refrigerated centrifuge (Thermo Scientific, Waltham, MA, USA). Controlled incubation experiments were conducted using a MaxQ 6000 shaking incubator (Thermo Scientific, Waltham, MA, USA), while additional temperature-controlled procedures were performed in standard laboratory water baths. SDS-PAGE analysis was performed using a Mini-PROTEAN® Tetra Vertical Electrophoresis System (Bio-Rad Laboratories, Hercules, CA, USA).

Chromatographic instrument control, data acquisition, and calibration were performed using Chromeleon™ software (Thermo Fisher Scientific, Waltham, MA, USA).

5.2.4 Microorganism and inoculum preparation

The strain *A.faecalis* NZRM 836 was obtained from the New Zealand Reference Culture Collection (NZRM), PHF Science, New Zealand. Stock cultures were maintained on agar plates at 4 °C and sub-cultured monthly. Inocula were prepared by transferring a single colony into 50 mL nutrient broth and incubating at 30 °C with orbital shaking (180 rpm) until OD_{600} reached 0.80 ± 0.02 (late exponential phase). This standardized inoculum preparation was used to minimize variability in biomass input among experiments.

5.2.5 Preliminary media screening and inoculum size optimization

Media screening for extracellular MPLO-associated substrate oxidation activities was performed in 500 mL Erlenmeyer flasks containing 100 mL of LB, TSB, or minimal broth, supplemented with 4% (v/v) 12.5 mM (+)-catechin and/or 2% (v/v) 25 mM $CuSO_4 \cdot 5H_2O$ (filter-sterilized). Flasks were inoculated at 5% (v/v) and incubated at 37 °C with shaking (180 rpm) for 72 h. Growth was monitored by OD_{600}. The medium and supplement combination yielding the highest biomass

was selected for further evaluation, and ABTS-, L-DOPA-, catechol-, and pyrogallol-oxidizing activities were subsequently quantified. Inoculum size optimization (0.5–20% v/v) was conducted in the selected supplemented TSB medium. ABTS-oxidizing activity was used as the primary response variable during inoculum optimization following 72 h incubation.

5.2.6 Culture conditions and addition of inducer/cofactor for response surface methodology (RSM) optimization

Aliquots of TSB (50 mL in 250 mL Erlenmeyer flasks) were autoclaved at 121 °C for 15 min. After cooling, filter-sterilized (+)-catechin (12.5 mM in 50% v/v aqueous ethanol) and $CuSO_4$ (25 mM in Milli-Q water) stock solutions were added aseptically according to the central composite design (Section 5.2.7). Flasks were inoculated with 5 mL of standardized inoculum (OD_{600} = 0.80, 5% v/v) and incubated at 30 °C with orbital shaking (180 rpm) for 12–96 h. All experiments were performed in triplicate. Cultures were centrifuged (12,000 × g, 10 min, 4 °C), and the cell-free supernatant was used directly as the crude enzyme extract.

5.2.7 Enzyme activity assays

Enzyme activity was determined based on the rate of substrate conversion under defined assay conditions. The activity labels ABTS-, L-DOPA-, catechol-, and pyrogallol-oxidizing activities are used operationally to describe substrate-dependent oxidation profiles measured using the respective assay systems and do not imply definitive assignment of individual enzyme identities.

One unit (U) of enzyme activity was defined as the amount of enzyme required to catalyze the formation of 1 µmol of product per minute. For spectrophotometric assays, the change in absorbance was monitored over time. Enzyme activity (U/mL) was calculated using the Beer–Lambert relationship (Equation 5.1):

$$\text{Activity (U/mL)} = \frac{\Delta A/\text{min} \times V_{total}}{\varepsilon \times l \times V_{enzyme}} \qquad \textbf{(5.1)}$$

where, ΔA/min is the change in absorbance per minute, V_{total} is the total reaction volume (mL), V_{enzyme} is the enzyme volume (mL), ε is the molar extinction coefficient (M^{-1} cm^{-1}), and l is the optical path length (cm). This calculation allowed the quantification of enzymatic activity in the

crude enzyme preparation, enabling comparisons across different temperatures, substrates, or reaction conditions. Specific activity was determined using Equation 5.2:

$$\text{Specific activity (U/mg)} = \frac{\text{Enzyme activity (U)}}{\text{Protein concentration (mg/mL)}} \quad \textit{(5.2)}$$

Table 5.1 summarizes the substrates, target activities, assay conditions, wavelengths, and molar extinction coefficients. All assays were performed in 24-well microplates (total volume 1 mL) at room temperature using a Thermo Scientific Varioskan LUX Multimode microplate reader. Boiled enzyme and substrate-only blanks served as controls.

5.2.8 Experimental design and statistical analysis

5.2.8.1 Central composite design

A three-factor central composite response surface design comprising 20 experimental runs was used to evaluate the effects of catechin stock addition, $CuSO_4$ stock addition, and cultivation time on extracellular ABTS-, pyrogallol-, catechol-, and L-DOPA-oxidizing activities. The design comprised eight factorial runs, six axial runs, and six replicated center-point runs. The center condition was 333 μL catechin stock, 333 μL $CuSO_4$ stock, and 54 h cultivation. The complete experimental design and observed responses are provided in Table S5.1(Appendix D).

Table 5.1: Assay conditions, wavelengths, and molar extinction coefficients used for the determination of substrate oxidation activities associated with the extracellular MPLO system.

Target activity	Assay Wavelength (nm)	Molar Extinction Coefficient (ε, $M^{-1}\cdot cm^{-1}$)	Substrate stock (mM) volume	Substrate volume (μL)	Buffer used	Buffer volume (μL)	Sample volume (μL)	Other additions
ABTS-oxidizing activity	420	36,000	20	100	100 mM Citrate-phosphate buffer, pH 3.4	850	50	-
L-DOPA-oxidizing activity	475	3,600	10	100	100 mM Phosphate buffer, pH 6.5	850	50	-
Catechol-oxidizing activity	410	1,470	10	100	50 mM Phosphate buffer, pH 6.5	800	50	0.065 mM EDTA (50 μL)
Pyrogallol-oxidizing activity	420	2,470	40	100	100 mM Phosphate buffer, pH 6.0	800	50	0.027% (v/v) H_2O_2 (50 μL)

(8 factorial, 6 axial, and 6 center points) was generated using Python 3.14. The independent variables were catechin stock addition (X_1: 20–646 μL), $CuSO_4$ stock addition (X_2: 20–646 μL), and culture duration (X_3: 12–96 h). The full design matrix and mean responses (n = 3) are provided in Table S5.1 (Appendix D).

5.2.8.2 Response surface modeling

Second-order polynomial models were fitted to each response (Y) as shown in Equation 5.3.

$$Y = \beta_0 + \Sigma \beta_i X_i + \Sigma \beta_{ii} X_i^2 + \Sigma \beta_{ij} X_i X_j \quad \textbf{(5.3)}$$

where:

Y = predicted response (e.g., enzyme activity)

$\boldsymbol{\beta_0}$ = intercept (constant term)

$\boldsymbol{\beta_i}$ = linear coefficient for the ith independent variable

$\mathbf{X_i}$ = coded value of the ith independent variable (e.g., pH, temperature, $CuSO_4$ concentration)

$\boldsymbol{\beta_{ii}}$ = quadratic coefficient for the ith variable (captures curvature)

$\boldsymbol{\beta_{ij}}$ = interaction coefficient between the ith and j^{th} variables (captures synergistic or antagonistic effects)

Model adequacy was evaluated by analysis of variance (ANOVA), coefficient of determination (R^2), adjusted R^2, predicted R^2, adequate precision and lack-of-fit testing. The ANOVA table of each substrate-based MPLO activity and the RSM model equations are given in Tables S5.3-S5.6 (Appendix D)

5.2.8.3 Multi-objective optimization by desirability function application

Simultaneous optimization of the four enzyme activities was performed using Derringer's desirability function (Derringer & Suich, 1980), with all responses set to maximization for each response. The condition yielding the highest overall desirability (D) was selected as the global optimum. Weights were assigned as follows: L-DOPA-oxidizing activity (0.30), ABTS-oxidizing activity (0.25), pyrogallol-oxidizing activity (0.25), and catechol-oxidizing activity (0.20) to

prioritize balanced extracellular polyphenol oxidation behavior during optimization (Table S5.7 of Appendix D).

5.2.8.4 Verification of the predicted optimum

The predicted optimum was validated experimentally in triplicate. Cell-free supernatants produced under the optimized cultivation conditions were prepared as described in Section 5.2.5, and MPLO-associated substrate oxidation activities were quantified according to Section 5.2.6. Observed values were compared with model predictions to confirm accuracy.

5.2.9 Production and partial purification of the MPLO enzyme preparation

Submerged fermentation was performed in a 5 L bench-scale fermentation vessel (2 L working volume) under continuous aeration and agitation at 150 rpm. Cultures were grown in TSB under the optimized conditions using a 10% (v/v) inoculum prepared from mid-exponential-phase *A. faecalis* NZRM 836 (OD_{600} = 0.80 ± 0.02). At the end of cultivation, cells were removed by centrifugation at 10,000 × g for 20 min at 4 °C, and the clarified supernatant was collected as the crude enzyme extract.

The crude supernatant was subjected to sequential ultrafiltration to fractionate and enrich the extracellular oxidoreductases. Initially, a 100 kDa molecular weight cut-off (MWCO) centrifugal ultrafiltration device (Cytiva Jumbosep, Merck Millipore, Darmstadt, Germany) was used to remove high-molecular-weight proteins and aggregates. Samples were centrifuged at 3,000 × g at 4 °C until the filtrate volume reached 80–90% of the original volume. The filtrate was then concentrated using 10 kDa MWCO centrifugal filter units (Amicon Ultra-15, Merck Millipore, Darmstadt, Germany) at 8,000 × g and 4 °C, thereby retaining enzymes in the 10–100 kDa range while removing low-molecular-weight components.

The resulting retentate was subjected to buffer exchange by dialysis (Slide-A-Lyzer, Thermo Scientific, Waltham, MA, USA) against 50 mM sodium phosphate buffer (pH 6.0) to remove residual catechin, $CuSO_4$, salts, and other small molecules. A final concentration step using the same 10 kDa device yielded the partially purified (PP) enzyme preparation. Purification fold and activity recovery were calculated relative to the crude supernatant.

5.2.10 Sodium dodecyl sulfate–polyacrylamide gel electrophoresis (SDS-PAGE)

SDS-PAGE was performed according to Laemmli (1970) using a 12% resolving gel and 5% stacking gel. Samples (20–30 µg protein) were mixed with 4× Laemmli buffer containing β-mercaptoethanol, heated at 95 °C for 5 min, and electrophoresed at 120 V. Gels were stained with Coomassie Brilliant Blue R-250 and destained overnight. Molecular weights were estimated using a pre-stained protein ladder (10–250 kDa).

5.2.11 *In silico* genome mining of reference *Alcaligenes faecalis* genomes associated with extracellular MPLO-associated activities

In silico genome mining was performed using a high-quality reference and draft genomes of reference *A. faecalis* strains and closely related *Alcaligenes* species, retrieved from the NCBI Genome database. In total, 40 reference genomes, including those from strains TD-94, Mc250 (GCA_001641975.2), DSM 30030 (type strain; ATCC 8750), and JQ135, were selected.

Genome annotations and predicted protein sequences were screened using keyword-based searches including “multicopper oxidase,” “laccase,” “polyphenol oxidase,” “tyrosinase,” “catechol oxidase,” “catecholase,” “bilirubin oxidase,” and “blue copper oxidase.” Searches were supported by Pfam domain analysis targeting the conserved Cu-oxidase domain PF00394 and by BLASTp searches for similarity against characterized bacterial multicopper oxidases. Additional sequence validation and annotation comparisons were performed using UniProtKB (https://www.uniprot.org/).

5.2.12 Characterization of the partially purified MPLO enzyme preparation

Total protein concentration was determined using the Qubit Protein Assay Kit (Invitrogen, Thermo Fisher Scientific, Waltham, MA, USA) on a Qubit 4 Fluorometer, with bovine serum albumin as the standard. Enzyme activities were expressed as U/mL, and specific activity (µmol·min^{-1}·mg^{-1} protein) was calculated when required. Characterization focused primarily on ABTS- and L-DOPA-oxidizing activities as representative indicators of extracellular MPLO-associated polyphenol oxidation capacity.

5.2.12.1 Optimum temperature and pH

Temperature optima were determined by pre-equilibrating reaction mixtures (without enzyme) at 20–90 °C for 5 min, followed by immediate activity measurement. pH optima were assessed across pH 2.5–10.0 using acetate (pH 2.5–5.0), phosphate (pH 6.0–7.0), and Tris-HCl (pH 8.0–10.0) buffers. Relative activity was expressed as a percentage of the maximum.

5.2.12.2 Thermal stability

Thermal stability was evaluated by pre-incubating the enzyme extract at 40, 50, 60, 70, and 80 °C for 0, 2, 4, 8, 12, and 24 h. After each interval, samples were cooled on ice for 5 min, and residual activity was measured under standard assay conditions using both ABTS and L-DOPA at their respective optimum pH and temperature. Relative residual activity was expressed as a percentage of the initial activity (0 h = 100%).

5.2.12.3 pH stability

pH stability was assessed by incubating the enzyme extract in 50 mM buffers at pH 3.0, 5.0, and 7.0 at 4 °C for 0, 2, 4, 8, 12, and 24 h. These pH values represent the acidic optimum, the natural pH range of green tea (5.0–7.5), and the neutral optimum. Residual activity was measured at the optimum temperature using ABTS and L-DOPA and expressed as a percentage of the untreated control (0 h = 100%).

5.2.12.4 Substrate specificity

Substrate specificity was evaluated using 1, 10, and 20 mM solutions of catechol, pyrogallol, L-DOPA, syringaldazine, ABTS, and guaiacol. Activity measurements were performed under standard assay conditions for each substrate as given in Table S5.12. Relative activity was calculated by assigning catechol oxidation activity as 100% and expressing all other substrate oxidation activities relative to this value. This analysis was used to evaluate the substrate oxidation behavior of the extracellular MPLO system toward structurally diverse phenolic compounds relevant to tea biotransformation.

5.2.12.5 Effect of inhibitors and metal ions

The effects of Cu^{2+}, Fe^{2+}, EDTA, ascorbic acid (0.5 mM), and caffeine (1–10 mM) were determined using ABTS and L-DOPA as substrates. The enzyme extract was pre-incubated with each additive for 10 min at room temperature before residual activity was measured under optimum conditions. All assays were performed in triplicate.

5.2.12.6 Enzyme kinetics

Kinetic parameters were determined using ABTS and L-DOPA as substrates at concentrations ranging from 0.1 to 10 mM under their respective optimum temperature and pH. All assays were performed in triplicate. The experimental data were fitted to the Michaelis-Menten equation 5.4

$$v = \frac{V_{\max} \cdot [S]}{K_m + [S]} \qquad \textbf{(5.4)}$$

where, v is the reaction velocity, $V_{\max}$is the maximum velocity, $K_m$is the Michaelis constant, and [S] is the substrate concentration.

Because the partially purified MPLO preparation represents a heterogeneous extracellular oxidoreductase mixture, the reported kinetic parameters (apparent $K_m$and $V_{\max}$) reflect collective substrate oxidation behavior under the assay conditions rather than intrinsic constants of individual purified enzymes. Non-linear regression analysis was performed using Python to estimate apparent $K_m$and $V_{\max}$values. A Lineweaver–Burk double-reciprocal plot was additionally generated for comparative visualization of substrate-dependent oxidation behavior.

Kinetic analyses for ABTS and L-DOPA were conducted independently as representative indicators of distinct MPLO-associated substrate oxidation profiles and were not interpreted as direct measurements of individual enzyme-specific activities.

5.2.13 *In-vitro* oxidation of EGCG (model system) using MPLO preparation

The oxidative biotransformation potential of the extracellular MPLO preparation was initially evaluated using a model catechin system. A 1 mM solution of epigallocatechin gallate (EGCG) was prepared in 50 mM sodium phosphate buffer (pH 6.5) containing 0.1% (v/v) orthophosphoric acid. Biotransformation reactions were carried out in a final volume of 500 µL and initiated by

adding 0.5% (v/v) partially purified MPLO preparation standardized to 250 U/mL based on ABTS-oxidizing activity, corresponding to 0.625 U per reaction.

Reaction mixtures were incubated at 50 °C, and aliquots were collected at 0, 10, 30, and 60 min. Reactions were immediately quenched with three volumes of ice-cold ethanol and stored at −20 °C until HPLC analysis.

5.2.14 Application of the MPLO preparation on green tea matrix

5.2.14.1 Preparation of green tea extract

Green tea infusion was prepared from fresh leaves of *C. sinensis* harvested at the two-leaves-and-a-bud stage from Somerset Estate, Nuwara Eliya, Sri Lanka (6.9497° N, 80.7891° E). The leaves were washed with distilled water, steamed for 15 min to inactivate endogenous enzymes (Maliepaard, 2009), freeze-dried, and finely ground using a coffee grinder (Breville, New Zealand). Ten grams of powdered material were extracted with 1 L of hot deionized water at 90 °C for 5 min and filtered through Whatman No. 1 filter paper.

5.2.14.2 Time–dose optimization of MPLO-mediated oxidation

A preliminary time-dose optimization experiment was conducted to identify conditions that supported theaflavin formation while maintaining controlled catechin oxidation. The partially purified MPLO preparation was standardized to 250 U/mL based on ABTS-oxidizing activity, consistent with the activity basis used for the EGCG model system. Aliquots of the standardized MPLO preparation (50, 100, 200, and 500 µL) were added separately to 100 mL portions of green tea extract, corresponding to 0.05, 0.10, 0.20, and 0.50% (v/v), respectively. Based on an activity concentration of 250 U/mL, these additions corresponded to 12.5, 25, 50, and 125 U of ABTS-oxidizing activity, respectively. Reaction mixtures were incubated at 50 °C with agitation at 150 rpm for 6 h.

Samples were collected at 1 h intervals (1, 2, 3, 4, 5, and 6 h), heat-inactivated, and analyzed for catechins and theaflavins using HPLC-DAD (Section 5.2.14). The complete dataset is provided in Supplementary Table S5.8 (Appendix D). Based on this preliminary evaluation, 100 µL of MPLO

preparation, corresponding to 0.10% (v/v) and 25 U of ABTS-oxidizing activity, was selected for subsequent kinetic evaluation.

5.2.14.3 Kinetic evaluation under optimized conditions

Following optimization, the reaction was monitored to evaluate the kinetics of biotransformation. Aliquots were collected at 0, 1, 2, 3, 5, and 10 h. The pH of the reaction mixture was measured immediately using a calibrated pH meter. Residual enzyme activity was determined using ABTS and L-DOPA assays under standard conditions and expressed relative to the initial activity (0 h). Changes in color were monitored by measuring absorbance at 420 nm.

For polyphenol profiling, aliquots were quenched with an equal volume of ice-cold methanol containing 0.1% (v/v) formic acid, vortexed, and centrifuged at 12,000 × g for 10 min at 4 °C. The supernatants were filtered and analyzed using reversed-phase HPLC as described in Section 5.2.14.

A heat-inactivated enzyme control (100 °C for 10 min) was included and processed under identical conditions. All experiments were performed in triplicate.

The Briskness index, defined as the percentage ratio of total theaflavins to the sum of total theaflavins and caffeine, and is used as an indicator of tea briskness index, was calculated according to the equation 5.5 given by UPASI TRI TRF (2026) as:

$$\text{Briskness Index (\%)} = \left(\frac{\text{Total Theaflavins}}{\text{Total Theaflavins+Caffeine}}\right) \times 100 \qquad \textbf{(5.5)}$$

The color Index was expressed as the percentage increase in absorbance at 420 nm relative to the initial value (0 h).

5.2.15 HPLC analysis of key polyphenols and spectrophotometric quantification of tea pigments.

Samples were analyzed using a Thermo Scientific Hypersil GOLD C18 column (150 × 4.6 mm, 5 µm) and UV detection at 280 nm, with a gradient of 0.1% formic acid (solvent A) and acetonitrile containing 0.1% formic acid (solvent B). The gradient elution was performed at a flow rate of 0.3 mL/min as follows: 8% B (0–5 min), increased to 11% B (5–8 min), 20% B (10 min), 28% B (16 min), 30% B (25 min), and 35% B (30–35 min), followed by a ramp to 90% B (36–38 min), then

returned to 8% B (39 min) and re-equilibrated until 45 min. Injection volume was 5 µL. The column temperature was 25 °C.

The tea pigments thearubigins and theabrownins were quantified spectrophotometrically using the method described by Wang et al. (2011). The percentages of TF, TRs, and TBs are calculated according to Equations 5.6, 5.7, and 5.8.

$$TFs(\%) = \frac{E_C \times 2.25}{\text{Dry weiight of Green tea}(\%)} \times 100 \quad \textbf{(5.6)}$$

$$TRs(\%) -= \frac{7.06 \times (2E_A + 2E_D - E_C - 2\,E_B)}{\text{Dry weiight of Green tea}(\%)} \times 100 \quad \textbf{(5.7)}$$

$$TBs(\%) = \frac{2E_B \times 7.06}{\text{Dry weiight of Green tea}(\%)} \times 100 \quad \textbf{(5.8)}$$

where:

$\boldsymbol{E_A}$= absorbance of solution A at 380 nm; $\boldsymbol{E_B}$= absorbance of solution B at 380 nm ;$\boldsymbol{E_C}$= absorbance of solution C at 380 nm; $\boldsymbol{E_D}$= absorbance of solution D at 380 nm; TFs (%) = percentage of total theaflavins; TRs (%) = percentage of total thearubigins; TBs (%) = percentage of total theabrownins; Weight of green tea (%) = dry weight equivalent concentration of green tea extract used as the reference basis for normalization; 2.25 and 7.06 = empirical conversion factors derived from the spectrophotometric method described by Wang et al. (2011).

5.2.16 Statistical data analysis

All experiments were performed in triplicate, and results are presented as mean ± standard deviation (SD). Statistical analysis was conducted using Python (version 3.12). For response surface methodology (RSM), second-order polynomial models were fitted to the experimental data using the statsmodels library. Analysis of variance (ANOVA), regression coefficients, lack-of-fit tests, and model diagnostics (R^2, adjusted R^2, predicted R^2, and adequate precision) were performed in Python. Model adequacy was evaluated based on the coefficient of determination (R^2), adjusted R^2, predicted R^2, adequate precision (> 4), and a non-significant lack-of-fit test ($p > 0.05$). Multi-objective optimization was carried out using Derringer's desirability function, implemented in Python with the scipy.optimize and pandas libraries. Pearson correlation

coefficients and associated p-values between polyphenol concentrations, enzyme activities, and pH in the green tea matrix were calculated using SciPy-Stats module. Data visualization (RSM contour plots, actual-versus-predicted plots, time-course profiles, and correlation heatmaps) was generated using the matplotlib and seaborn libraries.

5.3 Results and discussion

In this study, microbial polyphenol-oxidizing-like oxidoreductase (MPLO) activity refers operationally to the collective extracellular substrate-oxidizing activities detected using ABTS, L-DOPA, catechol, and pyrogallol assay systems. These correspond functionally to ABTS-oxidizing (laccase-like), L-DOPA-oxidizing (diphenolase/tyrosinase-like), catechol-oxidizing (catecholase-like), and pyrogallol-oxidizing (peroxidase-like) activities, respectively. Because the extracellular preparation was only partially purified, these activities are interpreted as functional oxidation profiles of a heterogeneous oxidoreductase system rather than evidence for individually purified or genomically confirmed classical laccase, tyrosinase, catechol oxidase, or peroxidase enzymes.

5.3.1 Preliminary media screening: Growth kinetics and MPLO activity profiling

Screening of lysogeny broth (LB), tryptic soy broth (TSB), and minimal broth (MB) demonstrated clear differences in the influence of nutrient composition and buffering capacity on the growth of *A. faecalis* NZRM 836 and extracellular MPLO-associated substrate oxidation activities. TSB supported the highest bacterial biomass (final OD600 ≈ 2.37), followed by LB (≈ 2.18) and MB (< 0.5) (Figure 5.1). The stronger performance of TSB was likely associated with its richer nutrient composition and phosphate buffering capacity, which stabilized culture pH and supported sustained bacterial metabolism.

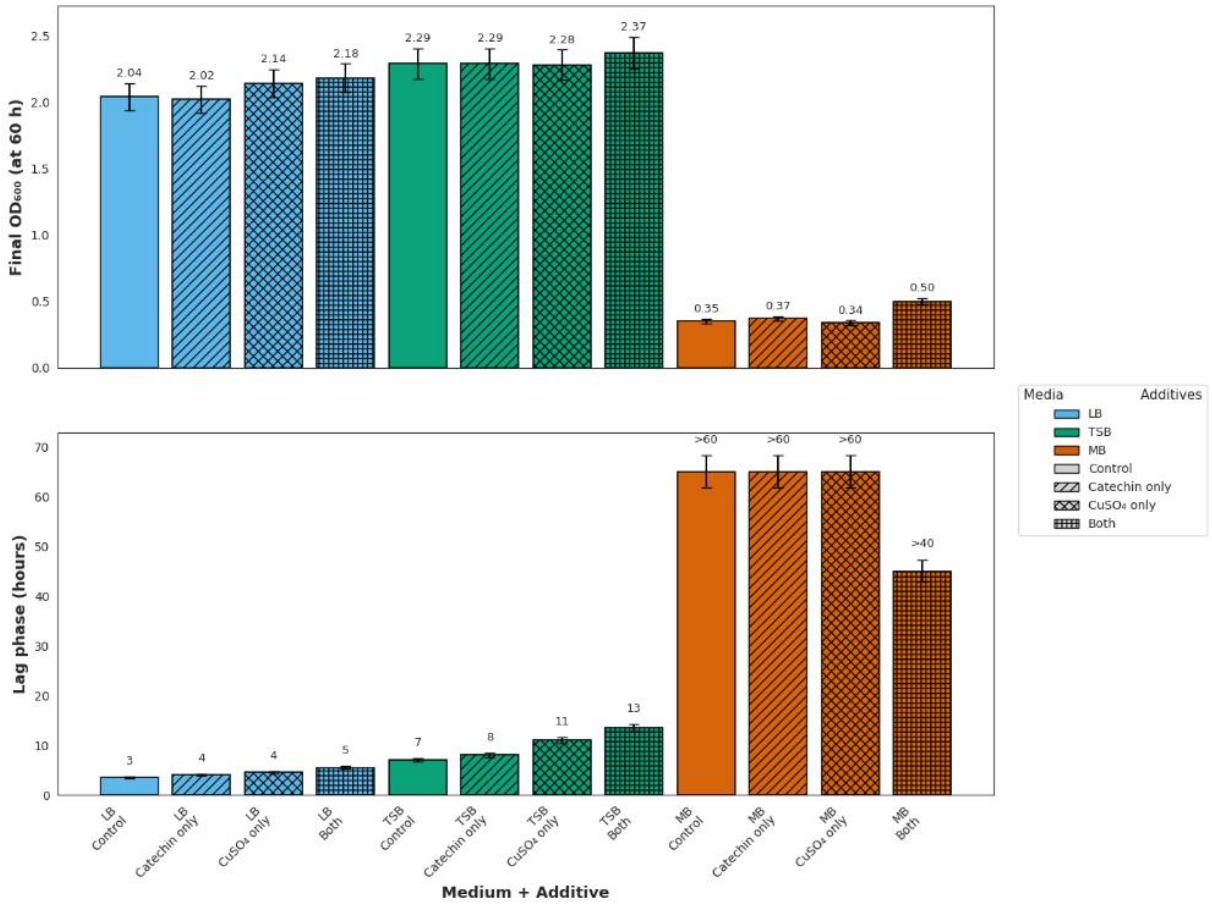

Figure 5.1: Growth of *Alcaligenes faecalis* NZRM 836 in lysogeny broth (LB), tryptic soy broth (TSB), and minimal broth (MB) supplemented with catechin, $CuSO_4$, or both. The upper panel shows the final OD_{600} at 60 h; the lower panel shows lag phase duration. Error bars = SD of mean (n=3). Hatching denotes additives (see legend). Values for longer lag phases in MB are indicated as >60 h or >40 h.

Supplementation with (+)-catechin and $CuSO_4$ extended the lag phase in all media, particularly in TSB, where the combination delayed growth by approximately 12–15 h (Figure 5.1). This delay likely reflects physiological adaptation to phenolic and copper-associated oxidative stress. Following adaptation, cultures in supplemented TSB exhibited the highest extracellular ABTS-, L-DOPA-, catechol-, and pyrogallol-oxidizing activities, support the interpretation that catechin functions both as of catechin as an oxidative inducer and Cu^{2+} as an essential cofactor for copper-containing oxidoreductase expression (Iwasaki et al., 2011).

Time-course analysis (Figure 5.2) demonstrated progressive increases in ABTS- and L-DOPA-oxidizing activities in TSB, with maximum activities observed around 60 h, whereas pyrogallol-oxidizing activity peaked earlier during cultivation. These trends suggested the coexistence of

multiple extracellular oxidoreductase components with distinct physiological roles and expression dynamics. Collectively, these findings identified supplemented TSB as the most suitable medium for extracellular MPLO production and supported subsequent optimization and biochemical characterization of the multifunctional extracellular oxidoreductase preparation.

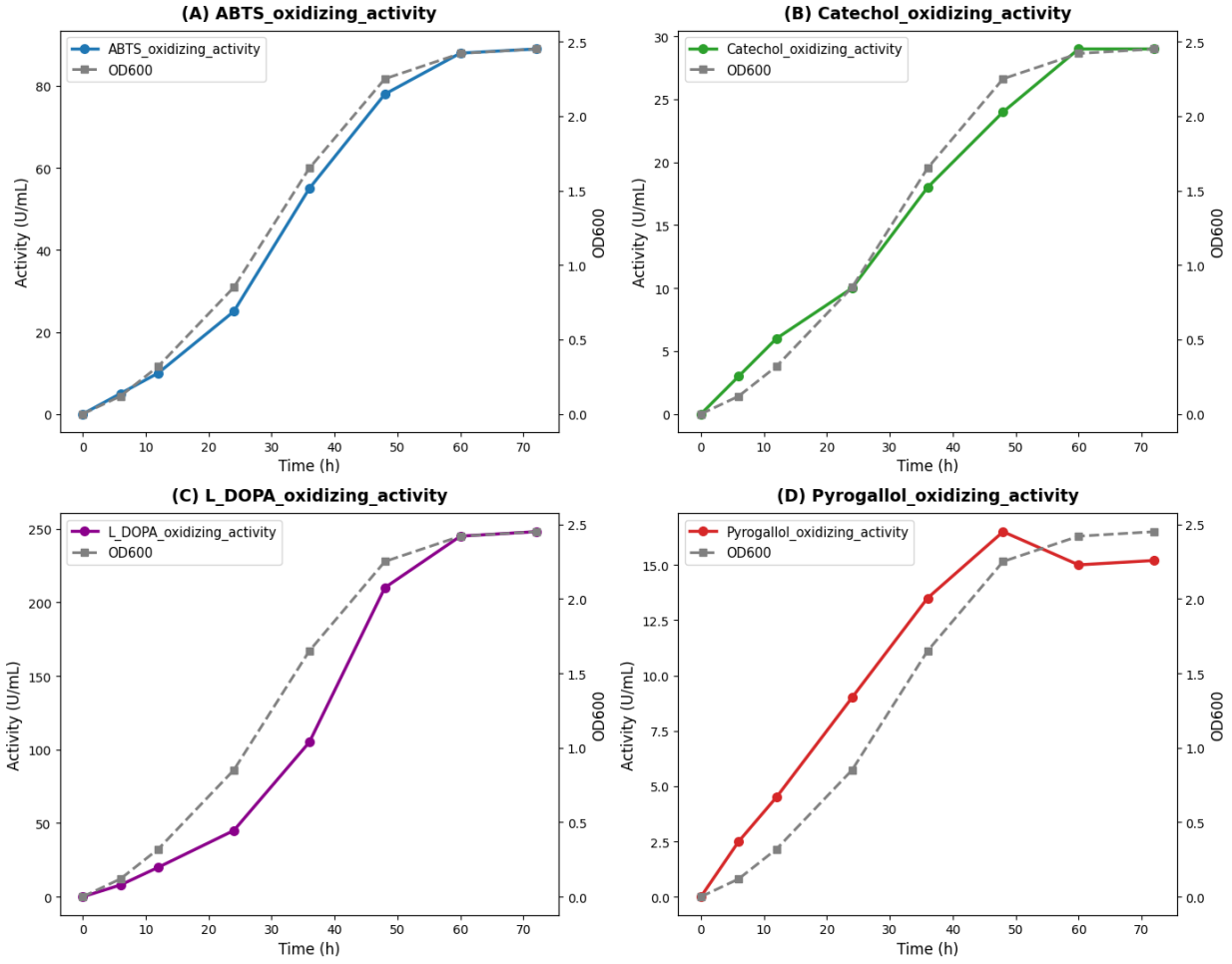

Figure 5.2: Time-course profiles of *Alcaligenes faecalis* NZRM 836 growth (OD_{600}) and extracellular MPLO-associated substrate oxidation activities during cultivation in Tryptic soy broth (TSB). Panels (A)–(D) show the production of ABTS-oxidizing activity (A), Catechol_oxidizing_activity (B), L_DOPA_oxidizing_activity (C), and Pyrogallol_oxidizing_activity (D), respectively, in relation to cell growth (OD_{600}, grey line). Enzyme activities are expressed in U/mL, while optical density at 600 nm reflects biomass accumulation.

Under optimized screening conditions (TSB supplemented with (+)-catechin and $CuSO_4$), inoculum size significantly influenced enzyme production (Figure 5.3). Increasing inoculum from

0.5% to 10% (v/v) enhanced MPLO activities, consistent with reports that moderate inoculum densities reduce lag phase and promote extracellular enzyme production (Gomathi et al., 2012; Kumar et al., 2022; Simair, 2017). Further increases to 20% resulted in only marginal improvements, likely due to nutrient depletion, oxygen limitation, or metabolic crowding at higher cell densities (Figure 5.3) (Lichtenberg et al., 2022; Nandal et al., 2013). A 10% inoculum was therefore selected as an optimal compromise, providing consistently high extracellular oxidoreductase activity without diminishing returns. Under these conditions, ABTS-, L-DOPA-, catechol-, and pyrogallol-oxidizing activities were consistently produced at levels suitable for subsequent response surface methodology optimization.

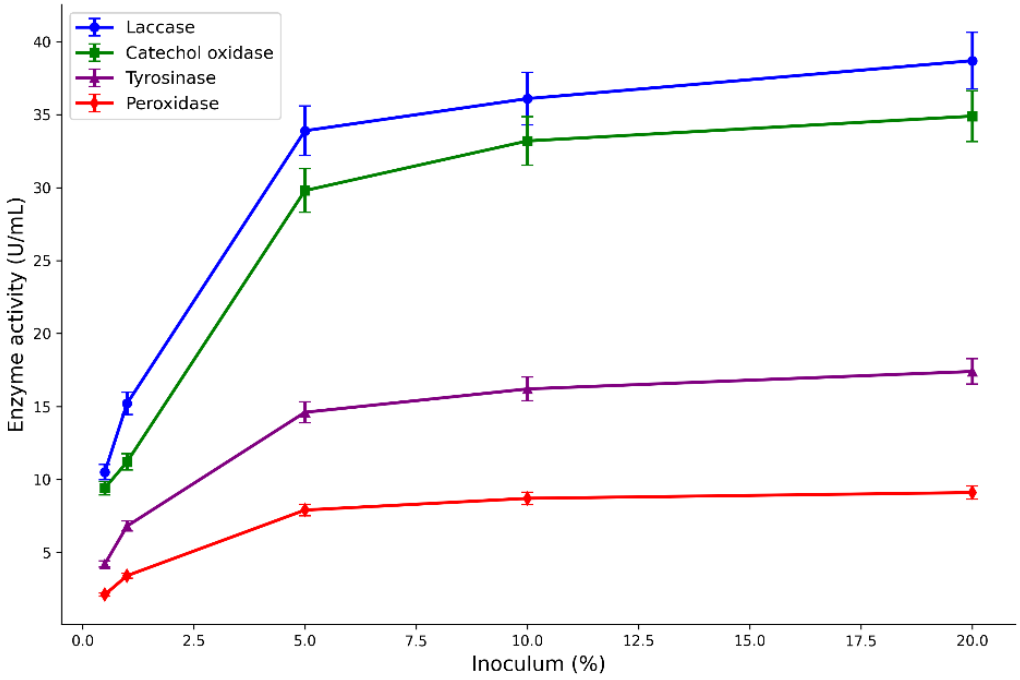

Figure 5.3: Effect of *Alcaligenes faecalis* NZRM 836 inoculum concentration (0.5–20% v/v) on extracellular MPLO-associated substrate oxidation activities in tryptic soy broth supplemented with (+)-catechin and $CuSO_4$ after 60 h cultivation. Curves show ABTS-, catechol-, pyrogallol-, and L-DOPA-oxidizing activities. Values represent mean ± SD (n = 3). Enzyme activities (U/mL) were determined using substrate-specific spectrophotometric assays under standardized reaction conditions.

5.3.2 RSM model fitting and statistical evaluation

The extracellular MPLO-associated substrate oxidation activities measured across the 20 experimental runs of the rotatable central composite design are summarized in Figure 5.4 and Table S5.2. The experimental design assessed the effects of catechin stock addition (X_1), $CuSO_4$

stock addition (X_2), and culture duration (X_3). Culture duration emerged as the dominant, consistently significant factor across all four activities, with $CuSO_4$ addition also contributing significantly to most responses; catechin addition alone did not reach statistical significance for any response, though a consistent upward trend with increasing concentration was observed. This pattern is broadly consistent with previous reports describing induction of microbial copper-containing oxidoreductase systems by phenolic substrates and copper ion (Munoz-Munoz et al., 2008; Piscitelli et al., 2011), while indicating that duration is the primary driver in this system.

As shown in Table 5.2, the four second-order quadratic models were statistically significant overall ($p < 0.05$), with R^2 values ranging from 0.787 to 0.841. Adjusted R^2 values (0.594–0.698) and adequate precision values (7.35–9.01, all exceeding the conventional threshold of 4) support that the models capture a substantial share of the variation in each response. However, Predicted R^2 values were negative for all four models, and lack-of-fit tests were statistically significant ($p < 0.05$) for all four responses, indicating that the quadratic model form does not fully capture the underlying response surface; this limitation is discussed further in Section 5.3. The model describing ABTS-oxidizing activity exhibited the best fit among the four ($R^2 = 0.841$), while L-DOPA-oxidizing activity showed the most modest fit ($R^2 = 0.787$). Actual versus predicted plots (Figure 5.4 B, D, F, H) showed reasonable but imperfect agreement between experimental and model-predicted values, consistent with the significant lack-of-fit identified above.

Table 5.2: Statistical parameters of the quadratic models.

Response	Model P-value	R^2	Adjusted R^2	Predicted R^2	Adequate Precision	Lack-of-Fit P-value
ABTS-oxidizing activity	0.0053	0.841	0.698	−0.188	8.56	0.0002 (significant)
Pyrogallol-oxidizing activity	0.0055	0.840	0.696	−0.195	9.01	0.0009 (significant)
Catechol-oxidizing activity	0.0113	0.811	0.641	−0.413	8.06	0.0002 (significant)
L-DOPA-oxidizing activity	0.0192	0.787	0.594	−0.569	7.35	0.0014 (significant)

Values regenerated directly from the complete central composite design dataset (n = 20 runs, proper rotatable design with $\alpha = 1.682$, Pure Error derived from the 6 individually reported center-point runs). All four models are statistically significant overall ($p < 0.05$). Lack-of-Fit is significant for all four responses, indicating the quadratic model does not fully capture the underlying response surface; this is discussed as a limitation in Section 5.3.

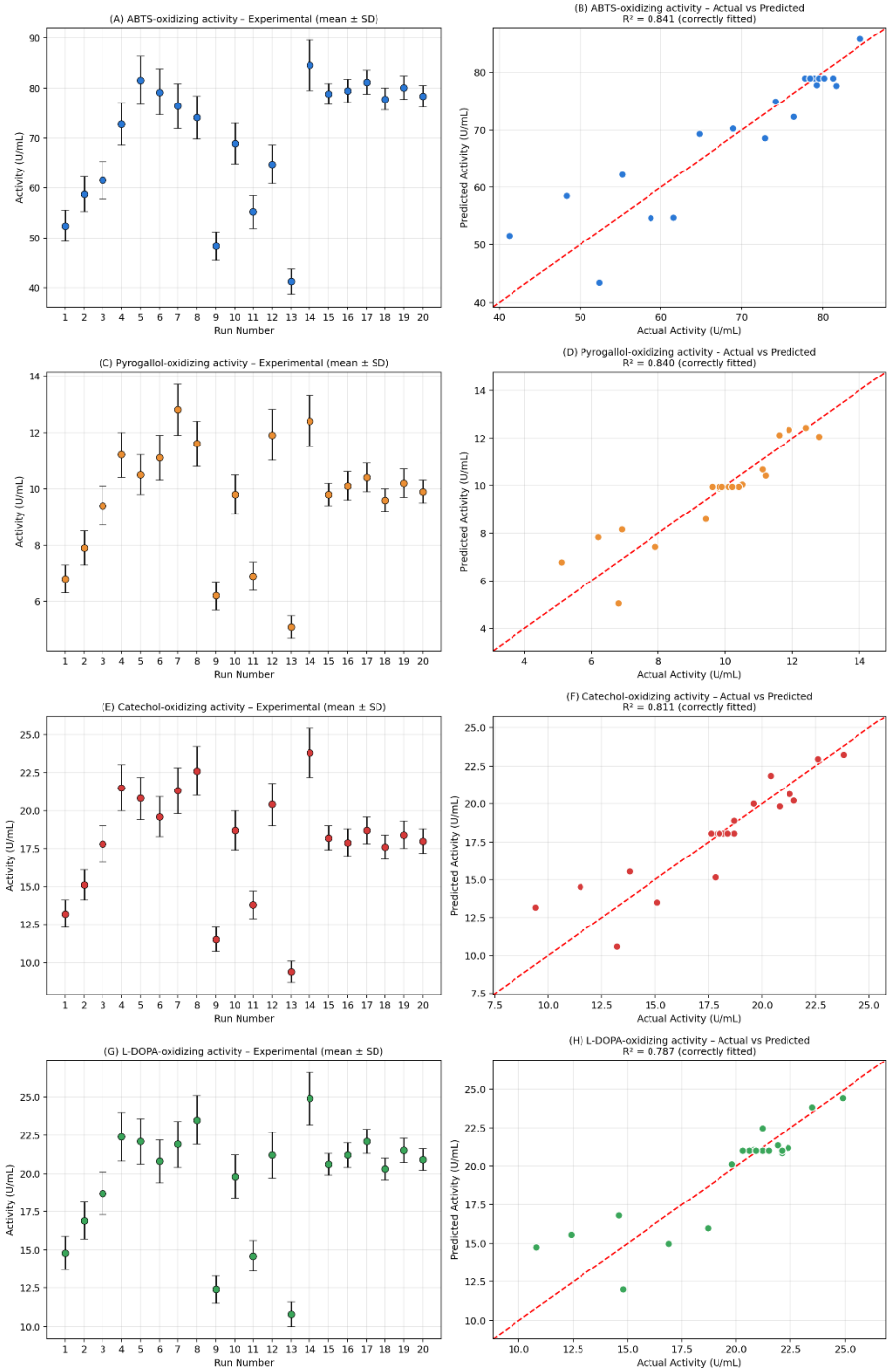

Figure 5.4: Experimental extracellular MPLO-associated substrate oxidation activities and model validation for *A. faecalis* NZRM 836 in the central composite design. Left panels (A, C, E, G): Mean ± SD of experimental ABTS-, pyrogallol-, catechol-, and L-DOPA-oxidizing activities, respectively, across all 20 design runs. Right panels (B, D, F, H): Actual versus predicted plots from the quadratic models. The dashed red line indicates the 1:1 reference. R^2 values are 0.841 (B), 0.840 (D), 0.811 (F), and 0.787 (H).

5.3.3 Response surface analysis and effect of culture duration

The three-dimensional response surface and contour plots (Figure 5.5) revealed distinct interactive effects of catechin (X_1) and $CuSO_4$ (X_2) at a fixed culture duration of 54 h. L-DOPA- and catechol-oxidizing activities increased markedly with higher concentrations of both catechin and $CuSO_4$, indicating synergistic effects of phenolic induction and copper availability on extracellular oxidoreductase production (Pretzler & Rompel, 2024). In contrast, ABTS-oxidizing activity peaked at intermediate inducer levels and declined at higher concentrations, suggesting mild substrate inhibition or metabolic burden (Shraddha et al., 2011). Pyrogallol-oxidizing activity showed a comparatively gradual increase with weaker interaction effects between the two variables.

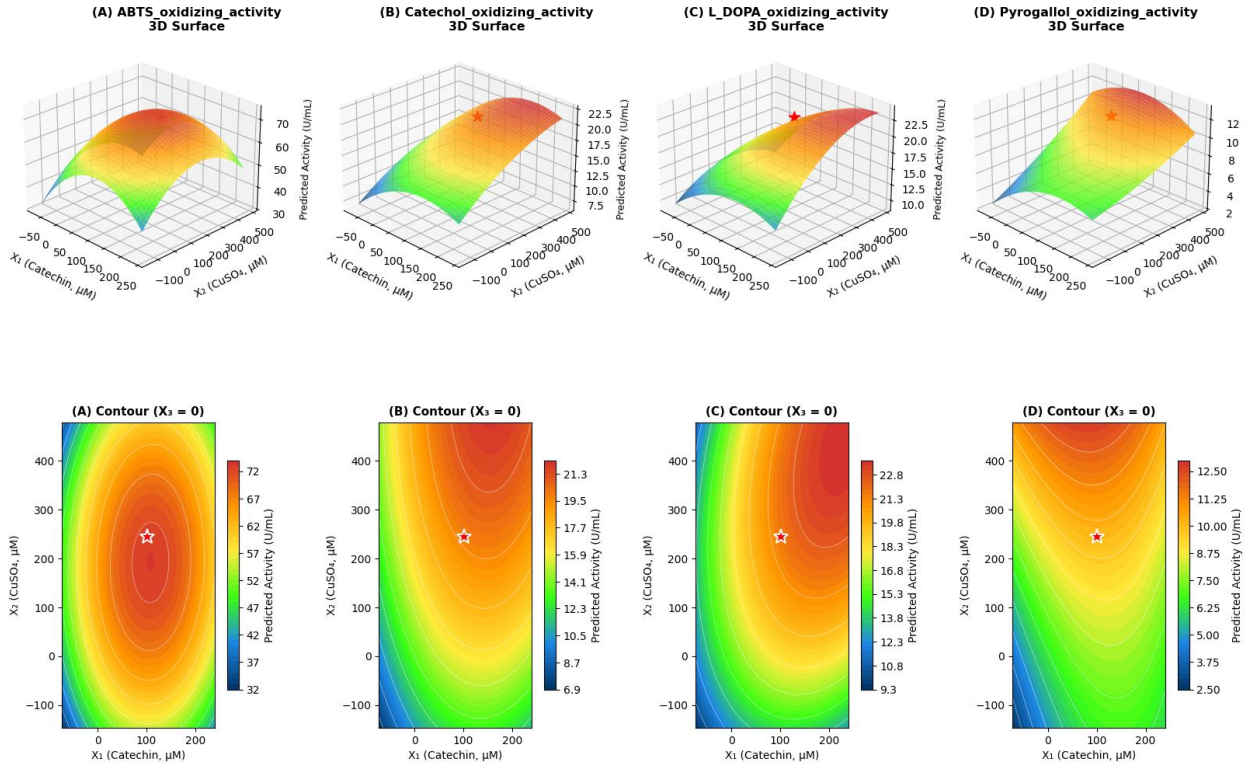

Figure 5.5: Response surface methodology (RSM) and contour plots illustrating the combined effects of catechin stock addition (X_1) and $CuSO_4$ stock addition (X_2) on the four MPLO-associated enzymatic activities of *Alcaligenes faecalis* NZRM 836 at a fixed culture duration of 54 h. Top row: 3D surfaces; bottom row: contour plots. The red star (★) indicates the X_1/X_2 position of the overall global optimum (occurring at 74 h; Table 5.3), projected onto this 54 h-fixed surface for visual reference; it does not represent a point directly calculated on this specific surface. Blue represents low activity; red represents high activity.

Table 5.3: Global optimum conditions, predicted activities, and experimental verification results.

Parameter	Optimized value	Predicted (U/mL)	Observed (mean ± SD, n=3)	Accuracy (%)
Catechin stock (µL of 12.5 mM)	405	-	-	-
Final catechin concentration	101 µM	-	-	-
$CuSO_4$ stock (µL of 25 mM)	490	-	-	-
Final $CuSO_4$ concentration	245 µM	-	-	-
Culture duration (h)	74	-	-	-
ABTS-oxidizing activity	-	81.5	79.2 ± 3.6	97.2
Pyrogallol-oxidizing activity	-	12.3	12.1 ± 0.5	98.4
Catechol-oxidizing activity	-	24.6	23.8 ± 1.3	96.7
L-DOPA-oxidizing activity	-	24.2	23.5 ± 0.9	97.1

Culture duration (X_3) exerted a predominantly positive effect on all four enzyme activities (Figure 5.6), with ABTS-oxidizing activity showing the strongest progressive increase during cultivation. This trend is consistent with the gradual accumulation of extracellular multicopper oxidase-associated systems during late exponential and early stationary growth phases (Ali et al., 2022; Wiśniewska et al., 2021).

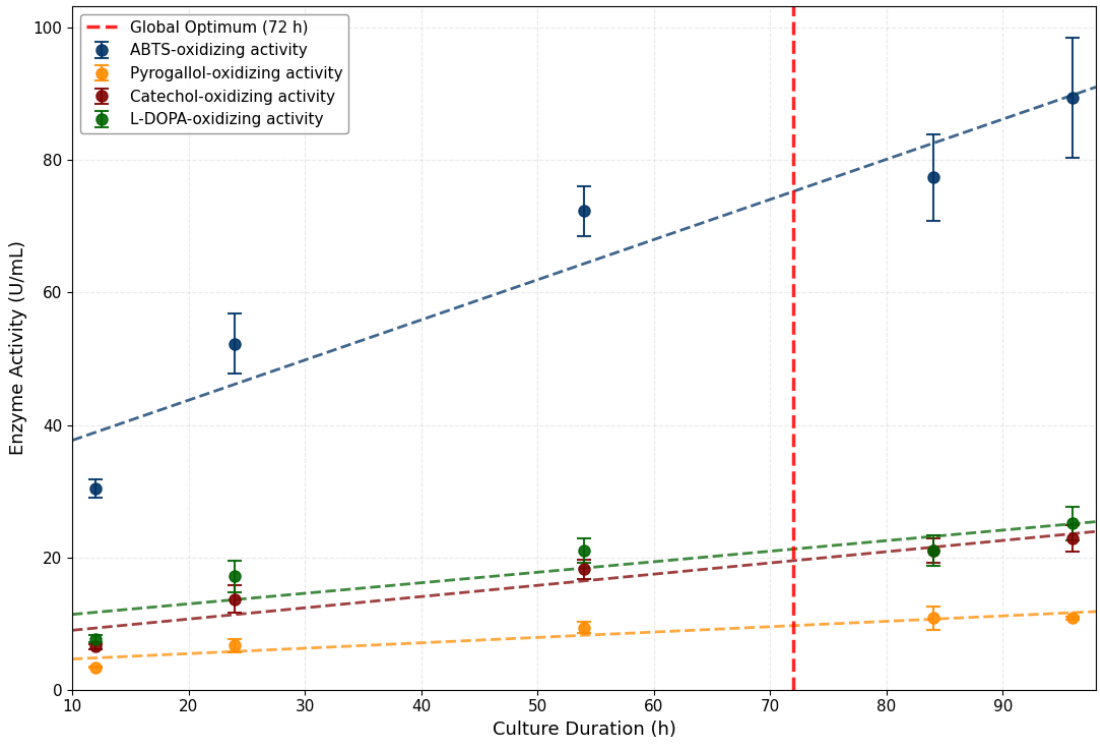

Figure 5.6: Effect of *Alcaligenes faecalis* NZRM 836 culture duration (12–96 h) on extracellular ABTS-, pyrogallol-, catechol-, and L-DOPA-oxidizing activities. Values represent mean ± SD (n = 3) with fitted linear trend lines. The red dashed line indicates the predicted global optimum at 74 h.

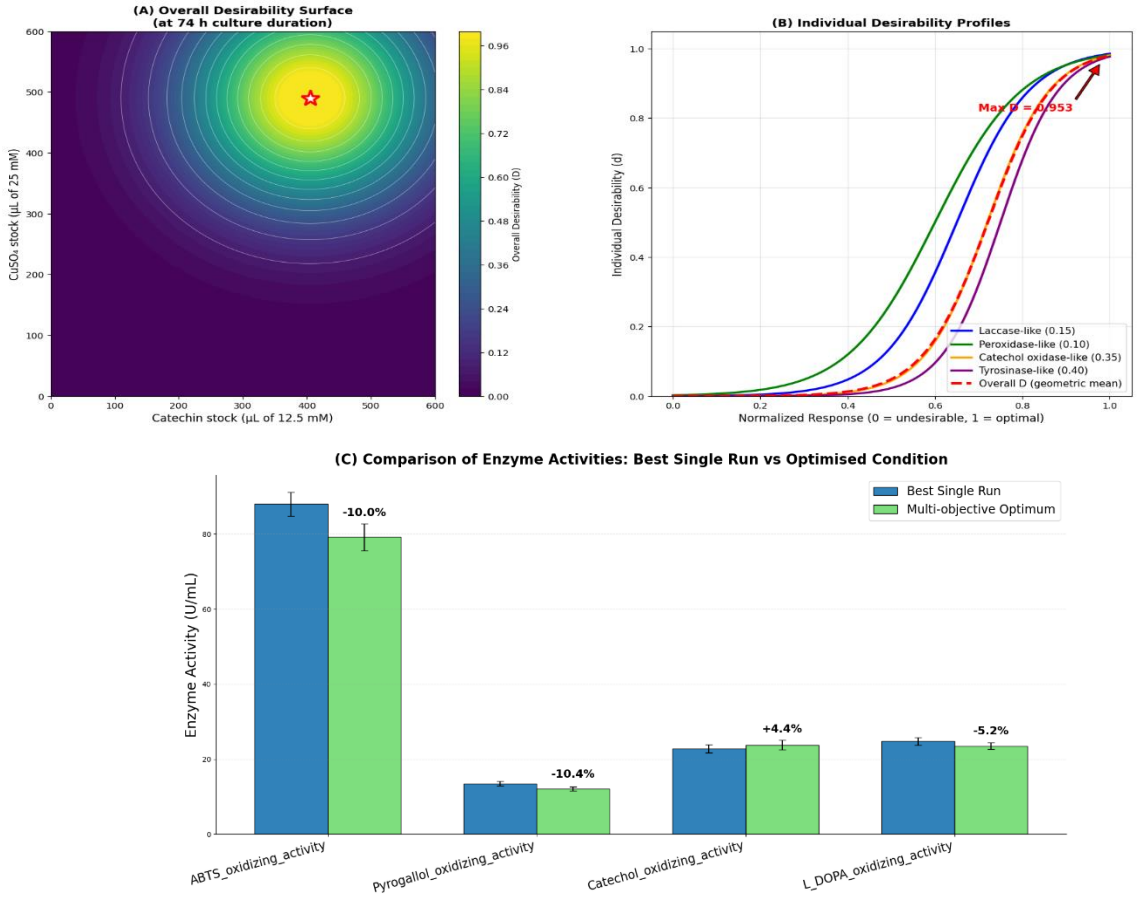

Figure 5.7: Derringer's desirability-based multi-objective optimization of extracellular MPLO-associated substrate oxidation activities from *Alcaligenes faecalis* NZRM 836. (A) Overall desirability surface showing the predicted global optimum at 74 h (101 µM catechin and 245 µM $CuSO_4$), indicated by a white star. (B) Individual desirability profiles for each substrate oxidation activity. (C) Comparison of substrate oxidation activities (U/mL) between the best experimental run and the globally optimized cultivation condition, with percentage improvements shown above bars.

The distinct response profiles observed among the four substrate oxidation activities further correspond with the interpretation that the extracellular MPLO preparation represents a heterogeneous multifunctional oxidoreductase system with partially overlapping substrate specificities and regulatory patterns. These differential responses also justified the application of Derringer's desirability function for simultaneous multi-objective optimization of extracellular MPLO production (Amdoun et al., 2018).

5.3.4 Partial purification and concentration

Three independent production batches were conducted in a 5 L bench-scale fermenter with a 2 L working volume under the optimized conditions. Each batch yielded 1991 ± 4.5 mL of clarified crude supernatant after centrifugation. The crude preparation contained 14.5 ± 1.2 mg/mL total protein and exhibited extracellular substrate oxidation activities of 37.66 ± 1.88 U/mL (ABTS-oxidizing), 5.04 ± 0.25 U/mL (pyrogallol-oxidizing), 9.38 ± 0.47 U/mL (catechol-oxidizing), and 9.35 ± 0.47 U/mL (L-DOPA-oxidizing).

This two-step ultrafiltration and dialysis process resulted in a 3.68–3.85-fold increase in specific activity across all measured substrate oxidation activities, with activity recovery ranging from 76.5% to 78.3% (Table 5.4). The relatively uniform purification fold and high activity recoveries suggest that the procedure effectively enriched the extracellular multifunctional oxidoreductase system while preserving its complementary substrate oxidation profile.

The partially purified preparation contained 20.04 ± 0.85 mg/mL total protein and was used for subsequent characterization and application studies. Compared with conventional multi-step chromatographic methods, this ultrafiltration-based approach offered a scalable, high-recovery method suitable for producing a functional biocatalyst rather than a highly purified single protein.

Table 5.4: Partial purification of the enzyme preparation produced by *Alcaligenes faecalis* NZRM 836

Enzyme	Crude activity (U/mL)	Crude specific activity (U/mg)	Partially purified MPLO activity (U/mL)	Partially purified MPLO specific activity (U/mg)	Activity recovery (%)	Purification fold
ABTS-oxidizing	37.66 ± 1.88	2.60 ± 0.25	191.2 ± 8.4	9.54 ± 0.41	76.5	3.75
Pyrogallol-oxidizing	5.04 ± 0.25	0.348 ± 0.033	26.2 ± 1.1	1.29 ± 0.05	78.3	3.85
Catechol-oxidizing	9.38 ± 0.47	0.647 ± 0.062	48.0 ± 2.1	2.35 ± 0.10	77.1	3.68
L-DOPA-oxidizing	9.35 ± 0.47	0.645 ± 0.062	47.7 ± 2.0	2.34 ± 0.09	76.8	3.72

The observed purification efficiency compares favorably with previous studies on bacterial oxidoreductases. Mehandia et al. (2020) reported a similar ~3.8-fold purification for an alkaline laccase from *A. faecalis*, although with substantially lower activity recovery following multi-step chromatographic purification. Similarly, Unuofin et al. (2019) reported comparable enrichment of laccases from *Achromobacter xylosoxidans*, often at the expense of reduced recovery due to additional purification steps. In contrast, the present ultrafiltration approach maintained high activity recovery (>76%), indicating minimal enzyme loss and suitability for producing a functional biocatalyst rather than a homogeneous single protein.

Overall, the optimized cultivation and ultrafiltration workflow provided a reproducible laboratory-scale strategy for generating a partially purified extracellular MPLO preparation with enhanced catalytic performance while retaining multifunctional oxidoreductase activity profiles relevant to tea catechin biotransformation.

5.3.5 SDS-PAGE analysis of the partially purified MPLO enzyme preparation

SDS-PAGE analysis of the partially purified enzyme preparation from *A. faecalis* NZRM 836 revealed multiple distinct protein bands, confirming the heterogeneous nature of the preparation (Figure 5.8). Prominent bands were observed in the approximate molecular weight ranges of 60–70 kDa and 35–40 kDa, along with several faint bands at lower and higher molecular weights.

The band at 60–70 kDa aligns with the reported size of bacterial laccase-like multicopper oxidases (LCMOs), which typically range from 55 to 80 kDa. The 35–40 kDa region may correspond to smaller extracellular oxidoreductase-associated proteins or truncated LMCO-related variants. However, because the extracellular preparation was only partially purified, definitive assignment of individual protein bands to specific oxidoreductase activities cannot be made solely on the basis of SDS-PAGE migration patterns.

The presence of multiple protein bands supports the interpretation that the extracellular MPLO preparation consisted of a heterogeneous multifunctional oxidoreductase system rather than a single purified enzyme species.

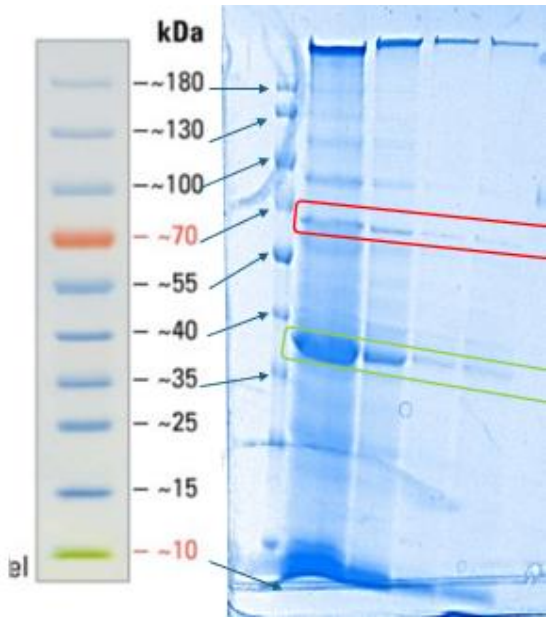

Figure 5.8: SDS-PAGE profile of the partially purified extracellular MPLO preparation from *Alcaligenes faecalis* NZRM 836. Lane M: molecular weight marker; lanes 1–4: partially purified extracellular enzyme preparations from independent production batches. Multiple protein bands were observed, including prominent bands within the ~60–70 kDa and ~35–40 kDa regions, supporting the heterogeneous composition of the extracellular oxidoreductase preparation.

5.3.6 Characterization of *Alcaligenes faecalis* NZRM 836 MPLO preparation

The partially purified MPLO enzyme preparation from *A. faecalis* NZRM 836 was characterized with respect to temperature and pH optima, thermal and pH stability, substrate specificity, kinetic parameters, and effects of inhibitors and metal ions. Characterization focused primarily on ABTS- and L-DOPA-oxidizing activities as representative indicators of the preparation's polyphenol-oxidizing capacity.

5.3.6.1 pH and temperature profiles

ABTS- and L-DOPA-oxidizing activities exhibited a clear temperature optimum at 70 °C (Figure 5.9A), consistent with the thermostable nature of many bacterial multicopper oxidases- associated systems and related extracellular oxidoreductases (Mehandia et al., 2020; Unuofin et al., 2019). Activity declined sharply above 70 °C, indicating thermal inactivation of the oxidoreductase components within the partially purified preparation.

The pH profiles were strongly substrate dependent. ABTS-oxidizing activity was maximal at pH 3.0, indicating the acidophilic behavior typical of many bacterial laccases (Abdelgalil et al., 2020). In contrast, L-DOPA-oxidizing activity reached its maximum at pH 7.0, which is characteristic of bacterial tyrosinases and diphenol oxidases that prefer near-neutral conditions (Chang, 2009). These contrasting pH optima further support the coexistence of multiple extracellular oxidoreductase components with partially overlapping substrate oxidation behavior.

5.3.6.2 Thermal and pH stability

Thermal stability studies showed that both ABTS- and L-DOPA-oxidizing activities retained approximately 45–58% of initial activity after 8 h at 40 °C and 50 °C, with further decline over extended incubation(Figure 5.9C, D). Significant inactivation occurred at temperatures ≥60 °C during prolonged incubation, with near-complete loss of activity at 80 °C after 24 h. This profile is comparable to other bacterial multicopper oxidases reported in the literature (Ausec et al., 2011; Reiss et al., 2013).

pH stability was assessed at pH 3.0, 5.0, and 7.0 (Figure 5.9E, F). ABTS-oxidizing activity showed the best retention among the pH conditions tested under acidic conditions, retaining approximately 80% of its initial activity at pH 3.0 after 24 h, the least decline observed across the three pH conditions, though not without measurable loss, in agreement with the acid tolerance commonly observed for bacterial laccases (Abdelgalil et al., 2020; Reiss et al., 2013). In contrast, L-DOPA-oxidizing activity exhibited greater stability at pH 5.0 and 7.0, suggesting the greater operational stability of bacterial o-diphenol-oxidizing systems under near-neutral conditions (Agunbiade & Le Roes-Hill, 2021; Chang, 2009).

These stability characteristics align well with the natural pH range of green tea infusions (approximately pH 5.0–7.5), supporting the suitability of the extracellular MPLO preparation for controlled tea biotransformation applications.

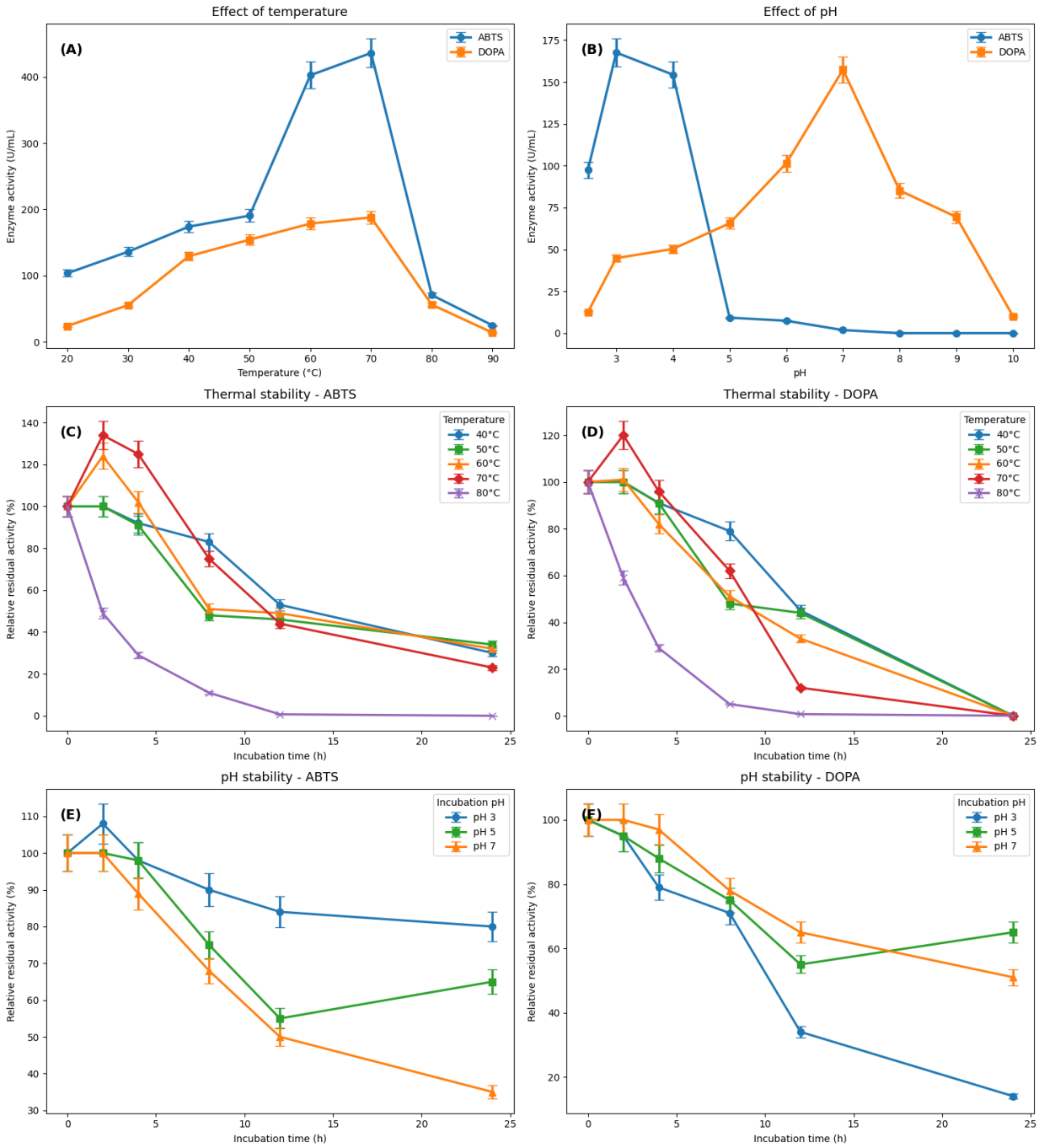

Figure 5.9: Effect of temperature (A) and pH (B) on the activity of the partially purified enzyme preparation from *Alcaligenes faecalis* NZRM 836 using ABTS and L-DOPA as substrates. Thermal stability of ABTS (C) and L-DOPA (D) after pre-incubation at different temperatures (40–80 °C) for 0–24 h. pH stability of ABTS (E) and L-DOPA (F) after pre-incubation at pH 3, 5, and 7 for 0–24 h. Relative residual activity (%) is expressed as a percentage of the initial activity at 0 h.

5.3.6.3 Substrate oxidation profiles

Substrate specificity of the partially purified MPLO enzyme preparation was evaluated using six phenolic substrates at final concentrations of 1, 10, and 20 mM (Table 5.5). The preparation displayed the highest activity toward ABTS, followed closely by L-DOPA, whereas moderate oxidation activity was observed toward catechol. Pyrogallol, guaiacol, and syringaldazine were oxidized at comparatively lower rates.

This substrate oxidation pattern is consistent with extracellular bacterial multicopper oxidases-associated systems, which typically show substantial apparent substrate interaction for ABTS and simple o-diphenolic compounds while exhibiting lower activity toward methoxylated phenolics such as guaiacol and syringaldazine (Janusz et al., 2020; Mehandia et al., 2020; Unuofin et al., 2019). The comparatively high activity toward L-DOPA, particularly at 20 mM, further supports the presence of strong o-diphenol oxidation capacity within the extracellular preparation (Song et al., 2021). Limited syringaldazine oxidation further supports the narrow substrate range often reported for bacterial oxidases relative to fungal laccases (Reiss et al., 2013).

Activity increased with rising substrate concentration for all compounds, most notably for ABTS and L-DOPA. This concentration-dependent behavior indicates substantial catalytic capacity under high polyphenol loads. This behavior is advantageous for tea biotransformation systems, where catechin concentrations are naturally high and dynamically change during processing (Abdelgalil et al., 2020; Brugnari et al., 2021).

Table 5.5: Substrate specificity of the enzyme preparation expressed by *Alcaligenes faecalis* NZRM 836 as activity (U/mL) at different substrate concentrations.

Substrate	λmax (nm)	ε ($M^{-1}cm^{-1}$)	1 mM (U/mL)	10 mM (U/mL)	20 mM (U/mL)
ABTS	420	36,000	65.23 ± 3.59	259.31 ± 14.52	405.01 ± 26.33
Pyrogallol	420	12,000	2.41 ± 0.14	10.56 ± 0.63	30.54 ± 1.98
Guaiacol	470	26,600	1.02 ± 0.06	3.76 ± 0.22	8.26 ± 0.50
Catechol	410	1470	10.21 ± 0.67	39.61 ± 2.57	75.32 ± 4.90
L-DOPA	475	3,600	48.96 ± 2.74	222.22 ± 13.11	265.00 ± 15.37
Syringaldazine	530	65,000	1.83 ± 0.11	18.30 ± 1.17	34.05 ± 2.21

Activities were measured at the respective λmax using corresponding molar extinction coefficients. Values represent the mean ± SD (n = 3).

5.3.6.4 Apparent kinetic behavior

The partially purified MPLO enzyme preparation displayed Michaelis–Menten-type kinetics when evaluated using ABTS and L-DOPA as representative substrates for extracellular polyphenol oxidation (Figure 5.10). Because the MPLO preparation in this experiment is a heterogeneous multi-enzyme preparation, all reported kinetic parameters are apparent values aligning with the aggregate behavior of multiple oxidoreductases rather than the intrinsic properties of a single purified enzyme.

Non-linear regression analysis yielded the following apparent kinetic parameters:

1. For ABTS (laccase-like activity): K_m = 10.87 ± 6.11 mM, V_{max} = 518.2 ± 181.2 U/mL
2. For L-DOPA (o-diphenolase (tyrosinase-like) activity): K_m = 7.36 ± 1.49 mM, V_{max} = 393.8 ± 43.8 U/mL

The higher apparent K_m observed with ABTS indicates lower overall substrate affinity compared with L-DOPA. However, ABTS oxidation did not reach clear saturation within the tested concentration range (up to 10 mM). Consequently, the estimated K_m and V_{max} values for ABTS should be interpreted with caution, as the V_{max} may be underestimated and the K_m less precisely defined due to the incomplete saturation curve (Abdelgalil et al., 2020; Dai et al., 2021).

In contrast, L-DOPA oxidation approached saturation more readily and exhibited a lower apparent K_m, reflecting higher overall substrate affinity under the assay conditions. This behavior is consistent with o-diphenolase oxidizing systems, which typically display efficient turnover of o-diphenolic substrates (Agunbiade & Le Roes-Hill, 2021; Fernandez-Julia et al., 2021).

The contrasting kinetic profiles observed with ABTS and L-DOPA further support the coexistence of multiple extracellular oxidoreductase components within the partially purified MPLO preparation. While the ABTS-derived parameters provide an operational estimate of laccase-like activity, the L-DOPA parameters more reliably represent the dominant o-diphenolase contribution in the mixture.

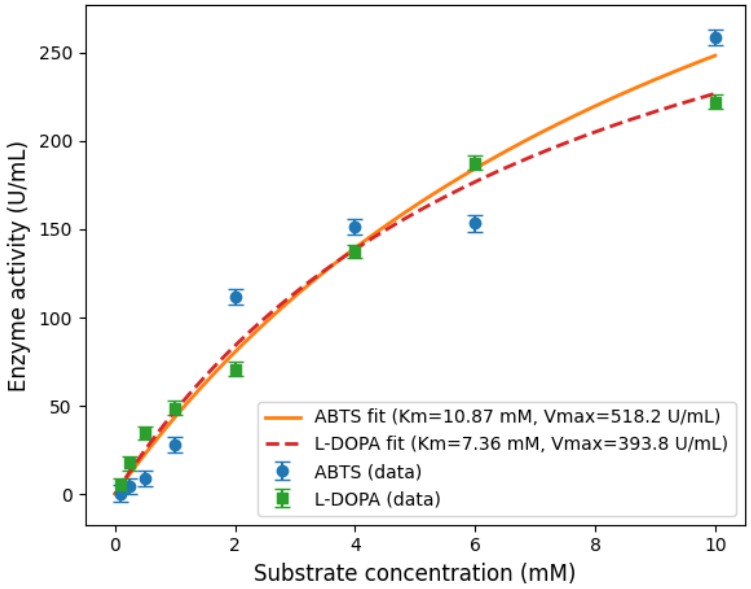

Figure 5.10: Michaelis–Menten kinetic profiles of extracellular ABTS- and L-DOPA-oxidizing activities of the partially purified MPLO preparation from *Alcaligenes faecalis* NZRM 836. Enzyme activity (U/mL) is plotted against substrate concentration (mM). Experimental values represent mean ± SD (n = 3), and curves were fitted using nonlinear Michaelis–Menten regression.

5.3.6.5 Effects of inhibitors and metal ions

The influence of metal ions, inhibitors, and caffeine on the partially purified MPLO enzyme preparation was evaluated to assess its performance in a complex tea matrix (Table 5.6). Cu^{2+} significantly enhanced ABTS-oxidizing activity (142% residual activity), consistent with its essential role as a catalytic cofactor in multicopper oxidases, where it facilitates electron transfer and oxygen reduction (Dai et al., 2021; Mehandia et al., 2020). This activation suggests that the extracellular oxidoreductase system likely retained accessible copper-binding sites capable of enhanced catalytic activity under copper-supplemented conditions.

In contrast, Fe^{2+} produced moderate inhibition, possibly through disruption of copper-associated redox cycling or interference with catalytic electron-transfer pathways (Abdelgalil et al., 2020; Dai et al., 2021). EDTA markedly inhibited both ABTS- and L-DOPA-oxidizing activities, supporting the dependence of the extracellular oxidoreductase system on metal-associated catalytic centers (Chang, 2009; Liu et al., 2024a). Similarly, ascorbic acid caused strong inhibition, likely through the reduction of quinone intermediates and the scavenging of oxidative radicals generated during substrate oxidation (Liu et al., 2024a; Unuofin et al., 2019).

Caffeine produced only modest inhibitory effects, even at 10 mM, suggesting limited direct interaction with extracellular oxidoreductase components. This observation corresponds to previous reports indicating that caffeine primarily interacts with tea polyphenols rather than directly inhibiting oxidoreductase activity (Couzinet-Mossion et al., 2010).

Table 5.6: Effect of metal ions, inhibitors, and caffeine on the activity of the partially purified enzyme preparation from *Alcaligenes faecalis* NZRM 836 (residual activity % of control).

Additive	Concentration (mM)	ABTS (U/mL)	ABTS (% residual)	L-DOPA (U/mL)	L-DOPA (% residual)
Control	–	259.3 ± 12.1	100	222.2 ± 11.4	100
Cu^{2+}	0.5	368.9 ± 18.2	142.3	249.1 ± 13.5	112.1
Fe^{2+}	0.5	198.7 ± 9.4	76.6	178.4 ± 7.2	80.3
EDTA	0.5	98.7 ± 5.2	38.1	112.4 ± 6.3	50.6
Ascorbic acid	0.5	31.8 ± 2.6	12.3	24.6 ± 2.1	11.1
Caffeine	1	248.7 ± 11.3	95.9	215.6 ± 10.8	97
	5	236.4 ± 9.8	91.2	204.8 ± 8.7	92.2
	10	219.8 ± 10.2	84.8	189.3 ± 9.4	85.2

Values are mean ± SD (n = 3).

The differing sensitivities of ABTS- and L-DOPA-oxidizing activities to these additives further confirm the coexistence of multiple oxidoreductase components, likely representing functionally distinct laccase-like and tyrosinase-like enzymes (Dai et al., 2021; Fernandez-Julia et al., 2021). The enhancement by Cu^{2+} highlights the importance of metal cofactor availability in tea matrices (Mehandia et al., 2020), whereas the strong inhibitory effect of ascorbic acid underscores the role of endogenous reducing compounds in modulating oxidation efficiency during processing (Najjari & Bodaghi, 2024). Given that ascorbic acid levels decrease during tea processing (Li et al., 2017), its residual presence may still influence enzymatic reactions in green tea systems. Overall, these results demonstrate that matrix composition, particularly metal ion availability and reducing capacity, can significantly affect the functional performance of the extracellular MPLO-mediated catechin oxidation efficiency.

5.3.7 *In-silico* genome mining of reference *Alcaligenes faecalis* genomes associated with extracellular MPLO-associated activities

Genome mining of reference *A. faecalis* genomes identified a diverse repertoire of putative blue copper-containing laccase-like multicopper oxidases (LMCOs) containing the conserved PF00394 Cu-oxidase domain characteristic of bacterial multicopper oxidases associated with extracellular phenolic oxidation (Table 5.7). Several homologs showed similarity to bilirubin oxidase-like proteins, whereas canonical tyrosinase (EC 1.14.18.1) and dedicated catechol oxidase/catecholase homologs were not identified in the analyzed genomes.

Table 5.7: Representative putative blue copper-containing multicopper oxidases and related oxidoreductases identified in reference *Alcaligenes faecalis* genomes.

Protein ID	Annotation	Key domain	Putative relevance to catechin oxidation	Interpretation
WP_042480682.1	Multicopper oxidase family protein	PF00394 (Cu-oxidase)	High	Representative Group A LMCO
WP_045931327.1	Multicopper oxidase family protein	PF00394 (Cu-oxidase)	High	Representative Group A LMCO
WP_270115582.1	Multicopper oxidase family protein	PF00394 (Cu-oxidase)	High	Strong Group A LMCO variant
ARP53812.1	Bilirubin oxidase	PF00394 (Cu-oxidase)	High	Blue copper LMCO potentially associated with extracellular polyphenol oxidation
KVX07323.1	Bilirubin oxidase	PF00394 (Cu-oxidase)	High	Blue copper LMCO potentially associated with extracellular polyphenol oxidation
ctg_03494 (TD-94)	Multicopper oxidase	PF00394.25	High	Direct genome annotation of putative LMCO
WP_316990414.1	Multicopper oxidase family protein	PF00394 (Cu-oxidase)	Moderate	Divergent LMCO-related variant
A0A2U2BQ30	Bilirubin oxidase	PF00394 (Cu-oxidase)	High	Likely associated with extracellular polyphenol oxidation
A0AAE9HGQ3	Multicopper oxidase family protein	PF00394 (Cu-oxidase)	High	Putative LMCO-associated oxidoreductase
A0ABY7MZI0	Multicopper oxidase family protein	PF00394 (Cu-oxidase)	High	Putative LMCO-associated oxidoreductase

More than 40 putative multicopper oxidase-related homologs were identified across the analyzed genomes. Multiple sequence alignment revealed two principal LMCO-associated subgroups retaining conserved T1 blue copper and trinuclear T2/T3 copper-binding motifs characteristic of bacterial multicopper oxidases. Several homologs also contained predicted N-terminal signal peptides, supporting possible extracellular or periplasmic localization. However, the actual expression, secretion, and catalytic activity of these candidate oxidoreductase-related proteins require transcriptomic, proteomic, and biochemical confirmation.

These genome-associated observations link well with the experimentally observed multifunctional extracellular MPLO-associated substrate oxidation activities. Bilirubin oxidase (BOD)-like proteins and related LMCO homologs catalyze the oxidation of model laccase substrates (ABTS), simple diphenols (catechol), amino acid derivatives (L-DOPA), and complex polyphenols via one-electron abstraction, generating phenoxyl radicals that can undergo coupling and polymerization, the similar oxidative chemistry associated with theaflavin and thearubigin formation from tea catechins (Detering et al., 2018; Khlupova et al., 2015; Khlupova et al., 2018).

The coexistence of multiple putative LMCO variants (including BOD-like enzymes) aligns well with the distinct ABTS-, L-DOPA-, catechol-, and pyrogallol-oxidizing profiles, heterogeneous SDS-PAGE banding patterns, and kinetic behavior observed in the partially purified extracellular MPLO preparation. Functionally, the strong ABTS-oxidizing activity reflects classic laccase-like behavior, while efficient oxidation of L-DOPA and catechol indicates diphenolase/catechol oxidase-like capacity toward the o-diphenolic moieties of tea catechins such as EGCG, ECG, and EC.

Although canonical tyrosinases (EC 1.14.18.1) or dedicated catechol oxidases homologs were not identified in the analyzed reference genomes, bacterial multicopper oxidase family proteins and bilirubin oxidase-like proteins are well documented to exhibit broad substrate specificity toward phenolic and polyphenolic compounds, often functioning effectively at neutral pH (Detering et al., 2018; Hiroshi & Shiro, 2003; Khlupova et al., 2015). Previous studies have also reported multicopper oxidase-associated phenolic oxidation activity together with phenol hydroxylase systems in *A. faecalis* (Li et al., 2023; Zhu et al., 2008). Genes encoding phenol hydroxylase- and catechol dioxygenase-related homologs were identified in reference *A. faecalis* genomes; however, these enzymes primarily function in hydroxylation and aromatic ring-cleavage pathways rather

than quinone-mediated oxidative polymerization (Li et al., 2023; Regar et al., 2023; Zeng et al., 2023b). Nevertheless, such enzymes may contribute to secondary catechin transformation reactions because the present study utilized a partially purified extracellular enzyme preparation rather than individually purified enzymes.

It should be noted, however, that the present study primarily focused on extracellular oxidoreductase-associated activities relevant to catechin oxidation. Comprehensive screening, quantification, and characterization of other extracellular enzyme classes potentially involved in secondary catechin transformation reactions, including hydrolases, esterases, and dioxygenases, were beyond the scope of this study.

Collectively, these findings support the interpretation that the extracellular MPLO preparation represents a multifunctional oxidoreductase system dominated by LMCO-associated polyphenol oxidation relevant to controlled tea catechin biotransformation.

5.3.8 *In-vitro* oxidation of EGCG and green tea extract using the MPLO enzyme preparation of *Alcaligenes faecalis* NZRM 836

5.3.8.1 *In-vitro* oxidation of the EGCG model system

The biotransformation potential of the partially purified MPLO preparation was initially evaluated using EGCG as a defined model substrate. A 1 mM EGCG solution was incubated with 0.5% (v/v) MPLO preparation, standardized to 250 U/mL ABTS-oxidizing activity, at 50 °C , and changes in EGCG and associated transformation products were monitored over 60 min. The theoretical EGCG concentration of the reaction mixture was 458.37 µg/mL. Following quenching with three volumes of ice-cold ethanol, a fourfold dilution was introduced, giving an expected concentration of approximately 114.6 µg/mL. The measured concentration at 0 min was 105.65 ± 5.28 µg/mL, which was reasonably consistent with the expected concentration after a fourfold dilution achieved by adding three volumes of ethanol to one volume of sample. The oxidation dynamics are shown in Table 5.8 and Figure 5.11.

Table 5.8: Changes in EGCG and associated catechin and oxidation products during treatment of a 1.00 mM EGCG model system with 0.5% (v/v) partially purified extracellular MPLO preparation from *Alcaligenes faecalis* NZRM 836 at 50 °C for 0, 10, 30, and 60 min, compared with a boiled-enzyme control at 60 min.

Time (mins)	Gallic acid	EGC	Catechin	EC	EGCG	GCG	ECG	CG	TF	TF3G	TF3'G	TF3-3'G
0	1.25± 0.06^{b}	0.66± 0.03^{b}	0.25±0 .01^{d}	0.22± 0.01^{c}	105.65 ±5.28^{a}	0.03± 0.00^{c}	2.54±0 .13^{c}	ND	ND	ND	ND	ND
10	4.62± 0.23^{a}	3.12± 0.16^{a}	8.64±0 .43^{c}	2.27± 0.11^{b}	53.93± 2.70^{b}	2.67± 0.13^{a}	4.54±0 .23^{b}	0.24± 0.01^{c}	ND	ND	ND	2.14± 0.11^{a}
30	0.73± 0.04^{c}	ND	38.77± 1.94^{a}	7.15± 0.36^{a}	31.41± 1.57^{c}	2.32± 0.12^{a}	11.64± 0.58^{a}	2.15± 0.11^{a}	0.07± 0.00^{a}	0.03± 0.00^{a}	0.02± 0.00^{a}	0.01± 0.00^{b}
60	0.91± 0.05^{c}	ND	32.57± 1.63^{b}	3.03± 0.15^{b}	22.13± 1.11^{c}	1.02± 0.05^{b}	10.48± 0.52^{a}	0.59± 0.03^{b}	0.07± 0.00^{a}	0.03± 0.00^{a}	0.02± 0.00^{a}	0.01± 0.00^{b}
60 *	0.93± 0.05^{c}	0.57± 0.03^{b}	0.19±0 .01^{d}	0.25± 0.01^{c}	92.02± 4.60^{a}	0.09± 0.00^{c}	2.04±0 .10^{c}	ND	ND	ND	ND	ND

Values are expressed as mean ± SD (n = 3). Different superscript letters within the same column indicate statistically significant differences ($p < 0.05$), * indicates boiled enzyme as control.

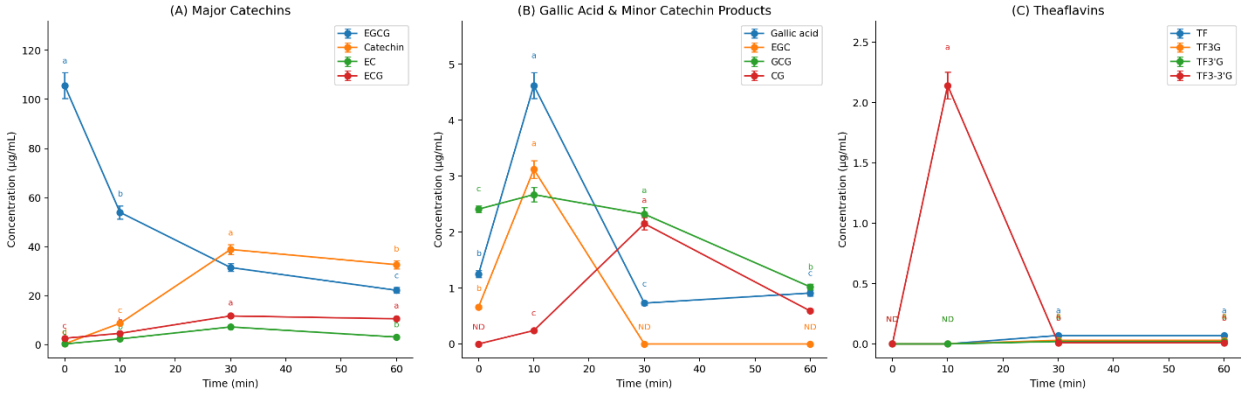

Figure 5.11: Time-course profiles of EGCG biotransformation by the partially purified MPLO preparation in the model system over 60 minutes. (A) Depletion of EGCG and formation of major catechin products (catechin, EC, ECG). (B) Gallic acid formation and minor catechin products (EGC, GCG, CG). (C)

Formation of individual theaflavins. Values not detected (ND) are plotted as zero; error bars represent ± standard deviation (n = 3).

EGCG underwent rapid depletion in the presence of active MPLO preparation. Within 10 min, its concentration decreased from 105.65 ± 5.28 to 53.93 ± 2.70 µg/mL, corresponding to a 49.0% reduction relative to the initial measured concentration. EGCG decreased further to 31.41 ± 1.57 µg/mL at 30 min and 22.13 ± 1.11 µg/mL at 60 min, representing an overall 79.1% reduction during the 60 min treatment. The rapid decrease in EGCG was accompanied by changes in several catechin-related compounds. At 10 min, gallic acid increased from 1.25 ± 0.06 to 4.62 ± 0.23 µg/mL, EGC from 0.66 ± 0.03 to 3.12 ± 0.16 µg/mL, (+)-catechin from 0.25 ± 0.01 to 8.64 ± 0.43 µg/mL, and EC from 0.22 ± 0.01 to 2.27 ± 0.11 µg/mL. GCG and ECG also increased relative to their initial concentrations. The transient accumulation of gallic acid together with changes in non-gallated and epimerized catechin-related compounds is consistent with multiple transformation reactions occurring during EGCG treatment, potentially including degallation and epimerization (Ishino et al., 2010; Sang et al., 2011).

By 30 min, (+)-catechin, EC, ECG, and CG reached 38.77 ± 1.94, 7.15 ± 0.36, 11.64 ± 0.58, and 2.15 ± 0.11 µg/mL, respectively. TF3-3′G was already detectable at 10 min, while all four quantified theaflavins, TF, TF3G, TF3′G, and TF3-3′G, were detectable at 30 min. The appearance of these theaflavins during progressive EGCG depletion is consistent with oxidative coupling reactions associated with catechin oxidation during tea processing (Li et al., 2022c; Takemoto & Takemoto, 2018).

At 60 min, EGCG decreased further to 22.13 ± 1.11 µg/mL, while several catechin-related products remained detectable. (+)-Catechin and ECG remained at 32.57 ± 1.63 and 10.48 ± 0.52 µg/mL, respectively, and all four quantified theaflavins remained detectable at low concentrations. This temporal pattern is consistent with continued conversion of EGCG and associated secondary transformations rather than accumulation of a single stable end product (Zhang et al., 2021).

The boiled-enzyme control retained 92.02 ± 4.60 µg/mL EGCG after 60 min, compared with 22.13 ± 1.11 µg/mL in the active MPLO treatment, and no theaflavins were detected in the control. The substantially greater EGCG depletion and the appearance of theaflavins in the active treatment support a major contribution of the MPLO preparation to the observed biotransformation (Abudureheman et al., 2022). Nevertheless, because the MPLO preparation contained multiple

extracellular substrate-oxidizing activities, the observed transformations cannot be attributed to a specific oxidoreductase component based on these data alone.

5.3.8.2 *In-vitro* oxidation of green tea matrix

Preliminary time–dose optimization in the green tea matrix showed that both enzyme concentration and incubation time significantly influenced catechin oxidation and tea pigments formation. In enzyme-treated samples, EGCG decreased progressively with increasing dose and time, indicating efficient substrate conversion. Two-way ANOVA confirmed significant effects of enzyme concentration, incubation time, and their interaction on EGCG levels (Dose: $F = 94.41$; Time: $F = 387.90$; Dose × Time: $F = 16.95$; $p < 0.001$), with time exerting the strongest influence.

Theaflavin formation followed a non-linear response, reaching maximal accumulation at moderate enzyme levels and intermediate incubation times (3–5 h). Significant effects of enzyme concentration, time, and their interaction were observed for total theaflavins (Dose: $F = 9412.15$; Time: $F = 2388.03$; Dose × Time: $F = 1316.67$; $p < 0.001$). One-way ANOVA further showed that the 100 µL treatment at 3–5 h produced significantly higher theaflavin levels than both lower and higher enzyme concentrations ($p < 0.05$; Table S5.10 (Appendix D)). At enzyme doses ≥200 µL or extended incubation times, theaflavin levels plateaued or declined despite continued catechin depletion. This pattern is consistent with the well-documented transient nature of theaflavins as reactive intermediates that undergo further oxidative polymerization into higher-molecular-weight pigments such as thearubigins (Haslam, 2003; Liang et al., 2003a).

Control samples without enzyme showed only minor changes over time, with slight EGCG reduction and ~90% increase in GCG attributable to thermal epimerization. Total theaflavin levels remained low and statistically unchanged ($p > 0.05$; Table S5.10 (Appendix D)), supporting that moderate heating alone promotes catechin interconversion without substantial oxidative polymerization (Friedman et al., 2009; Wang et al., 2008).

Correlation analysis (Figure 5.12 B) supported these trends, showing a strong inverse relationship between EGCG and total theaflavins ($r \approx -0.89$, $p < 0.001$), consistent with substrate–product conversion during tea oxidation (Liang et al., 2003a). In this context, the TF/TC ratio was used as an integrated indicator of oxidation efficiency, corresponding to the balance between catechin depletion and theaflavin formation. While classical quality indices such as the TF/TR ratio are

widely used in tea evaluation (Munim Khan et al., 2023; Roberts & Smith, 1961), ratio-based approaches linking precursor and product pools provide a mechanistically relevant measure of transformation efficiency under controlled conditions (Liang et al., 2003a). Accordingly, higher TF/TC values (Figure 5.12A) observed under optimal conditions indicate efficient conversion, whereas lower values at higher enzyme doses reflect progression beyond the theaflavin stage.

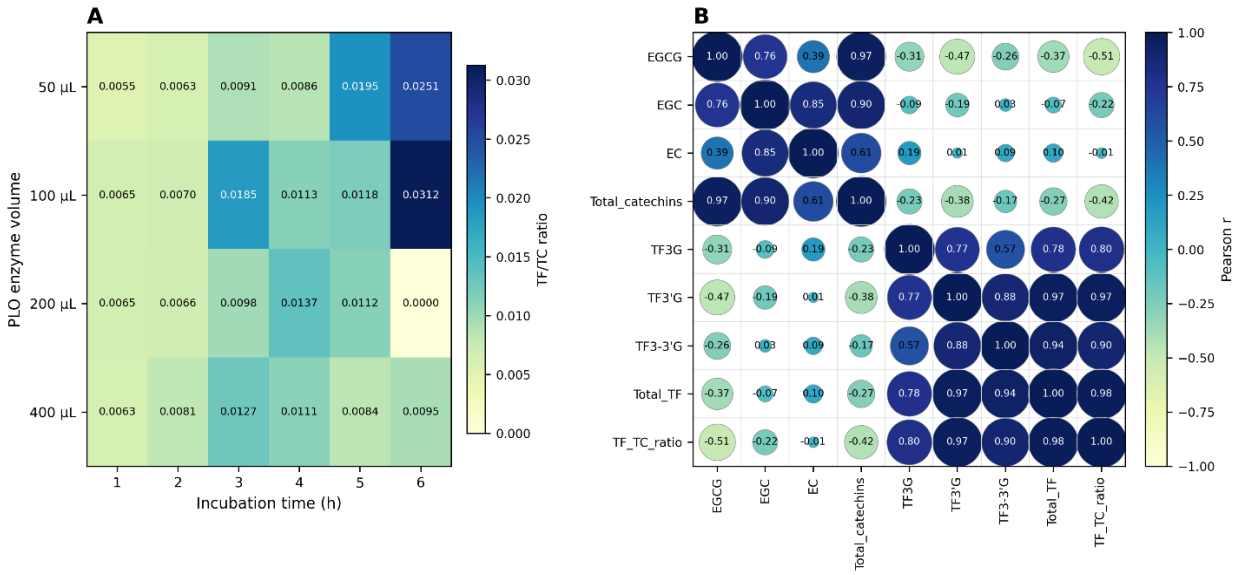

Figure 5.12: Effect of enzyme dose and incubation time on MPLO-mediated oxidation in a green tea matrix. (A) TF/TC ratio heatmap showing the time–dose dependence of oxidation efficiency. (B) Correlation matrix of major catechins, theaflavins, and derived indices, with circle size and color indicating Pearson correlation coefficients.

Overall, enzymatic oxidation dominated the transformation process, while thermal effects contribute only to limited structural rearrangements. Accordingly, 100 µL (0.2% v/v) of the partially purified MPLO enzyme preparation and 5 h incubation at 50 °C were selected as optimal conditions for subsequent experiments. The complete dataset supporting this optimization is provided in Table S5.10 (Appendix D).

The performance of the MPLO enzyme preparation was further evaluated in a green tea infusion system over 10 h, using 100 µL (250 units ABTS-based) of the preparation, with detailed analysis focused on the initial 0–6 h period, during which the most significant biochemical transformations occurred (Table 5.9, Figure 5.13). EGCG concentration decreased from 848.98 ± 42.45 µg/mL at 0 h to 117.27±9.77 µg/mL at 10 h, corresponding to an 86.2% reduction. Similar declines were

observed for EGC, EC, and GCG. Gallic acid showed a transient increase followed by a gradual decline, consistent with degallation of catechins. Theaflavins appeared within 1–2 h, peaked between 3–5 h, and subsequently declined, mirroring their transient role in classical black tea fermentation (Haslam, 2003; Tanaka & Matsuo, 2020).

Table 5.9: Changes in major catechins, theaflavins, caffeine, color development (A_{420}), and Briskness Index during the initial 0–6 h of enzymatic oxidation of green tea infusion by the MPLO enzyme preparation.

Time (h)	EGCG (µg/mL)	EGC (µg/mL)	ECG (µg/mL)	EC (µg/mL)	Gallic acid (µg/mL)	Total TF (µg/mL)	Caffeine (µg/mL)	A_{420}	Briskness Index (%)	TR (%)	TB (%)
0	848.98 ±42.45^{a}	442.38 ±22.12^{a}	137.40 ±6.87^{a}	98.33± 4.92^{b}	14.17± 0.71^{c}	0^{c}	233.89 ±11.69^{a}	0.534^{d}	0^{c}	0.03^{d}	0.10^{d}
1	811.27 ±40.56^{a}	433.94 ±21.70^{a}	137.27 ±6.86^{a}	92.87± 4.64^{c}	13.81± 0.69^{c}	2.02^{c}	232.85 ±11.64^{a}	0.582^{c}	0.86^{b}	1.25^{c}	1.14^{cd}
2	644.09 ±32.20^{b}	360.33 ±18.02^{c}	122.15 ±6.11^{b}	79.23± 3.96^{d}	15.78± 0.79^{b}	6.25^{a}	226.88 ±11.34^{b}	0.641^{c}	2.68^{a}	2.05^{b}	1.17^{c}
3	524.36 ±26.22^{c}	378.21 ±18.91^{b}	120.69 ±6.03^{b}	88.71± 4.44^{c}	17.55± 0.88^{a}	8.09^{a}	221.78 ±11.09^{b}	0.712^{b}	3.52^{a}	2.32^{ab}	1.21^{bc}
5	478.41 ±23.92^{c}	387.08 ±19.35^{b}	121.48 ±6.07^{b}	95.44± 4.77^{b}	19.34± 0.97^{a}	7.96^{a}	220.69 ±11.03^{b}	0.816^{a}	3.48^{a}	2.34^{a}	1.24^{b}
6	343.14 ±17.16^{d}	408.60 ±20.43^{b}	123.97 ±7.20^{a}	102.81 ±5.14^{a}	12.38± 0.62^{c}	8.01^{a}	226.18 ±11.31^{b}	0.845^{a}	3.42^{a}	2.38^{a}	1.45^{a}
10	117.27 ±9.77^{e}	118.50 ±20.43^{d}	93.97± 7.20^{c}	67.84± 5.14^{e}	10.38± 0.62^{d}	4.51^{b}	224.05 ±10.87^{b}	1.442^{a}	2.82^{a}	4.02	4.43

Values are expressed as mean ± SD (n = 3). Different superscript letters within the same column indicate statistically significant differences ($p < 0.05$).

Thearubigin content increased progressively from 0.03% to 2.38% over 6 h, while theabrownin accumulated more slowly (0.10% to 1.45%). As these fractions were estimated using spectrophotometric partitioning rather than direct structural quantification, the reported percentages should be interpreted as relative indices of oxidation-associated pigment formation rather than absolute concentrations of chemically defined compounds. The moderate theabrownin formation within the 0–6 h window supports this interval as an optimal reaction period.

Pearson correlation analysis revealed statistically significant relationships between polyphenol degradation, enzyme activity, and pH. EGCG, EGC, and EC showed strong positive correlations with pH ($r = 0.90–0.96$, $p < 0.01$). ABTS activity correlated positively with GCG and gallic acid, while L-DOPA activity declined as pH decreased, suggesting its greater pH sensitivity (Fernandez-Julia et al., 2021).

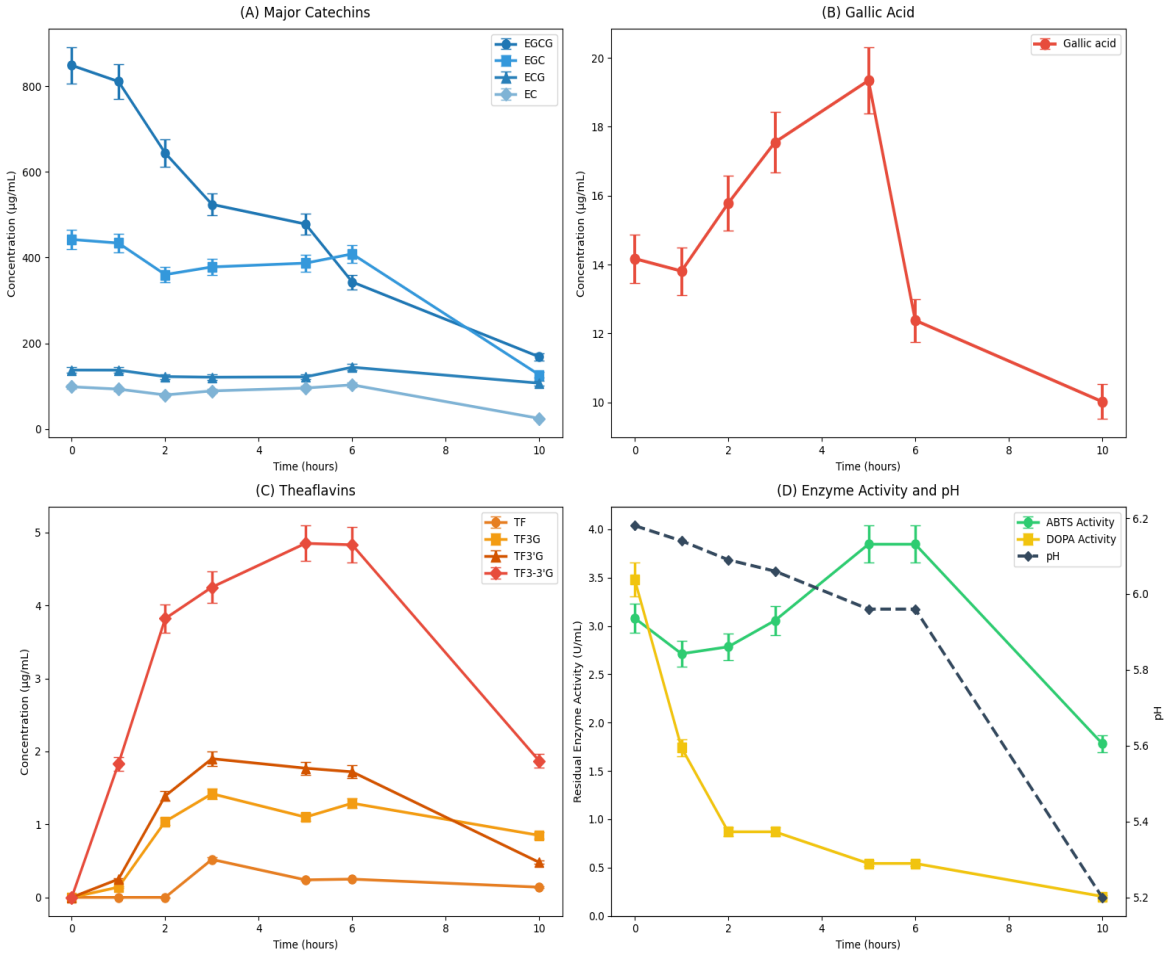

Figure 5.13: Time-course profiles of enzymatic oxidation using the MPLO preparation from *Alcaligenes faecalis* in green tea matrix over 10 hours. (A) Degradation of major catechins, (B) Trend of gallic acid, (C) Formation of individual theaflavins, and (D) Residual ABTS and L-DOPA activities with corresponding pH changes. Error bars represent ± standard deviation (n=3).

The initial 0–6 h period encompassed the most significant transformations, including rapid catechin depletion, peak theaflavin formation, and progressive color development (Figure 5.14 A&B). Within this window, the reaction reached a functional optimum at approximately 5 h, characterized by high theaflavin levels, a 53% increase in absorbance at 420 nm, and a Briskness

Index of 3.48% under moderately acidic conditions (pH 5.96). This value is substantially lower than the normal commercial range reported for fully processed CTC black tea (above 23%; UPASI TRI TRF, 2026), consistent with the short, partial, lab-scale nature of this reaction relative to an extensively optimized industrial fermentation process.

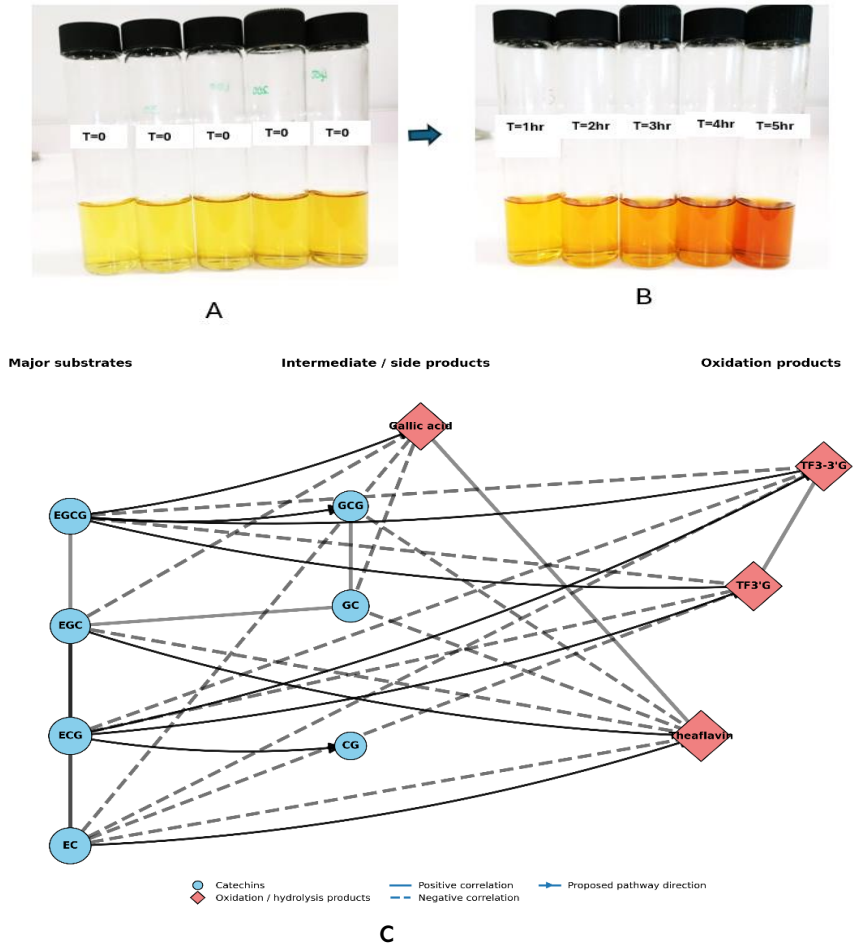

Figure 5.14: Visual progression of enzymatic oxidation of green tea infusion by the MPLO enzyme preparation from *Alcaligenes faecalis* NZRM 836. (A) The initial reaction mixture at 0 h, showing a pale-yellow color. (B) Time-dependent color development from 1 to 5 h, illustrating the transition from yellow to orange-brown associated with the formation of theaflavins and related oxidation-associated metabolites. (C) Proposed reaction network showing major substrates (blue circles), intermediates/side products (light blue), oxidation-associated metabolites (red diamonds), positive correlations (solid blue lines), negative correlations (dashed grey lines), and proposed pathway directions.

This optimum was further validated using Derringer's desirability function, the same multi-response optimization approach applied in the RSM analysis (Section 5.3.2), combining five

independent criteria (TF:TR ratio, Briskness Index, color development, gallic acid concentration, and pH stability) into a single composite score at each sampled timepoint (Table S5.11). The 5 h timepoint achieved the highest composite desirability (D = 0.925), clearly exceeding both the 3 h (D = 0.811) and 6 h (D = 0.690) timepoints. This result was driven by gallic acid reaching its absolute maximum concentration (19.34 μg/mL) at exactly 5 h, and by pH remaining stable within the 5.9–6.2 range throughout the 0–6 h window before declining sharply to approximately 5.2 by 10 h (Figure 5.13D), confirming that the favorable chemical conditions established by 3 h were maintained, rather than degraded, up to the 5 h mark. Similar optimal windows (3–5 h) have been reported in controlled tea oxidation systems, where balanced catechin oxidation and theaflavin accumulation contribute to desirable sensory attributes (Obanda et al., 2001).

Beyond 5 h, continued incubation resulted in further catechin depletion and a decline in theaflavins, accompanied by increased acidification (pH ~5.20) and reduced enzyme activity. This transition aligns with the conversion of theaflavins into higher-molecular-weight pigments such as thearubigins. The proposed reaction network, constructed based on Pearson correlation coefficients among the quantified metabolites, is presented in Figure 5.14C.

From a quality perspective, the balance between theaflavins, thearubigins, and theabrownins is critical. The dominance of theaflavins and moderate accumulation of thearubigins within the 3–5 h window is associated with desirable brightness, color, and briskness, whereas excessive theabrownin formation is typically linked to duller color and reduced quality.

Overall, the extracellular MPLO enzyme preparation effectively reproduced key oxidative transformations observed in tea fermentation under mild conditions. Its combined laccase-like and o-diphenolase (tyrosinase-like) activities enabled broad oxidation of phenolics. In the green tea matrix, it produced substantial catechin depletion and transient theaflavin formation followed by polymerization, closely mirroring established pathways. The well-defined 5 h reaction window supports the preparation's potential as a controllable laboratory-scale biocatalyst for targeted modification of tea polyphenols and associated functional markers under the conditions tested. Sensory implications remain inferential and require dedicated sensory and volatile validation in future studies.

5.4 Conclusions

This chapter demonstrated that a partially purified polyphenol-oxidizing-like oxidoreductase (MPLO) enzyme preparation produced by *A. faecalis* NZRM 836 acts as a multifunctional oxidoreductase system capable of driving controlled biotransformation of green tea catechins. Optimization using response surface methodology enabled simultaneous enhancement of extracellular ABTS-, L-DOPA-, catechol-, and pyrogallol-oxidizing activities, resulting in a balanced oxidation system with complementary catalytic functions.

Biochemical characterization showed distinct substrate-dependent catalytic properties, including acidic pH preference for ABTS oxidation and near-neutral pH preference for L-DOPA oxidation, supporting the coexistence of multiple extracellular oxidoreductase components within the partially purified preparation. The extracellular MPLO system also exhibited relatively high temperature optima and maintained operational stability within the natural pH range of green tea, indicating suitability for controlled tea biotransformation applications.

Application of the MPLO preparation in both a model EGCG system and a green tea matrix demonstrated efficient catechin transformation, characterized by substantial EGCG depletion, transient theaflavin formation, and progressive development of color and briskness. These transformation patterns reproduce key oxidative processes associated with tea fermentation while allowing controlled progression of the reaction

The most favorable transformation profile was achieved within an operational window of approximately 5 h, during which catechin oxidation, theaflavin accumulation, and color development remained balanced. Prolonged incubation beyond this period promoted further oxidation and decline of theaflavins together with increased formation of secondary polymerized pigments, emphasizing the importance of reaction-time control during enzymatic tea processing.

Genome mining of reference *A. faecalis* genomes identified multiple putative blue copper-containing laccase-like multicopper oxidases potentially associated with the observed extracellular MPLO activities, whereas canonical tyrosinase homologs were not detected. These findings support the interpretation that the observed extracellular diphenol-oxidation capacity was primarily associated with broad-substrate-specificity multicopper oxidase systems rather than with classical tyrosinases. However, because whole-genome sequencing was not performed for strain

NZRM 836, definitive assignment of the observed extracellular activities to specific genes or oxidoreductase isoforms remains unresolved. Future genomic sequencing and functional expression studies of NZRM 836 are therefore required to establish direct genotype–phenotype relationships and confirm the molecular basis of the observed MPLO activities.

Overall, this study provides a novel laboratory-scale proof of concept for the use of a co-produced bacterial extracellular oxidoreductase system to enable controlled catechin biotransformation in green tea. The extracellular MPLO preparation, therefore, represents a promising biocatalytic platform for targeted and potentially tunable modification of tea polyphenols and oxidation-associated quality attributes, although future food-related applications will require safety and regulatory assessment, pilot-scale validation, and comprehensive sensory and volatile characterization.

Chapter 6

Controlled biotransformation of tea catechins using microbial polyphenol oxidizing-like enzymes: Comparative metabolomic and functional valuation against green and black tea

Preface

This chapter evaluates the application of the extracellular MPLO preparation for controlled modification of green tea catechins. Changes in metabolite composition, antioxidant properties, enzyme inhibitory activities, pigment formation, and in vitro phenolic bioaccessibility were compared with untreated green tea and conventional black tea systems.

Abstract

Microbial oxidoreductases provide a controlled approach for the oxidative transformation of tea polyphenols. In this study, a partially purified, cell-free extracellular microbial polyphenol-oxidizing-like oxidoreductase (MPLO) preparation, derived from the bacterium *Alcaligenes faecalis* NZRM 836, was applied to green tea extract to achieve partial, controlled oxidative transformation of catechins. The resulting product, MPLO-treated tea (MPLO-T), was compared with untreated green tea (GT) and conventionally processed black tea (BT) in terms of chemical composition, selected functional properties, and *in vitro* digestive behavior.

Quantitative high-performance liquid chromatography with diode array detection (HPLC-DAD) analysis revealed substantial depletion of major catechins in MPLO-T, with epigallocatechin gallate (EGCG) decreasing in GT from 825.13 ± 57.76 µg/mL to 179.22 ± 12.55 µg/mL, together with the appearance of theaflavins. Untargeted liquid chromatography-tandem mass spectrometry (LC-MS/MS) metabolomics indicated that MPLO-T displayed an intermediate oxidative profile between GT and BT.

Despite the marked reduction in catechins, MPLO-T exhibited 2,2-diphenyl-1-picrylhydrazyl (DPPH) radical scavenging activity comparable to that of BT. MPLO-T also showed significantly higher inhibitory activity against α-glucosidase and α-amylase than both GT and BT. Simulated gastrointestinal digestion (INFOGEST protocol) demonstrated higher *in vitro* bioaccessibility of phenolic compounds and greater retention of EGCG in MPLO-T relative to GT. Multivariate analyses (Principal component analysis (PCA) and correlation) indicated associations between oxidation markers (theaflavins, thearubigins, and theabrownins) and enhanced enzyme inhibitory activity as well as bioaccessibility. These results suggest that MPLO-mediated oxidation enables reproducible, selective modification of tea polyphenol profiles, generating a product with an intermediate oxidative character and a distinct functional profile compared with traditional GT and BT.

Keywords: tea catechins, microbial oxidoreductases, controlled oxidation, metabolomics, enzyme inhibition, bioaccessibility

6.1 Introduction

Tea (*Camellia sinensis*) is a globally consumed beverage valued for its sensory properties and health-promoting potential, largely due to its diverse polyphenols and alkaloids, including catechins, theaflavins, gallic acid, caffeine, and theobromine. Notably, green tea retains high levels of native catechins, particularly epigallocatechin gallate (EGCG), epigallocatechin (EGC), epicatechin gallate (ECG), and epicatechin (EC), because endogenous oxidative enzyme activity is minimized during processing (Hilal & Engelhardt, 2007). In contrast, black tea undergoes considerable enzymatic oxidation during fermentation, thereby generating theaflavins, thearubigins, and related oxidation-associated metabolites that contribute to its characteristic color and sensory properties (Obanda et al., 2001; Sang et al., 2011).

Although conventional tea fermentation has been extensively studied, the process remains difficult to control due to variability in enzyme localization, oxygen availability, leaf structure, and processing conditions. These factors limit the ability to achieve consistent and targeted polyphenol transformation (Liang et al., 2003b). Building on the optimization and biochemical characterization presented in Chapter 5, this chapter investigates the application of a partially purified extracellular microbial polyphenol-oxidizing-like oxidoreductase (MPLO) preparation for controlled catechin oxidation in green tea extract.

In this study, MPLO refers operationally to the combined extracellular ABTS-oxidizing (laccase-like), L-DOPA-oxidizing (tyrosinase-like or diphenolase-like), catechol-oxidizing (catechol oxidase-like), and pyrogallol-oxidizing (peroxidase-like) activities detected in the extracellular preparation derived from *Alcaligenes faecalis* NZRM 836. This terminology reflects the functional substrate oxidation profile of the preparation rather than definitive identification of individual purified enzymes.

The resulting MPLO-treated tea (MPLO-T) was compared with untreated green tea (GT) and conventionally processed black tea (BT). MPLO-T was generated directly from the same GT batch used for untreated controls to minimize variation arising from raw material differences, whereas commercial BT was included as a conventionally oxidized reference rather than a directly equivalent processing control.

The objectives of this chapter were to characterize chemical changes induced by MPLO treatment, evaluate selected *in vitro* functional properties, including α-glucosidase and α-amylase inhibitory activities and phenolic bioaccessibility during simulated digestion, and assess relationships between compositional and functional changes using multivariate analyses. Whereas Section 5.3.9 optimized enzyme dose and incubation time using chemical markers alone, this chapter applies that single optimized condition (0.2% v/v, 5 h) to evaluate MPLO-T's broader functional properties, namely metabolomics, antioxidant capacity, enzyme inhibition, and digestibility, against GT and BT.

Although *A. faecalis* is not classified as Generally Recognized as Safe (GRAS), this study used a cell-free, partially purified extracellular preparation obtained through centrifugation, membrane filtration, and ultrafiltration to remove viable bacterial cells prior to application. Safety assessment of food enzymes primarily focuses on the characteristics of the final enzyme preparation rather than solely on the production organism (EFSA FCA Panel et al., 2021; FAO/WHO, 2006).

Collectively, this chapter examines whether controlled extracellular MPLO-associated oxidation can generate an intermediate oxidative profile between GT and BT while preserving selected functional and compositional attributes relevant to tea biotransformation research.

6.2 Materials and methods

6.2.1 Chemicals and reagents

All chemicals were of analytical grade or higher. (+)-Catechin hydrate, gallic acid, Folin–Ciocalteu reagent, sodium carbonate, ninhydrin, 2,2-diphenyl-1-picrylhydrazyl (DPPH), 2,2′-azinobis-(3-ethylbenzothiazoline-6-sulfonic acid) (ABTS), Trolox, and chloramphenicol were obtained from Sigma-Aldrich (St. Louis, MO, USA). HPLC- and LC–MS-grade methanol, acetonitrile, and formic acid were purchased from Fisher Scientific (Waltham, MA, USA). Ammonium formate was obtained from Merck (Darmstadt, Germany). Ultrapure water (18.2 MΩ·cm) was produced using a Milli-Q water purification system (Millipore, Billerica, MA, USA).

Commercial assay kits for α-glucosidase (ab284520) and α-amylase (ab283391) inhibition were obtained from Abcam (Cambridge, UK).

6.2.2 Instruments and analytical equipment

All analytical measurements were performed using calibrated laboratory instruments. UV–Vis absorbance measurements were conducted using a UV-3600 spectrophotometer (Shimadzu, Tokyo, Japan). Microplate-based assays were performed using a Varioskan LUX multimode microplate reader (Thermo Scientific, Waltham, MA, USA) operated through SkanIt PC software (Research Edition).

Chromatographic analysis of non-volatile compounds was carried out using a Vanquish HPLC system (Thermo Fisher Scientific, Waltham, MA, USA) equipped with a binary solvent pump, autosampler, column oven, and diode array detector. High-resolution metabolite profiling was performed using an Accela 1250 UHPLC system (Thermo Scientific, Waltham, MA, USA) coupled to a Q Exactive Orbitrap mass spectrometer with a heated electrospray ionization (HESI) source.

Protein quantification was conducted using a Qubit 4 Fluorometer with the Qubit Protein Assay Kit (Invitrogen, Thermo Fisher Scientific, Waltham, MA, USA). Electrophoretic analyses were performed using a Mini-PROTEAN Tetra vertical electrophoresis system (Bio-Rad Laboratories, Hercules, CA, USA).

Centrifugation steps were carried out using an X1 Pro benchtop refrigerated centrifuge (Thermo Scientific, Waltham, MA, USA). Incubation and agitation experiments were performed using a MaxQ™ 6000 shaking incubator (Thermo Scientific, Waltham, MA, USA) operated at the specified temperatures and agitation rates. Additional temperature-controlled procedures were conducted using standard laboratory water baths.

Chromatographic data acquisition, instrument control, and calibration for HPLC analysis were performed using Chromeleon software (Thermo Fisher Scientific, Waltham, MA, USA). LC–MS data acquisition was conducted using Xcalibur software (Thermo Scientific). Metabolomics data processing was performed using MS-DIAL (v5.5.260323), and statistical and multivariate analyses were carried out using MetaboAnalyst.

6.2.3 Microorganism and enzyme preparation

The bacterium *A. faecalis* NZRM 836 was used to produce the extracellular microbial polyphenol-oxidizing-like oxidoreductase (MPLO). Cultures were maintained on nutrient agar at 4 °C and subcultured periodically. MPLO-associated activity production was performed in tryptic soy broth (TSB) under the optimized conditions described in Chapter 5. The global optimum had a desirability value of 0.953 and used 101 µM catechin, 245 µM $CuSO_4$, 74 h of cultivation at 37 °C, and agitation at 150 rpm.

Following incubation, the extracellular fraction (cell-free fraction containing secreted proteins) was obtained by centrifugation at 10,000 × g for 15 min at 4 °C to separate cells from the supernatant, followed by filtration through 0.22 µm membranes to remove residual bacteria. The clarified extracellular fraction was then concentrated by ultrafiltration using a 10-kDa molecular-weight cut-off membrane to generate the partially purified extracellular MPLO preparation for subsequent tea oxidation experiments.

The extracellular MPLO preparation had a mean ABTS-oxidizing activity of 245.3 ± 18.6 U/mL (n = 3) and a protein concentration of 20.04 mg/mL. This corresponded to a specific activity of 12.24 U/mg protein. Sterility of the extracellular preparation was verified by plating aliquots on nutrient agar and incubating at 37 °C to confirm the absence of microbial growth.

Enzyme activity was determined using the ABTS oxidation assay described in Chapter 5. One unit (U) of ABTS-oxidizing activity was defined as the amount of extracellular preparation required to oxidize 1 µmol of ABTS per minute. Activity was monitored spectrophotometrically at 420 nm under the assay conditions.

6.2.4 Preparation of tea samples

Fresh leaves of *C. sinensis* (two leaves and a bud stage) were handpicked from Somerset Estate, Nuwara Eliya, Sri Lanka (6.9497° N, 80.7891° E) and used for the preparation of green tea. The leaves were washed with distilled water and steamed for 15 min to inactivate endogenous enzymes (Maliepaard, 2009). The material was then freeze-dried and finely milled using a coffee grinder (Breville, New Zealand) to obtain a uniform powder.

Commercial black tea samples were similarly ground to a fine powder prior to analysis. The moisture content of both green and black tea samples was determined by measuring mass loss at 103 °C according to the ISO 1573 method (ISO, 1980). Sample weights were subsequently adjusted to a dry weight basis to ensure comparability between tea types. All sample weights were normalized on dry weight basis prior to extraction to improve comparability among treatments

Green tea and black tea were extracted on a dry-weight basis to ensure comparability between samples. The dry matter content of each tea was determined, and the corresponding fresh weight required to obtain 2.5 g dry weight (DW) was calculated. The measured fresh weights were 2.5 g DW equivalent for green tea (corresponding fresh weight: 2.56 g) and black tea (corresponding fresh weight: 2.55 g). Each sample was extracted with 250 mL of boiling distilled water (100 °C) for 10 min. The infusions were cooled to room temperature and centrifuged at approximately 7000 × g for 10 min. The resulting supernatants were filtered through 0.22 µm membrane filters to remove residual particulates. The clarified extracts were stored at −20 °C until further analysis.

MPLO-treated tea (MPLO-T) was prepared using the same GT extract batch to minimize variation due to raw-material differences. The partially purified extracellular MPLO preparation described in Section 6.2.3 was added to the GT extract at 0.2% (v/v) and incubated at 50 °C for 5 h under controlled conditions optimized in Chapter 5 (Section 5.3.9). Incubation was performed using a MaxQ™ 6000 shaking incubator (Thermo Scientific, Waltham, MA, USA) at 150 rpm. The reaction was terminated by heating at 80 °C for 10 min, consistent with established enzyme inactivation practice in aqueous systems, where this exact temperature–time combination has been confirmed via residual-activity assay to achieve complete inactivation (Le Maux et al., 2017). The resulting MPLO-T extract was centrifuged, filtered through 0.22 µm membranes, and stored at −20 °C until further analysis.

Commercial BT was included as a conventionally oxidized reference sample rather than as a directly equivalent processing control because it represents an industrially leaf-fermented product generated under manufacturing conditions distinct from the extract-based MPLO treatment system.

6.2.5 Chemical composition analysis

6.2.5.1 Determination of tea polyphenols

Total tea polyphenol content was determined using the Folin–Ciocalteu colorimetric assay, a widely used method for estimating total phenolic content in plant-derived extracts (Johnson et al., 2023; Singleton et al., 1999). Because the Folin–Ciocalteu assay is based on overall reducing capacity, the results represent total reducing phenolic equivalents rather than absolute concentrations of individual phenolic compounds.

Briefly, 1 mL of sample or gallic acid standard solution (0–100 mg/L) was transferred into a 10 mL volumetric flask, followed by the addition of 5 mL of Folin–Ciocalteu reagent (10%, v/v). After 5 min, 4 mL of sodium carbonate solution (7.5%, w/v) was added. The mixture was allowed to react at room temperature for 60 min, and absorbance was measured at 765 nm using a UV–Vis spectrophotometer (UV-3600, Shimadzu, Tokyo, Japan). Results were expressed as mg gallic acid equivalents (GAE) per mL of infusion.

6.2.5.2 Determination of free amino acids

The total concentration of free amino acids in tea infusions was determined using the ninhydrin colorimetric method (Yemm et al., 1955). L-Theanine was used as the calibration standard, and results are expressed as theanine equivalents rather than as a complete amino acid profile. This assay, therefore, provides an estimate of total free amino acid-associated content rather than direct quantification of individual amino acids. L-theanine was selected because it is the predominant free amino acid in *C. sinensis* and is commonly used as a representative compound in tea amino acid analysis (Horanni & Engelhardt, 2013).

Briefly, 1 mL of sample or L-theanine standard solution (0–0.9 mg/mL) was transferred into a 25 mL volumetric flask, followed by the addition of 0.5 mL of phosphate buffer (pH 8.0) and 0.5 mL of 2% (w/v) ninhydrin solution. The reaction mixture was heated in a boiling water bath for 15 min, cooled to room temperature, and diluted to volume with distilled water. After standing for 10 min, absorbance was measured at 570 nm using a UV–Vis spectrophotometer. Results were expressed as mg theanine equivalents per mL of infusion.

6.2.5.3 Determination of total reducing sugars

Total reducing sugars were determined using the 3,5-dinitrosalicylic acid (DNS) colorimetric method (Miller, 1959), adapted to a microplate format, and supported by recent applications in food analysis (Goncalves et al., 2021). Glucose and fructose are the principal reducing sugars in tea leaves; maltose served as the calibration standard, with results expressed as maltose equivalents. Tea extracts were diluted appropriately and centrifuged to obtain clear supernatants before analysis. Briefly, 150 µL of sample or maltose standard solution (0–3 mg/mL) was mixed with 75 µL of DNS reagent and heated in a boiling water bath for 15 min. The reaction was rapidly cooled in an ice bath, followed by the addition of 675 µL of distilled water to stabilize the color. An aliquot of 200 µL of the reaction mixture was transferred to a 96-well microplate, and absorbance was measured at 540 nm using a microplate reader. A calibration curve was constructed using maltose standards, and reducing sugar content was calculated from the linear regression equation. Results were expressed as mg maltose equivalents per mL of extract or per g of dry tea sample.

6.2.6 Chromatographic and metabolomic analysis

6.2.6.1 HPLC-DAD analysis of non-volatile compounds and spectrophotometric quantification of tea pigments

Non-volatile compounds were quantified using high-performance liquid chromatography with diode-array detection (HPLC–DAD) on a Hypersil GOLD C18 column (150 × 2.1 mm, 2.6 µm; Thermo Scientific, Waltham, MA, USA). Detection was performed at 210 nm and 280 nm.

The mobile phase consisted of solvent A (0.1% v/v formic acid in Milli-Q water) and solvent B (acetonitrile). The column was maintained at 25 °C, with a flow rate of 0.3 mL/min and an injection volume of 10 µL.

The gradient elution program was as follows: 8–11% B (0–5 min), 11–20% B (5–10 min), 20% B (10–16 min), 20–28% B (16–25 min), 28–30% B (25–30 min), 30–35% B (30–34 min), 35–90% B (34–36 min), followed by 90% B (36–39 min) and re-equilibration to initial conditions (8% B) for 6 min.

Quantification was performed using external calibration curves prepared with authentic standards. The standards used were gallic acid, theobromine, gallocatechin (GC), epigallocatechin (EGC), epicatechin (EC), epigallocatechin gallate (EGCG), epicatechin gallate (ECG), gallocatechin gallate (GCG), catechin gallate (CG), theaflavin (TF), theaflavin-3-gallate (TF3G), theaflavin-3′-gallate (TF3′G), theaflavin-3,3′-digallate (TF3-3′G), rutin, kaempferol, quercetin, and myricetin. Calibration curves, concentration ranges, correlation coefficients (R^2), limits of detection (LOD), and limits of quantification (LOQ) are provided in Supplementary Table S6.1 (Appendix E).

Tea pigments (TFs, TRs and TBs) were also estimated spectrophotometrically using the solvent-partitioning method of Wang et al. (2011), as described in Section 5.2.15, with the sequential extraction steps detailed in Section 4.2.7.2. Briefly, four solutions (A–D) were prepared from each infusion by partitioning between ethyl acetate, sodium bicarbonate (2.5%, w/v), *n*-butanol and saturated oxalic acid, and diluted with 95% ethanol. Absorbance (E_A–E_D) was read at 380 nm in a 1-cm cell, and TFs, TRs and TBs (%) were calculated using Equations 5.6–5.8, normalized to the dry weight of tea in the infusion analyzed (2.5 g DW per 250 mL; Section 6.2.4). All measurements were performed in triplicate. Because this method separates pigment classes by partitioning behavior, TR and TB values are relative indices of oxidation-associated pigment formation rather than absolute concentrations. They allow comparison among GT, MPLO-T and BT analyzed under identical conditions but are not directly comparable with gravimetric or other fractionation-based estimates in the literature.

6.2.6.2 LC–MS/MS metabolite profiling

Untargeted metabolite profiling was performed using an Accela 1250 UHPLC system coupled to a Q Exactive Orbitrap mass spectrometer equipped with a heated electrospray ionization (HESI) source (Thermo Scientific, Waltham, MA, USA). Samples were introduced using a PAL autosampler with an injection volume of 5 µL. Chromatographic separation was achieved on a Hypersil GOLD C18 column (150 × 2.1 mm, 2.6 µm; Thermo Scientific, Waltham, MA, USA). The mobile phase consisted of deionized water containing 0.1% formic acid (eluent A) and acetonitrile (eluent B), with a flow rate maintained at 300 µL/min. The gradient elution program was as follows: 8–11% B (0–5 min), 11–20% B (5–10 min), 20% B (10–16 min), 20–28% B (16–

25 min), 28–30% B (25–30 min), 30–35% B (30–34 min), 35–90% B (34–36 min), followed by 90% B (36–39 min) and a 6 min re-equilibration period.

Mass spectrometric detection was carried out using the HESI source operating in both positive and negative ionization modes. The spray voltage was set at 3.5 kV in positive mode and 3.0 kV in negative mode. The capillary temperature was maintained at 325 °C, and the probe heater temperature was set at 250 °C. Sheath gas, auxiliary gas, and spare gas flow rates were set at 40, 10, and 5 arbitrary units, respectively. The S-lens RF level was 50, and the maximum spray current was 100. Data acquisition was performed in full scan MS^1 mode and parallel reaction monitoring (PRM) mode. Full scan MS^1 spectra were acquired over a mass range of m/z 100–1500.

Quality control (QC) samples were prepared by pooling equal volumes of all study samples and were injected every 5–6 samples throughout the analytical batch to monitor instrument performance and correct for signal drift. Blank samples (solvent only) were injected regularly to assess carry-over and enable blank subtraction. Raw data were processed using MS-DIAL (version 5.5).

6.2.6.3 Data processing and multivariate chemometric analysis

The aligned feature matrix generated in MS-DIAL was exported for subsequent statistical and multivariate analyses. Data were log-transformed and auto-scaled prior to analysis to reduce heteroscedasticity and improve comparability among metabolites with different abundance ranges.

Principal component analysis (PCA) and heatmap visualization were performed using Python 3.14, incorporating the libraries NumPy, SciPy, pandas, scikit-learn, matplotlib, and seaborn. PCA was used to evaluate clustering patterns and compositional differences among GT, MPLO-T, and BT samples.

Metabolite annotation followed established metabolomics reporting guidelines (Salek et al., 2013; Sumner et al., 2007). Detected features were classified into three confidence levels. Level 1 corresponded to compounds confirmed using authentic reference standards based on matching retention time, accurate mass, and MS/MS fragmentation patterns. Level 2 included putatively annotated compounds identified through spectral matching against databases and comparison with published literature. Level 3 represented putatively characterized compound classes for which

structural information could be inferred from mass spectral features but could not be assigned to a specific compound. This classification framework was used to distinguish experimentally confirmed metabolites from tentative or putative annotations and to avoid overinterpretation of untargeted metabolomics data.

6.2.7 Antioxidant activity evaluation

6.2.7.1 DPPH free radical scavenging activity

The antioxidant capacity of tea extracts was evaluated using the 2,2-diphenyl-1-picrylhydrazyl (DPPH) radical scavenging assay, based on a modified method of Sembiring et al. (2018). This assay provides an *in vitro* estimate of free radical scavenging capacity based on electron- or hydrogen-donating activity under defined chemical conditions.

This assay is based on the reduction of the stable DPPH radical, which exhibits a strong absorbance at 517 nm. Upon reaction with antioxidant compounds, DPPH is reduced, resulting in decreased absorbance and a visible color change from purple to yellow. A 10 mM stock solution of DPPH was prepared in absolute ethanol and diluted to a 0.1 mM working solution before analysis. In a 96-well microplate, 5 µL of sample at different concentrations (or ethanol as blank) was mixed with 195 µL of DPPH working solution. The mixture was incubated in the dark at room temperature for 30 min, and absorbance was measured at 517 nm using a microplate reader (Varioskan™ LUX, Thermo Scientific, USA). Radical scavenging activity was expressed as percentage inhibition (%RSA) using the following equation (6.1):

$$\%\text{RSA} = \frac{A_{\text{control}} - A_{\text{sample}}}{A_{\text{control}}} \times 100 \quad (6.1)$$

where:

$\mathbf{A_{control}}$ = absorbance of the DPPH solution with ethanol (blank) at 517 nm

$\mathbf{A_{sample}}$ = absorbance of the DPPH solution with the tea extract (sample) at 517 nm

6.2.7.2 FRAP antioxidant activity

The ferric reducing antioxidant power (FRAP) assay was used to evaluate the reducing capacity of tea infusions, following a modified method described by Benzie and Strain (1996). The FRAP

assay estimates antioxidant-associated reducing capacity based on conversion of ferric (Fe^{3+}) to ferrous (Fe^{2+}) ions under acidic conditions and therefore reflects overall reducing potential rather than direct biological antioxidant activity.

Briefly, 100 µL of appropriately diluted sample was mixed with 3 mL of freshly prepared FRAP reagent, consisting of 300 mM acetate buffer (pH 3.6), 10 mM 2,4,6-tripyridyl-s-triazine (TPTZ) solution, and 20 mM ferric chloride solution in a ratio of 10:1:1 (v/v/v). The reaction mixture was incubated at room temperature for 4 min, and absorbance was measured at 593 nm. A calibration curve was constructed using $FeSO_4$, and results were expressed as µmol Fe^{2+} equivalents per g dry weight of tea. The concentration of Fe^{2+} equivalents was determined from the calibration curve of $FeSO_4$. The antioxidant capacity was expressed as µmol Fe^{2+} equivalents per g dry weight (DW) of tea, calculated using the following equation 6.2:

$$FRAP(\mu mol\ Fe^{2+}/gDW) = \left(\frac{A_{sample}-C}{m}\right) \times \frac{V_{total}}{m_{sample}} \quad \textbf{(6.2)}$$

where:

A_{sample}= absorbance of the sample

m= slope of the $FeSO_4$ calibration curve

c= intercept of the calibration curve

V_{total}= total extract volume (L)

m_{sample}= mass of tea sample (g dry weight basis)

6.2.8 *In vitro* enzyme inhibition assays

6.2.8.1 Alpha-glucosidase inhibition assay

α-Glucosidase inhibitory activity was determined using a colorimetric assay kit (ab284520, Abcam, Cambridge, UK) following the manufacturer's instructions with minor modifications. This assay provides an *in vitro* estimate of the ability of tea extracts to interfere with α-glucosidase activity under controlled assay conditions and does not directly predict *in vivo* glycemic responses or physiological efficacy.

The assay is based on the hydrolysis of a synthetic substrate by α-glucosidase, releasing a chromophore measured at 410 nm. Test samples were prepared as concentrated stock solutions and diluted to working concentrations using assay buffer. Aliquots (10 µL) of diluted samples were added to a 96-well clear flat-bottom microplate. Acarbose was used as a positive control inhibitor, while assay buffer served as enzyme and background controls. The enzyme solution was prepared by diluting the supplied α-glucosidase and adding 10 µL to each well, followed by adjustment of the reaction volume to 80 µL with assay buffer. After incubation at room temperature for 15–20 min, 20 µL of the reaction mixture containing the assay buffer and substrate was added to initiate the reaction.

Absorbance was measured kinetically at 410 nm for 60 min at room temperature using a temperature-controlled microplate reader. The rate of reaction (ΔA/min) was calculated from the linear portion of the curve. Percentage inhibition was calculated relative to the enzyme control after subtraction of background absorbance.

6.2.8.2 Alpha-amylase inhibition assay

α-Amylase inhibitory activity was evaluated using a colorimetric assay kit (ab283391, Abcam, Cambridge, UK) according to the manufacturer's instructions. This assay provides a comparative *in vitro* measure of α-amylase inhibition potential and should not be interpreted as direct evidence of physiological glucose-lowering activity. The assay quantifies enzymatic hydrolysis of starch into reducing sugars, detected spectrophotometrically at 405 nm.

Test samples were prepared as concentrated stocks and diluted in assay buffer. A volume of 50 µL of each sample was added to a 96-well microplate. Appropriate controls included an inhibitor control (the manufacturer-supplied positive control inhibitor provided with kit ab283391, the specific composition of which is proprietary and not disclosed by the manufacturer), enzyme control, solvent control, and background control. The α-amylase enzyme solution was prepared by diluting the stock enzyme in assay buffer, and 50 µL was added to each well. After incubation at room temperature for 10 min, 50 µL of diluted substrate solution was added to initiate the reaction.

Absorbance was measured at 405 nm in kinetic mode for 20–25 min at room temperature. Reaction rates were calculated from the linear portion of absorbance versus time plots. Percentage inhibition was determined relative to the enzyme control after background correction.

6.2.8.3 Calculation of inhibitory activity

For both assays, enzymatic activity was expressed as the rate of change in absorbance per minute (ΔA/min). Percentage inhibition was calculated using the following Equation 6.3:

$$\% \text{ Inhibition} = \frac{(\text{Slope}_{EC} - \text{Slope}_{S})}{\text{Slope}_{EC}} \times 100 \qquad \textbf{(6.3)}$$

where:

$Slope_{EC}$= reaction rate of the enzyme control

$Slope_{S}$= reaction rate in the presence of the sample

6.2.9 Simulated gastrointestinal digestion

Simulated gastrointestinal digestion was conducted according to the standardized INFOGEST static *in vitro* digestion protocol, with minor modifications to evaluate the stability, transformation, and bioaccessibility of phenolic compounds in tea samples (Brodkorb et al., 2019; Morales et al., 2025). Because this model represents a simplified *in vitro* digestion system, the results should be interpreted as estimates of digestive stability and bioaccessibility rather than direct measures of *in vivo* bioavailability or intestinal absorption. Three tea preparations were investigated: green tea (GT), black tea (BT), and enzymatically oxidized tea (MPLO-T). The MPLO-T sample was prepared by treating GT infusion with microbial enzyme solution at a concentration of 0.2% (v/v; 400 µL enzyme per 20 mL tea infusion).

For the oral phase, 5 mL of tea infusion was mixed with 5 mL of simulated salivary fluid (SSF, pH 7.0) containing α-amylase (30 U/mL; Sigma-Aldrich, St. Louis, MO, USA). The mixture was adjusted to pH 7.0 and incubated at 37 °C in a shaking water bath at 100 rpm for 2 min. At the end of the oral phase, a 2 mL aliquot was collected, and enzymatic activity was immediately terminated by acidification using hydrochloric acid.

For the gastric phase, 6 mL of the oral bolus was combined with 8 mL of simulated gastric fluid (SGF) containing pepsin (2000 U/mL, final gastric phase activity). The pH was adjusted to 3.0 using 6.0 M HCl, and the mixture was incubated at 37 °C under continuous agitation (100 rpm) for 120 min. Samples (2 mL) were collected at 30, 60, 90, and 120 min. Enzymatic activity was

quenched immediately after sampling by the addition of pepstatin, and samples were rapidly cooled on ice.

For the intestinal phase, 6 mL of gastric chyme (the volume remaining after sequential 2 mL sampling at 30, 60, 90, and 120 min from the 14 mL gastric-phase mixture) was mixed with 8 mL of simulated intestinal fluid (SIF) containing bile salts (10 mM) and pancreatin (providing 2000 U lipase activity/mL of intestinal phase). The pH was adjusted to 7.0 using 1.0 M NaOH, and digestion was performed at 37 °C with continuous shaking at 100 rpm for 120 min. Samples (2 mL) were collected at 30, 60, 90, and 120 min, with an additional sample collected at 240 min to assess extended intestinal stability. Enzymatic reactions were terminated by the addition of a protease inhibitor, and all samples were immediately placed on ice.

All digested samples were centrifuged at 10,000 × g for 10 min at 4 °C and filtered through 0.22 μm membrane filters prior to analysis. The total phenolic content (TPC) was determined using the Folin–Ciocalteu method as described in Section 6.2.4. Individual catechins, theaflavins, caffeine, and phenolic degradation products were quantified using high-performance liquid chromatography (HPLC) as described in Section 6.2.6.1. All experiments were performed in triplicate, and results were expressed as mean ± standard deviation.

To account for the progressive reduction in digestion volume due to sampling, concentrations were corrected by back-calculation. The total amount of each analyte present in the digestion vessel at a given time point was calculated by multiplying the measured concentration by the corresponding digestion volume immediately prior to sampling. To enable direct comparison among time points, values were normalized to the initial phase volume.

The retention (%) of each compound during digestion was calculated relative to the first sampling point of the respective phase using the following equation (6.4):

$$\text{Retention (\%)} = \frac{A_i}{A_{0,\text{phase}}} \times 100 \qquad \textbf{(6.4)}$$

where, A_i is the amount of analyte at time i, and $A_{0,\text{phase}}$ is the amount at the beginning of the phase.

The bioaccessibility (%) of phenolic compounds was determined based on the amount present at the end of the intestinal phase relative to the initial amount in the undigested sample, as shown in Equation 6.5

$$\text{Bioaccessibility (\%)} = \frac{A_{\text{intestinal, final}}}{A_{\text{initial}}} \times 100 \quad \textit{(6.5)}$$

where, $A_{\text{intestinal, final}}$ represents the analyte content at the final intestinal time point (240 min), and A_{initial} corresponds to the initial concentration of the respective compound in the tea infusion prior to digestion.

In this study, bioaccessibility refers operationally to the fraction of compounds remaining soluble and detectable following simulated gastrointestinal digestion and does not imply intestinal uptake or systemic bioavailability.

6.2.10 Statistical analysis

All experiments were performed in triplicate (n = 3), except for the DPPH radical scavenging and enzyme inhibitory assays, which were performed in quadruplicate (n = 4), and results are presented as mean ± standard deviation (SD). Statistical analyses were conducted using Python 3.14, incorporating the libraries NumPy, SciPy, pandas, statsmodels, and scikit-learn.

Differences among sample groups were evaluated using one-way analysis of variance (ANOVA) followed by Tukey's honestly significant difference (HSD) post-hoc test for multiple comparisons. Statistical significance was established at $p < 0.05$. Prior to analysis, data were assessed for normality and homogeneity of variance using the Shapiro–Wilk and Levene's tests, respectively.

For LC–MS-based metabolomics data, peak intensities were log-transformed and auto-scaled prior to multivariate analysis. Principal component analysis (PCA) was performed using the scikit-learn framework to evaluate compositional differences and clustering patterns among GT, MPLO-T, and BT samples. Because the metabolomics component of this study was exploratory in nature and involved a limited number of biological replicates, interpretation focused primarily on comparative trend analysis and metabolite pattern visualization rather than predictive classification. To reduce false-positive associations in metabolomics datasets, multiple hypothesis testing correction was performed using the false discovery rate (FDR) approach based on the Benjamini–Hochberg procedure. Variables with adjusted p-values < 0.05 were considered statistically significant. Graphical outputs, including bar plots, heatmaps, and PCA score plots, were generated using matplotlib and seaborn.

6.3 Results and discussion

6.3.1 Changes in bulk chemical composition (total phenolics, amino acids, and reducing sugars)

The bulk composition of green tea (GT), MPLO-treated tea (MPLO-T), and black tea (BT) differed significantly, indicating that processing altered the chemical balance of the infusions (Table 6.1; Figure 6.1A-C). Overall, MPLO-T showed an intermediate profile between GT and BT, although the extent of change varied depending on the component measured.

Table 6.1: Statistical analysis of compositional parameters.

Parameter	Sample	Mean ± SD	F-value	p-value	η^2 (effect size)
TPC (mg GAE/mL)	GT	0.76 ± 0.04^{a}	6.12	0.035	0.67
	MPLO-T	0.74 ± 0.04^{a}			
	BT	0.71 ± 0.04^{b}			
TFAA (µg/mL)	GT	481.20 ± 55.80^{b}	18.45	0.003	0.86
	MPLO-T	474.30 ± 86.10^{b}			
	BT	257.10 ± 31.20^{a}			
TRS (mg/mL)	GT	0.94 ± 0.01^{a}	412.60	<0.001	0.99
	MPLO-T	0.86 ± 0.01^{b}			
	BT	0.68 ± 0.01^{c}			

Values are expressed as mean ± SD (n = 3). Different superscript letters within the same parameter indicate significant differences among samples ($p < 0.05$) based on one-way ANOVA followed by Tukey's Honestly Significant Difference (HSD) test.

Total phenolic content (TPC) remained statistically comparable between GT and MPLO-T, while BT showed a slight but significant reduction ($F = 6.12$, $p = 0.035$, $\eta^2 = 0.67$). This observation suggests that MPLO treatment altered phenolic structure without substantial loss of overall reducing capacity. Such behavior is consistent with the Folin–Ciocalteu assay, which measures total reducing potential rather than specific phenolic compounds (Singleton et al., 1999). During conventional BT processing, catechins undergo extensive oxidation to theaflavins and thearubigins, which may reduce assay responsiveness despite continued phenolic presence (Haslam, 2003; Sang et al., 2011). The relatively stable TPC observed in MPLO-T therefore

supports the occurrence of controlled phenolic biotransformation rather than extensive oxidative degradation.

Total free amino acids (TFAA) followed a similar pattern, with GT and MPLO-T showing comparable levels, both significantly higher than BT ($F = 18.45$, $p = 0.003$, $\eta^2 = 0.86$). This trend aligns with previous findings that GT retains higher amino acid content, particularly L-theanine, compared to BT (Horanni & Engelhardt, 2013). The reduced TFAA in BT is likely due to amino acid consumption during oxidative and thermal processes, including Strecker degradation and Maillard-type reactions that contribute to flavor development (Friedman et al., 2005; Li et al., 2025a; Rizzi, 1999). In contrast, preservation of TFAA in MPLO-T suggests that the extracellular MPLO preparation promoted comparatively milder oxidative conversion with comparatively limited secondary reactions involving amino compounds.

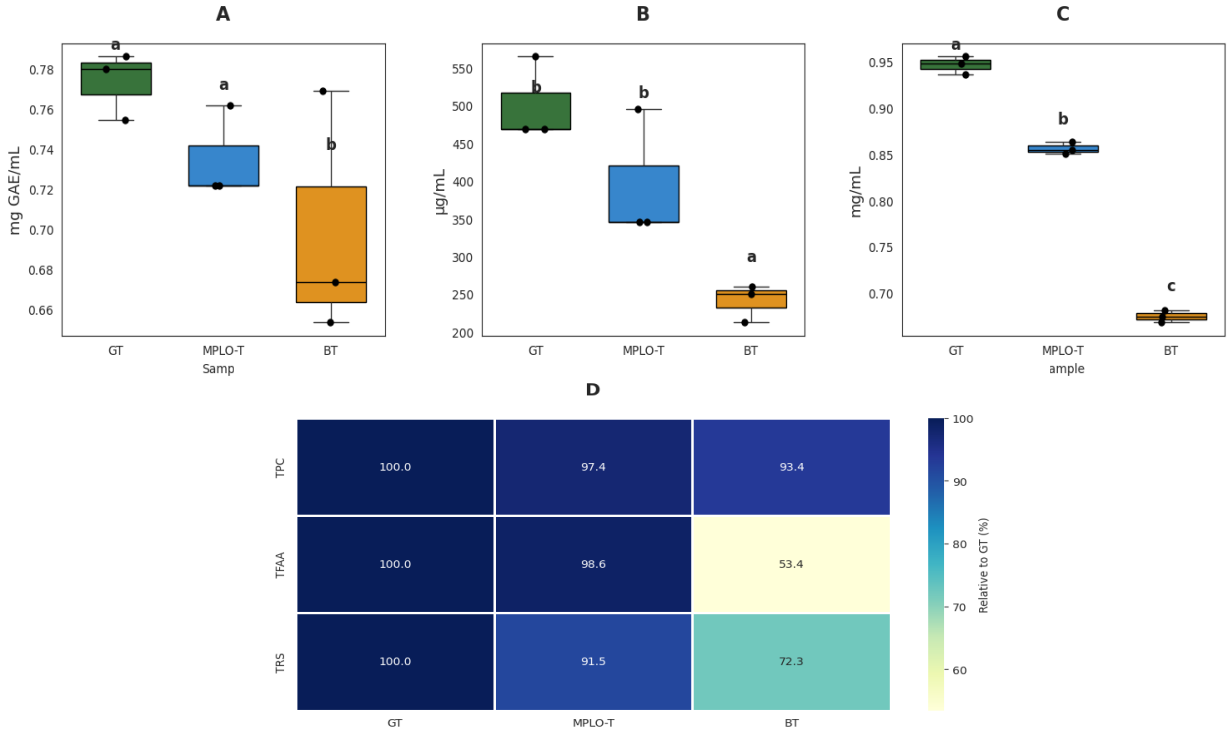

Figure 6.1: Integrated compositional comparison of green tea (GT), MPLO-treated tea (MPLO-T), and black tea (BT). Panels show (A) total phenolic content (TPC), (B) total free amino acids (TFAA), (C) total reducing sugars (TRS), and (D) normalized compositional heatmap expressed relative to GT (GT = 100). Bars in panels A–C represent mean ± SD (n = 3), and different letters indicate significant differences among samples within each parameter at $p < 0.05$.

Total reducing sugars (TRS) exhibited the most pronounced response to processing, decreasing progressively from GT to MPLO-T to BT ($F = 412.6$, $p < 0.001$, $\eta^2 = 0.99$). This indicates that carbohydrates are highly sensitive to processing intensity. The reduction in TRS is consistent with their involvement in oxidative transformations and thermal reactions, including Maillard pathways, which are more extensive in BT production (Sarker et al., 2007). The intermediate TRS level in MPLO-T suggests partial carbohydrate utilization or transformation during extracellular enzymatic treatment while avoiding the more extensive depletion observed in BT.

Multivariate analysis further supported these trends. The normalized compositional heatmap (Figure 6.1D) showed that MPLO-T retained near-GT levels of TPC and TFAA, while displaying a moderate reduction in TRS. Collectively, these findings demonstrate that extracellular MPLO-mediated oxidation selectively modified tea composition while preserving major phenolic- and amino acid-associated characteristics. Compared with conventional BT processing, the MPLO treatment system produced a milder, more controlled oxidative transformation, supporting its potential as a targeted biotransformation strategy to modulate tea composition without extensive depletion of key functional constituents.

6.3.2 MPLO-induced biotransformation of tea metabolites

6.3.2.1 Quantitative profiling of major tea metabolites by HPLC–DAD

Quantitative HPLC–DAD profiling revealed substantial differences in major tea metabolites among green tea (GT), MPLO-treated tea (MPLO-T), and black tea (BT) (Table 6.2). GT was characterized by high concentrations of catechins, particularly epigallocatechin gallate (EGCG), epigallocatechin (EGC), epicatechin gallate (ECG), and epicatechin (EC), consistent with the composition of minimally oxidized tea and previous reports describing GT flavan-3-ol profiles (Hilal & Engelhardt, 2007; Lee et al., 2018).

All major catechins (EGCG, EGC, ECG, and EC) were significantly reduced in MPLO-T relative to GT ($F > 60$, $p < 0.001$), indicating substantial consumption of these substrates during enzymatic treatment. This depletion is evident in Figure 6.2 A, where catechins are enriched in GT and reduced in MPLO-T. Such coordinated loss is consistent with established oxidation systems in tea processing, where catechins undergo enzymatic oxidation to quinones followed by condensation into theaflavins and higher molecular weight products (Deka et al., 2021). Similar catechin

declines associated with enzymatic oxidation and pigment formation have been described for both endogenous and microbial polyphenol oxidase systems (Abudureheman et al., 2022; Sang et al., 2011). In contrast, GC and GCG concentrations increased significantly in MPLO-T relative to GT (Figure 6.2C). These changes are consistent with redistribution within the catechin pool during incubation and may reflect epimerization, differential oxidation susceptibility, or selective enrichment of residual catechin subclasses. However, because the experimental system involved both enzymatic treatment and elevated incubation temperature, the relative contributions of enzymatic versus non-enzymatic transformation cannot be conclusively distinguished from HPLC–DAD data alone.

Table 6.2: Quantitative profiling of major tea metabolites with ANOVA statistics.

Compound	GT (mg/g DW)	MPLO-T (mg/g DW)	BT (mg/g DW)	F-value	p-value
EGCG	83.97 ± 5.87^{a}	18.24 ± 1.28^{c}	8.83 ± 0.62^{d}	187.52	< 0.0001*
EGC	41.67 ± 2.92^{a}	33.79 ± 2.37^{b}	8.65 ± 0.61^{c}	96.84	< 0.0001*
ECG	13.49 ± 0.94^{a}	10.13 ± 0.71^{b}	6.92 ± 0.48^{c}	64.37	< 0.0001*
EC	9.66 ± 0.68^{a}	7.39 ± 0.52^{b}	3.94 ± 0.28^{c}	72.91	< 0.0001*
GC	9.36 ± 0.66^{b}	11.60 ± 0.81^{a}	0.97 ± 0.07^{c}	154.22	< 0.0001*
GCG	1.15 ± 0.08^{b}	1.72 ± 0.12^{a}	0.20 ± 0.01^{c}	118.63	< 0.0001*
CG	0.21 ± 0.01^{c}	0.49 ± 0.03^{a}	0.32 ± 0.02^{b}	92.45	< 0.0001*
Gallic acid	1.68 ± 0.12^{c}	2.31 ± 0.16^{b}	7.05 ± 0.49^{a}	136.08	< 0.0001*
Theaflavin	ND	0.019 ± 0.001^{b}	0.95 ± 0.07^{a}	—	—
TF3′G	ND	0.20 ± 0.01^{b}	0.29 ± 0.02^{a}	58.11	< 0.0001*
TF3-3′G	ND	0.46 ± 0.03^{b}	0.66 ± 0.05^{a}	74.66	< 0.0001*
Rutin	1.80 ± 0.13^{c}	2.89 ± 0.20^{b}	7.09 ± 0.50^{a}	165.77	< 0.0001*
Myricetin	0.27 ± 0.02^{c}	0.58 ± 0.04^{a}	0.33 ± 0.02^{b}	109.34	< 0.0001*
Quercetin	ND	0.021 ± 0.001^{b}	0.098 ± 0.007^{a}	—	—
Caffeine	23.44 ± 1.64^{a}	21.15 ± 1.48^{b}	17.59 ± 1.23^{c}	8.92	0.016 **
Theobromine	4.34 ± 0.30^{a}	2.93 ± 0.21^{b}	1.85 ± 0.13^{c}	45.21	< 0.001
Theophylline	1.11 ± 0.08^{b}	1.37 ± 0.10^{a}	0.39 ± 0.03^{c}	39.87	< 0.001
Theanine	19.34 ± 1.35^{a}	19.80 ± 1.39^{a}	15.28 ± 1.07^{b}	2.11	0.19 (ns)

Values are expressed as mean ± SD (n = 3). Different superscript letters within the same row indicate significant differences between samples ($p < 0.05$). One-way ANOVA was performed to evaluate statistical differences among GT, MPLO-T, and BT. Significance levels are indicated as follows: *$p < 0.05$; **$p < 0.01$; **$p < 0.001$; ns, not significant. ND, not detected.

Theaflavins were not detected in GT but were present in both MPLO-T and BT. Their presence in MPLO-T indicates that oxidation-derived dimeric products were formed during enzymatic treatment. However, concentrations remained markedly lower than in BT. It is important to note

that MPLO-T was generated from a GT extract, whereas BT represents a commercially processed leaf-based product. Although values were normalized to a dry weight basis, differences in matrix structure and processing conditions limit direct quantitative comparison. These results are therefore best interpreted as reflecting relative oxidation extent rather than absolute equivalence.

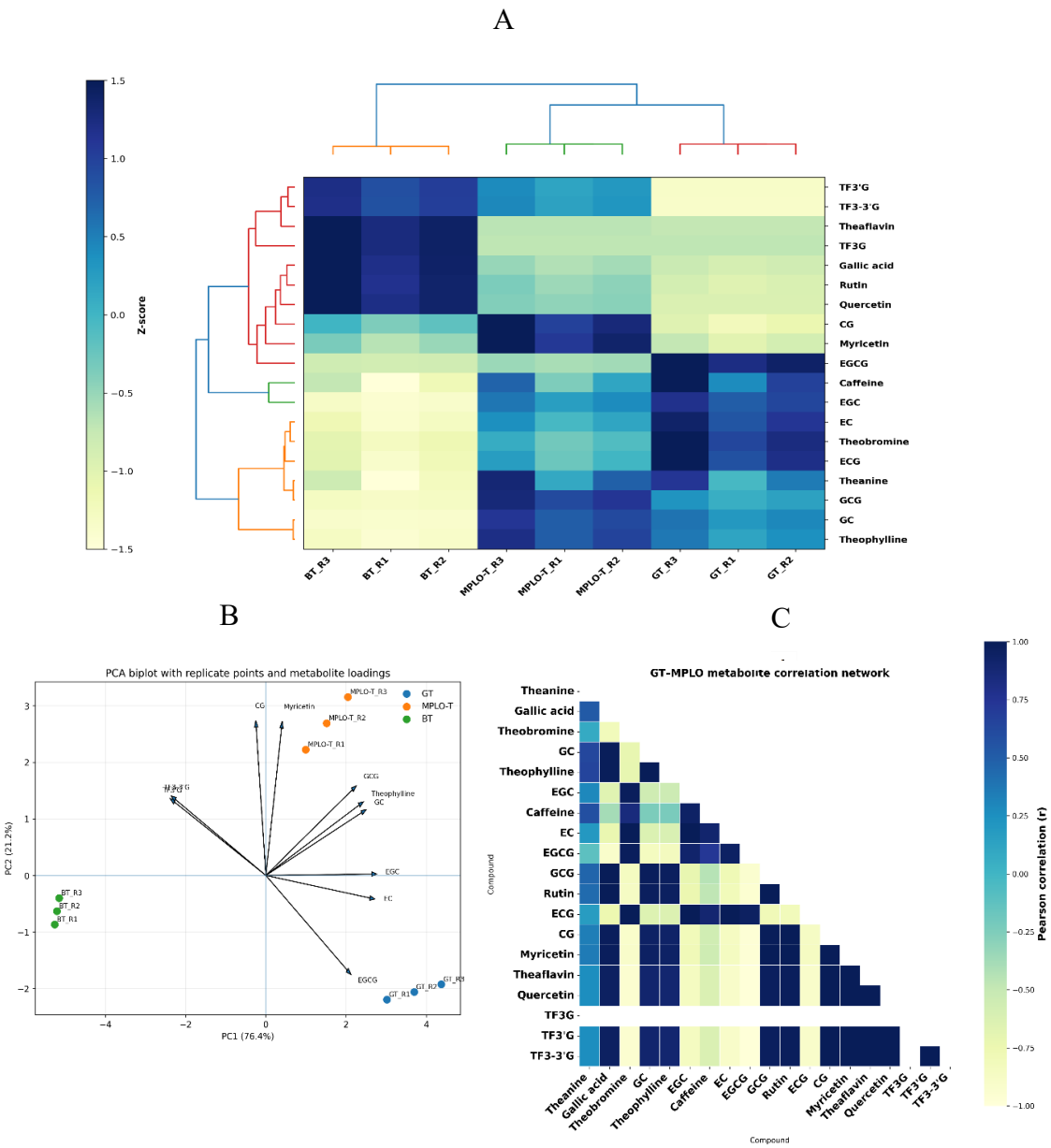

Figure 6.2: Multivariate analysis of green tea (GT) and microbial polyphenol-oxidizing-like oxidoreductase-treated tea (MPLO-T) metabolite profiles showing (A) clustered heatmap of Z-score-normalized data, (B) PCA score plot with loading vectors, and (C) correlogram illustrating metabolite correlations. The analyses collectively demonstrate catechin depletion and formation of oxidation-associated metabolites during MPLO treatment.

Gallic acid increased significantly in MPLO-T relative to GT, while gallated catechins such as EGCG and ECG decreased. This inverse relationship mirrors patterns observed during both plant and microbial polyphenol oxidase-mediated degradation of EGCG, where ester hydrolysis and oxidative cleavage release gallic acid and non-gallated catechins (Abudureheman et al., 2022; Zhang et al., 2019). Although the present HPLC data cannot definitively resolve the sequence of reactions, the compositional association strongly supports a linked transformation between gallated catechins and free gallic acid.

Flavonols, including rutin and myricetin derivatives, were also higher in MPLO-T than in GT. Similar increases in flavonol aglycones or enhanced extractability have been reported during tea processing and have been attributed to cell wall disruption, glycoside hydrolysis, or matrix softening under oxidative or thermal conditions (Lee et al., 2018; Lin et al., 2003). In the context of MPLO-T, this may reflect improved release of flavonols from the leaf matrix during enzymatic treatment rather than *de novo* synthesis.

In contrast, alkaloids such as caffeine and theanine showed minimal variation across GT, MPLO-T, and BT, and contributed little to compositional separation. This stability aligns with previous studies showing that caffeine is largely conserved during BT processing and that theanine is more sensitive to withering and fermentation than to mild oxidative treatments (Deka et al., 2021; Li et al., 2013a).

Overall, the HPLC constrained profiling demonstrates that MPLO treatment induces a distinct yet partial shift in the tea metabolite profile. Catechin depletion, increased GC and GCG, modest theaflavin formation, and elevated gallic acid and flavonols collectively indicate controlled biotransformation that moves the chemical composition of MPLO-T toward a BT-like state without reaching the full extent of conventional fermentation. These findings are consistent with recent work on microbial polyphenol oxidases in tea biotransformation and support the concept of MPLO-T as a chemically intermediate and potentially tunable tea system (Faustina et al., 2022; Li et al., 2022b; Li et al., 2013a).

6.3.2.2 Transformation of tea pigments (thearubigins and theabrownins)

The relative distribution of oxidation-derived pigments is presented in Table 6.3 and Figure 6.3. Because thearubigin (TR) and theabrownin (TB) fractions were estimated using

spectrophotometric partitioning methods, the reported values should be interpreted as relative indices of oxidation-associated pigment formation rather than absolute concentrations of chemically defined compounds.

TR increased markedly with processing. GT exhibited negligible TR, consistent with minimal oxidation, whereas MPLO-T showed a substantial increase, approaching but remaining lower than BT ($p < 0.05$). This progressive increase is evident in Figure 6.3, where TR follows the order GT < MPLO-T < BT. The intermediate TR level in MPLO-T indicates that enzymatic treatment promotes catechin oxidation and condensation into polymeric intermediates but does not fully replicate the extent of transformation achieved during conventional BT fermentation (Haslam, 2003; Roberts & Smith, 1961).

Table 6.3: Thearubigin (TR) and theabrownin (TB) content of tea samples.

Sample	TR (%)	TB (%)
GT	0.08 ± 0.00^{c}	0.09 ± 0.003^{b}
BT	2.27 ± 0.15^{a}	1.33 ± 0.11^{a}
MPLO-T	2.01 ± 0.10^{b}	1.34 ± 0.03^{a}

Values are expressed as mean ± SD (n = 3). Different superscript letters within the same column indicate significant differences among samples ($p < 0.05$) based on one-way ANOVA followed by Tukey's Honestly Significant Difference (HSD) test.

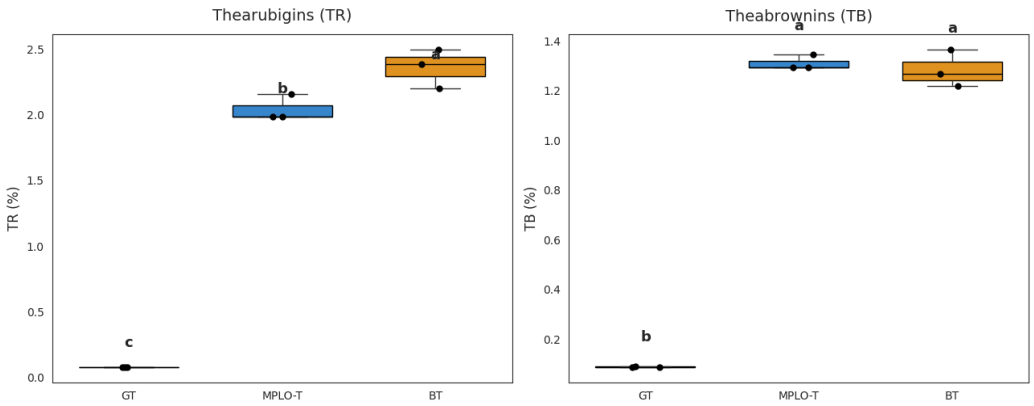

Figure 6.3: Thearubigin (TR) and theabrownin (TB) contents (%) of green tea (GT), MPLO-treated tea (MPLO-T), and black tea (BT). Values are expressed as mean ± SD (n = 3). Different letters indicate significant differences within each parameter ($p < 0.05$).

The absolute TR values here (2.27% in BT) are lower than the 10–20% of dry weight commonly reported for black tea, because the spectrophotometric partitioning method used (Section 6.2.6.1)

captures only the fraction extracted into the assay's aqueous layer and applies a calibration specific to that method. Values are therefore comparable across the three teas but not with literature gravimetric estimates.

Total free amino acids (TFAA) followed a similar pattern, with GT and MPLO-T showing comparable levels, both significantly higher than BT ($F = 18.45$, $p = 0.003$, $\eta^2 = 0.86$). This trend aligns with previous findings that GT retains higher amino acid content, particularly L-theanine, compared to BT (Horanni & Engelhardt, 2013). The reduced TFAA in BT is likely due to amino acid consumption during oxidative and thermal processes, including Strecker degradation and Maillard-type reactions that contribute to flavor development (Friedman et al., 2005; Li et al., 2025a; Rizzi, 1999). In contrast, preservation of TFAA in MPLO-T suggests that the extracellular MPLO preparation promoted comparatively milder oxidative conversion with comparatively limited secondary reactions involving amino compounds.

Overall, the results demonstrate that extracellular MPLO treatment induced a distinct oxidative pigment profile characterized by intermediate TR accumulation and substantial TB formation. This combination suggests controlled progression along the catechin oxidation pathway, generating a pigment composition that was chemically differentiated from both catechin rich GT and conventionally fermented BT.

6.3.2.3 Non-targeted LC–MS metabolomics

Untargeted LC–MS analysis revealed substantial differences in the metabolite composition of GT, MPLO-T, and BT, suggesting progressive chemical modification during oxidation. Following data filtering and annotation, approximately 124 metabolites were retained, with the dataset dominated by polyphenolic compounds and their derivatives. The list of identified metabolites is given in Table S6.2 (Appendix E). The class distribution (Figure 6.4) indicated that catechins, flavonoids, phenolic acids, and oxidation-associated metabolites constituted the major chemical groups, consistent with recent tea metabolomics studies reporting that oxidation shifts the metabolome from monomeric catechins toward structurally diverse phenolic derivatives (Su et al., 2024a). The metabolite classification map further demonstrated enrichment of flavonoid glycosides, catechin gallates, hydrolyzable tannins, and oxidation-associated intermediates, highlighting the chemical diversity generated during controlled enzymatic oxidation.

Principal component analysis (PCA) showed clear separation among the three tea types (Figure 6.5), with GT distinctly clustered due to its high catechin content. While MPLO-T and BT were separated along the primary axis of variation, reflecting the transition toward oxidation-derived metabolite profiles. The intermediate positioning of MPLO-T between GT and BT indicates that enzymatic treatment altered the metabolome substantially but did not fully reproduce the compositional state of conventional BT, a pattern that has also been observed in controlled or partial oxidation systems (Chen et al., 2021; Zhou et al., 2022). These differences carry plausible sensory implications: GT's high catechin content aligns with sharper astringency, while MPLO-T and BT's oxidation-derived metabolites favor reduced astringency and greater color and briskness, with MPLO-T's intermediate profile suggesting an intermediate sensory character. This inference is not sensory-tested and warrants future validation.

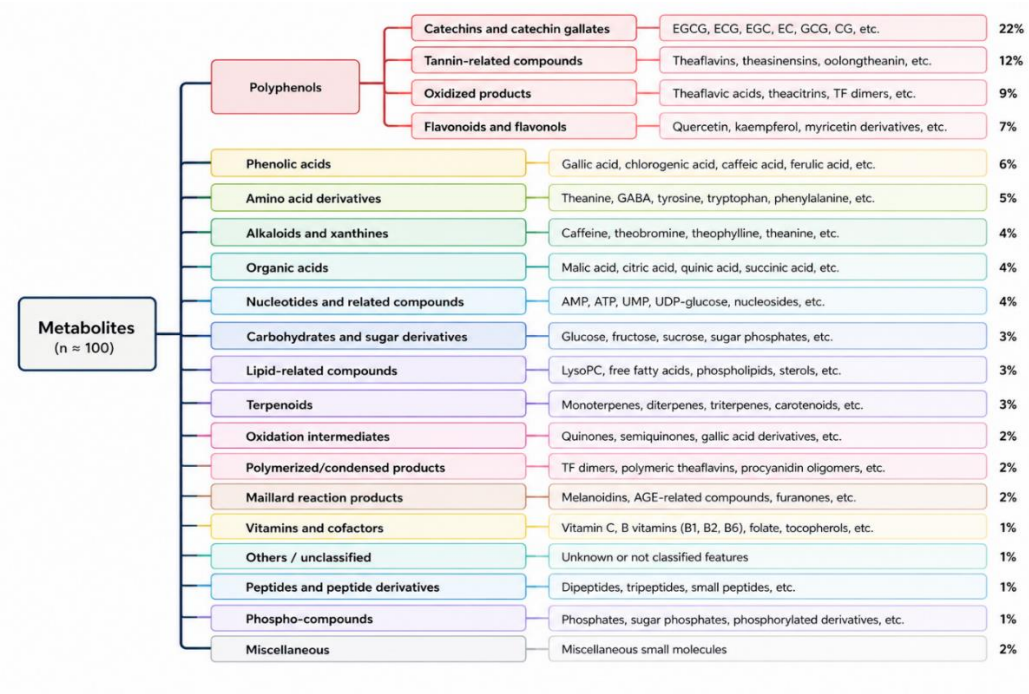

Figure 6.4: Distribution of metabolite classes identified in green tea (GT), MPLO-treated tea (MPLO-T), and black tea (BT) based on untargeted LC–MS profiling. Compounds are grouped into major chemical classes, including catechins, flavonoids, phenolic acids, alkaloids, and oxidation-associated metabolites. Percentages represent the relative abundance of each class within the annotated dataset after filtering and alignment. This classification provides an overview of the compositional diversity and highlights the predominance of polyphenolic compounds across samples.

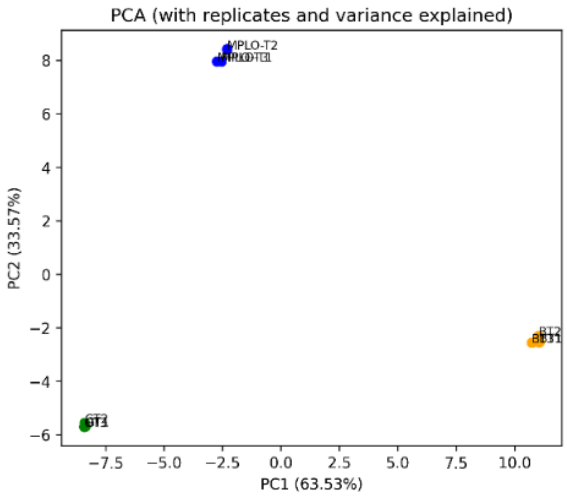

Figure 6.5: Multivariate analysis of LC–MS metabolomic profiles of green tea (GT), MPLO-treated tea (MPLO-T), and black tea (BT). Principal component analysis (PCA) score plot showing unsupervised separation of samples based on major sources of variance.

These multivariate trends were further supported by heatmap analysis (Figure S6.1, Appendix E), in which GT showed a high relative abundance of catechins, BT was enriched in oxidation-associated metabolites, and MPLO-T displayed a mixed profile characterized by reduced catechin abundance and increased levels of oxidation-derived intermediates. The clustered catechin biotransformation heatmap (Figure 6.6) further resolved these relationships, showing coordinated depletion of native catechins together with accumulation of theaflavins, catechin dimers, gallated oxidation products, and downstream phenolic degradation metabolites in MPLO-T and BT. Hierarchical clustering grouped metabolites based on progressive oxidation behavior, separating early-stage catechins from intermediate- and advanced-oxidation-associated products.

In agreement with HPLC quantification, major catechins such as EGCG (m/z 457.08), ECG (m/z 441.08), EGC (m/z 305.07), gallocatechin, and catechin were most abundant in GT and showed marked reductions in MPLO-T, confirming their role as primary substrates during oxidation. Metabolites associated with oxidative transformation, including theaflavin (TF1), TF3G, TF3′G, TF3-3′G, neotheaflavin, theasinensin C, theasinensin F, and hydroxytheaflavin or degalloyl-oolongtheanin, exhibited higher relative abundance in MPLO-T and BT. The presence of these compounds indicates that enzymatic treatment promoted oxidative coupling reactions that generated structurally more complex phenolics, consistent with established catechin oxidation chemistry (Kuhnert, 2010; Li et al., 2022b; Sang et al., 2011).

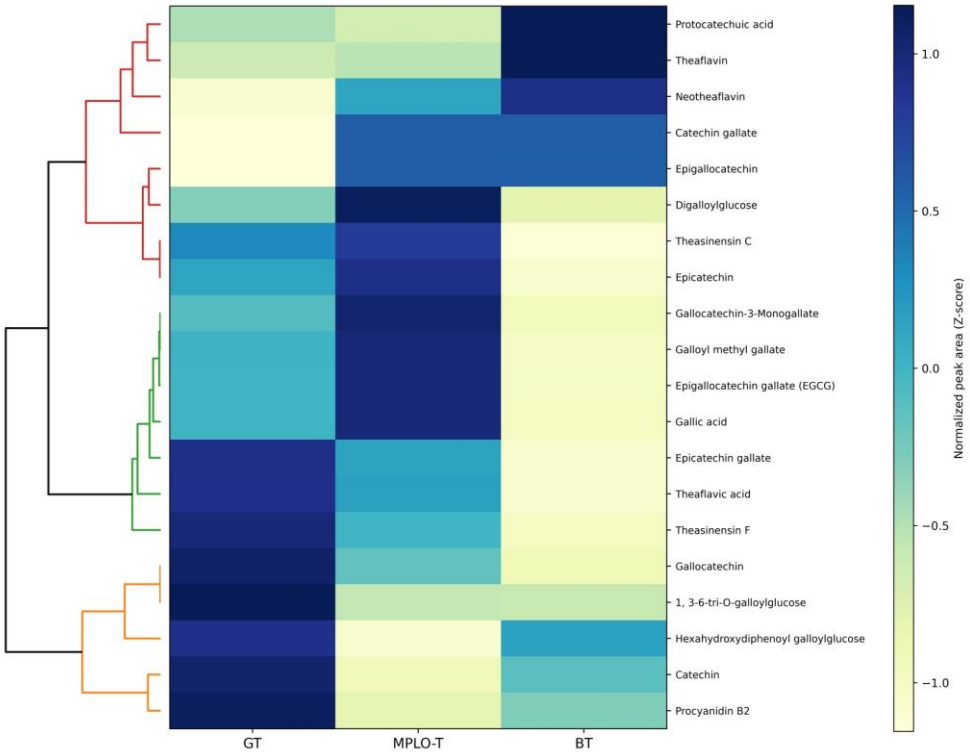

Figure 6.6: Clustered heatmap illustrating relative changes in catechin biotransformation-associated metabolites among minimally oxidized green tea (GT), MPLO-treated tea (MPLO-T), and black tea (BT) based on normalized LC–MS peak areas. Hierarchical clustering was performed using Z-score normalized data to visualize similarities in metabolite abundance patterns across samples. The heatmap includes major catechins, catechin gallates, catechin dimers, theaflavins, oxidation intermediates, and downstream phenolic degradation products associated with catechin oxidation systems. Color intensity represents relative abundance, ranging from pale yellow (low abundance) to dark blue (high abundance). The dendrogram on the left indicates clustering relationships among metabolites based on their abundance profiles.

In addition to these oxidation-associated metabolites, several higher molecular weight features associated with advanced oxidation stages were detected in MPLO-T, including theacitrin A and putative thearubigin-associated intermediates (Table 6.4). Importantly, metabolite annotations were classified according to MSI confidence criteria, with Class 1 metabolites confirmed using authentic standards and Class 2 metabolites representing putative annotations based on accurate mass, retention behavior, and spectral similarity. This conservative annotation framework minimizes over-interpretation while still enabling mechanistic interpretation of oxidation-associated pathways.

Table 6.4: Oxidation-associated metabolites detected by LC–MS in green tea (GT), MPLO-treated tea (MPLO-T), and black tea (BT).

Compound / Feature	Annotation confidence	Approx. MW (g/mol)	GT (normalized peak area)	BT (normalized peak area)	MPLO-T (normalized peak area)	Oxidation stage
Epigallocatechin gallate (EGCG)	Class 1	458.4	High	Trace	Moderate	Native catechin substrate
Epicatechin gallate (ECG)	Class 1	442.4	High	Moderate	High	Native catechin substrate
Epigallocatechin (EGC)	Class 1	306.3	High	High	High	Native catechin substrate
Gallocatechin	Class 1	306.3	Moderate	Moderate	Moderate	Native catechin substrate
Catechin	Class 1	290.3	Very high	Moderate	Moderate	Native catechin substrate
Epicatechin	Class 1	290.3	High	Moderate	Very high	Native catechin substrate
Catechin gallate	Class 1	442.4	Moderate	Very high	Very high	Intermediate oxidation product
Gallocatechin-3-monogallate	Class 2	458.4	Moderate	Moderate	Very high	Intermediate catechin substrate
Theaflavin (TF1)	Class 1	564.5	ND	Very high	Low	Early dimerization
Theaflavin-3-gallate (TF3G)	Class 1	716.6	ND	High	Low	Early
Theaflavin-3′-gallate (TF3′G)	Class 1	716.6	ND	Moderate	Low	Early
Theaflavin-3,3′-digallate (TF3-3′G)	Class 1	868.7	ND	Low	Low	Early
Neotheaflavin	Class 2	564.5	Low	Moderate	Low	Early
Hydroxytheaflavin / degalloyl-oolongtheanin	Class 2	580	Trace	Trace	Trace	Intermediate
Theaflavic acid	Class 2	427.3	Trace	Trace	Trace	Intermediate
Theacitrin A	Class 2	759.6	Trace	Trace	Trace	Intermediate
Theasinensin C	Class 2	913.2	Trace	Trace	Trace	Intermediate
Theasinensin F	Class 2	911.2	Trace	Trace	Trace	Intermediate
Procyanidin B2	Class 2	578.5	Moderate	Moderate	Low	Intermediate
Digalloylglucose	Class 2	484.1	Low	Low	Low	Intermediate
Galloyl methyl gallate	Class 2	336.1	Moderate	Low	Very high	Intermediate
Hexahydroxydiphenoyl galloylglucose	Class 2	634.1	High	Mod.-high	Low	Advanced
1,3,6-tri-O-galloylglucose	Class 2	636.1	Very high	Moderate	Low	Advanced
Gallic acid	Class 1	170.1	High	High	Very high	Intermediate
Protocatechuic acid	Class 2	154.1	Moderate	Very high	Moderate	Advanced

Normalized peak areas are reported qualitatively because untargeted LC–MS data were normalized and auto-scaled prior to analysis. Qualitative descriptors were assigned based on relative normalized abundance as follows: very high (>15%), high (8–15%), moderate (3–8%), low (0.5–3%), and trace (<0.5%). "ND" indicates not detected. Annotation confidence levels follow the Metabolomics Standards Initiative (MSI) framework: Class 1 = confirmed using authentic standards; Class 2 = putatively annotated based on accurate mass, retention behavior, and literature/database comparison; Class 3 = putative compound class or unresolved feature without definitive structural assignment. Oxidation stages were interpreted relative to established catechin oxidation systems and represent biochemical progression rather than an absolute reaction sequence.

These compounds have previously been reported in oxidized tea systems and are generally associated with further transformation of initial catechin dimers into more complex structures (Li et al., 2025b; Yang et al., 2024). However, because several assignments are based on MS/MS similarity and database matching, they should be considered putative, and the LC–MS data alone do not allow definitive structural confirmation. Nevertheless, their presence in MPLO-T, particularly when absent or less abundant in GT, suggests progression beyond initial dimer formation. The enrichment of theasinensin-type dimers together with theaflavin derivatives suggests that multiple oxidative pathways operated simultaneously within the MPLO-treated system (Chen et al., 2021; Su et al., 2024a).

Chromatographic profiles (Figure 6.7) further illustrate these compositional changes, showing progressive reduction of early-eluting catechin peaks and the emergence of broader peaks associated with more complex compounds. These chromatographic changes were accompanied by visible differences in infusion color, transitioning from pale yellow in GT to amber in MPLO-T and deeper reddish-brown in BT, consistent with increasing accumulation of oxidation-associated metabolites and polymeric pigments. This observation aligns with previous reports linking catechin oxidation to the formation of colored compounds contributing to tea liquor characteristics (Haslam, 2003).

Mechanistically, the observed metabolite patterns are consistent with a multi-stage oxidation process initiated by extracellular MPLO components. The reduction of catechins together with the appearance of dimeric and higher molecular weight phenolics suggests that enzymatic activity likely facilitated the formation of reactive quinone intermediates that subsequently underwent coupling and further transformation. Based on the detected oxidation-associated metabolites and previously characterized activity profile of the enzyme preparation, possible oxidoreductase-, hydroxylase-, esterase-, and peroxidase-associated activities may have contributed cooperatively to catechin oxidation and downstream biotransformation reactions. Subsequent dimerization, rearrangement, polymerization, and degradation reactions likely proceeded through both enzymatic and non-enzymatic pathways. The concurrent detection of TF-type compounds, theasinensin-type dimers, galloylated oxidation products, and downstream phenolic acids suggests that the MPLO system promoted a complex reaction network rather than a single linear

transformation pathway, consistent with current understanding of tea polyphenol oxidation chemistry (Itoh et al., 2007; Kuhnert, 2010; Li et al., 2025b).

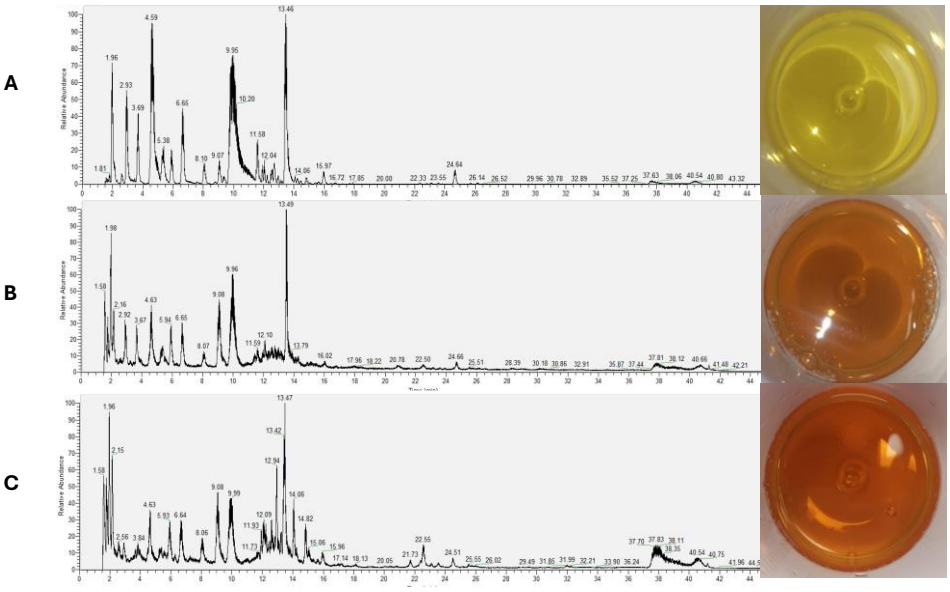

Figure 6.7: Representative total ionization chromatogram (TIC) profiles and corresponding infusion colors of (A) green tea (GT), (B) MPLO-treated tea (MPLO-T), and (C) black tea (BT). Chromatograms illustrate the reduction of early-eluting catechin peaks, and the emergence of broader peaks associated with more complex compounds in oxidized samples. The accompanying images show the transition in liquor color from pale yellow (GT) to amber (MPLO-T) and reddish-brown (BT), reflecting increasing accumulation of oxidation-derived pigments.

To integrate these observations, the proposed metabolic pathway (Figure 6.8) summarizes the progression of catechin oxidation in MPLO-treated tea. In this model, primary catechins undergo oxidative conversion into catechin dimers and theaflavins, followed by formation of oxidation-associated intermediates such as theacitrins and hydroxytheaflavin-type compounds, with continued transformation yielding downstream phenolic degradation products including gallic acid and protocatechuic acid. The pathway also highlights the accumulation of galloylated intermediates and hydrolyzable tannin-related metabolites detected in MPLO-T, supporting the hypothesis that controlled extracellular oxidation promoted both oxidative condensation and partial hydrolytic reactions within the tea matrix. The pathway integrates experimentally detected metabolites with established tea oxidation chemistry while acknowledging that several intermediate steps remain putative (Li et al., 2022b; Verloop et al., 2016).

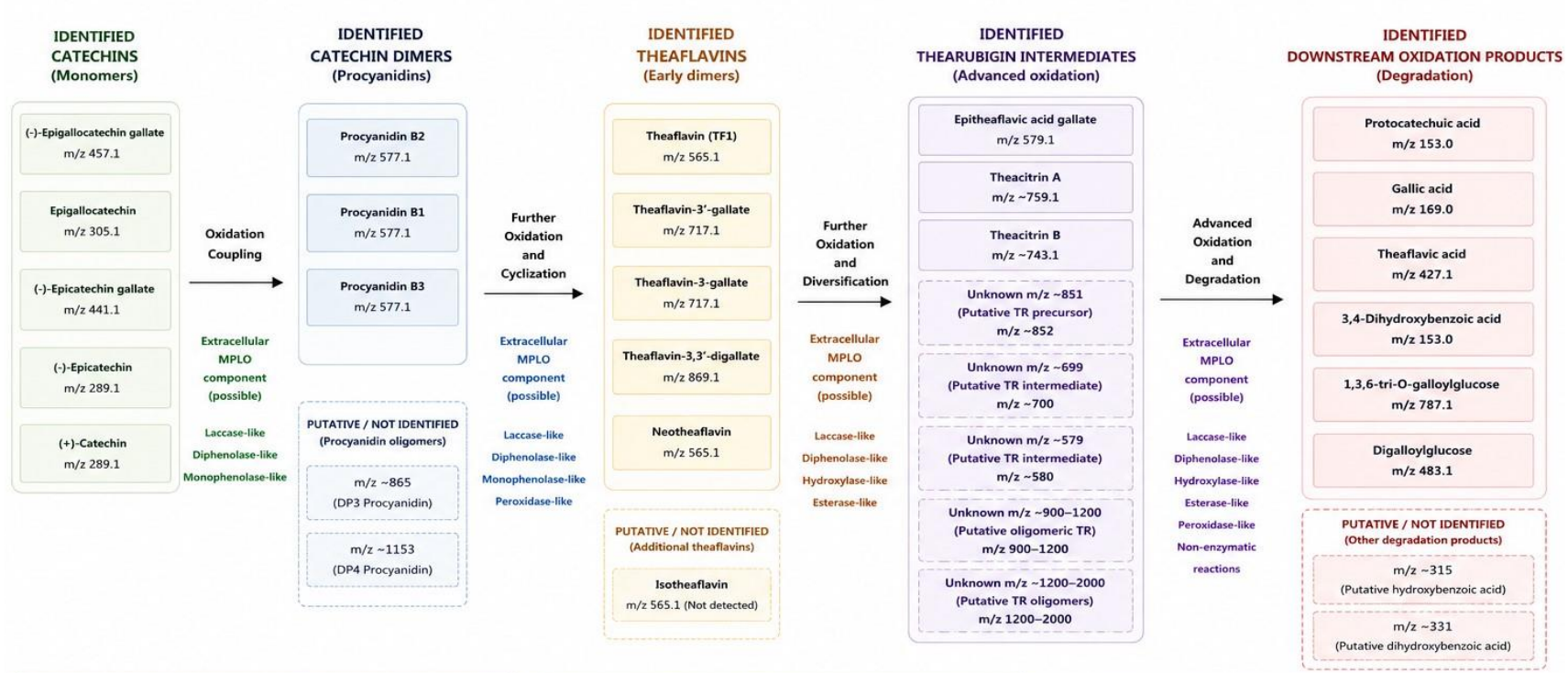

Figure 6.8: Proposed catechin biotransformation pathway in MPLO-treated tea (MPLO-T) based on LC–MS metabolomic profiling and the inferred activity of extracellular microbial polyphenol-oxidizing-like oxidoreductase (MPLO) components. The pathway illustrates the progression from native catechins to catechin dimers, theaflavins, thearubigin-associated intermediates, and downstream oxidation-associated metabolites detected during enzymatic treatment. Solid boxes represent metabolites detected in MPLO-T, whereas dashed boxes indicate putative or non-confirmed intermediates inferred from accurate mass and known tea oxidation systems. Proposed transformations include oxidative coupling, hydroxylation, ester hydrolysis, polymerization, and secondary oxidative degradation mediated by possible oxidoreductase-, hydroxylase-, esterase-, and peroxidase-associated activities.

Although MPLO-T shared several oxidation-associated metabolites with BT, the overall metabolite distribution remained distinct. This difference is expected because MPLO-T was generated from a tea extract system, whereas BT is produced through leaf-based fermentation involving intact cellular structure, oxygen gradients, endogenous plant enzymes, and prolonged oxidation conditions. Even though results were normalized on a dry-weight basis, these fundamental differences limit direct quantitative comparison. Therefore, the LC–MS data should be interpreted as reflecting differences in oxidation systems and processing environments rather than differences in reaction completeness. Within this context, MPLO treatment can be described as inducing a controlled and partial oxidation process that generates a broad range of oxidation-associated metabolites without fully reproducing the complexity of conventional BT chemistry.

Overall, the LC–MS results demonstrate that MPLO treatment induces coordinated transformation of tea polyphenols characterized by catechin depletion, formation of multiple oxidation-derived metabolites, and emergence of higher molecular weight features associated with advanced oxidation stages. The combined HPLC, LC–MS, clustered heatmap, and pathway analyses collectively indicate that MPLO treatment promotes selective and potentially tunable catechin biotransformation rather than uncontrolled oxidation, resulting in a tea system with intermediate oxidative characteristics positioned between minimally oxidized GT and fully oxidized BT.

6.3.3 Functionality assessment

All functional outcomes reported in this chapter (antioxidant capacity, digestive enzyme inhibition, and simulated digestion bioaccessibility) were derived from *in vitro* assays and therefore indicate comparative activity under assay conditions rather than confirmed *in vivo* efficacy.

6.3.3.1 Antioxidant activity (DPPH and FRAP assays)

The DPPH radical scavenging activity of aqueous tea extracts was consistently high across all three samples, ranging from 87.33% to 88.61% (Table 6.5, Figure 6.9), with no statistically significant differences observed between GT, MPLO-T, and BT (one-way ANOVA, $p = 0.73$).

Table 6.5: Antioxidant activity of aqueous tea extracts (DPPH and FRAP).

Sample	DPPH Scavenging (%)	FRAP (µmol Fe^{2+}/g DW)
GT	87.33 ± 2.42	2590.93 ± 132.04[a]
MPLO-T)	88.37 ± 1.11	1219.13 ± 98.86[b]
BT	88.61 ± 1.06	1044.45 ± 51.62[b]

Values are expressed as mean ± SD (n = 4). Different superscript letters within the same column indicate significant differences at $p < 0.05$ (one-way ANOVA followed by Tukey's Honestly Significant Difference (HSD) test).

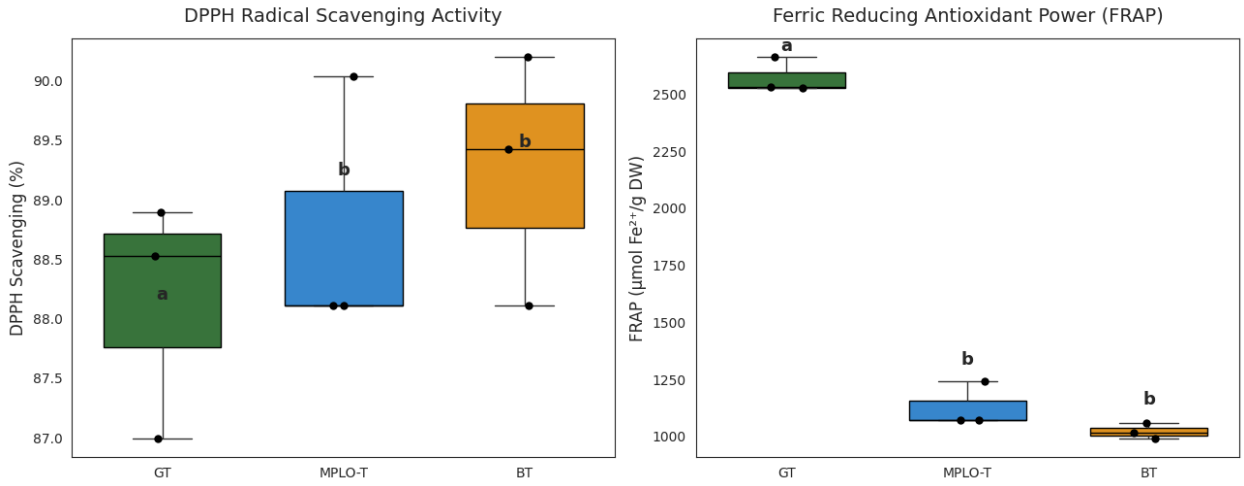

Figure 6.9: Comparison of antioxidant activities of GT, BT, and MPLO-T aqueous tea extracts using DPPH (left axis) and FRAP (right axis) assays. Values are expressed as mean ± standard deviation (n = 4). Superscripts with different letters within the same assay denote statistically significant differences at $p < 0.05$ according to one-way ANOVA followed by pairwise comparisons.

In contrast, FRAP values were markedly higher in GT than in MPLO-T and BT, which did not differ significantly from each other. This pattern is consistent with FRAP's particular sensitivity to intact, unmodified catechins as strong iron-reducing agents, a pool that declines progressively with increasing oxidation (Leung et al., 2001; Prior et al., 2005), rather than oxidation-derived compounds such as TFs and TRs enhancing overall antioxidant capacity in this assay system. MPLO-T exhibited FRAP activity comparable to black tea, consistent with its intermediate degree of catechin oxidation.

The absence of any significant DPPH difference across all three samples, despite their markedly different oxidation states and FRAP profiles, indicates that overall radical-scavenging capacity, as

measured by this assay, was maintained regardless of the substantial compositional change occurring during oxidation. This aligns with previous reports highlighting that controlled enzymatic oxidation can preserve antioxidant properties through selective biotransformation of catechins (Li et al., 2022a; Wang et al., 2022d; Yan et al., 2020).

Because tea is primarily consumed as a water-based infusion, the consistently high and statistically indistinguishable DPPH scavenging activity across all three samples is practically relevant: it suggests aqueous MPLO-T extracts retain the same overall radical-scavenging capacity as conventionally processed black tea, even though the two differ substantially in FRAP-measured reducing capacity. MPLO-T therefore demonstrates promising potential as a functional tea product, offering DPPH antioxidant activity comparable to traditionally processed black tea while allowing greater control over the reaction inputs driving these biochemical transformations, specifically enzyme dose, reaction time, temperature, and pH, in contrast to conventional black tea manufacture, where oxidation depends entirely on the leaf's own endogenous, cultivar- and season-dependent PPO activity.

6.3.3.2 Enzyme inhibitory activity (α-glucosidase and α-amylase)

Enzyme inhibitory activity varied significantly among treatments for both α-glucosidase and α-amylase (Table 6.6; Figure 6.10), with MPLO-T showing the highest inhibition, followed by BT, while GT exhibited the lowest activity.

Table 6.6: α-Glucosidase and α-Amylase inhibitory activity of tea infusions.

Sample	α-Glucosidase (%)	α-Amylase (%)
GT	21.97 ± 2.45^{b}	21.56 ± 10.29^{c}
BT	23.99 ± 2.28^{b}	56.45 ± 18.04^{b}
MPLO-T	30.67 ± 0.98^{a}	75.28 ± 10.32^{a}
Negative control (Inhibitor)	96.04 ± 0.68	97.23± 0.22

Values are expressed as mean ± SD (n = 4). Different superscript letters within the same column indicate significant differences at $p < 0.05$ (one-way ANOVA followed by Tukey's Honestly Significant Difference (HSD) test).

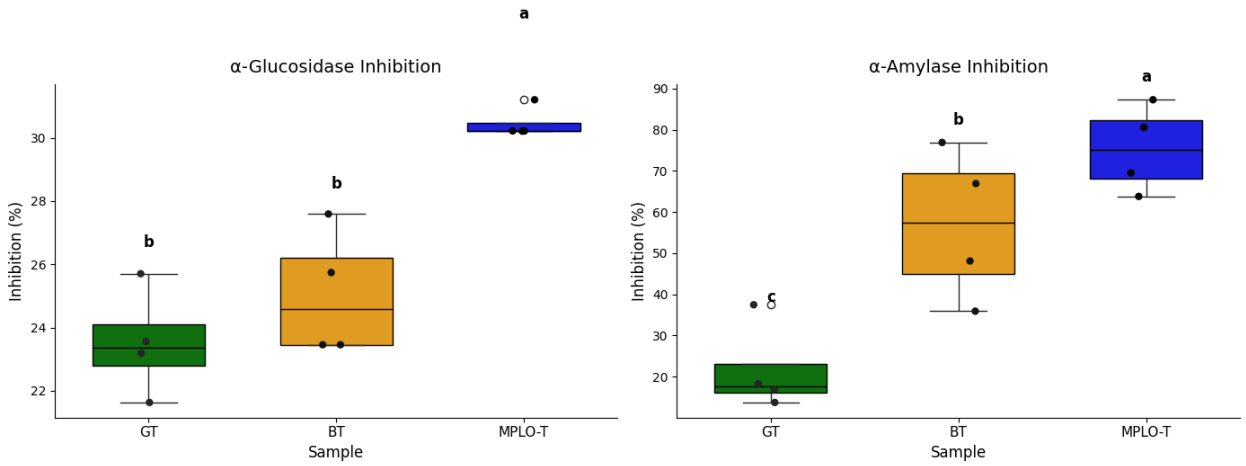

Figure 6.10: Inhibitory activity of tea infusions against α-glucosidase and α-amylase. Bars show mean ± SD (n = 4). Different letters indicate significant differences ($p < 0.05$).

For α-glucosidase, MPLO-T showed significantly higher inhibition than both GT and BT, whereas no significant difference was observed between GT and BT. The moderate inhibition in GT is consistent with the presence of catechins, particularly EGCG, which have been reported to interact with α-glucosidase through hydrogen bonding and hydrophobic interactions (Chiang et al., 2022; Kan et al., 2021). This aligns with the HPLC results (Section 6.3.2), in which GT retained higher concentrations of intact catechins. The lack of a significant increase in BT suggests that extensive oxidative transformation during conventional processing does not necessarily enhance α-glucosidase inhibition under the conditions tested.

In contrast, the higher inhibition observed in MPLO-T coincides with compositional changes identified by LC–MS, including the presence of theaflavin derivatives and other oxidation-associated metabolites. While it is not possible to attribute activity to specific compounds without targeted assays, the results suggest that controlled enzymatic oxidation generates polyphenolic structures with altered interaction potential toward the enzyme. Similar trends have been reported where oxidized or polymerized catechin derivatives exhibit modified inhibitory behavior compared to monomeric forms (Chen et al., 2023b; Kan et al., 2021).

For α-amylase, a clearer separation among treatments was observed, with inhibition following the trend MPLO-T > BT > GT. These results indicate that MPLO-T has enhanced *in vitro* inhibitory

activity against carbohydrate-digesting enzymes; any implication for diabetes management remains speculative without *in vivo* evidence.

The relatively low activity in GT is consistent with recent reports showing that monomeric catechins, particularly EGCG and EGC, exhibit only weak α-amylase inhibition at physiologically relevant concentrations, due to limited affinity for the enzyme's catalytic pocket (Ćorković et al., 2022; Zeng et al., 2023a). The increased inhibition in BT likely reflects the formation of oxidized and polymerized polyphenolic structures, such as theaflavins and early thearubigins, which possess greater hydrophobic surface area and enhanced protein-binding capacity, enabling stronger interaction with α-amylase (Liang et al., 2023; Liu et al., 2024b).

The further increase observed in MPLO-T is consistent with the broader distribution of intermediate- and higher-molecular-weight oxidation-associated metabolites detected by LC–MS, which have been shown to exhibit modified inhibitory behavior compared with both monomeric catechins and fully oxidized BT pigments (Chen et al., 2023b). These findings suggest that controlled enzymatic oxidation generates a unique polyphenolic profile with improved α-amylase inhibitory potential.

Overall, the consistent ranking across both assays suggests that the degree and nature of polyphenol oxidation influence enzyme inhibitory activity. Integration of HPLC and LC–MS data indicates that MPLO treatment produces a compositional profile distinct from both GT and BT, contributing to its superior inhibitory performance. Importantly, these assays were performed using tea infusions prepared under typical consumption conditions, providing a more realistic assessment of functional efficacy.

6.3.3.3 *In vitro* gastrointestinal digestion and bioaccessibility

The phase-wise evolution of TPC, EGCG, caffeine, and total catechins during simulated gastrointestinal digestion is presented in Table 6.7 and Figure 6.11. Two-way ANOVA revealed that both the digestion phase and treatment significantly influenced all measured compounds ($p < 0.001$), with phase exerting the strongest effect for EGCG and total catechins ($\eta^2 > 0.90$), while treatment effects were more pronounced for caffeine ($\eta^2 = 0.84$).

TPC values in the oral phase were comparable between GT and MPLO-T (45.86 ± 2.30 and 46.58 ± 2.33 mg GAE/g DW, respectively; $p > 0.05$), and significantly higher than BT (19.68 ± 0.98 mg GAE/g DW; $p < 0.05$). This indicates that enzymatic oxidation did not substantially reduce the total phenolic pool, consistent with the formation of oxidized derivatives rather than complete degradation.

During gastric digestion, TPC decreased in GT but increased in BT (32.09 ± 1.10 mg GAE/g DW), leading to convergence among treatments ($p > 0.05$). This apparent increase in BT aligns with matrix softening and enhanced release of bound phenolics under acidic conditions, as previously reported (Eran Nagar et al., 2020; Governa et al., 2022). A moderate decline was observed in the intestinal phase across all samples, with retention values of 34–42%, indicating partial instability but sustained phenolic availability.

EGCG exhibited the most pronounced degradation (Phase effect: $F = 412.8$, $p < 0.001$, $\eta^2 = 0.95$), confirming its well-established susceptibility to pH and enzymatic conditions. GT showed a sharp decrease from 270.44 ± 13.52 mg/g DW in the oral phase to 74.57 ± 3.73 mg/g DW after gastric digestion, followed by near depletion in the intestinal phase (~2.6 mg/g DW).

In contrast, MPLO-T maintained significantly higher EGCG during gastric digestion (120.95 ± 6.05 mg/g DW; $p < 0.05$), suggesting that partial enzymatic oxidation may stabilize catechins through structural modification or complex formation. Similar enhancements in catechin stability following microbial pre-transformation have been reported (Tkacz et al., 2025). However, both GT and MPLO-T exhibited low intestinal bioaccessibility (<5%), consistent with rapid degradation, epimerization, and interaction with bile salts (Rha et al., 2019).

Table 6.7: Changes in (A) total phenolic content, (B) Epigallocatechin gallate (EGCG), (C) caffeine, and (D) total catechins during simulated gastrointestinal digestion of green tea (GT), black tea (BT), and MPLO-treated tea (MPLO-T). Values are expressed on a dry weight basis.

Parameter	Metric	GT	BT	MPLO-T
Total Phenolic Content (TPC; mg GAE/g DW)	Oral	46.09 ± 2.31^{a}	19.91 ± 1.00^{c}	46.81 ± 2.34^{a}
	Gastric 120 min	34.88 ± 1.74^{a}	32.48 ± 1.11^{b}	36.78 ± 1.84^{a}
	Intestinal 120 min	36.68 ± 1.84^{a}	31.98 ± 1.60^{b}	36.58 ± 1.83^{a}
	Intestinal 240 min	29.25 ± 1.47^{a}	24.90 ± 1.25^{b}	31.05 ± 1.56^{a}
	Retention (%)	63.5^{b}	125.1^{a}	66.3^{b}
	Bioaccessibility (%)	38.2^{a}	34.4^{b}	41.5^{a}
EGCG (mg/g DW)	Oral	271.80 ± 13.59^{a}	11.29 ± 0.57^{c}	230.48 ± 11.53^{b}
	Gastric 120 min	74.94 ± 3.75^{b}	3.29 ± 0.71^{c}	121.56 ± 6.08^{a}
	Intestinal 120 min	2.17 ± 0.11^{c}	2.86 ± 0.14^{c}	7.60 ± 0.38^{b}
	Intestinal 240 min	2.63 ± 0.13^{c}	2.36 ± 0.12^{c}	7.46 ± 0.37^{b}
	Retention (%)	1.0^{c}	20.9^{a}	3.2^{b}
	Bioaccessibility (%)	0.3^{c}	1.9^{b}	4.1^{a}
Caffeine (mg/g DW)	Oral	103.8 ± 5.2^{b}	48.3 ± 2.4^{c}	131.3 ± 6.6^{a}
	Gastric 120 min	98.7 ± 2.2^{b}	46.6 ± 0.9^{c}	127.1 ± 3.2^{a}
	Intestinal 120 min	90.3 ± 1.0^{b}	40.9 ± 0.5^{c}	125.4 ± 1.4^{a}
	Intestinal 240 min	81.0 ± 1.0^{b}	41.9 ± 0.6^{c}	111.7 ± 1.6^{a}
	Retention (%)	78.0^{b}	86.7^{a}	85.1^{a}
	Bioaccessibility (%)	35.0^{b}	22.0^{c}	53.5^{a}
Total Catechins (mg/g DW)	Oral	61.41 ± 3.07^{a}	14.17 ± 0.71^{c}	65.02 ± 3.25^{a}
	Gastric 120 min	9.45 ± 0.47^{c}	ND	19.10 ± 0.96^{b}
	Intestinal 120 min	5.53 ± 0.28^{c}	1.32 ± 0.07^{d}	8.64 ± 0.43^{b}
	Intestinal 240 min	4.82 ± 0.24^{c}	1.72 ± 0.09^{d}	7.24 ± 0.36^{b}
	Retention (%)	7.8^{b}	12.1^{a}	11.1^{a}
	Bioaccessibility (%)	3.1^{b}	2.9^{b}	8.8^{a}

Values represent (Mean ± SD; n=3; different superscript letters (a–c) within a row indicate significant differences ($p < 0.05$); TPC values given in mg gallic acid equivalents per gram of dry weight (mg GAE/g DW); ND = not detected).

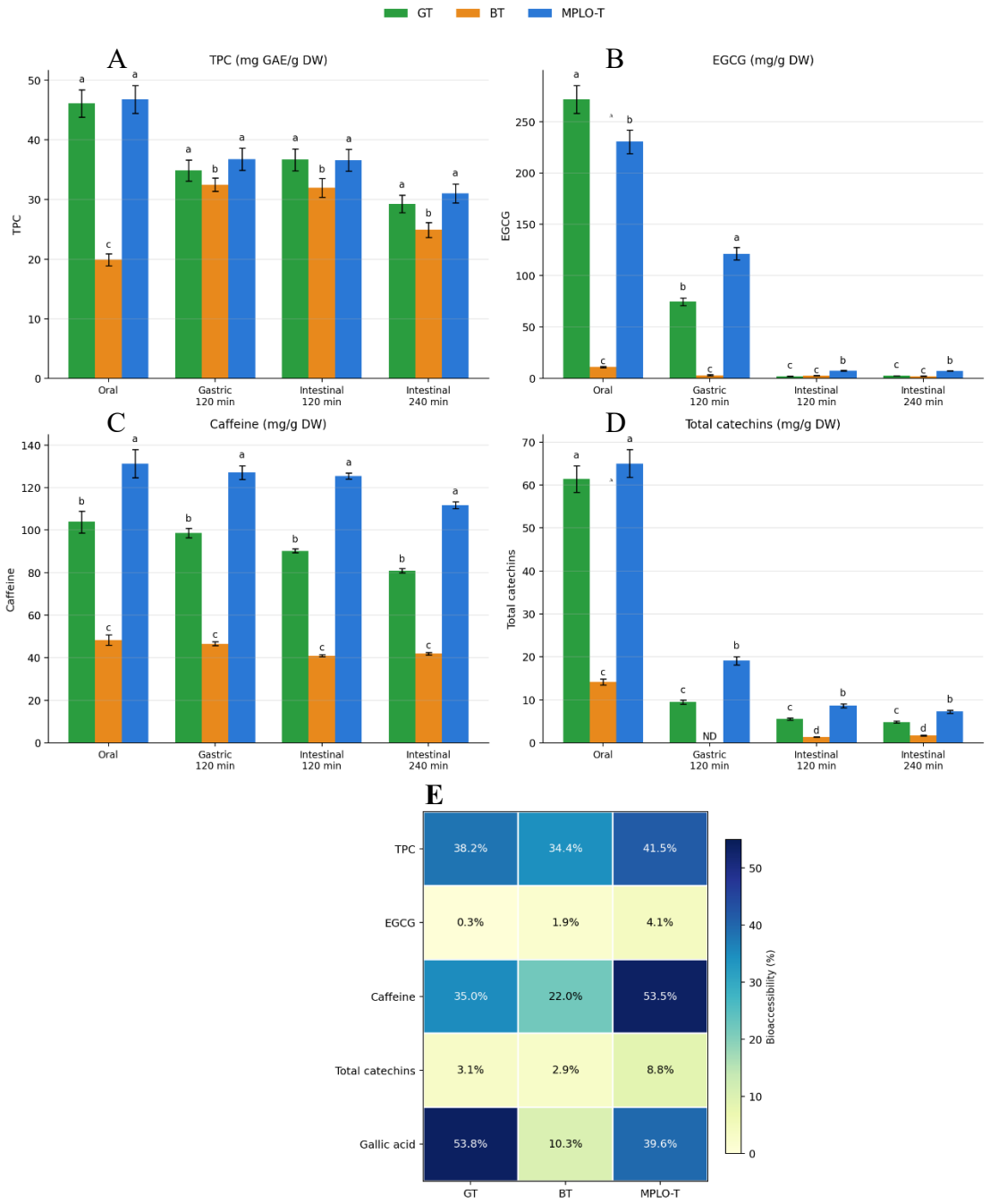

Figure 6.11: Phase-wise changes in phenolic compounds during simulated gastrointestinal digestion of green tea (GT), black tea (BT), and MPLO-treated tea (MPLO-T, 0.2% v/v). Panels show (A) total phenolic content (TPC), (B) epigallocatechin gallate (EGCG), (C) caffeine, (D) total catechins and (E) bioaccessibility heatmap. Values represent mean ± standard deviation (n = 3). Different superscript letters indicate significant differences between treatments within each digestion phase ($p < 0.05$). ND = not detected.

Total catechins followed a similar trend, with substantial losses during gastric digestion in GT (61.10 ± 3.05 to 9.40 ± 0.47 mg/g DW), while MPLO-T retained significantly higher levels (19.00 ± 0.95 mg/g DW; $p < 0.05$). This supports the hypothesis that controlled enzymatic oxidation enhances catechin stability by generating intermediate oxidation-associated metabolites that are less susceptible to degradation. Despite this, intestinal-phase concentrations remained low in all samples, indicating the inherent instability of catechins under alkaline conditions and their transformation into smaller phenolic metabolites (Eran Nagar et al., 2020).

Caffeine followed a different pattern from the other measured compounds. Although statistically significant reductions were observed across digestion phases (Phase effect: $F = 24.6$, $p < 0.001$), the magnitude of change was modest, with retention exceeding 75% in all samples. MPLO-T consistently showed the highest caffeine concentration at every phase, including the Oral phase (131.3 ± 6.6 mg/g DW), exceeding both GT (103.8 ± 5.2) and BT (48.3 ± 2.4). Since caffeine is not a substrate for MPLO-associated oxidoreductase activity, this difference cannot reflect enzymatic action. Instead, it reflects differential retention during the oral-phase simulation: MPLO-T retained 62.8% of its initial caffeine content through the Oral phase, compared with 44.8% for GT and 25.4% for BT, indicating that the three tea preparations underwent proportionally different dilution during oral-phase processing rather than a compositional or analytical artifact (Eran Nagar et al., 2020; Qin & Ketnawa, 2025).

TF were not detected in the digested samples due to their low relative proportion in the initial infusions and further degradation under intestinal conditions; therefore, they were not included in the quantitative analysis. Gallic acid exhibited an inverse trend, increasing markedly in the intestinal phase due to hydrolysis of gallated catechins (Neilson et al., 2009).

Overall, MPLO-T showed higher *in vitro* phenolic bioaccessibility compared to GT and BT, particularly for EGCG and total catechins. Bioaccessibility values for TPC and caffeine were highest in MPLO-T (41.5% and 53.5%, respectively), indicating enhanced release and stability during simulated digestion. The improved bioaccessibility observed at the intestinal phase relative to the gastric phase is consistent with two well-documented mechanisms: bile-salt micellization, in which bile salts act as natural surfactants that solubilize otherwise poorly-soluble phenolic compounds into mixed micelles (Zheng et al., 2023), and pH-driven dissociation of protein-phenolic complexes formed during the acidic gastric phase, as the shift to neutral intestinal pH

reduces the electrostatic and hydrophobic interactions stabilizing these complexes (Zheng et al., 2023). A directly comparable example has been reported for catechins in another food matrix, where release increased from 25.8% at the gastric phase to 69.5% at the intestinal phase, attributed to this same combination of effects (Wu et al., 2026).

These findings suggest that microbial enzyme-mediated oxidation can modulate the digestive fate of tea polyphenols, promoting a balance between structural transformation and functional preservation. Importantly, these results reflect *in vitro* bioaccessibility under simulated gastrointestinal conditions; human absorption and bioavailability cannot be inferred from *in vitro* data alone and would require dedicated *in vivo* studies (Tkacz et al., 2025).

6.3.4 Integrative multivariate analysis and overall insights

Multivariate statistical analyses were conducted to integrate chemical, metabolomic, and functional datasets and to identify the major factors contributing to differences among GT, MPLO-T, and BT. PCA of the bulk composition parameters (TPC, TFAA, and TRS) revealed clear separation among the three tea types (Figure 6.12B). GT clustered in the positive region of PC1, reflecting its comparatively higher TPC, TFAA, and TRS. BT was positioned in the negative PC1 quadrant, consistent with its markedly lower levels of these constituents. MPLO-T occupied an intermediate position but was distinctly separated along PC2, indicating a compositional profile that is neither fully green-tea-like nor black-tea-like.

When all measured variables were included, such as major catechins and gallic acid from HPLC, TF, TR, TB, LC-MS oxidation-associated metabolites, antioxidant capacity (DPPH and FRAP), enzyme inhibitory activities (α-glucosidase and α-amylase), and phenolic bioaccessibility, the overall PCA (Figure 6.12B) again showed clear differentiation among GT, MPLO-T, and BT. PC1 accounted for 66.2 percent of the total variance and was primarily associated with TPC, TFAA, and monomeric catechins. PC2 explained 33.8 percent of the variance and was more strongly associated with oxidation-related pigments, including TF, TR, and TB, as well as functional parameters such as α-amylase inhibition. These patterns suggest that variation in both primary polyphenols and oxidation-associated metabolites contribute to the multivariate separation observed among the three tea types.

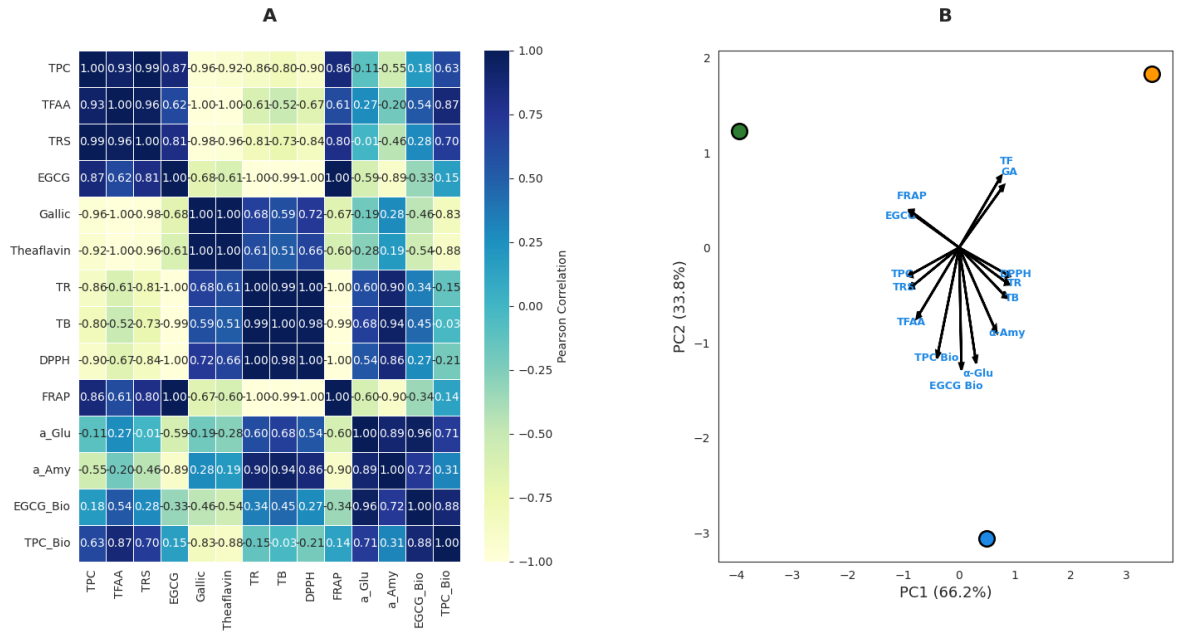

Figure 6.12: Integrative multivariate analysis combining chemical and functional data of green tea (GT), microbial polyphenol-oxidizing-like oxidoreductase-treated tea (MPLO-T), and black tea (BT). (A) Pearson correlation heatmap between chemical and functional parameters. (B) Principal component analysis (PCA) score plot with loading vectors. PC1 accounts for 66.2%, and PC2 accounts for 33.8% of the total variance.

Correlation analysis further highlighted several meaningful associations (Figure 6.12A). TPC values showed a strong positive association with DPPH radical-scavenging activity ($r = 0.89$, $p < 0.05$). Monomeric catechins, particularly EGCG, were positively associated with α-glucosidase inhibition in GT. In contrast, oxidation-derived compounds (TF, TR, and TB) were positively associated with phenolic bioaccessibility ($r = 0.78–0.85$) and α-amylase inhibitory activity ($r = 0.90–0.94$) in MPLO-T and BT. MPLO-T exhibited an intermediate pattern in which moderate levels of oxidation-associated metabolites were associated with enhanced enzyme inhibitory activity and improved EGCG bioaccessibility.

The magnitude of these differences is reflected in the effect sizes (η^2) summarized in Table 6.8. Parameters such as TRS, EGCG, total TF, and FRAP exhibited very large effect sizes ($\eta^2 \geq 0.97$), indicating strong differentiation among the three tea types. In contrast, DPPH scavenging showed only a medium effect size ($\eta^2 = 0.22$), consistent with the high and relatively similar radical-scavenging capacity across all samples.

Table 6.8: Summary of key parameters and effect sizes (η^2) from one-way ANOVA.

Parameter	η^2	Effect Size Interpretation	MPLO-T Position Relative to GT and BT
TPC	0.67	Large	Comparable to GT
TFAA	0.86	Large	Comparable to GT
TRS	0.99	Very large	Intermediate
EGCG	0.98	Very large	Strong reduction vs GT
Total Theaflavins	0.97	Very large	Intermediate (new formation)
Total Pigments (TR + TB)	0.95	Very large	Intermediate to high
DPPH Scavenging	0.22	Medium	Comparable to BT
FRAP	0.99	Very large	Lower than GT
α-Glucosidase Inhibition	0.80	Large	Highest
α-Amylase Inhibition	0.81	Large	Highest

Note: η^2 values were calculated from one-way ANOVA. Effect sizes are interpreted as: 0.01 = small, 0.06 = medium, 0.14 = large (Cohen, 1988). For total theaflavins, GT was set to 0 μg/mL for statistical calculation due to non-detected values.

Although untargeted LC–MS analysis detected a broad range of flavonoids, flavonols, and alkaloids, the integrative analysis focused on the major and functionally relevant compounds (catechins, TF, TR, TB, TPC, TFAA, and TRS). Minor metabolites such as rutin, myricetin, quercetin, caffeine, and theobromine exhibited limited variation across the three tea types and contributed minimally to PCA separation or functional differences. Focusing on the dominant polyphenolic transformations, therefore, enabled clearer interpretation of the key drivers of differentiation—namely, the conversion of catechins into oxidation-associated metabolites and their associated impacts on bioactivity and bioaccessibility. A more comprehensive evaluation of minor metabolites would be valuable in future work but was beyond the primary scope of this study.

These findings are consistent with recent reports on enzymatic and microbial oxidation of tea catechins. Abudureheman et al. (2022) demonstrated that controlled enzymatic oxidation can generate TF and TR while retaining higher phenolic content than conventional fermentation. Liu et al. (2023c) reported that polyphenol oxidase-mediated oxidation yields intermediate products with enhanced functional properties, including improved enzyme inhibitory effects. Similarly, Su et al. (2024b) showed that microbial oxidoreductases can modulate catechin polymerization, producing tunable bioactive profiles.

In summary, the integrative multivariate analysis indicates that MPLO treatment produces a distinct intermediate oxidative state. MPLO-T retains several compositional features of GT while forming selected oxidation markers characteristic of BT. Functionally, MPLO-T exhibits antioxidant activity comparable to BT and the highest α-glucosidase and α-amylase inhibitory activities among the three teas. Under simulated gastrointestinal digestion, MPLO-T also demonstrated higher *in vitro* bioaccessibility of key polyphenols than GT. These results suggest that MPLO offers a promising controlled biotechnological approach for tailoring tea polyphenol composition and functionality.

6.4 Conclusions

The present study shows that microbial polyphenol-oxidizing-like oxidoreductases from *A. faecalis* NZRM 836 can support a controlled oxidative transformation of green tea catechins, resulting in a product (MPLO-T) with an intermediate chemical and functional profile between green and black tea. MPLO-T retained substantial levels of phenolics and amino acids that are typical of green tea while forming moderate quantities of oxidation-associated metabolites such as theaflavins, thearubigins, and theabrownins. These outcomes are consistent with recent reports describing controlled enzymatic and microbial oxidation of tea polyphenols (Abudureheman et al., 2022; Su et al., 2024b).

Multivariate integration of chemical, metabolomic, and functional datasets positioned MPLO-T between the two conventional tea types, reflecting both the preservation of monomeric catechins and the formation of selected oxidative pigments. Functionally, MPLO-T showed antioxidant capacity comparable to black tea and higher inhibitory activity against α-glucosidase and α-amylase under the *in vitro* conditions used. Simulated gastrointestinal digestion also indicated higher *in vitro* bioaccessibility of key polyphenols, particularly EGCG, which suggests that controlled enzymatic oxidation may influence the release and stability of bioactive compounds.

Several limitations should be acknowledged. The study used tea extracts rather than whole-leaf material, which does not fully represent the structural and physicochemical environment of leaf-based processing. All functional assessments, including antioxidant activity, enzyme inhibition, and digestion models, were conducted *in vitro*, and these results cannot be assumed to translate

directly to *in vivo* outcomes. The MPLO preparation is derived from a microbial source that is not currently used in food processing, and its safety, regulatory status, and consumer acceptability require systematic evaluation before any commercial application can be considered.

Nevertheless, the observed chemical distinctions between MPLO-mediated and conventional black tea oxidation are based on a limited number of replicates and a single black tea variety. Further studies involving more biological and technical replicates, multiple tea cultivars, and deeper untargeted metabolomic analysis will be required to fully confirm the extent of these distinctions and to obtain a more complete picture of the chemical divergence between the two systems.

Future research should also focus on scaling and optimizing the enzymatic process, characterizing sensory attributes, and conducting *in vivo* studies to verify the functional effects suggested by the current findings. Additional work on enzyme dosage, reaction time, and substrate concentration may allow more precise control of the oxidative profile. Overall, the results indicate that microbial oxidoreductases have potential as a controlled and reproducible approach for modulating tea polyphenol composition, although further investigation is needed to establish feasibility, safety, and practical relevance.

Chapter 7

General discussion, conclusions, and recommendations

Preface

This chapter integrates the findings from all experimental chapters and evaluates the broader significance of microbial oxidoreductase-mediated tea biotransformation. It discusses mechanistic insights, analytical and biotechnological implications, study limitations, and future research directions for developing controllable microbial oxidation platforms for tea processing.

7.1 Synthesis of key findings

This thesis addressed the core challenge identified in Chapter 1: the limited controllability and high variability of endogenous polyphenol oxidase and peroxidase activities during black tea manufacture. These limitations arise primarily from fluctuations linked to cultivar, season, and leaf physiology. The overarching aim was to develop and evaluate an extracellular microbial polyphenol-oxidizing-like oxidoreductase (MPLO) platform capable of delivering controlled and reproducible catechin oxidation. The thesis progressed through a three-phase structure comprising (i) analytical platform development, (ii) microbial discovery and enzyme optimization, and (iii) application and validation of the MPLO system in tea catechin oxidation. This structure directly reflects the conceptual foundations established in **Chapters 1 and 2**, where the limitations of endogenous polyphenol oxidase (PPO)/peroxidase (POD) systems and the need for a controllable microbial alternative were identified.

In this thesis, the term "microbial polyphenol-oxidizing-like oxidoreductases (MPLOs)" refers to microbial phenol-oxidizing enzymes, including laccase-like multicopper oxidases, tyrosinase-like oxidoreductases, catechol oxidase-like activities, and peroxidase-associated phenol-oxidizing systems, that catalyze analogous transformations of tea polyphenols through distinct catalytic mechanisms. The term MPLO is operational and function-based rather than strictly structural or taxonomic, reflecting the shared ability of these oxidoreductase systems to generate quinone intermediates associated with pigment formation and polyphenol polymerization. In the present study, these activities were inferred from substrate-based functional assays performed on the extracellular enzyme preparation rather than from purification or molecular identification of individual enzymes.

Chapter 3 developed and validated a high-performance liquid chromatography with diode array detection (HPLC-DAD) method for the simultaneous quantification of 12 key non-volatile tea constituents. This analytical tool enabled reliable comparisons across tea types and precise monitoring of catechin oxidation and pigment development. This analytical capability proved essential for evaluating both endogenous enzyme-driven oxidation and the MPLO platform.

Chapter 4 provided evidence that tea-associated environments contain culturable microorganisms capable of secreting extracellular MPLO-associated activities. Screening of 83 isolates in this research identified the bacterium *Alcaligenes faecalis* as exhibiting the highest extracellular

catechol-oxidizing activity. This outcome supports the initial research hypothesis and aligns with ecological observations that certain bacteria in plant-associated settings can contribute to phenolic transformations through secreted oxidoreductases.

Chapter 5 optimized the production of a multifunctional extracellular MPLO preparation using response surface methodology. The optimized preparation achieved a three- to four-fold increase in activity and demonstrated suitable kinetic and stability properties under tea-relevant conditions. The preparation exhibited complementary oxidation-associated activities consistent with both one-electron and two-electron phenolic oxidation pathways, supporting the proposed role of the preparation in controlled catechin biotransformation.

Chapter 6 applied the optimized MPLO preparation to green tea extract, producing a MPLO-treated tea (MPLO-T) product. Comparative analyses using HPLC-DAD and LC-MS/MS showed that MPLO-T occupied a reproducible intermediate oxidative state. Substantial catechin depletion occurred relative to green tea, while residual monomeric catechins remained higher than in conventional black tea. Theaflavins and thearubigin-like pigments formed at levels approaching those of black tea, and principal component analysis of the metabolomic profile positioned MPLO-T between green tea and black tea. Functionally, MPLO-T exhibited antioxidant capacity comparable to black tea and significantly higher inhibitory activity against α-glucosidase and α-amylase than both green tea and black tea. It also showed improved phenolic bioaccessibility during simulated digestion.

Mechanistically, the extracellular deployment of the MPLO preparation changes catechin oxidation kinetics relative to endogenous leaf PPO and POD systems. Traditional oxidation depends on intracellular enzymes activated upon leaf disruption, creating variable oxygen gradients and heterogeneous polymerization pathways that often progress to complex thearubigins. In contrast, the external, cell-free microbial system allows precise control through enzyme dosage, reaction time, temperature, and oxygen exposure. This control favors balanced formation of benzotropolone-containing dimers (theaflavins) with moderate further polymerization. This intermediate chemical profile can be described quantitatively through higher residual catechin levels than black tea, combined with measurable theaflavin markers and pigment proxies.

The enhanced carbohydrate-digesting enzyme inhibition observed after partial oxidation is mechanistically plausible. Mixed phenolic profiles (retained monomers plus theaflavins and early

polymers) may enhance binding interactions at enzyme active sites through combined hydrogen bonding and hydrophobic effects. Molecular docking studies in related work have shown that theaflavins, particularly galloylated forms, exhibit strong binding affinities to the active sites of α-glucosidase and α-amylase, often outperforming or complementing monomeric catechins due to specific interactions with key residues. Alternative explanations, such as contributions from side hydrolytic activities in the crude preparation, remain possible and require purified enzyme studies or molecular docking on individual components to definitively exclude. Overall, the findings across Chapters 3 to 6 support a model in which extracellular MPLOs enable controlled catechin oxidation by decoupling the reaction from leaf-intrinsic variability. Table 7.1 summarizes the fundamental differences between the microbial MPLO-mediated oxidation developed in this thesis and the conventional endogenous PPO-driven process in orthodox black tea manufacturing.

Table 7.1: Key differences between the MPLO-mediated and conventional black tea oxidation systems.

Aspect	Conventional PPO/POD pathway (Plant)	MPLO preparation pathway (*Alcaligenes faecalis*)	Advantages of the microbial approach
Enzyme source and location	Endogenous, intracellular	Extracellular, secreted multi-enzyme preparation	External dosage control
Activation	*In situ*, triggered by leaf disruption	External addition of cell-free enzyme preparation	Precise tuning of reaction time and load
Catalytic mechanisms	Primarily two-electron oxidation	Complementary one-electron, two-electron, and peroxide-dependent pathways	Balanced dimer formation with moderated polymerization
Degree of control	Low; highly variable	High; tunable dosage, time, oxygen, temperature, though final product composition remains only partially controllable	Improved batch-to-batch consistency
Degallation and side reactions	Limited	Prominent ester hydrolysis	Reduced astringency; additional substrates
Metabolite profile	Extensive catechin depletion; heterogeneous thearubigins	Intermediate oxidative state; controlled pigment formation	Potentially tunable functional properties
Kinetics	Prolonged, uncontrolled	Rapid, controlled reaction window	Faster and more controllable under laboratory conditions

Evidence basis: Targeted markers (Table 6.2), metabolomic features (Table 6.4), and statistical effect sizes/significance (Table 6.8).

While both systems rely on quinone-mediated oxidative polymerization, they differ significantly in catalytic mechanism, process controllability, degree of oxidation, and resulting chemical and functional outcomes. This control applies to reaction inputs, not cultivar, season, or leaf physiology, which were not experimentally varied; MPLO-T's intermediate GT/BT positioning (Section 6.3.1) confirms input control does not equate to full product control. These distinctions highlight the complementary advantages of the bacterial MPLO platform, particularly in terms of reproducibility and tunability.

7.2 Broader implications for tea biotechnology

The results indicate that extracellular MPLOs can function as controllable biocatalysts for tea polyphenol transformation. Because the enzymes are applied externally in a cell-free form, oxidation can be regulated through defined parameters such as dosage, reaction time, temperature, and oxygen availability. This means the reaction no longer depends on the leaf's own, naturally variable PPO and POD activity, which is known to fluctuate with cultivar, season, and leaf physiology (Li et al., 2024b); instead, the oxidation outcome is set directly by the externally applied enzyme dose and conditions. Such external control aligns with broader developments in enzymatic food processing, where microbial oxidoreductases support more consistent phenolic outcomes (Espina et al., 2021; Kumar et al., 2024a).

The most immediate applications may involve systems requiring standardized phenolic profiles. These include the production of ready-to-drink tea extracts with reproducible color and catechin-to-pigment ratios, the development of functional tea ingredients with enhanced carbohydrate-enzyme inhibition characteristics, and the creation of hybrid products that combine selected attributes of green and black tea. The platform may also serve as a preprocessing step in conventional black tea manufacture to establish a more consistent oxidative baseline before blending or sensory adjustment. Comparable enzyme-assisted strategies have shown promise for improving consistency and functionality in other beverage systems (Aregbe et al., 2025). For such products, controlled functionality matters most for batch-to-batch reproducibility, meeting both consumer expectations of consistency and industrial quality-control needs, arguably the single most important outcome for commercial viability.

Nevertheless, several practical constraints must be recognized. Enzyme production costs and scalability could limit viability, particularly where high loadings are needed. Oxygen transfer in extract-based systems may restrict efficiency and require optimized aeration at larger scales. Downstream processing, including enzyme inactivation, clarification, and removal of residual proteins, would be necessary to meet beverage quality and safety standards. Regulatory considerations are also important, as the MPLO preparation derives from a non–generally recognized as safe (non-GRAS) organism and would require thorough safety evaluation consistent with guidelines for microbial enzyme preparations used in food.

Taken together, these findings represent a laboratory-scale demonstration rather than a fully validated industrial alternative to traditional fermentation. The work shows that microbial extracellular oxidoreductases can modulate tea polyphenol composition in a controlled manner, yet further scale-up, sensory validation, and regulatory assessment will be required to determine practical translation.

7.3 Limitations and critical evaluation

Several limitations define the scope of this study and indicate priorities for future research. These are presented in order of their impact on broader applicability. The most significant limitation is the exclusive reliance on laboratory-scale systems. Factors such as mass transfer, oxygen delivery, and enzyme stability were not assessed under pilot or industrial conditions, although these parameters strongly influence oxidation kinetics in phenolic-rich matrices (Hu et al., 2022). To address this, controlled pilot-scale fermenter trials with defined aeration, mixing, and thermal control would be required to evaluate reproducibility at scale. Direct precedent exists for this kind of scale-up: bacterial laccase-type enzyme production has been demonstrated at industrial bioreactor volumes of up to 5 tons (Liu et al., 2016), with key process variables such as dissolved oxygen and agitation rate already characterized in the literature (Ma et al., 2025). However, this enzyme class is also documented to frequently show reduced activity at larger scale relative to laboratory conditions, indicating that pilot-scale trials would likely require dedicated re-optimization rather than a simple linear scale-up of the conditions established here (Liu et al., 2016).

Additionally, these findings are based on a limited number of replicates and a single black tea variety. Further studies involving more biological and technical replicates, multiple tea cultivars, and more comprehensive untargeted metabolomic analysis will be required to fully confirm the extent of these distinctions and to obtain a more complete picture of the chemical divergence between MPLO-mediated and conventional black tea oxidation pathways.

A second limitation concerns the bacterial strain used for enzyme production. Although initial screening identified a high-activity *A. faecalis* isolate from Sri Lankan tea environments, import regulations necessitated the use of a strain from the New Zealand Reference Culture Collection (*A. faecalis* NZRM 836). This substitution introduces uncertainty regarding potential strain-specific differences in oxidoreductase profiles. Comparative activity assays and genomic analyses of both strains would be valuable to confirm their functional equivalence. Further, the screening conducted in this study was restricted to isolates obtained from tea-associated environments and therefore does not capture the full diversity of potential oxidoreductase-producing microorganisms. While this targeted approach was hypothesis-driven, broader screening across diverse ecological niches may reveal microorganisms with enzymes that have higher oxidoreductase-associated activity, wider substrate specificity, or novel functional properties.

Third, enzyme production occurred in a small-scale fermenter with limited continuous monitoring of dissolved oxygen and pH. The system relied on the buffering capacity of tryptic soy broth and basic aeration and agitation. Although adequate for proof-of-concept work, this setup does not replicate industrial bioreactor control. Future studies should employ fully instrumented bioreactors with continuous parameter monitoring to better define effects on oxidoreductase expression.

Fourth, functionality evaluation relied primarily on *in vitro* enzyme inhibition assays (α-glucosidase and α-amylase) and static simulated digestion models. While these approaches provided useful preliminary insights into carbohydrate-digesting enzyme inhibition and phenolic bioaccessibility, they do not fully capture cellular uptake, metabolism, or physiological responses. Cell-based models (e.g., intestinal or adipocyte models) and *in vivo* studies are needed to better assess bioavailability and bioefficacy (Dilkalal et al., 2024; Yang et al., 2025b). The absence of structural modeling, such as molecular docking, also limits atomic-level understanding of enzyme-substrate or inhibitor-enzyme interactions. To address these gaps, future work should incorporate

cell-based models such as Caco-2 or HepG2 lines for transport and metabolic studies, alongside dynamic gastrointestinal simulators.

Fifth, the study did not include sensory evaluation or comprehensive volatile profiling. While chemical and functional data provide clear insights, the impact on tea aroma and overall acceptability remains unknown. Integration of gas chromatography–mass spectrometry (GC–MS) or comprehensive two-dimensional gas chromatography–olfactometry–mass spectrometry (GC×GC-O-MS) with trained sensory panels would be necessary to assess flavor outcomes (Guan et al., 2024).

Sixth, experiments used green tea extract rather than intact or mechanically disrupted leaves. Extract systems simplify enzyme-substrate contact but do not replicate the structural environment of leaf-based oxidation, including oxygen gradients and cell-wall influences. Comparative trials with whole-leaf or partially disrupted matrices would help determine how structural context affects performance.

Seventh, genomic characterization of the *A. faecalis* NZRM 836 strain was not performed. Without whole-genome sequencing, the specific genes potentially associated with the observed MPLO activities, and any accessory pathways, remain unidentified. Sequencing, gene annotation, and targeted disruption studies would provide stronger mechanistic evidence (Assad et al., 2023).

Analytical limitations also apply. The structural heterogeneity of thearubigins continues to challenge detailed characterization, and several LC-MS/MS features observed in this work would benefit from further structural elucidation using advanced MS/MS, authentic standards, or nuclear magnetic resonance (NMR) spectroscopy, which provides direct evidence of atomic connectivity rather than the indirect, fragmentation-based inference MS/MS relies on, and could resolve several compounds currently identified only tentatively (Long et al., 2023; Moreira et al., 2024).

Finally, the non-GRAS origin of the production organism raises regulatory considerations for food use. A comprehensive safety dossier, including purity profiling, confirmation of the absence of viable cells or residual DNA, and assessments of allergenicity and toxicology, would be required.

These limitations define the scope of the present work and identify priorities for future development without diminishing the proof-of-concept value of the findings. Instead, they clarify the boundaries of the present work and provide focused directions for subsequent development.

7.4 Potential industrial and research applications

The MPLO platform shows potential in contexts where controlled polyphenol oxidation is beneficial, although successful deployment will depend on further scale-up, regulatory clearance, sensory validation, and expanded functionality testing. The laboratory findings support several near-term applications that could be explored with additional development.

One immediate application is the production of enzyme-oxidized green tea extracts for ready-to-drink beverages requiring standardized black-tea-like color and consistent catechin-to-pigment ratios. The reproducible intermediate oxidative state achieved by MPLO-T suggests that the microbial system could help stabilize product quality in formulations where batch-to-batch variation is a concern. Similarly, powdered functional ingredients with enhanced α-glucosidase and α-amylase inhibitory profiles may be feasible, subject to appropriate safety assessment; because these two enzymes act sequentially in starch digestion, a preparation capable of inhibiting both represents a more complete blockade of the digestive pathway than single-enzyme inhibitors, a recognized advantage in functional-food development. Controlled microbial oxidation could also serve as a preprocessing step in conventional tea manufacture, establishing a more defined oxidative baseline before blending or sensory tuning.

Enzyme immobilization strategies may substantially improve the industrial feasibility of this platform by enhancing enzyme stability, enabling reusability across multiple cycles, and reducing overall production costs. Recent studies on microbial laccases and related oxidoreductases have demonstrated that immobilized preparations often exhibit improved storage stability, broader pH tolerance, and retained activity after repeated use in phenolic oxidation systems (Kyomuhimbo & Brink, 2023; Li et al., 2024a; Patti et al., 2025). Such approaches would be particularly valuable for extract-based tea processing, where enzyme recovery and reuse could address scalability constraints.

Beyond tea, the general concept of deploying controlled extracellular oxidoreductases may extend to other polyphenol-rich matrices, such as fruit juices, wine intermediates, cocoa extracts, or herbal infusions, to modulate color, bitterness, astringency, and antioxidant profiles. These applications remain exploratory and would require matrix-specific optimization, sensory evaluation, and regulatory review.

Longer-term research directions may include transferring putative oxidoreductase-associated genes into GRAS-status microbial hosts following complete genome sequencing of the *A. faecalis* strain. This strategy could enhance safety, scalability, and regulatory compatibility. Additional opportunities involve integrating the MPLO preparation with complementary enzymes such as tannase to refine aroma and flavor outcomes, as well as metagenomic screening for GRAS-compatible oxidoreductase variants. All such extensions should be viewed as future possibilities that build upon the current proof-of-concept rather than immediate outcomes.

7.5 Summary of outcomes and answers to research questions

This thesis demonstrates that a bacterial extracellular MPLO platform can support controlled catechin biotransformation and generate a chemically intermediate tea product with promising functional characteristics. The outcomes for each research question are summarized below.

Research Question 1: Can traditionally processed Sri Lankan orthodox black tea provide a suitable analytical and metabolite reference framework for evaluating microbial tea catechin biotransformation?

Yes. Traditionally processed Sri Lankan orthodox black tea provided a suitable comparative reference framework for evaluating microbial catechin biotransformation. Chapter 3 established and validated an HPLC-DAD analytical platform capable of simultaneously quantifying major catechins, theaflavins, alkaloids, and related polyphenolic compounds across green tea and black tea matrices. Comparative profiling of black tea processing stages and commercially processed black tea enabled identification of characteristic oxidation-associated metabolites, pigment trends, and catechin depletion patterns that subsequently served as benchmarks for interpretation.

Research Question 2: Can MPLO-active microorganisms be isolated from tea-associated environments, and does the selected bacterial strain exhibit sufficient extracellular MPLO activity to serve as a biocatalyst for catechin oxidation?

Yes. Culture-dependent screening of 83 isolates from various stages of orthodox black tea processing (Chapter 4) successfully identified multiple MPLO-active microorganisms. *A. faecalis* was selected as a high-performing strain. However, due to import and biosafety restrictions, subsequent optimization and biotransformation studies were conducted using *Alcaligenes faecalis* NZRM 836 obtained from the New Zealand Reference Culture Collection. The NZRM 836 strain exhibited extracellular substrate-based oxidoreductase activities consistent with laccase-like, catechol oxidase-like, tyrosinase-like, and peroxidase-associated phenol-oxidizing functions. The resulting extracellular MPLO preparation efficiently catalyzed oxidation of major tea catechins, particularly EGCG and related gallated catechins, confirming the suitability of selected *A. faecalis* strains as controllable biocatalytic systems for tea catechin biotransformation under laboratory conditions.

Research Question 3: Can crude extracellular enzyme preparations from selected bacterial strains catalyze oxidative transformation of major tea catechins and generate black tea-related oxidation-associated metabolites under controlled laboratory conditions?

Yes. Crude extracellular enzyme preparations obtained from selected bacterial strain catalyzed oxidative transformation of major tea catechins under controlled laboratory conditions. In the model EGCG oxidation system, crude 36 h extracellular enzyme filtrates from *A. faecalis* NZRM 836 oxidized EGCG in a concentration-dependent manner, reducing EGCG from 795.82 ± 55.71 mg/L in the heat-inactivated control to 333.33 ± 20.00 mg/L at the highest enzyme dosage (500 µL), representing approximately 58% depletion. Simultaneously, gallic acid increased from 1.06 ± 0.02 mg/L at t = 0 to 29.81 ± 1.79 mg/L, while epigallocatechin (EGC) increased from 1.14 ± 0.09 mg/L to 3.97 ± 0.24 mg/L, indicating oxidative degradation and transformation of gallated catechins. Significant accumulation of gallocatechin gallate was also observed, aligning with substantial epimerization under the incubation conditions.

Research Question 4: How do culture conditions and reaction parameters influence microbial oxidoreductase production and tea catechin biotransformation efficiency?

Culture conditions and reaction parameters strongly influenced extracellular MPLO production and catechin biotransformation efficiency. Response surface optimization identified 101 μM catechin, 245 μM $CuSO_4$, and 74 h cultivation at 37 °C and 150 rpm as optimal conditions, yielding an extracellular MPLO activity of 245.3 ± 18.6 U/mL. The enzyme preparation exhibited activity across the natural tea pH range and remained stable at elevated temperatures relevant to tea processing. In the green tea system, incubation at 50 °C for approximately 5 h provided optimal catechin oxidation and transient theaflavin formation, whereas prolonged incubation promoted secondary polymerization and decline of intermediate oxidation-associated metabolites. These findings demonstrate that both cultivation and reaction conditions critically determine the efficiency and selectivity of MPLO-mediated catechin biotransformation.

Research Question 5: What biochemical characteristics, substrate preferences, apparent kinetic behavior, and operational stability properties are exhibited by partially purified MPLO from the selected bacterial strain?

The partially purified extracellular MPLO preparation exhibited multiple oxidoreductase-associated activities with distinct substrate-dependent behavior. Laccase-like activity showed acidic pH optima, whereas tyrosinase-like activity exhibited near-neutral optima, supporting the presence of complementary phenol-oxidizing functions within the preparation. The enzyme system retained activity across the natural pH range of tea and demonstrated relatively high-temperature operational stability under tea-relevant processing conditions. Substrate specificity assays confirmed activity toward multiple phenolic substrates, while apparent kinetic analyses indicated substantial oxidation activity toward catechin-related compounds. Collectively, these characteristics support the suitability of the extracellular MPLO preparation as a promising biocatalytic system for controlled tea catechin biotransformation.

Research Question 6: How does the polyphenolic composition of microbially oxidized green tea compare with that of traditionally processed black tea and unoxidized green tea?

MPLO-treated tea (MPLO-T) exhibited an intermediate polyphenolic profile positioned between minimally oxidized green tea (GT) and traditionally processed black tea (BT). Targeted HPLC-

DAD analysis showed substantial depletion of major catechins following MPLO treatment, with EGCG decreasing from 83.97 ± 5.87 mg/g DW in GT to 18.24 ± 1.28 mg/g DW in MPLO-T, accompanied by formation of oxidation-associated metabolites including theaflavins and increased thearubigin content. Untargeted LC–MS metabolomics further identified catechin dimers, putative theaflavin-associated intermediates, galloylated oxidation-associated metabolites, and downstream phenolic degradation metabolites in MPLO-T. Multivariate analysis demonstrated clear compositional separation among GT, MPLO-T, and BT, while clustered heatmap analysis confirmed coordinated depletion of native catechins together with accumulation of oxidation-associated metabolites. Overall, MPLO-T partially reproduced several key features of black tea oxidation while retaining higher residual catechin levels and exhibiting a milder degree of polymerization than conventional BT.

Research Question 7: How does MPLO-mediated oxidation influence selected functional properties, including total phenolic content, antioxidant capacity, and in vitro bioaccessibility, relative to traditional black tea and unoxidized green tea?

MPLO-mediated oxidation altered several functional properties while preserving substantial antioxidant potential. Total phenolic content remained relatively stable between GT and MPLO-T, indicating that MPLO treatment modified phenolic composition without extensive loss of overall reducing potential. Antioxidant assays demonstrated that MPLO-T retained strong radical scavenging and ferric reducing activities relative to GT and BT, despite substantial catechin transformation. *In vitro* gastrointestinal digestion studies further showed that several oxidation-associated metabolites exhibited improved retention during simulated digestion, while MPLO-T maintained measurable bioaccessible phenolic fractions throughout the intestinal phase. However, these findings reflect *in vitro* bioaccessibility rather than *in vivo* bioavailability or physiological efficacy. Collectively, the results indicate that controlled MPLO-mediated oxidation can modify tea polyphenol composition while retaining important functional characteristics associated with tea bioactivity.

7.6 Recommendations for future work

Future work should progress through short-, mid-, and long-term priorities that build on the findings of this thesis and address the limitations identified in Section 7.3. In the short term, pilot-scale laboratory validation is needed to determine whether the reproducibility observed at the small scale can be maintained under conditions that more closely resemble industrial processing. Instrumented benchtop bioreactors would allow systematic evaluation of oxygen transfer, mixing efficiency, thermal stability, and enzyme performance, all of which strongly influence phenolic oxidation kinetics in complex matrices (Al-Sharify et al., 2025). Parallel to this, genomic characterization of the *A. faecalis* strain should be undertaken. In the present study, MPLO activities were inferred from substrate-based biochemical assays performed on the extracellular enzyme preparation rather than from genomic and proteomic data, or from purified enzyme characterization. Consequently, the specific genes, enzymes, and catalytic systems responsible for the observed catechin biotransformation reactions remain unresolved.

Whole-genome sequencing and gene annotation should be integrated with transcriptomic analysis and proteomic profiling of the extracellular enzyme preparation to identify not only putative oxidoreductase-associated genes, but also extracellular proteins actively expressed and secreted under MPLO-inducing conditions. This multi-omics approach would provide stronger evidence for identifying the candidate laccase-like, tyrosinase-like, catechol oxidase-like, and peroxidase-like enzymes responsible for the observed MPLO activities and could support future strategies such as targeted overexpression or heterologous expression in GRAS hosts (Amin et al., 2025). Short-term work should also include enhanced analytical characterization of oxidation-associated metabolites using high-resolution MS/MS, molecular networking, and NMR to clarify intermediate structures and polymerization pathways, particularly for thearubigin-like fractions that remain analytically challenging (Kuhnert et al., 2010b; Long et al., 2023; Moreira et al., 2024; Saalwächter, 2019). Initial sensory and volatile profiling using GC-MS, GC×GC-O-MS, and small sensory panels would provide early insights into aroma attributes and guide optimization of reaction conditions (Guan et al., 2024).

Mid-term priorities should focus on expanding the substrate scope and improving process consistency. Evaluating the MPLO system using whole leaves, partially disrupted leaves, and other polyphenol-rich matrices such as cocoa, fruit extracts, or herbal infusions would clarify how matrix

structure influences enzyme accessibility, oxygen gradients, and polymerization behavior (Aregbe et al., 2025). Process engineering efforts should explore enzyme immobilization strategies, as immobilized oxidoreductases often exhibit enhanced thermal tolerance, broader pH stability, and improved reusability across multiple cycles, which can significantly reduce production costs (Kyomuhimbo & Brink, 2023; Li et al., 2024b; Patti et al., 2025). Mid-term work should also include a comprehensive sensory evaluation with trained panels to assess flavor, aroma, and overall acceptability of MPLO-T and related products, integrating sensory outcomes with chemical and functional data. Expanded functional and bioavailability studies using cell culture models and *in vivo* systems would provide deeper insight into physiological relevance, complementing the *in vitro* digestion and enzyme inhibition assays used in this thesis (Dilkalal et al., 2024; Wang et al., 2022a).

Long-term priorities should address regulatory readiness, industrial translation, and the development of GRAS-compatible production systems. Once the *A. faecalis* genome is sequenced, transferring relevant oxidoreductase genes into GRAS microbial hosts would enhance safety, scalability, and regulatory compatibility for food applications. Regulatory and safety assessments will be essential, including purity profiling, confirmation of the absence of viable cells or residual DNA, allergenicity evaluation, and toxicological testing, consistent with international guidelines for microbial enzyme use in foods (Devi et al., 2025; Espina et al., 2021; Kumar et al., 2024a). Long-term work should also include pilot-scale production trials in industrially relevant reactors to evaluate process stability, cost efficiency, and integration with existing tea manufacturing workflows. These studies will determine whether MPLO systems can be incorporated into commercial tea processing or functional ingredient production. Finally, product development and commercialization pathways should be explored, including standardized tea extracts, functional beverages, or hybrid tea products that leverage controlled microbial oxidation, in collaboration with industry partners to assess market potential and refine product specifications.

7.7 Contribution to knowledge

This thesis makes several contributions to the field of tea biotechnology and to the broader study of controlled phenolic oxidation in food systems. First, it provides clear evidence that tea-associated environments harbor microorganisms capable of secreting extracellular

polyphenol-oxidizing-like oxidoreductase (MPLO) activity. Although microbial oxidoreductases have been studied in other plant-associated contexts (e.g., rhizosphere and phyllosphere microbiomes of various crops), their systematic isolation and characterization from tea environments remain limited. By screening 83 isolates and identifying *A. faecalis* as a high-activity strain, this work expands current understanding of tea-associated microbial contributors to phenolic transformations in tea ecosystems.

Second, it establishes a validated HPLC-DAD method for the simultaneous quantification of 12 key non-volatile tea constituents, and a semi-validated method for 19 tea compounds, including catechin and theaflavins, facilitating consistent monitoring of oxidation dynamics across green tea, black tea, and microbially oxidized products. Further, an optimized ultrasonic-based extraction for tea polyphenols is also presented in this study.

Third, the thesis demonstrates that a multifunctional extracellular MPLO preparation can be produced, optimized, and applied to tea catechin oxidation in a controlled manner. The integration of response surface methodology for enzyme production, combined with detailed kinetic and stability characterization, provides a methodological framework for developing microbial oxidoreductase systems tailored to specific food matrices. This adds to the growing body of research on microbial enzymes as tools for modulating phenolic composition in food and beverage processing.

Fourth, the application of the optimized MPLO preparation on green tea extract resulted in a reproducible intermediate oxidation profile between green tea (GT) and black tea (BT) that differs from both green tea and conventional black tea. The combined use of HPLC-DAD, LC-MS/MS, and multivariate analysis allowed detailed characterization of this intermediate state, demonstrating that microbial oxidation can generate a distinct and potentially tunable chemical profile. Such a finding extends current understanding by showing that controlled microbial oxidation can decouple catechin transformation from the variability inherent in endogenous PPO and POD systems.

Fifth, the thesis provides new insights into the functional implications of controlled microbial oxidation. MPLO-T showed higher *in vitro* inhibition of α-glucosidase and α-amylase than GT and BT under the assay conditions used (Table 6.6; Figure 6.10), along with improved phenolic bioaccessibility during simulated digestion, suggests that partial oxidation may optimize the

balance between monomeric catechins and early-stage polymers. This contributes to ongoing discussions about how oxidation state influences bioactivity and suggests potential of microbial systems to generate functional tea ingredients with tailored health-related properties.

Finally, the work establishes a conceptual and methodological foundation for future development of MPLO platforms. By identifying key limitations, outlining a staged roadmap for scale-up, and highlighting regulatory considerations, the thesis provides a realistic framework for translating laboratory findings into practical applications. Collectively, these contributions advance scientific understanding of microbial oxidoreductases in tea processing and open new avenues for controlled phenolic modification in food biotechnology.

7.8 Closing Statement

This thesis addresses a long-standing challenge in tea biotechnology: the limited controllability and high variability of endogenous PPO and POD activities that drive black tea oxidation. By developing and evaluating a bacterial extracellular MPLO platform, the work demonstrates that controlled and reproducible catechin biotransformation is achievable outside the constraints of leaf-intrinsic enzymatic systems. The findings show that microbial oxidoreductases can generate a chemically intermediate tea product with distinct functional properties, including enhanced inhibition of carbohydrate-digesting enzymes and improved phenolic bioaccessibility. These outcomes highlight the potential of microbial systems to complement or extend traditional tea processing methods.

At the same time, the thesis acknowledges the limitations of laboratory-scale experimentation and outlines a clear roadmap for future development, including pilot-scale validation, genomic characterization, advanced analytical work, sensory evaluation, and regulatory assessment. The staged recommendations emphasize that translation to industrial practice will require coordinated progress across biochemical, engineering, sensory, and regulatory domains.

Overall, this research contributes new knowledge to the field by demonstrating that microbial extracellular oxidoreductases can be harnessed to modulate the composition of tea polyphenols in a controlled and potentially tunable manner. It establishes a foundation for future work to develop standardized tea extracts, functional beverages, and hybrid products that leverage controlled

microbial oxidation. The insights gained here provide both conceptual and practical pathways for advancing tea biotechnology and for exploring broader applications of microbial oxidoreductases in food systems.

Bibliography

Aaqil, M., Kamil, M., Kamal, A., Nawaz, T., Peng, C., Alaraidh, I. A., Al-Amri, S. S., Okla, M. K., Hou, Y., Fahad, S., & Gong, J. (2024). Metabolomics reveals a differential attitude in phytochemical profile of black tea (*Camellia sinensis* Var. *assamica*) during processing. *Food Chemistry: X*, *24*, 101899.

Abdallah, N., Elmansi, H., & Ibrahim, F. (2024). Facile green spectrophotometric approaches for the determination of three natural edible antioxidant polyphenols in different matrices. *Spectrochimica Acta Part A: Molecular and Biomolecular Spectroscopy*, *318*, 124428.

Abdelgalil, S. A., Attia, A. R., Reyed, R. M., & Soliman, N. A. (2020). Partial purification and biochemical characterization of a new highly acidic NYSO laccase from *Alcaligenes faecalis*. *Journal of Genetic Engineering and Biotechnology*, *18*(1), 79.

Aboulwafa, M. M., Youssef, F. S., Gad, H. A., Sarker, S. D., Nahar, L., Al-Azizi, M. M., & Ashour, M. L. (2019). Authentication and discrimination of green tea samples using UV-vis, FTIR and HPLC techniques coupled with chemometrics analysis. *Journal of Pharmaceutical and Biomedical Analysis*, *164*, 653-658.

Abudureheman, B., Yu, X., Fang, D., & Zhang, H. (2022). Enzymatic oxidation of tea catechins and its mechanism. *Molecules*, *27*(3), 942.

Adak, M., & Abdel-Gabbar, M. (2011). Green tea as a functional food for better health: A brief review. *Research Journal of Pharmaceutical, Biological and Chemical Sciences*, *2*, 645-664.

Adhikary, B., Kashyap, B., Kanrar, B., Gogoi, R. C., Varghese, S., & Babu, A. (2024). Comparative evaluation of the impact of processing methods in determining the levels of health promoting chemical constituents and quality of green tea. *Beverage Plant Research*, *4*(1), 0-0.

Agarwal, P., Singh, M., Singh, J., & Singh, R. P. (2019). Microbial tyrosinases: A novel enzyme, structural features, and applications. In *Applied Microbiology and Bioengineering* (pp. 3-19).

Aguilar, C. N., Rodríguez, R., Gutiérrez-Sánchez, G., Augur, C., Favela-Torres, E., Prado-Barragan, L. A., Ramírez-Coronel, A., & Contreras-Esquivel, J. C. (2007). Microbial tannases: Advances and perspectives. *Applied Microbiology and Biotechnology*, *76*(1), 47-59.

Agunbiade, M., & Le Roes-Hill, M. (2021). Application of bacterial tyrosinases in organic synthesis. *World Journal of Microbiology and Biotechnology*, *38*(1), 2.

Ai, Y., Wu, Q., Yuan, H., He, Y., Jiang, Y., & Niu, S. (2024). Development of a rapid, accurate and efficient HPLC method for simultaneous determination of catechins and theaflavins in black tea. *Journal of Food Composition and Analysis*, *128*, 105990.

Akuli, A., Joshi, R., Dey, T., Pal, A., Gulati, A., & Bhattacharyya, N. (2012). A new method for rapid detection of total colour (TC),theaflavins (TF), thearubigins (TR) and brightness (TB) in orthodox teas. In *2012 Sixth International Conference on Sensing Technology (ICST), Sensing Technology (ICST), 2012 Sixth International Conference on* (pp. 23-28): IEEE.

Al-Sharify, Z. T., Onyeaka, H., Al-Sharify, N. T., AL-Sharify, T. A., Al-Dabooni, N. M., Alshrefy, Z. A. I., Tamasiga, P., & Akinsemolu, A. A. (2025). Optimizing beverage production: the role of fluid dynamics in microbial fermentation. *Journal of Food Processing and Preservation*, *2025*(1), 8811731.

Al-Shwaiyat, M., Denisenko, T., Miekh, Y., & Vishnikin, A. (2018). Spectrophotometric determination of polyphenols in green teas with 18-Molybdodiphosphate. *Chemistry & Chemical Technology*, *12*(2), 135-142.

Ali, N. S., Huang, F., Qin, W., & Yang, T. C. (2022). Identification and characterization of a new *Serratia proteamaculans* strain that naturally produces significant amount of extracellular laccase. *Frontiers in Microbiology*, *Volume 13 - 2022*.

Alshammari, O. A. O., Almulgabsagher, G. A. A., Ryder, K. S., & Abbott, A. P. (2021). Effect of solute polarity on extraction efficiency using deep eutectic solvents. *Green Chemistry*, *23*(14), 5097-5105.

Altunkaya, A. (2014). Partial purification and characterization of polyphenol oxidase from Turkish tea leaf (*Camellia sinensis* L.). *International Journal of Food Properties, 17*(7), 1490–1497.

Amdoun, R., Khelifi, L., Khelifi-Slaoui, M., Amroune, S., Asch, M., Assaf-Ducrocq, C., & Gontier, E. (2018). The desirability optimization methodology; A tool to predict two antagonist responses in biotechnological systems: Case of biomass growth and hyoscyamine content in elicited *Datura starmonium* hairy roots. *Iranian Journal of Biotechnology*, *16*(1), e1339.

Amin, K. A., Elbait, G. D., Yousef, A. F., Al Safar, H., & Ashraf, S. S. (2025). Genomic, bioinformatics, and functional analysis of a novel bioremediation bacterial strain from mangrove sediment. *Case Studies in Chemical and Environmental Engineering*, *11*, 101226.

Aminianfar, A., Fatemi, M. H., & Azimi, F. (2024). Comprehensive characterization of volatile compounds in Iranian black teas using chemometric analysis of GC-MS fingerprints. *Food Chemistry X*, *24*(101859-), 101859.

AOAC. (2023). AOAC official method 2017.13-Total phenolic content in extracts: Folin-C (Folin and Ciocalteu) colorimetric method. In G. W. Latimer, Jr. (Ed.), *Official Methods of Analysis of AOAC Iinternational* (pp. 0). Oxford University Press.

Apak, R., Özyürek, M., Güçlü, K., & Çapanoğlu, E. (2016). Antioxidant Activity/Capacity Measurement. 1. Classification, Physicochemical principles, mechanisms, and electron transfer (ET)-based assays. *Journal of Agricultural and Food Chemistry*, *64*(5), 997-1027.

Aregbe, A. Y., Murtaza, S., Falade, E. O., Rahman, M. H., & Ma, Y. (2025). Synergistic effect of enzyme-assisted fermentation on phytochemical content, volatile profile, antioxidant, antidiabetic, and ACE inhibitory properties of Sea Buckthorn-based cereal beverages. *Food Science and Nutrition*, *13*(12), e71217.

Arifah, M. F., Agustina, A. M. B. H., & Abdul, R. (2022). Application of molecular spectroscopy and chemometrics for authentication and quality control of tea (*Camellia sinensis* L.): A review. *Indonesian Journal of Pharmacy*, *33*(4).

Assad, M., Ashaolu, T. J., Khalifa, I., Baky, M. H., & Farag, M. A. (2023). Dissecting the role of microorganisms in tea production of different fermentation levels: a multifaceted review of their action mechanisms, quality attributes and future perspectives. *World Journal of Microbiology and Biotechnology*, *39*(10), 265.

Athirojthanakij, W., & Rashidinejad, A. (2024). Optimizing catechin extraction from green tea waste: Comparative analysis of hot water, ultrasound-assisted, and ethanol methods for enhanced antioxidant recovery. *Food Science & Nutrition*, *12*(7), 5121-5130.

Ausec, L., Zakrzewski, M., Goesmann, A., Schlüter, A., & Mandic-Mulec, I. (2011). Bioinformatic analysis reveals high diversity of bacterial genes for laccase-like enzymes. *PLoS One*, *6*(10), e25724.

Baldrian, P. (2006). Fungal laccases – Occurrence and properties. *FEMS Microbiology Reviews*, *30*(2), 215-242.

Bastola, K. P., Yadhu Nath, G., Vamsi, B., & Praveen Venkata, V. (2017). Evaluation of standards and interfering compounds in the determination of phenolics by Folin-Ciocalteu assay method for effective bioprocessing of biomass. *American Journal of Analytical Chemistry*, *8*(6), 416-431.

Batt, C. A. (2014). *Alcaligenes*. In C. A. Batt & M. L. Tortorello (Eds.), *Encyclopedia of Food Microbiology (Second Edition)* (pp. 38-41). Academic Press.

Belle, C. (2013). Catechol oxidase and tyrosinase. In R. H. Kretsinger, V. N. Uversky, & E. A. Permyakov (Eds.), *Encyclopedia of Metalloproteins* (pp. 574-579). Springer New York.

Bhuyan, L. P., Borah, P., Sabhapondit, S., Gogoi, R., & Bhattacharyya, P. (2015). Spatial variability of theaflavins and thearubigins fractions and their impact on black tea quality. *Journal of Food Science and Technology*, *52*(12), 7984-7993.

Biswas, A., & Radhakrishna, M. (2025). Exploring catechol binding to laccase with insights into enzyme dynamics for biosensing applications. *The Journal of Physical Chemistry B*, *129*(15), 3761-3775.

Bittner, S. (2006). When quinones meet amino acids: chemical, physical and biological consequences. *Amino Acids*, *30*(3), 205-224.

Bourbonnais, R., & Paice, M. G. (1990). Oxidation of non-phenolic substrates: An expanded role for laccase in lignin biodegradation. *FEBS Letters*, *267*(1), 99-102.

Brodkorb, A., Egger, L., Alminger, M., Alvito, P., Assunção, R., Ballance, S., Bohn, T., Bourlieu-Lacanal, C., Boutrou, R., Carrière, F., Clemente, A., Corredig, M., Dupont, D., Dufour, C., Edwards, C., Golding, M., Karakaya, S., Kirkhus, B., Le Feunteun, S., Recio, I. (2019). INFOGEST static *in vitro* simulation of gastrointestinal food digestion. *Nature Protocols*, *14*(4), 991-1014.

Brugnari, T., Braga, D. M., dos Santos, C. S. A., Torres, B. H. C., Modkovski, T. A., Haminiuk, C. W. I., & Maciel, G. M. (2021). Laccases as green and versatile biocatalysts: from lab to enzyme market—An overview. *Bioresources and Bioprocessing*, *8*(1), 131.

Cabrera, C., Artacho, R., & Gimenez, R. (2006). Beneficial effects of green tea-A review. *Journal of the American College of Nutrition*, *25*(2), 79-99.

Cai, Z.-Y., Li, X.-M., Liang, J.-P., Xiang, L.-P., Wang, K.-R., Shi, Y.-L., Yang, R., Shi, M., Ye, J.-H., Lu, J.-L., Zheng, X.-Q., & Liang, Y.-R. (2018). Bioavailability of tea catechins and its improvement. *Molecules*, *23*(9), 2346.

Camarero, S., Ibarra, D., Martínez María, J., & Martínez Ángel, T. (2005). Lignin-derived compounds as efficient laccase mediators for decolorization of different types of recalcitrant dyes. *Applied and Environmental Microbiology*, *71*(4), 1775-1784.

Campuzano, S., Pedrero, M., Gamella, M., Serafín, V., Yáñez-Sedeño, P., & Pingarrón, J. M. (2020). Beyond sensitive and selective electrochemical biosensors: Towards continuous, real-time, antibiofouling and calibration-free devices. *Sensors*, *20*(12), 3376.

Casanova, E., Salvado, J., Crescenti, A., & Gibert-Ramos, A. (2019). Epigallocatechin gallate modulates muscle homeostasis in type 2 diabetes and obesity by targeting energetic and redox pathways: A narrative review. *International Journal of Molecular Sciences*, *20*(3).

Centers for Disease Control and Prevention, C. N. I. o. H., NIH. (2020). Biosafety in Microbiological and Biomedical Laboratories, 6th ed. U.S. Department of Health and Human Services.

Chance, B., & Maehly, A. C. (1955). Assay of catalases and peroxidases. *Methods in Enzymology, 2*, 773–775.

Chandini, S. K., Jaganmohan Rao, L., & Subramanian, R. (2011). Influence of extraction conditions on polyphenols content and cream constituents in black tea extracts. *International Journal of Food Science & Technology*, *46*(4), 879-886.

Chang, T.-S. (2009). An updated review of tyrosinase inhibitors. *International Journal of Molecular Sciences*, *10*(6), 2440-2475.

Chaudhary, P., Mitra, D., Das Mohapatra, P. K., Oana Docea, A., Mon Myo, E., Janmeda, P., Martorell, M., Iriti, M., Ibrayeva, M., Sharifi-Rad, J., Santini, A., Romano, R., Calina, D., & Cho, W. C. (2023). *Camellia sinensis*: Insights into its molecular mechanisms of action towards nutraceutical, anticancer potential and other therapeutic applications. *Arabian Journal of Chemistry*, *16*(5), 104680.

Chen, C. T., Yang, C. Y., & Tzen, J. T. C. (2022a). Molecular characterization of polyphenol oxidase between small and large leaf tea cultivars. *Scientific Reports*, *12*(1), 12870.

Chen, G., Peng, Y., Xie, M., Xu, W., Chen, C., Zeng, X., & Liu, Z. (2023a). A critical review of Fuzhuan brick tea: Processing, chemical constituents, health benefits and potential risk. *Critical Reviews in Food Science and Nutrition*, *63*(22), 5447-5464.

Chen, L., Liu, F., Yang, Y., Tu, Z., Lin, J., Ye, Y., & Xu, P. (2021). Oxygen-enriched fermentation improves the taste of black tea by reducing the bitter and astringent metabolites. *Food Research International*, *148*, 110613.

Chen, L., Wang, H., Ye, Y., Wang, Y., & Xu, P. (2023b). Structural insight into polyphenol oxidation during black tea fermentation. *Food Chemistry X*, *17*, 100615.

Chen, S., Li, M., Zheng, G., Wang, T., Lin, J., Wang, S., Wang, X., Chao, Q., Cao, S., Yang, Z., & Yu, X. (2018). Metabolite profiling of 14 Wuyi Rock tea cultivars using UPLC-QTOF MS and UPLC-QqQ MS combined with chemometrics. *Molecules*, *23*(2).

Chen, X., Hu, Y., Wang, B., Chen, Y., Yuan, Y., Zhou, W., Song, W., Wu, Z., & Li, X. (2022b). Characterization of theabrownins prepared from tea polyphenols by enzymatic and chemical oxidation and their inhibitory effect on colon cancer cells. *Frontiers in Nutrition*, *Volume 9 - 2022*.

Chen, Y., Gao, R., Xiang, J., Lin, Z., Chen, C., & Yu, W. (2025a). Progress of near infrared spectroscopy in tea research. *Food Chemistry*, *487*, 144691.

Chen, Y., Lai, L., You, Y., Gao, R., Xiang, J., Wang, G., & Yu, W. (2023c). Quantitative analysis of bioactive compounds in commercial teas: Profiling catechin alkaloids, phenolic acids, and flavonols using targeted statistical approaches. *Foods*, *12*(16), 3098.

Chen, Z., Sui, Y., & Wisniewski, M. (2025b). Current and future perspectives on tea production. *Industrial Crops and Products*, *235*, 121663.

Chiang, S.-H., Yang, K.-M., Wang, S.-Y., & Chen, C.-W. (2022). Enzymatic treatment in black tea manufacturing processing: Impact on bioactive compounds, quality, and bioactivities of black tea. *LWT - Food Science & Technology*, *163*, 113560.

Cieńska, M., Labus, K., Lewańczuk, M., Koźlecki, T., Liesiene, J., & Bryjak, J. (2016). Effective L-Tyrosine hydroxylation by native and Immobilized tyrosinase. *PLoS One*, *11*(10), e0164213.

Cisneros-Yupanqui, M., & Lante, A. (2020). Tea from the food science perspective: An overview. *The Open Biotechnology Journal*, *14*(1), 78-83.

Claus, H. (2004). Laccases: Structure, reactions, distribution. *Micron*, *35*(1-2), 93-96.

Claus, H. (2010). Copper-containing oxidases: Occurrence in soil microorganisms, properties, and applications. In I. Sherameti & A. Varma (Eds.), *Soil heavy metals* (Soil Biology, Vol. 19, pp. 281–313). Springer.

Claus, H., & Decker, H. (2006). Bacterial tyrosinases. *Systematic and Applied Microbiology*, *29*(1), 3-14.

Cohen, J. (1988). *Statistical power analysis for the behavioral sciences* (2nd ed.). Lawrence Erlbaum Associates.

Coll, P. M., Fernández-Abalos, J. M., Villanueva, J. R., Santamaría, R., & Pérez, P. (1993). Purification and characterization of a phenoloxidase (laccase) from the lignin-degrading basidiomycete PM1 (CECT 2971). *Applied and Environmental Microbiology*, *59*(8), 2607-2613.

Cordero, C., Canale, F., Del Rio, D., & Bicchi, C. (2009). Identification, quantitation, and method validation for flavan-3-ols in fermented ready-to-drink teas from the Italian market using HPLC-UV/DAD and LC-MS/MS. *Journal of Separation Science*, *32*(21), 3643-3651.

Ćorković, I., Gašo-Sokač, D., Pichler, A., Šimunović, J., & Kopjar, M. (2022). Dietary polyphenols as natural inhibitors of α-amylase and α-glucosidase. *Life (Basel)*, *12*(11).

Couzinet-Mossion, A., Balayssac, S., Gilard, V., Malet-Martino, M., Potin-Gautier, M., & Behra, P. (2010). Interaction mechanisms between caffeine and polyphenols in infusions of *Camellia sinensis* leaves. *Food Chemistry*, *119*(1), 173-181.

Custodio-Mendoza, J. A., Pokorski, P., Aktas, H., Carro, A. M., & Kurek, M. A. (2024). Simultaneous determination of six catechins and caffeine in tea and wine using salting-out assisted liquid-liquid extraction and high-performance liquid chromatography with ultraviolet detection. *Journal of Separation Science*, *47*(9-10), e2400142.

Dai, S., Yao, Q., Yu, G., Liu, S., Yun, J., Xiao, X., Deng, Z., & Li, H. (2021). Biochemical characterization of a novel bacterial laccase and improvement of its efficiency by directed evolution on dye degradation. *Frontiers in Microbiology*, *Volume 12 - 2021*.

De, D., Deb, M., & Ray, S. (2024). Comprehensive Isolation and characterization of theaflavins, thearubigins and caffeine as bioactive compounds from Darjeeling black tea. *Asian Journal of Chemistry*, *36*, 2443-2451.

Deka, H., Sarmah, P. P., Devi, A., Tamuly, P., & Karak, T. (2021). Changes in major catechins, caffeine, and antioxidant activity during CTC processing of black tea from North East India. *RSC Advances*, *11*(19), 11457-11467.

Demesa, A. G., Saavala, S., Poysa, M., & Koiranen, T. (2024). Overview and toxicity assessment of ultrasound-assisted extraction of natural ingredients from plants. *Foods*, *13*(19), 3066.

Derringer, G., & Suich, R. (1980). Simultaneous Optimization of Several Response Variables. *Journal of Quality Technology*, *12*(4), 214-219.

Detering, T., Linke, D., Gounel, S., Mano, N., & Berger, R. G. (2018). Laccase-catalysed cleavage of malvidin-3-O-galactoside to 2,6-dimethoxy-1,4-benzoquinone and a coumarin galactoside. *Mycological Progress*, *17*(6), 681-690.

Devi, M., Sarma, A. D., Kalita, P., Parasar, D. P., Hiremath, V., Choudhary, N., Kumar, D., & Babu Kondaveeti, S. (2025). Advances in microbial enzyme technology for food processing strategies and applications. *Discover Food*, *6*(1), 56.

Dilkalal, A., Annapurna, A. S., & Umesh, T. G. (2024). *In vitro* antioxidant, anticancer and *in silico* studies of polyphenol enriched leaf extract of Asystasia gangetica. *Scientific Reports*, *14*(1), 28374.

Dimcheva, V., Kaloyanov, N., Karsheva, M., Peycheva, M. F., & Stoilova, N. (2019). HPLC-DAD method for simultaneous determination of natural polyphenols. *Open Journal of Analytical and Bioanalytical Chemistry*, *3*(1), 039-043.

Dirks-Hofmeister, M. E., Kolkenbrock, S., & Moerschbacher, B. M. (2013). Parameters that enhance the bacterial expression of active plant polyphenol oxidases. *PLoS ONE, 8*(10), e77291.

Drynan, J. W., Clifford, M. N., Obuchowicz, J., & Kuhnert, N. (2010). The chemistry of low molecular weight black tea polyphenols. *ChemInform*, *41*(24).

Du, S., Chang, J., & Zhou, Z. (2025). A Comprehensive Review of Theaflavins: Physiological Activities, Synthesis Techniques, and Future Challenges. *Food Science and Nutrition*, *13*(8), e70762.

EFSA FCA Panel, o. F. C. M., Enzymes, Aids, P., Lambré, C., Barat Baviera, J. M., Bolognesi, C., Cocconcelli, P. S., Crebelli, R., Gott, D. M., Grob, K., Lampi, E., Mengelers, M., Mortensen, A., Rivière, G., Steffensen, I.-L., Tlustos, C., Van Loveren, H., Vernis, L., Zorn, H., Glandorf, B., Chesson, A. (2021). Scientific guidance for the submission of dossiers on food enzymes. *EFSA Journal*, *19*(10), e06851.

Eicken, C., Zippel, F., Büldt-Karentzopoulos, K., & Krebs, B. (1998). Biochemical and spectroscopic characterization of catechol oxidase from sweet potatoes (*Ipomoea batatas*) containing a type-3 dicopper center. *FEBS Letters*, *436*(2), 293-299.

El-Sayed, S. E., Abdelaziz, N. A., Alshahrani, M. Y., El-Housseiny, G. S., & Aboshanab, K. M. (2024). Biologically active metabolites of *Alcaligenes faecalis*: diversity, statistical optimization, and future perspectives. *Future Science OA*, *10*(1), 2430452.

Engelhardt, U. H. (2010). Chemistry of tea. In H.-W. Liu & L. Mander (Eds.), *Comprehensive Natural Products II* (pp. 999-1032). Elsevier.

Engelhardt, U. H. (2023). Different types of tea: Chemical composition, analytical methods and authenticity. In J.-M. Mérillon, C. Riviere, & G. Lefèvre (Eds.), *Natural Products in Beverages: Botany, Phytochemistry, Pharmacology and Processing* (pp. 1-44). Springer International Publishing.

Eran Nagar, E., Okun, Z., & Shpigelman, A. (2020). Digestive fate of polyphenols: updated view of the influence of chemical structure and the presence of cell wall material. *Current Opinion in Food Science*, *31*, 38-46.

Ergün, B. G., Berrios, J., Binay, B., & Fickers, P. (2021). Recombinant protein production in *Pichia pastoris*: from transcriptionally redesigned strains to bioprocess optimization and metabolic modelling. *FEMS Yeast Research*, *21*(7).

Espín, J. C., Morales, M., García-Ruiz, P. A., Tudela, J., & García-Cánovas, F. (1997). Improvement of a continuous spectrophotometric method for determining the monophenolase and diphenolase activities of mushroom polyphenol oxidase. *Journal of Agricultural and Food Chemistry*, *45*(4), 1084-1090.

Espina, G., Atalah, J., & Blamey, J. M. (2021). Extremophilic oxidoreductases for the industry: Five successful examples with promising projections. *Frontiers in Bioengineering and Biotechnology*, *9*, 710035.

Fang, X., Du, M., Liu, T., Fang, Q., Liao, Z., Zhong, Q., Chen, J., Meng, X., Zhou, S., & Wang, J. (2019). Changes in the biotransformation of green tea catechins induced by different carbon and nitrogen sources in *Aspergillus niger* RAF106. *Frontiers in Microbiology*, *10*, 2521.

FAO. (2022). International tea market: Market situation, prospects and emerging issues. 11p. https://openknowledge.fao.org/items/6af87b3d-5b2b-424c-817e-6a049a48668c

FAO. (2024). *Current global market situation and medium-term outlook*. F. a. A. O. o. t. U. Nations. https://openknowledge.fao.org/server/api/core/bitstreams/c1cad039-4e40-4888-bc74-3073d3ed7963/content

FAO/WHO. (2006). General specifications and considerations for enzyme preparations used in food processing. *Combined Compendium of Food Additive Specifications*, *4*. https://www.fao.org/4/a0691e/A0691E03.htm

Faustina, D. R., Gunadi, R., Fitriani, A., & Supriyadi, S. (2022). Alteration of phenolic and volatile compounds of tea leaf extract by tyrosinase and β-glucosidase during preparation of ready-to-drink tea on farm. *International Journal of Food Science*, *2022*(1), 1977762.

Feng, Z., Li, Y., Li, M., Wang, Y., Zhang, L., Wan, X., & Yang, X. (2019). Tea aroma formation from six model manufacturing processes. *Food Chemistry*, *285*, 347-354.

Fernandez-Julia, P. J., Tudela-Serrano, J., Garcia-Molina, F., Garcia-Canovas, F., Garcia-Jimenez, A., & Munoz-Munoz, J. L. (2021). Study of tyrosine and dopa enantiomers as tyrosinase substrates initiating l- and D-melanogenesis pathways. *Biotechnology and Applied Biochemistry*, *68*(4), 823-831.

Frańska, M., & Frański, R. (2024). Application of mass spectrometry for analysis of nucleobases, nucleosides and nucleotides in tea and selected herbs: A critical review of the mass spectrometric data. *Foods*, *13*(18).

Friedman, M., Kim, S. Y., Lee, S. J., Han, G. P., Han, J. S., Lee, K. R., & Kozukue, N. (2005). Distribution of catechins, theaflavins, caffeine, and theobromine in 77 teas consumed in the United States. *Journal of Food Science*, *70*(9), C550-C559.

Friedman, M., Levin, C. E., Lee, S.-U., & Kozukue, N. (2009). Stability of green tea catechins in commercial tea leaves during storage for 6 months. *Journal of Food Science*, *74*(2), H47-H51.

García-Molina, F., Fenoll, L. G., Morote, J. C., García-Ruiz, P. A., Rodríguez-López, J. N., García-Cánovas, F., & Tudela, J. (2005). Opposite effects of peroxidase in the initial stages of tyrosinase-catalysed melanin biosynthesis. *The International Journal of Biochemistry & Cell Biology*, *37*(6), 1179-1196.

Gascoyne, K., Marchand, F., Desharnais, J., & Americi, H. (2018). *Tea: History, terroirs, varieties* (Third Edition (revised and updated) ed.). Firefly Books.

Ge, Y., Bian, X., Sun, B., Zhao, M., Ma, Y., Tang, Y., Li, N., & Wu, J. L. (2019). Dynamic profiling of phenolic acids during Pu-erh tea fermentation using derivatization liquid chromatography-mass spectrometry approach. *Journal of Agricultural and Food Chemistry*, *67*(16), 4568-4577.

Gigault, J., El Hadri, H., Reynaud, S., Deniau, E., & Grassl, B. (2017). Asymmetrical flow field flow fractionation methods to characterize submicron particles: application to carbon-based aggregates and nanoplastics. *Analytical and Bioanalytical Chemistry*, *409*(29), 6761-6769.

Gomathi, D., Muthulakshmi, C., Kumar, D. G., Ravikumar, G., Kalaiselvi, M., & Uma, C. (2012). Submerged fermentation of wheat bran by *Aspergillus flavus* for production and characterization of carboxy methyl cellulase. *Asian Pacific Journal of Tropical Biomedicine*, *2*(1, Supplement), S67-S73.

Goncalves, B. D., Windson Isidoro Haminiuk, C., Cristina Pedro, A., de Andrade Arruda Fernandes, I., & Maria Maciel, G. (2021). Processing, chemical signature and food industry applications of *Camellia sinensis* teas: An overview. *Food Chemistry X*, *12*, 100160.

Governa, P., Manetti, F., Miraldi, E., & Biagi, M. (2022). Effects of *in vitro* simulated digestion on the antioxidant activity of different *Camellia sinensis* (L.) Kuntze leaves extracts. *European Food Research and Technology*, *248*(1), 119-128.

Govindarajan, R. K., Khanongnuch, C., Mathivanan, K., Shyu, D. J. H., Sharma, K. P., & De Mandal, S. (2021). In-vitro biotransformation of tea using tannase produced by *Enterobacter cloacae* 41. *Journal of Food Science and Technology*, *58*(8), 3235-3242.

Guan, X., Chen, Q., & Guo, T. (2024). Variation of taste and odor compounds in tea beverage after microbial fermentation by HPLC–MS, GC×GC–O–MS, GC–MS, and sensory evaluation. *Journal of Food Composition and Analysis*, *128*, 106075.

Guo, X., Wang, L., Huang, X., & Zhou, Q. (2025). Characterization of the volatile compounds in tea (*Camellia sinensis* L.) flowers during blooming. *Frontiers in Nutrition*, *Volume 11 - 2024*.

Gupta, A., Kagliwal, L. D., & Singhal, R. S. (2013). Biotransformation of polyphenols for improved bioavailability and processing stability. In J. Henry (Ed.), *Advances in Food and Nutrition Research* (Vol. 69, pp. 183-217). Academic Press.

Hakim, S., Naqqash, T., Nawaz, M. S., Laraib, I., Siddique, M. J., Zia, R., Mirza, M. S., & Imran, A. (2021). Rhizosphere engineering with plant growth-promoting microorganisms for agriculture and ecological sustainability. *Frontiers in Sustainable Food Systems*, *Volume 5 - 2021*.

Harbowy, M. E., Balentine, D. A., Davies, A. P., & Cai, Y. (2010). Tea chemistry. *Critical Reviews in Plant Sciences*, *16*(5), 415-480.

Harvey, N., Takis, P. G., Lindon, J. C., Li, J. V., & Jiménez, B. (2023). Optimization of diffusion-ordered NMR spectroscopy experiments for high-throughput automation in human metabolic phenotyping. *Analytical Chemistry*, *95*(6), 3147-3152.

Hasan, S., Anwar, Z., Khalid, W., Afzal, F., Zafar, M., Ali, U., Refai, M. Y., Afifi, M., AL-Farga, A., & Aljobair, M. O. (2023). Laccase production from local biomass using solid-state fermentation. *Fermentation*, *9*(2), 179.

Hashiguchi, K., Teramoto, S., Katayama, K., Matsuo, Y., Saito, Y., & Tanaka, T. (2023). Oligomerization mechanisms of tea catechins involved in the production of black tea thearubigins. *Journal of Agricultural and Food Chemistry*, *71*(41), 15319-15330.

Haslam, E. (2003). Thoughts on thearubigins. *Phytochemistry*, *64*(1), 61-73.

He, H. F. (2017). Research progress on theaflavins: efficacy, formation, and preparation. *Food & Nutrition Research*, *61*(1), 1344521.

He, S., Deng, X., Han, Y., Gong, Z., Wang, J., Tao, X., Tong, H., & Chen, Y. (2023). Metabolites and metagenomic analysis reveals the quality of Pu-erh "tea head". *Food Chemistry*, *429*, 136992.

Hearing, V. J., & Tsukamoto, K. (1991). Enzymatic control of pigmentation in mammals. *The FASEB Journal*, *5*(14), 2902-2909.

Hidayat, M., Jannah, F., & Kuswandi, B. (2016). Development of paper based sensor for the determination of total phenolic content in green tea beverages. *Agriculture and Agricultural Science Procedia*, *9*, 424-430.

Hilal, Y., & Engelhardt, U. (2007). Characterisation of white tea – Comparison to green and black tea. *Journal für Verbraucherschutz und Lebensmittelsicherheit*, *2*(4), 414-421.

Hiroshi, U., & Shiro, K. (2003). Enzymatic synthesis of polyphenols. *Current Organic Chemistry*, *7*(13), 1387-1397.

Ho, C.-T., Zhu, N., & Huang, T.-C. (2001). Oxidative transformation of tea catechins. In *Chemistry and physiology, food colorants selected* (Vol. 775, pp. 102-112). American Chemical Society.

Holm, K. A., Nielsen, D. M., & Eriksen, J. (1998). Automated colorimetric determination of recombinant fungal laccase activity in fermentation samples using syringaldazine as chromogenic substrate. *Journal of Analytical Methods in Chemistry*, *20*(6), 913298.

Hong, B. X., Ichihashi, M., & Ngoc, N. T. B. (2024). Analysis of consumer preferences for green tea products: A randomized conjoint analysis in Thai Nguyen, Vietnam. *Sustainability*, *16*(11), 4521.

Horanni, R., & Engelhardt, U. H. (2013). Determination of amino acids in white, green, black, oolong, pu-erh teas and tea products. *Journal of Food Composition and Analysis*, *31*(1), 94-100.

Hu, T., Shi, S., & Ma, Q. (2022). Modulation effects of microorganisms on tea in fermentation. *Frontiers in Nutrition*, *9*, 931790.

Huang, C. (2020). Extensively drug-resistant *Alcaligenes faecalis* infection. *BMC Infectious Diseases*, *20*(1), 833.

Huang, S., Zhao, H., Hu, Y., Ren, D., & Yi, L. (2022). Comprehensive analysis of chemical constituents of tea flowers by ultra-performance liquid chromatography-high resolution mass spectrometry combined with integrated filtering strategy. *Chinese Journal of Chromatography*, *40*(3), 242-252.

Huang, Y., Goh, R. M. V., Pua, A., Jublot, L., Liu, S. Q., Yu, B., & Huang, D. (2025). Advanced analytical techniques for bioactive compounds in tea. In V. R. Preedy & V. B. Patel (Eds.), *Tea in Health and Disease Prevention (Second Edition)* (pp. 887-897). Academic Press.

Huda, H.-S.-A., Majid, N. B. A., Chen, Y., Adnan, M., Ashraf, S. A., Roszko, M., Bryła, M., Kieliszek, M., & Sasidharan, S. (2024). Exploring the ancient roots and modern global brews of tea and herbal beverages: A comprehensive review of origins, types, health benefits, market dynamics, and future trends. *Food Science & Nutrition*, *12*(10), 6938-6955.

Ishino, N., Yanase, E., & Nakatsuka, S. (2010). Epimerization of tea catechins under weakly acidic and alkaline conditions. *Bioscience, Biotechnology, and Biochemistry*, *74*(4), 875-877.

ISO. (1980). ISO 1573:1980 Tea- Determination of loss in mass at 103 degrees C. In: International Organization for Standardization.

ISO. (2005). ISO 14502-1:2005 Determination of substances characteristic of green and black tea; Part 1: Content of total polyphenols in tea — Colorimetric method using Folin-Ciocalteu reagent. In. Vernier (Geneva), Switzerland.: International Organization for Standardization.

ISO. (2021). ISO 18447:2021 Tea — Determination of theaflavins in black tea — Method using high performance liquid chromatography. In: International Organization for Standardization.

Ito, A., & Yanase, E. (2022). Study into the chemical changes of tea leaf polyphenols during Japanese black tea processing. *Food Research International*, *160*, 111731.

Itoh, N., Katsube, Y., Yamamoto, K., Nakajima, N., & Yoshida, K. (2007). Laccase-catalyzed conversion of green tea catechins in the presence of gallic acid to epitheaflagallin and epitheaflagallin 3-O-gallate. *Tetrahedron*, *63*(38), 9488-9492.

Iwasaki, Y., Hirasawa, T., Maruyama, Y., Ishii, Y., Ito, R., Saito, K., Umemura, T., Nishikawa, A., & Nakazawa, H. (2011). Effect of interaction between phenolic compounds and copper ion on antioxidant and pro-oxidant activities. *Toxicology in Vitro*, *25*(7), 1320-1327.

John, A., Riaz, S., Taihid Ali, S. K., & Selvarajan, E. (2025). Laccase and polyphenol oxidase: Biochemistry and biotechnological applications. In I. K. H. Leung (Ed.), *Laccase and*

polyphenol oxidase: Biochemistry and biotechnological applications (pp. 69–83). Academic Press.

Jan, M., Sharba, M., Falih, S., Rdam, R., & Mohammed, A. (2023). Isolation and Characterization of tannase from isolated *Bacillus subtilis Ymer*, *21*.

Janusz, G., Pawlik, A., Swiderska-Burek, U., Polak, J., Sulej, J., Jarosz-Wilkolazka, A., & Paszczynski, A. (2020). Laccase properties, physiological functions, and evolution. *International Journal of Molecular Sciences*, *21*(3), 966.

Jayasinghe, S. L., Kumar, L., & Hasan, M. K. (2020). Relationship between environmental covariates and Ceylon tea cultivation in Sri Lanka. *Agronomy*, *10*(4).

Jia, W. B., Zhao, Y. Q., Liao, S. Y., Li, P. W., Zou, Y., Chen, S. X., Chen, W., He, C. L., Du, X., Zhu, M. Z., & Xu, W. (2022). Dynamic changes in the diversity and function of bacterial community during black tea processing. *Food Research International 161*, 111856.

Jiang, C. K., Ma, J. Q., Apostolides, Z., & Chen, L. (2019a). Metabolomics for a millenniums-old crop: tea plant (*Camellia sinensis*). *Journal of Agricultural and Food Chemistry*, *67*(23), 6445-6457.

Jiang, H., Yu, F., Qin, L., Zhang, N., Cao, Q., Schwab, W., Li, D., & Song, C. (2019b). Dynamic change in amino acids, catechins, alkaloids, and gallic acid in six types of tea processed from the same batch of fresh tea (*Camellia sinensis* L.) leaves. *Journal of Food Composition and Analysis*, *77*, 28-38.

Jiang, J., Zhang, M., An, T., Zu, Z., Song, P., Chen, M., Yue, P., & Gao, X. (2022). Preparation of instant dark tea by liquid-state fermentation using sequential inoculation with *Eurotium cristatum* and *Aspergillus niger*: Processes optimization, physiochemical characteristics and antioxidant activity. *LWT - Food Science & Technology*, *162*, 113379.

Johnson, J. B., Mani, J. S., & Naiker, M. (2023). Microplate methods for measuring phenolic content and antioxidant capacity in chickpea: impact of shaking. *Engineering Proceedings*, *48*(1), 57.

Juneja, L. R., Chu, D.-C., Okubo, T., Nagato, Y., & Yokogoshi, H. (1999). L-theanine—a unique amino acid of green tea and its relaxation effect in humans. *Trends in Food Science & Technology*, *10*(6), 199-204.

Kakuda, T. (2011). Neuroprotective effects of theanine and its preventive effects on cognitive dysfunction. *Pharmacological Research*, *64*(2), 162-168.

Kan, L., Capuano, E., Fogliano, V., Verkerk, R., Mes, J. J., Tomassen, M. M. M., & Oliviero, T. (2021). Inhibition of α-glucosidases by tea polyphenols in rat intestinal extract and Caco-2 cells grown on Transwell. *Food Chemistry*, *361*, 130047.

Karas, D., Ulrichova, J., & Valentova, K. (2017). Galloylation of polyphenols alters their biological activity. *Food and Chemical Toxicology*, *105*, 223-240.

Karyakin, A. A. (2001). Prussian blue and its analogues: Electrochemistry and analytical applications. *Electroanalysis*, *13*(10), 813-819.

Khan, A. L., Hussain, J., Al-Harrasi, A., Al-Rawahi, A., & Lee, I. J. (2015). Endophytic fungi: Resource for gibberellins and crop abiotic stress resistance. *Critical Reviews in Biotechnology*, *35*(1), 62-74.

Khlupova, M. E., Vasil'eva, I. S., Shumakovich, G. P., Morozova, O. V., Chertkov, V. A., Shestakova, A. K., Kisin, A. V., & Yaropolov, A. I. (2015). Enzymatic polymerization of dihydroquercetin using bilirubin oxidase. *Biochemistry (Mosc)*, *80*(2), 233-241.

Khlupova, M. E., Vasil'eva, I. S., Shumakovich, G. P., Morozova, O. V., Zaitseva, E. A., Chertkov, V. A., Shestakova, A. K., Kisin, A. V., & Yaropolov, A. I. (2018). Multicopper oxidase-catalyzed biotransformation of dihydroquercetin. *Moscow University Chemistry Bulletin*, *73*(5), 237-243.

Kidist, T. (2019). Effect of tea processing methods on biochemical composition and sensory quality of black tea (*Camellia sinensis* (L.) O. Kuntze): A review. *Journal of Horticulture and Forestry*, *11*(6), 84-95.

Kikkawa, H. S., Kobayashi, M., Minamimoto, A., Ono, H., & Tsuge, K. (2022). Simultaneous determination of eight catechins and four theaflavins in bottled tea by liquid chromatography-tandem mass spectrometry for forensic analysis. *Journal in Forensic Science*, *67*(1), 309-320.

Kleks, G., Holland, D. C., Porter, J., & Carroll, A. R. (2021). Natural products dereplication by diffusion ordered NMR spectroscopy (DOSY). *Chemical Science*, *12*(32), 10930-10943.

Kong, J., Yang, X., Zuo, X., Su, X., Hu, B., & Liang, X. (2022). High-quality instant black tea manufactured using fresh tea leaves by two-stage submerged enzymatic processing. *Food Science and Human Wellness*, *11*(3), 676-685.

Korenblum, E., Massalha, H., & Aharoni, A. (2022). Plant–microbe interactions in the rhizosphere via a circular metabolic economy. *The Plant Cell*, *34*(9), 3168-3182.

Koros, D., Tshelang, C., & Masangano, M. (2023). Current trend in Kenya's tea industry. *Agricultural Socio-Economics Journal*, *23*, 231-238.

Kuhnert, N. (2010). Unraveling the structure of the black tea thearubigins. *Archives of Biochemistry and Biophysics*, *501*(1), 37-51.

Kuhnert, N., Drynan, J. W., Obuchowicz, J., Clifford, M. N., & Witt, M. (2010a). Mass spectrometric characterization of black tea thearubigins leading to an oxidative cascade hypothesis for thearubigin formation. *Rapid Commun Mass Spectrom*, *24*(23), 3387-3404.

Kumar, A., & Azmi, W. (2016). Analysis of physicochemical variables and their interactive effect on uricase production from *Alcaligenes faecalis*. *Journal of Applied Microbiology*, *2*(6), 275-284.

Kumar, A., Dhiman, S., Krishan, B., Samtiya, M., Kumari, A., Pathak, N., Kumari, A., Aluko, R. E., & Dhewa, T. (2024a). Microbial enzymes and major applications in the food industry: a concise review. *Food Production, Processing and Nutrition*, *6*(1), 85.

Kumar, A., Kumar, S., & Kumar, S. (2005). Biodegradation kinetics of phenol and catechol using *Pseudomonas putida* MTCC 1194. *Biochemical Engineering Journal*, *22*(2), 151-159.

Kumar, B. S. S., Golla, N., Kumar, K. D., Geetha, K. S., & Reddy, B. R. (2024b). Bacterial polyphenol oxidases and their applications in bioremediation. In V. Pradeep, A. Komal, & P. S. Maulin (Eds.), *Polyphenol Oxidases* (pp. 25-68).

Kumar, P., Chaudhary, S., Sood, S., Mahant, S., Pundir, S., Kalia, P., & Kumar, R. (2025). Tea beyond the cup: a comprehensive review of *Camellia sinensis* (L.) O. Kuntze. *Clinical Phytoscience*, *11*(1), 23.

Kumar, V. V., Venkataraman, S., Kumar, P. S., George, J., Rajendran, D. S., Shaji, A., Lawrence, N., Saikia, K., & Rathankumar, A. K. (2022). Laccase production by *Pleurotus ostreatus* using cassava waste and its application in remediation of phenolic and polycyclic aromatic hydrocarbon-contaminated lignocellulosic biorefinery wastewater. *Environmental Pollution*, *309*, 119729.

Kumbasaroglu, H. (2026). Global tea production forecasting using ARIMA models: A multi-country time-series analysis (1961–2028). *Sustainability*, *18*(2), 1005.

Kunamneni, A., Plou, F. J., Ballesteros, A., & Alcalde, M. (2008). Laccases and their applications: a patent review. *Recent Patents on Biotechnology*, *2*(1), 10-24.

Kyomuhimbo, H. D., & Brink, H. G. (2023). Applications and immobilization strategies of the copper-centred laccase enzyme; a review. *Heliyon*, *9*(2), e13156.

Laemmli, U. K. (1970). Cleavage of Structural Proteins during the Assembly of the Head of Bacteriophage T4. *Nature*, *227*(5259), 680-685.

Lee, L. S., Kim, Y. C., Park, J. D., Kim, Y. B., & Kim, S. H. (2016). Changes in major polyphenolic compounds of tea (*Camellia sinensis*) leaves during the production of black tea. *Food Science and Biotechnology*, *25*(6), 1523-1527.

Lee, M.-K., Kim, H.-W., Lee, S.-H., Kim, Y. J., Asamenew, G., Choi, J., Lee, J.-W., Jung, H.-A., Yoo, S. M., & Kim, J.-B. (2018). Characterization of catechins, theaflavins, and flavonols by leaf processing step in green and black teas (*Camellia sinensis*) using UPLC-DAD-QToF/MS. *European Food Research and Technology*, *245*(5), 997-1010.

Le Maux, S., Nongonierma, A. B., Lardeux, C., & FitzGerald, R. J. (2017). Impact of enzyme inactivation conditions during the generation of whey protein hydrolysates on their physicochemical and bioactive properties. *International Journal of Food Science and Technology, 53*(1), 219–227.

Leonard, W., Zhang, P., Ying, D., Adhikari, B., & Fang, Z. (2021). Fermentation transforms the phenolic profiles and bioactivities of plant-based foods. *Biotechnology Advances*, *49*, 107763.

Lei, J., Zhang, Y., Ni, X., Yu, X., & Wang, X. (2021). Degradation of epigallocatechin and epicatechin gallates by a novel tannase TanHcw from *Herbaspirillum camelliae*. *Microbial Cell Factories, 20*, Article 197.

Leung, L. K., Su, Y., Zhang, Z., Chen, Z.-Y., Huang, Y., & Chen, R. (2001). Theaflavins in black tea and catechins in green tea are equally effective antioxidants. *The Journal of nutrition*, *131*(9), 2248-2251.

Li, D., Dong, L., Li, J., Zhang, S., Lei, Y., Deng, M., & Li, J. (2022a). Optimization of enzymatic synthesis of theaflavins from potato polyphenol oxidase. *Bioprocess and Biosystems Engineering*, *45*(6), 1047-1055.

Li, H., Huang, W., Wang, G.-L., Wang, W.-L., Cui, X., & Zhuang, J. (2017). Transcriptomic analysis of the biosynthesis, recycling, and distribution of ascorbic acid during leaf development in tea plant (*Camellia sinensis* (L.) O. Kuntze). *Scientific Reports*, *7*(1), 46212.

Li, L., Zan, J., Chen, W., Zong, X., Yuan, H., Jiang, Y., & Zhu, H. (2025a). Maillard reaction inducing amino acids degradation can adjust the flavour characteristic of black tea. *Food Research International*, *201*, 115685.

Li, M., Dong, Y., Kang, M., Tao, T., Li, W., Zhang, S., Quan, W., & Liu, Z. (2024a). Potential anti-hyperglycemic activity of black tea theaflavins through inhibiting α-amylase. *Food Chem X*, *22*, 101296.

Li, M., Xiao, J., Zeng, Z., Zhang, T., & Ren, Y. (2023). Study on the biodegradation of phenol by *Alcaligenes faecalis* JH1 immobilized in rice husk biochar. *Frontiers in Environmental Science*, *Volume 11 - 2023*.

Li, M., Xiao, Y., Zhong, K., Wu, Y., & Gao, H. (2022b). Delving into the biotransformation characteristics and mechanism of steamed green tea fermented by Aspergillus niger PW-2 based on metabolomic and proteomic approaches. *Foods*, *11*(6), 865.

Li, M., Xu, H., Chen, H., Ding, F., Li, Q., Liu, Z., Wang, F., Jia, X., Wu, Y., Sun, Y., & Jin, S. (2025b). Metabolomics and transcriptomics reveal the quality formation mechanism during the processing of black tea. *npj Science of Food*, *9*(1), 131.

Li, N., Taylor, L. S., Ferruzzi, M. G., & Mauer, L. J. (2012). Kinetic study of catechin stability: effects of pH, concentration, and temperature. *Journal of Agricultural and Food Chemistry*, *60*(51), 12531-12539.

Li, N., Xu, J., Zhao, Y., Zhao, M., Liu, Z., Wang, K., Huang, J., & Zhu, M. (2024b). The influence of processing methods on polyphenol profiling of tea leaves from the same large-leaf cultivar (*Camellia sinensi*s var. assamica cv. Yunkang-10): nontargeted/targeted polyphenomics and electronic sensory analysis. *Food Chemistry*, *460*(Pt 2), 140515.

Li, S., Lo, C.-Y., Pan, M.-H., Lai, C.-S., & Ho, C.-T. (2013). Black tea: Chemical analysis and stability. *Food & Function*, *4*(1), 10-18.

Li, S., Zhang, L., Wan, X., Zhan, J., & Ho, C.-T. (2022c). Focusing on the recent progress of tea polyphenol chemistry and perspectives. *Food Science and Human Wellness*, *11*(3), 437-444.

Li, T., Xu, S., Wang, Y., Wei, Y., Shi, L., Xiao, Z., Liu, Z., Deng, W. W., & Ning, J. (2021). Quality chemical analysis of crush-tear-curl (CTC) black tea from different geographical regions based on UHPLC-Orbitrap-MS. *Journal of Food Science*, *86*(9), 3909-3925.

Li, Y., Hao, J., Zhou, J., He, C., Yu, Z., Chen, S., Chen, Y., & Ni, D. (2022d). Pile-fermentation of dark tea: Conditions optimization and quality formation mechanism. *LWT - Food Science & Technology*, *166*.

Liang, J., Wu, H., Lu, M., & Li, Y. (2024). HS-SPME-GC-MS untargeted metabolomics reveals key volatile compound changes during Liupao tea fermentation. *Food Chemistry: X*, *23*, 101764.

Liang, Y.-R., Lu, J., Zhang, L., Wu, S., & Wu, Y. (2003a). Estimation of black tea quality by analysis of chemical composition and colour difference of tea infusions. *Food Chemistry*, *80*, 283-290.

Liang, Y., Lu, J., Zhang, L., Wu, S., & Wu, Y. (2003b). Estimation of black tea quality by analysis of chemical composition and colour difference of tea infusions. *Food Chemistry*, *80*(2), 283-290.

Liang, Z., Huang, Y., Zhang, P., & Fang, Z. (2023). Impact of fermentation on the structure and antioxidant activity of selective phenolic compounds. *Food Bioscience*, *56*, 103147.

Lichtenberg, M., Kvich, L., Larsen, S. L. B., Jakobsen, T. H., & Bjarnsholt, T. (2022). Inoculum concentration influences *Pseudomonas aeruginosa* phenotype and biofilm architecture. *Microbiology Spectrum*, *10*(6), e0313122.

Lin, H., Liu, C., Peng, Z., Tan, B., Wang, K., & Liu, Z. (2022). Distribution pattern of endophytic bacteria and fungi in tea plants. *Frontiers in Microbiology*, *13*, 872034.

Lin, Y.-S., Tsai, Y.-J., Tsay, J.-S., & Lin, J.-K. (2003). Factors affecting the levels of tea polyphenols and caffeine in tea leaves. *Journal of Agricultural and Food Chemistry*, *51*(7), 1864-1873.

Liu, C., Lin, H., Wang, K., Zhang, Z., Huang, J., & Liu, Z. (2023a). Study on the trend in microbial changes during the fermentation of black tea and Its effect on the quality. *Foods*, *12*(10).

Liu, C., Zhou, J., Huang, J., Xu, W., & Liu, Z. (2023b). Study on the synthesis of theaflavin-3,3′-digallate catalyzed by *Escherichia coli* expressing tea tree polyphenol oxidase isozymes and its enzymatic solution. *Fermentation, 9*(8), 770.

Liu, F., Wang, Y., Corke, H., & Zhu, H. (2022a). Dynamic changes in flavonoids content during congou black tea processing. *LWT - Food Science & Technology*, *170*.

Liu, J., Liang, C., Jiang, H., Yu, Z., Zou, L., Zhou, L., & Liu, W. (2024a). Identification of polyphenol oxidase inhibitors from the root of *Pueraria Lobata*: Inhibitor profiles, kinetics analysis and molecular interaction. *Food Biophysics*, *19*(3), 730-744.

Liu, J. Y., Yu, Z. H., Liao, X. R., Liu, J. H., Mao, F. J., & Huang, Q. G. (2016). Scalable production, fast purification, spray drying of native *Pycnoporus* laccase and circular dichroism characterization. *Journal of Cleaner Production, 127*, 600–609.

Liu, K., Chen, Q., Luo, H., Li, R., Chen, L., Jiang, B., Liang, Z., Wang, T., Ma, Y., & Zhao, M. (2023c). An in-vitro catalysis of tea polyphenols by polyphenol oxidase. *Molecules*, *28*(4), 1722.

Liu, K., Han, L., Wang, Q., Yang, L., Liu, X., Jiang, B., Zeng, X., Liu, Y., Li, M., Jiao, W., & Liu, M. (2023c). Interaction and metabolic function of microbiota during Tibetan tea fermentation through bioaugmentation with *Aspergillus niger*. *Fermentation*, *9*(7), 690.

Liu, L., Shi, J., Yuan, Y., & Yue, T. (2022b). Changes in the metabolite composition and enzyme activity of fermented tea during processing. *Food Research International*, *158*, 111428.

Liu, Y., Wang, D., Li, J., Zhang, Z., Wang, Y., Qiu, C., Sun, Y., & Pan, C. (2024b). Research progress on the functions and biosynthesis of theaflavins. *Food Chemistry*, *450*, 139285.

Long, P., Rakariyatham, K., Ho, C.-T., & Zhang, L. (2023). Thearubigins: Formation, structure, health benefit and sensory property. *Trends in Food Science & Technology*, *133*, 37-48.

Lu, X., Lin, Y., Tuo, Y., Liu, L., Du, X., Zhu, Q., Hu, Y., Shi, Y., Wu, L., & Lin, J. (2023). Optimizing processing techniques of oolong tea: Balancing between high retention of catechins and sensory quality. *Foods*, *12*(23).

Ma, Y., Liu, M., Gu, R., Zhang, R., Ji, X., Zhang, J., Wen, W., & Peng, Z. (2025). Optimization of the scale-up production process for high-yield laccase from white-rot fungi. *Frontiers in Bioengineering and Biotechnology, 13*, 1631687.

Maliepaard, R. (2009). *Inactivation of polyphenol oxidase in Camellia sinensis for the production of high quality instant green tea* [Doctoral dissertation, University of Pretoria]. University of Pretoria Institutional Repository. https://repository.up.ac.za/handle/2263/26839

Martins, R. O., Borsatto, J. V. B., Will, C., & Lanças, F. M. (2025). Advancements in microextraction by packed sorbent: Insights into sorbent phases and automation strategies. *Separations*, *12*(1), 11.

Matsuo, Y., Li, Y., Watarumi, S., Tanaka, T., & Kouno, I. (2011). Production and degradation mechanism of theacitrin C, a black tea pigment derived from epigallocatechin-3-O-gallate via a bicyclo[3.2.1]octane-type intermediate. *Tetrahedron*, *67*(11), 2051-2059.

Mayer, A. M. (2006). Polyphenol oxidases in plants and fungi: Going places? A review. *Phytochemistry*, *67*(21), 2318-2331.

Mehandia, S., Sharma, S. C., & Arya, S. K. (2020). Isolation and characterization of an alkali and thermostable laccase from a novel *Alcaligenes faecalis* and its application in decolorization of synthetic dyes. *Biotechnology Reports(Amst)*, *25*, e00413.

Miller, G. L. (1959). Use of dinitrosalicylic acid reagent for determination of reducing sugar. *Analytical Chemistry*, *31*(3), 426-428.

Mondal, S., Karande, M., Srivastava, S., Sharma, A., Sharma, S., & Ghosh, A. (2025). Unravelling the microbiome perspective to variations in tea metabolome. *Industrial Crops and Products*, *223*, 120129.

Morales, D., Iriondo-DeHond, A., & Fernández-Tomé, S. (2025). Application of the INFOGEST 2.0 standardized method to study the behavior of phenolic compounds throughout gastrointestinal digestion. *Food Chemistry*, *492*, 145531.

Moreira, J., Aryal, J., Guidry, L., Adhikari, A., Chen, Y., Sriwattana, S., & Prinyawiwatkul, W. (2024). Tea quality: an overview of the analytical methods and sensory analyses used in the most recent studies. *Foods*, *13*(22), 3580.

Morya, R., Salvachúa, D., & Thakur, I. S. (2020). *Burkholderia*: An untapped but promising bacterial genus for the conversion of aromatic compounds. *Trends in Biotechnology*, *38*(9), 963-975.

Mukhtar, H., & Ahmad, N. (2000). Tea polyphenols: prevention of cancer and optimizing health. *American Journal of Clinical Nutrition*, *71*(6 Suppl), 1698S-1702S; discussion 1703S-1694S.

Munim Khan, M. R., Islam, M. A., Uddin, R., Kalam, M. A., Baishakh, N. N., Barua, P., Rahman Talukder, M. H., & Ahmad, I. (2023). Biochemical investigation of Bangladeshi black tea and their correlation to organoleptic quality evaluation. *Heliyon*, *9*(6), e16802.

Muniraj, I., Shameer, S., & Uthandi, S. (2021). Tyrosinase and laccase-producing *Bacillus aryabhatta*i TFG5 and its role in the polymerization of phenols. *BMC Microbiology*, *21*(1), 187.

Munoz-Munoz, J. L., García-Molina, F., Molina-Alarcón, M., Tudela, J., García-Cánovas, F., & Rodríguez-López, J. N. (2008). Kinetic characterization of the enzymatic and chemical oxidation of the catechins in green tea. *Journal of Agricultural and Food Chemistry*, *56*(19), 9215-9224.

Murugesan, G. S., Angayarkanni, J., & Swaminathan, K. (2002). Effect of tea fungal enzymes on the quality of black tea. *Food Chemistry*, *79*, 411-417.

Myers, R. H., Montgomery, D. C., & Anderson-Cook, C. M. (2016). Response surface methodology: Process and product optimization using designed experiments. Wiley.

Myo, H., Yaowiwat, N., Pongkorpsakol, P., Aonbangkhen, C., & Khat-udomkiri, N. (2023). Butylene glycol used as a sustainable solvent for extracting bioactive compounds from *Camellia sinensis* Flowers with Ultrasound-Assisted Extraction. *ACS Omega*, *8*(5), 4976-4987.

Najjari, M., & Bodaghi, H. (2024). Inhibitory effect of ascorbic acid in enzymatic browning and preservation of quality in fresh pistachios (*Pistacia Vera* L.). *Applied Fruit Science*, *66*(2), 609-620.

Nandal, P., Ravella, S. R., & Kuhad, R. C. (2013). Laccase production by *Coriolopsis caperata* RCK2011: Optimization under solid state fermentation by Taguchi DOE methodology. *Scientific Reports*, *3*(1), 1386.

Neilson, A. P., George, J. C., Janle, E. M., Mattes, R. D., Rudolph, R., Matusheski, N. V., & Ferruzzi, M. G. (2009). Influence of chocolate matrix composition on cocoa flavan-3-ol bioaccessibility *in vitro* and bioavailability in humans. *Journal of Agricultural and Food Chemistry*, *57*(20), 9418-9426.

Nguyen Ngoc, T., Phan Phuoc, H., & Huynh Ngoc, O. (2015). Change of polyphenol oxidase activity during oolong tea process. *Journal of Food and Nutrition Sciences*, *3*(1-2), 88-93.

Nikolaivits, E., Dimarogona, M., Karagiannaki, I., Chalima, A., Fishman, A., & Topakas, E. (2018). Versatile fungal polyphenol oxidase with chlorophenol bioremediation potential: Characterization and protein engineering. *Applied and Environmental Microbiology*, *84*(23), e01628-01618.

Nuraini, V. A., Falasca, V., Wenholz, D. S., Black, D. S., & Kumar, N. (2025). Synthesis of fused-ring systems and diarylmethane flavonoids via ortho-quinone methide intermediates. *RSC Advances*, *15*(4), 2912-2929.

Obanda, M., Okinda Owuor, P., & Mang'oka, R. (2001). Changes in the chemical and sensory quality parameters of black tea due to variations of fermentation time and temperature. *Food Chemistry*, *75*(4), 395-404.

Obanda, M., Owuor, P. O., & Taylor, S. J. (1997). Flavanol composition and caffeine content of green leaf as quality potential indicators of Kenyan black teas. *Journal of the Science of Food and Agriculture*, *74*(2), 209-215.

Parveen, A., Qin, C.-Y., Zhou, F., Lai, G., Long, P., Zhu, M., Ke, J., & Zhang, L. (2023). The chemistry, sensory properties and health benefits of aroma compounds of black tea produced by *Camellia sinensis* and *Camellia assamica*. *Horticulturae*, *9*(12), 1253.

Patti, S., Magrini Alunno, I., Pedroni, S., Riva, S., Ferrandi, E. E., & Monti, D. (2025). Advances and Challenges in the Development of Immobilized Enzymes for Batch and Flow Biocatalyzed Processes. *ChemSusChem*, *18*(8), e202402007.

Peng, L., Song, X., Shi, X., Li, J., & Ye, C. (2008). An improved HPLC method for simultaneous determination of phenolic compounds, purine alkaloids and theanine in Camellia species. *Journal of Food Composition and Analysis*, *21*(7), 559-563.

Pérez, M., Dominguez-López, I., & Lamuela-Raventós, R. M. (2023). The chemistry behind the Folin–Ciocalteu method for the estimation of polyphenol content in food: Total phenolic intake in a Mediterranean dietary pattern. *Journal of Agricultural and Food Chemistry*, *71*(46), 17543-17553.

Perva-Uzunalić, A., Škerget, M., Knez, Ž., Weinreich, B., Otto, F., & Grüner, S. (2006). Extraction of active ingredients from green tea (*Camellia sinensis*): Extraction efficiency of major catechins and caffeine. *Food Chemistry*, *96*(4), 597-605.

Piscitelli, A., Giardina, P., Lettera, V., Pezzella, C., Sannia, G., & Faraco, V. (2011). Induction and transcriptional regulation of laccases in fungi. *Current Genomics*, *12*, 104 - 112.

Pitt, J. I., & Hocking, A. D. (2009). *Fungi and Food Spoilage*. Springer US.

Pou, K. R. J., Paul, S. K., & Malakar, S. (2019). Industrial Processing of CTC Black Tea. In A. M. Grumezescu & A. M. Holban (Eds.), *Caffeinated and Cocoa Based Beverages* (pp. 131-162). Woodhead Publishing.

Pretzler, M., & Rompel, A. (2024). Tyrosinases: A family of copper-containing metalloenzymes. *ChemTexts*, *10*(4), 12.

Prior, R. L., Wu, X., & Schaich, K. (2005). Standardized methods for the determination of antioxidant capacity and phenolics in foods and dietary supplements. *Journal of Agricultural and Food Chemistry*, *53*(10), 4290-4302.

Punyasiri, P. A., Jeganathan, B., Dananjaya Kottawa-Arachchi, J., Ranatunga, M. A., Abeysinghe, I. S., Gunasekare, M. T., & Bandara, B. M. (2015). New sample preparation method for quantification of phenolic compounds of tea (*Camellia sinensis* L. Kuntze): A polyphenol-rich plant. *Journal of Analytical Methods in Chemistry*, *2015*, 964341.

Qin, W., & Ketnawa, S. (2025). Exploring the bioaccessibility of roasted Japanese green tea: Impact of simulated gastrointestinal digestion. *Foods*, *14*(2).

Qiu, Y., Liu, X., Lyu, F., & Zhang, A. (2025). Effects of fermentation of *Eurotium cristatum* on the flavor quality of Anji Baicha (*Camellia sinensis*) based on LC-MS and GC–MS. *Food Chemistry*, *493*, 145663.

Ray, R. R., & Pattnaik, S. (2024). *Alcaligenes faecalis*: A bacterium for sustainable management of environment. *Environmental Quality Management*, *34*(1), e22189.

Regar, R. K., Singh, D., Gaur, V. K., Thakur, R. S., & Manickam, N. (2023). Functional genomic analysis of an efficient indole degrading bacteria strain *Alcaligenes faecalis* IITR89 and its

biodegradation characteristics. *Environmental Science and Pollution Research*, *30*(18), 51770-51781.

Rehder, A. P., Silva, P. B., Xavier, A. M. F., & Barrozo, M. A. S. (2021). Optimization of microwave-assisted extraction of bioactive compounds from a tea blend. *Journal of Food Measurement and Characterization*, *15*(2), 1588-1598.

Reiss, R., Ihssen, J., Richter, M., Eichhorn, E., Schilling, B., & Thöny-Meyer, L. (2013). Laccase versus laccase-like multi-copper oxidase: A comparative study of similar enzymes with diverse substrate spectra. *PLoS One*, *8*(6), e65633.

Rha, C.-S., Choi, Y.-M., Kim, J.-C., & Kim, D.-O. (2021). Cost-effective simultaneous separation and quantification of phenolics in green and processed tea using HPLC–UV–ESI single-quadrupole MS detector and Python script. *Separations*, *8*(4), 45.

Rha, C. S., Seong, H., Jung, Y. S., Jang, D., Kwak, J. G., Kim, D. O., & Han, N. S. (2019). Stability and fermentability of green tea flavonols in *in vitro* simulated gastrointestinal digestion and human fecal fermentation. *International Journal of Molecular Sciences*, *20*(23).

Rizzi, G. P. (1999). The Strecker degradation and its contribution to food flavor. In R. Teranishi, E. L. Wick, & I. Hornstein (Eds.), *Flavor Chemistry: Thirty Years of Progress* (pp. 335-343). Springer US.

Roberts, E. A. H., & Smith, R. F. (1961). Spectrophotometric measurements of theaflavins and thearubigins in black tea liquors in assessments of quality in teas. *Analyst*, *86*(1019), 94-98.

Romers, T., Saurina, J., Sentellas, S., & Nunez, O. (2023). Targeted HPLC-UV polyphenolic profiling to detect and quantify adulterated tea samples by chemometrics. *Foods*, *12*(7), 1501.

Romers, T., Sentellas, S., Saurina, J., & Núñez, O. (2024). Potential of high-throughput FIA-MS/MS and LC-MS/MS polyphenolic profiling to assess tea authenticity-Application to tea adulterations with chicory. *Microchemical Journal*, *207*, 111723.

Rong, Y., Xie, J., Yuan, H., Wang, L., Liu, F., Deng, Y., Jiang, Y., & Yang, Y. (2023). Characterization of volatile metabolites in Pu-erh teas with different storage years by combining GC-E-Nose, GC–MS, and GC-IMS. *Food Chemistry: X*, *18*, 100693.

Saad, W. F., Othman, A. M., Abdel-Fattah, M., & Ahmad, M. S. (2021). Response surface methodology as an approach for optimization of α-amylase production by the new isolated thermotolerant *Bacillus licheniformis* WF67 strain in submerged fermentation. *Biocatalysis and Agricultural Biotechnology*, *32*, 101944.

Saadati, N., Abdullah, M. P., Zakaria, Z., Sany, S. B. T., Rezayi, M., & Hassonizadeh, H. (2013). Limit of detection and limit of quantification development procedures for organochlorine pesticides analysis in water and sediment matrices. *Chemistry Central Journal*, *7*(1), 63.

Saalwächter, K. (2019). Applications of NMR in polymer characterization – An introduction. In R. Zhang, T. Miyoshi, & P. Sun (Eds.), *NMR Methods for Characterization of Synthetic and Natural Polymers* (pp. 0). The Royal Society of Chemistry.

Salek, R. M., Steinbeck, C., Viant, M. R., Goodacre, R., & Dunn, W. B. (2013). The role of reporting standards for metabolite annotation and identification in metabolomic studies. *GigaScience*, *2*(1).

Samanta, T., Cheeni, V., Das, S., Roy, A. B., Ghosh, B. C., & Mitra, A. (2015). Assessing biochemical changes during standardization of fermentation time and temperature for manufacturing quality black tea. *Journal of Food Science and Technology*, *52*(4), 2387-2393.

Sanaeifar, A., Huang, X., Chen, M., Zhao, Z., Ji, Y., Li, X., He, Y., Zhu, Y., Chen, X., & Yu, X. (2020). Nondestructive monitoring of polyphenols and caffeine during green tea processing using Vis-NIR spectroscopy. *Food Science & Nutrition*, *8*(11), 5860-5874.

Sang, S., Lambert, J. D., Ho, C.-T., & Yang, C. S. (2011). The chemistry and biotransformation of tea constituents. *Pharmacological Research*, *64*(2), 87-99.

Sarker, S. D., Nahar, L., & Kumarasamy, Y. (2007). Microtitre plate-based antibacterial assay incorporating resazurin as an indicator of cell growth, and its application in the *in vitro* antibacterial screening of phytochemicals. *Methods*, *42*(4), 321-324.

Schantz, M., Erk, T., & Richling, E. (2010). Metabolism of green tea catechins by the small human intestine. *Biotechnology Journal*, *5*(10), 1050-1059.

Sembiring, E. N., Berna, E., & Rani, S. (2018). Phytochemical screening, total flavonoid and total phenolic content, and antioxidant activity of different parts of *Caesalpinia bonduc* (L.) Roxb. *Pharmacognosy Journal*, *10*(1).

Sewalt, V., Shanahan, D., Gregg, L., La Marta, J., & Carrillo, R. (2016). The generally recognized as safe (GRAS) process for industrial microbial enzymes. *Industrial Biotechnology*, *12*(5), 295-302.

Sharma, P., Tamang, S., Thakur, N., & Das, S. (2024). 8 Application, current and future trends of bacterial and fungal polyphenol oxidases (laccases). In V. Pradeep, A. Komal, & P. S. Maulin (Eds.), *Polyphenol Oxidases* (pp. 189-222). De Gruyter.

Shaukat, H., Ali, A., Zhang, Y., Ahmad, A., Riaz, S., Khan, A., Mehany, T., & Qin, H. (2023). Tea polyphenols: extraction techniques and its potency as a nutraceutical. *Frontiers in Sustainable Food Systems*, *Volume 7 - 2023*.

Shi, J., Zhu, Y., Zhang, Y., Lin, Z., & Lv, H.-P. (2019). Volatile composition of Fu-brick tea and Pu-erh tea analyzed by comprehensive two-dimensional gas chromatography-time-of-flight mass spectrometry. *LWT - Food Science & Technology*, *103*, 27-33.

Shiquan, L., Li, T., Yu, S., Zhou, X., Liu, Z., Zhang, X., Cai, H., & Hu, Z. (2023). Analysis of bacterial community structure of Fuzhuan tea with different processing techniques. *Open Life Sciences*, *18*(1).

Shraddha, Shekher, R., Sehgal, S., Kamthania, M., & Kumar, A. (2011). Laccase: Microbial sources, production, purification, and potential biotechnological applications. *Enzyme Research*, *2011*(1), 217861.

Simair, A. (2017). Study of nutrient media components and cultivation conditions of *Bacillus licheniformis* BCC-02-50 for protease production using molasses as energy source. *International Journal of Research*, *4*, 552-562.

Singh, R., Kumar, M., Mittal, A., & Mehta, P. K. (2016). Microbial enzymes: industrial progress in 21st century. *3 Biotech*, *6*(2), 174.

Singleton, V. L., Orthofer, R., & Lamuela-Raventós, R. M. (1999). Analysis of total phenols and other oxidation substrates and antioxidants by means of Folin-Ciocalteu reagent. *Methods in Enzymology*, *299*, 152-178.

Sodhi, A. S., Bhatia, S., & Batra, N. (2024). Laccase: Sustainable production strategies, heterologous expression and potential biotechnological applications. *International Journal of Biological Macromolecules*, *280*, 135745.

Solano, F., Briganti, S., Picardo, M., & Ghanem, G. (2006). Hypopigmenting agents: an updated review on biological, chemical and clinical aspects. *Pigment Cell Res*, *19*(6), 550-571.

Solano, F., Lucas-Elío, P., Fernández, E., & Sanchez-Amat, A. (2000). *Marinomonas mediterranea* MMB-1 transposon mutagenesis: isolation of a multipotent polyphenol oxidase mutant. *Journal of Bacteriology*, *182*(13), 3754-3760.

Soliva-Fortuny, R. C., Grigelmo-Miguel, N., Odriozola-Serrano, I., Gorinstein, S., & Martín-Belloso, O. (2001). Browning evaluation of ready-to-eat apples as affected by modified atmosphere packaging. *Journal of Agricultural and Food Chemistry, 49*(8), 3685–3690.

Song, H., Lee, P.-G., Kim, H., Lee, U.-J., Lee, S.-H., Kim, J., & Kim, B.-G. (2021). Polyphenol-hydroxylating tyrosinase activity under acidic pH enables efficient synthesis of plant catechols and gallols. *Microorganisms*, *9*(9), 1866.

Souza, M. C., Santos, M. P., Sumere, B. R., Silva, L. C., Cunha, D. T., Martínez, J., Barbero, G. F., & Rostagno, M. A. (2019). Isolation of gallic acid, caffeine and flavonols from black tea by on-line coupling of pressurized liquid extraction with an adsorbent for the production of functional bakery products. *LWT - Food Science & Technology*, Not Available.

Steffany, B., Vivek, V., Cristina, L., & Luna., E. (2024). *Global market report: Tea prices and sustainability* (Sustainable Commodities Marketplace Series, Issue. I. I. f. S. Development. https://www.iisd.org/system/files/2024-01/2024-global-market-report-tea.pdf

Su, S., Long, P., Zhang, Q., Wen, M., Han, Z., Zhou, F., Ke, J., Wan, X., Ho, C.-T., & Zhang, L. (2024a). Chemical, sensory and biological variations of black tea under different drying temperatures. *Food Chemistry*, *446*, 138827.

Su, Y., Hu, K., Li, D., Guo, H., Sun, L., & Xie, Z. (2024b). Microbial-transferred metabolites and improvement of biological activities of green tea catechins by human gut microbiota. *Foods*, *13*(5).

Subramanian, N., Venkatesh, P., Ganguli, S., & Sinkar, V. P. (1999). Role of polyphenol oxidase and peroxidase in the generation of black tea theaflavins. *Journal of Agricultural and Food Chemistry*, *47*(7), 2571-2578.

Sumner, L. W., Amberg, A., Barrett, D., Beale, M. H., Beger, R., Daykin, C. A., Fan, T. W. M., Fiehn, O., Goodacre, R., Griffin, J. L., Hankemeier, T., Hardy, N., Harnly, J., Higashi, R., Kopka, J., Lane, A. N., Lindon, J. C., Marriott, P., Nicholls, A. W., . . . Viant, M. R. (2007). Proposed minimum reporting standards for chemical analysis. *Metabolomics*, *3*(3), 211-221.

Sun, M.-F., Jiang, C.-L., Kong, Y.-S., Luo, J.-L., Yin, P., & Guo, G.-Y. (2022a). Recent Advances in Analytical Methods for Determination of Polyphenols in Tea: A Comprehensive Review. *Foods*, *11*(10), 1425.

Sun, M. F., Jiang, C. L., Kong, Y. S., Luo, J. L., Yin, P., & Guo, G. Y. (2022b). Recent advances in analytical methods for determination of polyphenols in tea: A comprehensive review. *Foods*, *11*(10), 1425.

Surwase, S. N., & Jadhav, J. P. (2011). Bioconversion of L-tyrosine to L-DOPA by a novel bacterium *Bacillus* sp. JPJ. *Amino Acids*, *41*(2), 495-506.

Suryanarayanan, T. S. (2013). Endophyte research: Going beyond isolation and metabolite documentation. *Fungal Ecology*, *6*(6), 561-568.

Takemoto, M., & Takemoto, H. (2018). Synthesis of theaflavins and their functions. *Molecules*, *23*(4).

Takeo, T. (2014). Tea Leaf Polyphenol Oxidase. *Agricultural and Biological Chemistry*, *30*(6), 529-535.

Tanaka, T., & Kouno, I. (2003). Oxidation of tea catechins: Chemical structures and reaction mechanism. *Food Science and Technology Research*, *9*(2), 128-133.

Tanaka, T., & Matsuo, Y. (2020). Production mechanisms of black tea polyphenols. *Chemical & Pharmaceutical Bulletin (Tokyo)*, *68*(12), 1131-1142.

Tang, M., Zhang, S., Xiong, L.., Zhou, J., Huang, J., Zhao, A., Liu, Z.-h., & Liu, A. (2023). A comprehensive review of polyphenol oxidase in tea (*Camellia sinensis*): Physiological characteristics, oxidation manufacturing, and biosynthesis of functional constituents. *Comprehensive Reviews in Food Science and Food Safety*, *22*(3), 2267-2291.

Tang, P., Shen, D.-Y., Xu, Y.-Q., Zhang, X.-C., Shi, J., & Yin, J.-F. (2018). Effect of fermentation conditions and plucking standards of tea leaves on the chemical components and sensory quality of fermented juice. *Journal of Chemistry*, *2018*, 1-7.

Tao, W., Zhou, Z., Zhao, B., & Wei, T. (2016). Simultaneous determination of eight catechins and four theaflavins in green, black and oolong tea using new HPLC-MS-MS method. *Journal of Pharmaceutical and Biomedical Analysis*, *131*, 140-145.

TBI. (2024). *Tea Board India annual report for the year 2024-25*. https://www.teaboard.gov.in/pdf/Tea_Board_Annual_Report_2024_25_pdf287.pdf

Teng, J., Gong, Z., Deng, Y., Chen, L., Li, Q., Shao, Y., Lin, L., & Xiao, W. (2017). Purification, characterization and enzymatic synthesis of theaflavins of polyphenol oxidase isozymes from tea leaf (*Camellia sinensis*). *LWT - Food Science & Technology*, *84*, 263-270.

Teng, J., Liu, Y., Zeng, W., Zhou, M., Liu, Y., Huang, Y., & Chen, Q. (2021). In-vitro enzymatic synthesis of a monomeric theaflavin using a polyphenol oxidase isozyme from tea (*Camellia sinensis*) leaf. *International Journal of Food Science and Technology*, *57*(9), 5621-5631.

Theuma, M., & Attard, E. (2020). From herbal substance to infusion: The fate of polyphenols and trace elements. *Journal of Herbal Medicine*, *21*, 100347.

Tibpromma, S., Karunarathna, S. C., Bhat, J. D., Suwannarach, N., Stephenson, S. L., Elgorban, A. M., Al-Rejaie, S., Xu, J., & Mortimer, P. E. (2022). Using culture-dependent and molecular techniques to identify endophytic fungi associated with tea leaves (*Camellia* spp.) in Yunnan Province, China. *Diversity*, *14*(4), 287.

Timofeeva, I., Stepanova, K., & Bulatov, A. (2021). In-a-syringe surfactant-assisted dispersive liquid-liquid microextraction of polycyclic aromatic hydrocarbons in supramolecular solvent from tea infusion. *Talanta*, *224*, 121888.

Tkacz, K., Połomska, X., Turkiewicz, I. P., & Wojdyło, A. (2025). Enhancement of bioaccessibility and modulation of green tea phenolic compounds through pre-transformation by *Lactobacillus* and *Bifidobacterium* strains. *Food Research International*, *217*, 116848.

Tonami, H., Uyama, H., Nagahata, R., & Kobayashi, S. (2004). Guaiacol oxidation products in the enzyme-activity assay reaction by horseradish peroxidase catalysis. *Chemistry Letters*, *33*(7), 796-797.

Tong, W., Yu, J., Wu, Q., Hu, L., Tabys, D., Wang, Y., Wei, C., Ling, T., Ali Inayat, M., & Bennetzen, J. L. (2021). Black tea quality is highly affected during processing by its leaf surface microbiome. *Journal of Agricultural and Food Chemistry*, *69*(25), 7115-7126.

Tounekti, T., Joubert, E., Hernández, I., & Munné-Bosch, S. (2013). Improving the Polyphenol Content of Tea. *Critical Reviews in Plant Sciences*, *32*(3), 192-215.

TRF, U. (2026). *Tea quality parameters*. UPASI Tea Research Foundation Tea Research Institute, Nirar Dam (po), Valparai – 642 127, Coimbatore District, Tamil Nadu, INDIA. Retrieved 01/02/2026 from https://www.upasitearesearch.org/tea-quality-parameters/

Unuofin, J. O., Moubasher, H. A., Okoh, A. I., & Nwodo, U. U. (2019). Production of polyextremotolerant laccase by *Achromobacter xylosoxidans* HWN16 and *Citrobacter freundii* LLJ16. *Biotechnology Reports*, *22*, e00337.

Veetil, A. K. T., James, J., Subash, S. M., Joy, D., Dev, L., & Thankamani, V. (2012). Characterization of *Alcaligenes faecalis* GPA-1 producing thermostable extracellular α-amylase. *Research in Biotechnology*, *3*, 19-27.

Verloop, A. J. W., Gruppen, H., Bisschop, R., & Vincken, J.-P. (2016). Altering the phenolics profile of a green tea leaves extract using exogenous oxidases. *Food Chemistry*, *196*, 1197-1206.

Vivekanandhan, K., Soundari., P. G., Jeyasundar., A., Vellingiri, M. M., & Ayyappadas, M. P. (2024). Isolation and molecular identification of polyphenol oxidase and associated enzyme production from *Bacillus* spp. *Journal of Applied and Natural Science*, *16*(2), 663 - 673.

Vuong, Q. V., Golding, J. B., Stathopoulos, C. E., Nguyen, M. H., & Roach, P. D. (2011). Optimizing conditions for the extraction of catechins from green tea using hot water. *Journal of Separation Science*, *34*(21), 3099-3106.

Wang, A., Lei, Q., Zhang, B., Wu, J., Fu, Z., He, J., Wang, Y., & Wu, X. (2024). Revealing novel insights into the enhancement of quality in black tea processing through microbial intervention. *Food Chemistry: X*, *23*, 101743.

Wang, H., Provan, G. J., & Helliwell, K. (2000). Tea flavonoids: their functions, utilization and analysis. *Trends in Food Science & Technology.*, *11*(4/5), 152-160.

Wang, H., Provan, G. J., & Helliwell, K. (2003). HPLC determination of catechins in tea leaves and tea extracts using relative response factors. *Food Chemistry*, *81*(2), 307-312.

Wang, M., Li, J., Hu, T., & Zhao, H. (2022a). Metabolic fate of tea polyphenols and their crosstalk with gut microbiota. *Food Science and Human Wellness*, *11*(3), 455-466.

Wang, Q., Peng, C., & Gong, J. (2011). Effects of enzymatic action on the formation of theabrownin during solid state fermentation of Pu-erh tea. *Journal of the Science of Food and Agriculture*, *91*(13), 2412-2418.

Wang, R., Sun, J., Lassabliere, B., Yu, B., & Liu, S. Q. (2020). Biotransformation of green tea (*Camellia sinensis*) by wine yeast *Saccharomyces cerevisiae*. *Journal of Food Science*, *85*(2), 306-315.

Wang, R., Sun, J., Lassabliere, B., Yu, B., & Liu, S. Q. (2022b). UPLC-Q-TOF-MS based metabolomics and chemometric analyses for green tea fermented with *Saccharomyces boulardii* CNCM I-745 and *Lactiplantibacillus plantarum* 299V. *Current Research in Food Science*, *5*, 471-478.

Wang, R., Zhou, W., & Jiang, X. (2008). Reaction kinetics of degradation and epimerization of epigallocatechin gallate (EGCG) in aqueous system over a wide temperature range. *Journal of Agricultural and Food Chemistry*, *56*(8), 2694-2701.

Wang, S., Liu, P., Feng, L., Teng, J., Ye, F., Gui, A., Wang, X., Zheng, L., Gao, S., & Zheng, P. (2022c). Rapid determination of tea polyphenols content in Qingzhuan tea based on near infrared spectroscopy in conjunction with three different PLS algorithms. *Food Science and Technology*, *42*.

Wang, T., Li, R.-y., Liu, K.-y., Chen, Q.-y., Bo, N.-g., Wang, Q., Xiao, Y.-q., Sha, G., Chen, S.-q., Lei, X., Lu, Y., Ma, Y., & Zhao, M. (2023a). Changes in sensory characteristics, chemical composition and microbial succession during fermentation of ancient plants Pu-erh tea. *Food Chemistry: X*, *20*, 101003.

Wang, W., Chi-Tang, H., & Shiming, L. (2022d). Selection of polyphenol oxidase affects biotransformation efficacy of targeted theaflavins. *Journal of Food Bioactives*, *17*(0).

Wang, W., Le, T., Wang, W., Yu, L., Yang, L., & Jiang, H. (2023b). Effects of key components on the antioxidant activity of black tea. *Foods*, *12*(16), 3134.

Wang, W., Zhang, S., Lv, L., & Sang, S. (2018). A new method to prepare and redefine black tea thearubigins. *Journal of Chromatography A*, *1563*, 82-88.

Wang, X. P., Shan, R. Y., Li, Z. L., Kong, X. R., Hou, R. T., Wu, H. N., & Chen, C. S. (2023c). Metabolic improvements of novel microbial fermentation on black tea by *Eurotium cristatum*. *Frontiers in Microbiology*, *14*, 1287802.

Wang, Y., Yang, X., Li, K., Li, C., Li, L., Li, J., Huang, H., He, Y., Ye, C., & Song, X. (2010). Simultaneous determination of theanine, gallic acid, purine alkaloids, catechins, and theaflavins in black tea using HPLC. *International Journal of Food Science & Technology*, *45*(6), 1263-1269.

Weisburg, W. G., Barns, S. M., Pelletier, D. A., & Lane, D. J. (1991). 16S ribosomal DNA amplification for phylogenetic study. *Journal of Bacteriology*, *173*(2), 697-703.

Westphal, A. H., & van Berkel, W. J. H. (2021). Techniques for enzyme purification. In *Biocatalysis for Practitioners* (pp. 1-31).

White, T. J., Bruns, T., Lee, S., & Taylor, J. (1990). Amplification and direct sequencing of fungal ribosomal RNA genes for phylogenetics. In M. A. Innis, D. H. Gelfand, J. J. Sninsky, & T. J. White (Eds.), *PCR Protocols* (pp. 315-322). Academic Press.

Widsten, P., & Kandelbauer, A. (2008). Laccase applications in the forest products industry: A review. *Enzyme and Microbial Technology*, *42*(4), 293-307.

Wijeratne, M. (2003). Harvesting policies of tea (*Camellia sinensis* L.) for higher productivity and quality. *Tropical Agricultural Research and Extension*, *6*, 91.

Wiśniewska, K. M., Twarda-Clapa, A., & Białkowska, A. M. (2021). Screening of novel laccase producers—Isolation and characterization of cold-adapted laccase from *Kabatiella bupleuri* G3 capable of synthetic dye decolorization. *Biomolecules*, *11*(6), 828.

Wu, Q., et al., & She, Y. (2026). Constraint of lignin-carbohydrate complex orchestrated on polyphenol in oil-water interface targeting ulcerative colitis therapy. *Advanced Science*, e2524070.

Xiao, Y., Li, M., Liu, Y., Xu, S., Zhong, K., Wu, Y., & Gao, H. (2021). The effect of *Eurotium cristatum* (MF800948) fermentation on the quality of autumn green tea. *Food Chemistry*, *358*, 129848.

Xie, H., Feng, X., Wang, M., Wang, Y., Kumar Awasthi, M., & Xu, P. (2020). Implications of endophytic microbiota in *Camellia sinensis*: a review on current understanding and future insights. *Bioengineered*, *11*(1), 1001-1015.

Xu, H., Hong, J. H., Kim, D., Jin, Y. H., Pawluk, A. M., & Mah, J.-H. (2022). Evaluation of bioactive compounds and antioxidative activity of fermented green Tea produced via one- and two-step fermentation. *Antioxidants*, *11*(8), 1425.

Xu, Y.-Q., Yu, P., & Zhou, W. (2019). Combined effect of pH and temperature on the stability and antioxidant capacity of epigallocatechin gallate (EGCG) in aqueous system. *Journal of Food Engineering*, *250*, 46-54.

Xu, Y. (2012). Research on the process of microbial solid-state fermentation of tea vinegar. *Process technology*, *37*(4), 4(85-87,91).

Yan, Z., Zhong, Y., Duan, Y., Chen, Q., & Li, F. (2020). Antioxidant mechanism of tea polyphenols and its impact on health benefits. *Animal Nutrition*, *6*(2), 115-123.

Yang, C. S. (1999). Tea and health. *Nutrition*, *15*(11-12), 946-949.

Yang, D., Chunmiao, T., & Xingyi, Z. (2025a). Extraction and separation of tea polyphenols and caffeine from tea leaves by mechanochemical pretreatment. *Boletín Latinoamericano y del Caribe de Plantas Medicinales y Aromáticas*, *24*(1), 101-110.

Yang, M., Zhang, X., & Yang, C. S. (2025b). Bioavailability of Tea Polyphenols: A Key Factor in Understanding Their Mechanisms of Action *In Vivo* and Health Effects. *J Agric Food Chem*, *73*(7), 3816-3825.

Yang, S., Pathak, S., Tang, H., Zhang, D., Chen, Y., Ntezimana, B., Ni, D., & Yu, Z. (2024). Non-targeted metabolomics reveals the effects of different rolling methods on black tea quality. *Foods*, *13*(2).

Yang, W., Yang, H., Bao, X., Hussain, M., Bao, Q., Zeng, Z., Xiao, C., Zhou, L., & Qin, X. (2023). *Brevibacillus brevis* HNCS-1: a biocontrol bacterium against tea plant diseases. *Frontiers in Microbiology*, *14*, 1198747.

Yang, Z., Baldermann, S., & Watanabe, N. (2013). Recent studies of the volatile compounds in tea. *Food Research International*, *53*(2), 585-599.

Yassin, G. H., Grun, C., Koek, J. H., Assaf, K. I., & Kuhnert, N. (2014). Investigation of isomeric flavanol structures in black tea thearubigins using ultraperformance liquid chromatography coupled to hybrid quadrupole/ion mobility/time of flight mass spectrometry. *Journal of Mass Spectrometry*, *49*(11), 1086-1095.

Yemm, E. W., Cocking, E. C., & Ricketts, R. E. (1955). The determination of amino-acids with ninhydrin. *Analyst*, *80*(948), 209-214.

Yoruk, R., & Marshal, M. R. (2003). Physicochemical properties and function of plant polyphenol oxidase: A review. *Journal of Food Biochemistry*, *27*(5), 361-422.

Yu, P., Huang, H., Zhao, X., Zhong, N., & Zheng, H. (2022). Dynamic variation of amino acid content during black tea processing: A review. *Food Reviews International*, *39*(7), 3970-3983.

Yue, Z.-X., & Cao, J. (2022). A rapid and sensitive method for the simultaneous determination of multipolar compounds in plant tea by supercritical fluid chromatography coupled to ion mobility quadrupole time-of-flight mass spectrometry. *Foods*, *11*(1), 111.

Zawistowski, J., Biliaderis, C., & Eskin, M. (1991). Polyphenol oxidase. In (pp. 217-273).

Zeb, A. (2021). Basics in analysis of phenolic antioxidants. In *Phenolic antioxidants in foods: Chemistry, biochemistry and analysis* (pp. 437–479). Springer.

Zeng, Z., Jin, S., Xiang, X., Yuan, H., Jin, Y., Shi, Q., Zhang, Y., Yang, M., Zhang, L., Huang, R., & Song, C. (2023a). Dynamical changes of tea metabolites fermented by *Aspergillus cristatus*, *Aspergillus neoniger* and mixed fungi: A temporal clustering strategy for untargeted metabolomics. *Food Research International*, *170*, 112992.

Zeng, Z., Xiao, J., Li, M., Wu, J., & Zhang, T. (2023b). Degradation of phenol by immobilized *Alcaligenes faecalis* strain JH1 in Fe3O4-modified biochar from pharmaceutical residues. *Water*, *15*(23), 4084.

Zhang, A., Li, Q., Song, W., Yan, S., Tang, A., & Liu, Y. (2023a). Whole-genome analysis of *Alcaligenes faecalis* JF101 based on phenol degradation. *Biotechnology Bulletin*, *39*(10), 292-303.

Zhang, F., Zhu, F., Chen, B., Su, E., Chen, Y., & Cao, F. (2022). Composition, bioactive substances, extraction technologies and the influences on characteristics of *Camellia oleifera* oil: A review. *Food Research International*, *156*, 111159.

Zhang, G., Zhao, L., Li, W., Yao, H., Lu, C., Zhao, G., Wu, Y., Li, Y., & Kong, G. (2023b). Changes in physicochemical properties and microbial community succession during leaf stacking fermentation. *AMB Express*, *13*(1), 132.

Zhang, K., Ren, T., Liao, J., Wang, S., Zou, Z., Ma, Y., Li, F., Fang, W., & Zhu, X. (2021). Targeted metabolomics reveals dynamic changes during the manufacturing process of Yuhua tea, a stir-fried green tea. *Beverage Plant Research*, *1*(1), 1-11.

Zhang, L., Cao, Q.-Q., Granato, D., Xu, Y.-Q., & Ho, C.-T. (2020). Association between chemistry and taste of tea: A review. *Trends in Food Science & Technology*, *101*, 139-149.

Zhang, L., Ho, C. T., Zhou, J., Santos, J. S., Armstrong, L., & Granato, D. (2019). Chemistry and biological activities of processed *Camellia sinensis* teas: A comprehensive review. *Compr Rev Food Sci Food Saf*, *18*(5), 1474-1495.

Zhang, M., Zhang, T., Wang, Y., Duan, X., Pu, L., Zhang, Y., Li, Q., & Liu, Y. (2024). Accurate prediction of tea catechin content with near-infrared spectroscopy by deep learning based on channel and spatial attention mechanisms. *Chemosensors*, *12*(9), 184.

Zhang, Q., & Zhang, J. (2024). Overview of *Eurotium cristatum* and its fermentation application in tea. *Future Integrative Medicine*, *3*(1), 11-20.

Zhang, X. B., & Du, X. F. (2015). Effects of exogenous enzymatic treatment during processing on the sensory quality of summer Tieguanyin oolong tea from the Chinese Anxi County. *Food Technology and Biotechnology*, *53*(2), 180-189.

Zhang, Y., Skaar, I., Sulyok, M., Liu, X., Rao, M., & Taylor, J. W. (2016). The microbiome and metabolites in fermented Pu-erh tea as revealed by high-throughput sequencing and quantitative multiplex metabolite analysis. *PLoS One*, *11*(6), e0157847.

Zhao, M., Zhou, Y., Xia, H., Peng, M., Li, J., Jin, L., Peng, L., & Wang, Y. (2022). Quantitative microbiome analysis reveals the microbial community assembly along with its correlation with the flavor substances during the manufacturing process of Qingzhuan brick tea at an industrial scale. *LWT - Food Science & Technology*, *167*, 113835.

Zheng, B., Zhou, H., & McClements, D. J. (2023). Co-encapsulation of multiple polyphenols in plant-based milks: Formulation, gastrointestinal stability, and bioaccessibility. *Foods, 12*(18), 3432.

Zheng, J., Yu, L., Aaqil, M., Wang, Q., Peng, W., Zhuang, L., Gong, W., Zheng, T., Zhao, M., Wang, C., Jiang, X., Yan, L., & Yang, R. (2024). Enhanced fermentation of Pu-erh tea with *Aspergillus niger*: Quality and microbial community analysis. *Molecules*, *29*(23), 5647.

Zheng, O. (2025). Thearubigins: A comprehensive study from formation mechanism to biological activity and application prospects. *Theoretical and Natural Science*, *77*, 24-33.

Zhou, J., Fang, T., Li, W., Jiang, Z., Zhou, T., Zhang, L., & Yu, Y. (2022). Widely targeted metabolomics using UPLC-QTRAP-MS/MS reveals chemical changes during the processing of black tea from the cultivar *Camellia sinensis* (L.) O. Kuntze cv. Huangjinya. *Food Research International*, *162*(Pt B), 112169.

Zhu, C., Zhang, L., & Zhao, L. (2008). Molecular cloning, genetic organization of gene cluster encoding phenol hydroxylase and catechol 2,3-dioxygenase in *Alcaligenes faecalis* IS-46. *World Journal of Microbiology and Biotechnology*, *24*(9), 1687-1695.

Zhu, K., Jie, O., Jianan, H., & and Liu, Z. (2021). Research progress of black tea thearubigins: A review. *Critical Reviews in Food Science and Nutrition*, *61*(9), 1556-1566.

Zhuang, Y., Quan, W., Wang, X., Cheng, Y., & Jiao, Y. (2024). Comprehensive review of EGCG modification: Esterification methods and their impacts on biological activities. *Foods*, *13*(8), 1232.

Zou, C., Zhang, X., Xu, Y., & Yin, J. (2024). Recent advances regarding polyphenol oxidase in *Camellia sinensis:* Extraction, purification, characterization, and application. *Foods*, *13*(4).

Zou, H., Li, R., Xuan, X., Jiang, Y., Yuan, H., & An, T. (2025a). Rapid and quantitative prediction of tea pigments content during the rolling of black tea by multi-source information fusion and system analysis methods. *Foods*, *14*(16), 2829.

Zou, H., Xiao, Q., Li, G., Wei, X., Tian, X., Zhu, L., Ma, F., & Li, M. (2025b). Revisiting the advancements in plant polyphenol oxidases research. *Scientia Horticulturae*, *341*, 113960.

Appendices

Appendix A: Declaration on AI Usage in the thesis

In accordance with Massey University guidelines on the responsible use of artificial intelligence (AI), the author declares that AI-assisted tools were used in a limited and supportive capacity during the preparation of this thesis. All intellectual content, including the research design, experimental work, data collection, analysis, interpretation, and conclusions presented in this thesis, is the original work of the author.

AI tools were used to support specific technical and editorial tasks. Python programming was employed for data analysis and graphical outputs, with scripts developed and executed in Google Colab https://colab.research.google.com). Google Gemini (https: GitHub Copilot (https://github.com/features/copilot) was used to enhance coding efficiency.

Grammarly (https://www.grammarly.com) was used to assist with grammar, clarity, and language refinement. ChatGPT (https://chat.openai.com) was used to support brainstorming of visual presentation approaches and to generate templates for figure layout, without contributing to scientific concepts, data interpretation, or scholarly argumentation. Final figures and graphical illustrations were independently created by the author using BioRender (https://www.biorender.com).

All AI-assisted outputs were critically evaluated, verified, and revised by the author to ensure accuracy, academic integrity, and compliance with scholarly standards. No AI tools were used to generate original research data, results, or conclusions. The author accepts full responsibility for the content of this thesis.

Appendix B: Supplementary data for Chapter 3

Table S3.1: Final concentrations (µg/mL) of each compound in the six-level mixed calibration standards.

Compound	Level 1	Level 2	Level 3	Level 4	Level 5	Level 6
Gallic acid	1.8750	3.75	7.5	15	30	60
Theobromine	0.9375	1.875	3.75	7.5	15	30
EGC	0.9375	1.875	3.75	7.5	15	30
Caffeine	4.6875	9.375	18.75	37.5	75	150
Catechin	0.9375	1.875	3.75	7.5	15	30
EC	0.9375	1.875	3.75	7.5	15	30
EGCG	4.6875	9.375	18.75	37.5	75	150
ECG	0.9375	1.875	3.75	7.5	15	30
TF	2.8125	5.625	11.25	22.5	45	90
TF3G	2.8125	5.625	11.25	22.5	45	90
TF3′G	2.8125	5.625	11.25	22.5	45	90
TF3-3′G	2.8125	5.625	11.25	22.5	45	90

Table S3.2: Preparation of mixed calibration standards, Levels 1–6 (volumes in µL; final volume 10,000 µL)

Component	Stock conc. (µg/mL)	Level 1	Level 2	Level 3	Level 4	Level 5	Level 6
Individual stock solutions							
Gallic acid	300	62.5	125	250	500	–	–
Theobromine	300	31.25	62.5	125	250	–	–
EGC	300	31.25	62.5	125	250	–	–
Caffeine	300	156.25	312.5	625	1,250	–	–
Catechin	300	31.25	62.5	125	250	–	–
EC	300	31.25	62.5	125	250	–	–
EGCG	300	156.25	312.5	625	1,250	–	–
ECG	300	31.25	62.5	125	250	–	–
TF	300	93.75	187.5	375	750	–	–
TF3G	300	93.75	187.5	375	750	–	–
TF3′G	300	93.75	187.5	375	750	–	–
TF3-3′G	300	93.75	187.5	375	750	–	–
Intermediate mixed solution (IM)†	See note	–	–	–	–	2,500	5,000
Total stock/IM volume		906.25	1,812.5	3,625	7,250	2,500	5,000
Solvent balance							
Acetonitrile from stock/IM (20%)		181.25	362.5	725	1,450	500	1,000
Additional acetonitrile		1,818.75	1,637.5	1,275	550	1,500	1,000
Stabilization solution from stock/IM (10%)		90.625	181.25	362.5	725	250	500
Additional stabilization solution		909.375	818.75	637.5	275	750	500
Diluent (HPLC-grade water) to volume		6,365.625	5,731.25	4,462.5	1,925	5,250	3,500
Final volume		10,000	10,000	10,000	10,000	10,000	10,000
Total acetonitrile, µL (% v/v)		2,000 (20)	2,000 (20)	2,000 (20)	2,000 (20)	2,000 (20)	2,000 (20)
Total stabilization solution, µL (% v/v)		1,000 (10)	1,000 (10)	1,000 (10)	1,000 (10)	1,000 (10)	1,000 (10)
Final concentrations (µg/mL)							
Gallic acid		1.875	3.75	7.5	15	30	60
Theobromine, EGC, catechin, EC, ECG (each)		0.9375	1.875	3.75	7.5	15	30
Caffeine, EGCG (each)		4.6875	9.375	18.75	37.5	75	150
TF, TF3G, TF3′G, TF3-3′G (each)		2.8125	5.625	11.25	22.5	45	90

Levels 1–4 were prepared directly from the individual 300 µg/mL stock solutions (each containing 20% acetonitrile and 10% stabilization solution). †Levels 5–6 were prepared from an intermediate mixed solution (IM) containing gallic acid at 120 µg/mL; theobromine, EGC, catechin, EC and ECG at 60 µg/mL each; caffeine and EGCG at 300 µg/mL each; and TF, TF3G, TF3′G and TF3-3′G at 180 µg/mL each, i.e. twice the Level 6 concentrations. The IM was prepared by dissolving the weighed standards in acetonitrile (1 min ultrasonication), adding stabilization solution at 10% (v/v), and making up to 10 mL with HPLC-grade water, so that it contained 20% acetonitrile and 10% stabilization solution. "–" indicates that the individual stock was not used for that level. Final concentrations = (stock or IM concentration × volume) ÷ 10,000 µL.

Table S3.3. The comparison of different extraction methods and the yield of gallic acid, caffeine, total catechins, and total theaflavins.

Tea Type	Extraction Method	Solvent	Conc. (%)	Abbrev.	Gallic Acid (mg/g)	Caffeine (mg/g)	Total Catechins (mg/g)	Total TF (mg/g)
Green tea	Hot Water	Water	100	GT_HW	0.64 ± 0.03^{a}	34.35 ± 1.20^{a}	159.52 ± 5.44^{c}	0.08 ± 0.00^{d}
	Ultra sonication-assisted	Water	100	GT_U_W	0.65 ± 0.14^{a}	34.67 ± 0.85^{a}	161.52 ± 5.21^{c}	0.12 ± 0.00^{d}
		Ethanol	20	GT_U_E20	0.53 ± 0.01^{b}	34.42 ± 0.18^{a}	177.63 ± 0.24^{b}	0.21 ± 0.20^{c}
		Ethanol	50	GT_U_E50	0.33 ± 0.05^{c}	28.05 ± 2.67^{b}	138.14 ± 17.63^{d}	0.19 ± 0.23^{c}
		Ethanol	70	GT_U_E70	0.23 ± 0.08^{d}	23.87 ± 2.34^{c}	115.33 ± 12.60^{e}	0.03 ± 0.03^{d}
		Ethanol	90	GT_U_E90	0.09 ± 0.04^{e}	15.59 ± 1.72^{d}	40.38 ± 3.87^{f}	ND
		Methanol	20	GT_U_M20	0.00 ± 0.00^{f}	2.17 ± 0.26^{e}	170.98 ± 8.51^{b}	0.07 ± 0.00^{d}
		Methanol	50	GT_U_M50	0.48 ± 0.01^{b}	35.52 ± 1.51^{a}	191.18 ± 10.28^{a}	0.10 ± 0.01^{d}
		Methanol	70	GT_U_M70	0.52 ± 0.04^{b}	37.72 ± 2.23^{a}	214.30 ± 12.86^{a}	0.52 ± 0.02^{a}
		Methanol	90	GT_U_M90	0.44 ± 0.01^{c}	34.10 ± 2.18^{a}	189.72 ± 10.80^{a}	0.36 ± 0.09^{b}
	ISO 14502-1:2005	Methanol	70	GT_ISO	0.33 ± 0.05^{c}	34.42 ± 0.18^{a}	165.60 ± 6.36^{b}	0.07 ± 0.00^{d}
Black tea	Hot Water	Water	100	BT_HW	1.49 ± 0.02^{b}	21.79 ± 0.88^{c}	10.91 ± 0.93^{e}	2.12 ± 0.01^{e}
	Ultra sonication-assisted	Water	100	BT_U_W	0.33 ± 0.05^{d}	35.18 ± 0.55^{b}	16.48 ± 0.91^{d}	4.09 ± 0.33^{d}
		Ethanol	20	BT_U_E20	1.75 ± 0.13^{b}	41.31 ± 2.76^{a}	27.32 ± 1.52^{a}	9.21 ± 0.30^{c}
		Ethanol	50	BT_U_E50	0.90 ± 0.22^{c}	28.41 ± 2.51^{b}	16.96 ± 1.33^{d}	7.89 ± 2.11^{c}
		Ethanol	70	BT_U_E70	1.09 ± 0.17^{c}	31.17 ± 3.18^{b}	17.96 ± 3.25^{d}	8.84 ± 1.84^{c}
		Ethanol	90	BT_U_E90	0.08 ± 0.03^{e}	7.17 ± 0.29^{d}	3.11 ± 0.36^{f}	1.03 ± 0.30^{e}
		Methanol	20	BT_U_M20	1.50 ± 0.12^{b}	44.21 ± 4.46^{a}	18.01 ± 1.14^{d}	11.30 ± 0.24^{b}
		Methanol	50	BT_U_M50	1.89 ± 0.09^{b}	46.90 ± 0.35^{a}	25.75 ± 2.80^{b}	15.08 ± 1.15^{b}
		Methanol	70	BT_U_M70	2.35 ± 0.29^{a}	48.62 ± 0.90^{a}	23.97 ± 1.58^{b}	19.73 ± 1.33^{a}
		Methanol	90	BT_U_M90	1.77 ± 0.07^{b}	47.08 ± 2.57^{a}	24.97 ± 1.37^{b}	15.11 ± 1.88^{b}
	ISO 14502-1:2005	Methanol	70	BT_ISO	0.90 ± 0.22^{c}	41.31 ± 2.76^{a}	17.46 ± 1.16^{d}	15.07 ± 1.25^{b}

Values are expressed as mean ± standard deviation (n = 3). Within each column, values followed by different superscript letters (a–f) are significantly different at $p < 0.05$ based on one-way ANOVA followed by Tukey's post-hoc test. ND: Not Detected.

Table S3.4: Major polyphenolic content during black tea processing (mg/g DW ± SD, n=18).

Processing Stage	FTL	WTL	ROL	RTL	OTL 1	OTL 2	OTL 3	FBT
Gallic acid	15.10 ± 0.06^{a}	6.89 ± 0.04^{d}	9.50 ± 0.06^{b}	9.18 ± 0.12^{b}	4.14 ± 0.07^{f}	5.41 ± 0.08^{e}	4.47 ± 0.08^{f}	4.88 ± 0.08^{e}
Theobromine	4.42 ± 0.04^{a}	4.26 ± 0.03^{a}	4.79 ± 0.03^{c}	3.50 ± 0.04^{d}	3.60 ± 0.06^{d}	3.40 ± 0.05^{d}	3.67 ± 0.06^{d}	3.08 ± 0.05^{e}
EGC	32.77 ± 0.14^{a}	17.33 ± 0.11^{b}	18.66 ± 0.12^{b}	1.07 ± 0.01^{c}	0.27 ± 0.00^{d}	2.00 ± 0.03^{c}	0.90 ± 0.02^{c}	0.47 ± 0.01^{d}
Caffeine	101.70 ± 0.54^{a}	101.62 ± 0.69^{a}	98.51 ± 0.68^{c}	95.89 ± 1.20^{d}	94.77 ± 1.49^{e}	96.89 ± 1.28^{f}	95.70 ± 1.45^{g}	95.67 ± 1.47^{g}
Catechin	16.02 ± 0.07^{a}	6.77 ± 0.04^{b}	6.99 ± 0.04^{b}	3.26 ± 0.04^{c}	2.03 ± 0.03^{d}	1.37 ± 0.02^{e}	1.01 ± 0.02^{f}	1.37 ± 0.02^{e}
EC	42.65 ± 0.18^{a}	23.92 ± 0.14^{b}	31.34 ± 0.20^{c}	13.00 ± 0.16^{d}	4.12 ± 0.07^{e}	4.00 ± 0.06^{e}	2.80 ± 0.05^{f}	3.07 ± 0.05^{f}
EGCG	186.66 ± 0.79^{a}	111.68 ± 0.69^{b}	88.57 ± 0.57^{c}	9.31 ± 0.12^{d}	7.65 ± 0.03^{e}	5.80 ± 0.20^{d}	4.70 ± 0.04^{e}	3.29 ± 0.06^{e}
ECG	50.26 ± 0.21^{a}	31.25 ± 0.19^{b}	34.70 ± 0.22^{b}	14.25 ± 0.18^{c}	8.80 ± 0.14^{d}	9.99 ± 0.15^{d}	7.35 ± 0.13^{e}	6.13 ± 0.10^{f}
Theaflavin	ND^{e}	4.29 ± 0.03^{b}	6.21 ± 0.04^{a}	2.99 ± 0.04^{c}	1.68 ± 0.03^{d}	3.46 ± 0.05^{c}	2.70 ± 0.05^{c}	2.72 ± 0.05^{c}
TF3G	ND^{e}	2.94 ± 0.02^{a}	3.67 ± 0.02^{a}	3.43 ± 0.04^{a}	2.71 ± 0.04^{b}	3.36 ± 0.05^{a}	3.06 ± 0.05^{a}	3.57 ± 0.06^{a}
TF3'G	ND^{e}	2.26 ± 0.01^{b}	4.25 ± 0.03^{a}	2.79 ± 0.03^{b}	1.62 ± 0.03^{c}	2.73 ± 0.04^{b}	2.34 ± 0.04^{b}	2.32 ± 0.04^{b}
TF3-3G	ND^{e}	2.91 ± 0.01^{b}	1.84 ± 0.03^{c}	3.25 ± 0.03^{b}	2.71 ± 0.03^{c}	1.45 ± 0.04^{d}	1.42 ± 0.04^{d}	2.37 ± 0.04^{b}
TPC (GAE mg/g DW)	831.73± 23.32^{a}	436.22± I7.54^{c}	554.08± 18.65^{b}	517.25± 20.05^{b}	497.96± 10.61^{c}	391.74± 9.37^{d}	505.61± 19.77^{b}	374.18± 8.44^{d}

Data show concentrations (mg/g DW ± SD, n=18). ND = Not Detected (below LOD, treated as 0 mg/g for ANOVA and Tukey's HSD). Superscripts ($^{a–g}$) denote significant differences within rows ($p < 0.05$). LODs for theaflavins range from 0.03–1.68 µg/mL.

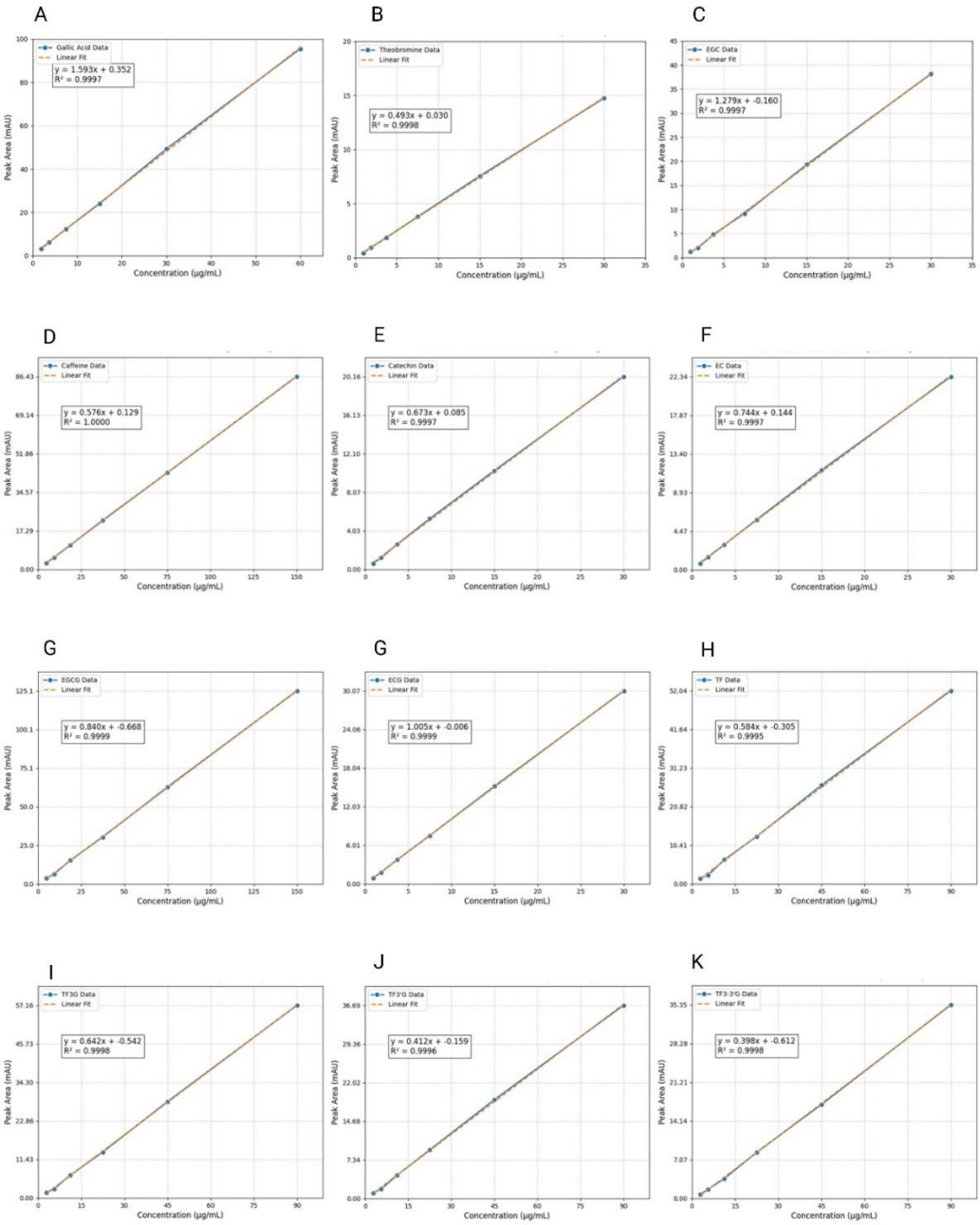

Figure S3.1. Calibration curves for 12 polyphenolic compounds detected at 210 nm using HPLC. The analytes include (A) Gallic acid, (B) Theobromine, (C) Epigallocatechin (EGC), (D) Caffeine, (E) Catechin, (F) Epicatechin (EC), (G) Epigallocatechin gallate (EGCG), (H) Epicatechin gallate (ECG), (I) Theaflavin (TF), (J) Theaflavin-3-gallate (TF3G), (K) Theaflavin-3′-gallate (TF3′G), and (L) Theaflavin-3,3′-digallate (TF3-3′G). Each calibration curve shows the linear relationship between concentration (µg/mL) and peak area (mAU), with corresponding regression equations and coefficients of determination (R^2), indicating excellent linearity ($R^2 > 0.999$ for most analytes).

Appendix C: Supplementary data for Chapter 4

Table S4.1: Molecular identification and polyphenol oxidase (PPO) activity of bacterial isolates recovered from different stages of black tea processing.

Isolate Code	*Isolation Source	Ref. GenBank Accession No.	Closest Match	% Identity	% Coverage	GenBank Accession No. (This Study)	MPLO Activity (U/mL, mean ± SD)
B12	OTL	KY744644.1	*Alcaligenes faecalis*	99	97	PP346132	132.57± 0.65
B23	OTL	MK617289.1	*A. faecalis*	99	100	PP346140	87.5 ± 0.5
B21	WTL	MZ068206.1	*Brevundimona*s sp.	95	100	PP346138	67 ± 0.2
B35	WT	OM293496.1	*A. faecalis*	100	100	PP346146	66.95 ± 0.05
B30	RS	EF011115.1	*A. faecalis*	99	100	PP346144	60.05 ± 4.15
B18	FTL	MH133190.1	*A. faecalis*	98	100	PP346136	41 ± 2.1
B08	WTL	MT378145.1	*A. faecalis*	100	100	PP346129	33.1 ± 0.3
B05	OTL	KR782275.1	*Brevibacillus parabrevis*	98	100	PP346126	31 ± 1.1
B33	FB	MN216192.1	*A. faecalis*	99	100	PP346145	28.8 ± 0.3
B24	OTL	KJ729607.1	*Alcaligenes* sp.	92	100	PP346141	23.25 ± 0.25
B20	FTL	MH793409.1	*A. faecalis*	99	100	PP346137	18.25 ± 0.75
B29	OTL	MN578054.1	*A. faecalis*	100	100	PP346143	18.05 ± 0.45
B15	ROL	MT605456.1	*Microbacterium testaceum*	100	100	PP346135	13.2 ± 0.2
B36	ROL	MH029146.1	*A. faecalis*	97	100	PP346147	11.5 ± 0.5
B10	RTL	MZ295250.1	*Mammaliicoccus* sp.	95	100	PP346130	11.35 ± 0.35
B26	OTL	MT378145.1	*Alcaligenes* sp.	90	92	PP346142	10 ± 0.54
B03	FTL	LC507944.1	*B. diminuta*	100	100	PP346124	5.75 ± 0.75
B01	WTL	KM203630.1	*B. parabrevis*	99	100	PP346122	4.55 ± 0.15
B11	OTL	CP125088.1	*Klebsiella pneumoniae*	100	100	PP346131	3.35 ± 0.85
B14	FTL	OQ780604.1	*Brevibacterium* sp.	99	100	PP346134	2.25 ± 0.15
B06	ROL	KR047782.1	*Brachybacterium rhamnosum*	100	100	PP346127	2.2 ± 0
B04	ROL	KT779213.1	*Staphylococcus sciuri*	100	100	PP346125	1.28 ± 0.58
B07	ROL	MF525127.1	*Brevundimonas* sp.	88	100	PP346128	1.23 ± 0.43
B13	OTL	MN880161.1	*Brevundimona*s sp.	94	100	PP346133	0.75 ± 0.01
B02	WTL	MK764985.1	*Staphylococcus succinus*	98	100	PP346123	0.3 ± 0
B22	ROL	MK847262.1	*Brevundimonas* sp.	90	98	PP346139	0.12 ± 0
B38	OTL	KF424684.1	*Kocuria palustris*	98	100	PP346148	0.07 ± 0

*Isolation sources: Fresh tea leaves (FTL); withered leaves (WTL); roller surfaces (RS); rotovaned leaves (RTL); oxidized leaves (OTL); fermentation beds (FB); and fired black tea (FBT); withering trays (WT); and rolling equipment (RE).

Table S4.2: Molecular identification and extracellular MPLO activity of fungal isolates associated with tea processing.

Isolate Code	*Isolation Source	Ref. GenBank Accession No.	Closest Match	% Identity	% Coverage	GenBank Accession No. (This Study)	MPLO Activity (U/mL, mean ± SD)
EP06	FTL	OQ933313.1	*Aspergillus fumigatus*	99	100	PP351846	77.67 ± 0.33
EP09	FTL	OQ933313.1	*A. fumigatus*	100	100	PP351848	119.03 ± 0.58
EP15	FTL	MT594361.1	*Aspergillus sydowii*	99	100	PP351850	34.00 ± 0.58
F15	FBT	OQ935466.1	*Aspergillus tubingensis*	100	100	PP351858	1.67 ± 0.33
EP03B	FTL	HQ443246.1	*Aspergillus versicolor*	100	100	PP354148	11.00 ± 0.58
EP05	FTL	MT609910.1	*A. versicolor*	99	100	PP351845	11.67 ± 0.33
PR04	RS	MN758930.1	*Colletotrichum* sp.	100	100	PP355769	32.67 ± 0.33
F8	ROL	MK590357.1	*Curvularia lunata*	100	100	PP351854	12.33 ± 1.45
F10	OTL	MT626601.1	*Daldinia eschscholtzii*	100	100	PP351856	4.33 ± 0.33
F1	FTL	MT197383.1	*Diaporthe* sp.	100	100	PP351853	23.00 ± 0.58
EP14	FTL	MH165845.1	*Fusarium* sp.	84	99	PP351849	2.00 ± 0.05
PR03	ROL	KX181288.1	*Lentinus sajor-caju*	100	100	PP351860	54.00 ± 1.00
F14	FBT	MT443931.1	*Lodderomyces* sp.	95	99	PP351857	23.33 ± 0.67
EP18	FTL	MT539193.1	*Meyerozyma* sp.	94	98	PP351851	2.33 ± 0.33
EP02	FTL	MT597827.1	*Nigrospora sphaerica*	100	100	PP351841	4.33 ± 0.33
EP02B	FTL	MT597827.1	*N. sphaerica*	100	100	PP351843	0.67 ± 0.33
PR09	FB	MG583911.1	*Rhizopus microsporus*	100	100	PP351863	3.33 ± 0.33
PR07	FB	LC269928.1	*Rigidoporus vinctus*	99	100	PP351862	2.00 ± 0.00
EP02A	FTL	MK336588.1	*Sarocladium strictum*	100	100	PP351842	1.00 ± 0.58
EP03A	FTL	MT557309.1	*Talaromyces pinophilus*	100	100	PP351844	24.00 ± 0.58
EP07	FTL	LC406460.1	*T.pinophilus*	100	100	PP351847	55.00 ± 0.58
F16	FBT	MT594355.1	*T.pinophilus*	98	100	PP351859	26.00 ± 0.58
PR05	RS	MT594355.1	*T. pinophilus*	100	100	PP351861	11.67 ± 0.33
F9	ROL	MT594355.1	*Talaromyces* sp.	82	94	PP351855	5.00 ± 0.58
EP18A	FTL	OQ933313.1	*Thyridium* sp.	94	98	PP351852	3.33 ± 0.33

***Isolation sources**: Fresh tea leaves (FTL); withered leaves (WTL); roller surfaces (RS); rotovaned leaves (RTL); oxidized leaves (OTL); fermentation beds (FB); and fired black tea (FBT); withering trays (WT); and rolling equipment (RE).

Appendix D: Supplementary data for Chapter 5

Table S5.1: Preparation and Incubation Chart (20 Runs).

Run No.	Coded X1	Coded X2	Coded X3	Catechin Stock (12.5 mM) (µL)	$CuSO_4$ Stock (25 mM) (µL)	Total Stock Volume (µL)	Phosphate buffer (50 mM, pH-7) (µL)	TSB Volume (mL)	Harvest Time (H)
1	-1	-1	-1	100	100	200	800	49.00	24
2	1	-1	-1	500	100	600	400	49.00	24
3	-1	1	-1	100	500	600	400	49.00	24
4	1	1	-1	500	500	1000	0	49.00	24
5	-1	-1	1	100	100	200	800	49.00	84
6	1	-1	1	500	100	600	400	49.00	84
7	-1	1	1	100	500	600	400	49.00	84
8	1	1	1	500	500	1000	0	49.00	84
9	+α	0	0	646	333	946	54	49.00	54
10	−α	0	0	20	333	302	698	49.00	54
11	0	+α	0	333	646	946	54	49.00	54
12	0	−α	0	333	20	320	680	49.00	54
13	0	0	+α	333	333	600	400	49.00	12
14	0	0	−α	333	333	600	400	49.00	96
15–20	0	0	0	333	333	600	400	49.00	54

Table S5.2: Rotatable Central Composite Design matrix with coded and actual factor levels and mean experimental enzyme activities (mean ± SD, n = 3 for factorial/axial points; n = 6 for center points).

Run	Coded X_1	Coded X_2	Coded X_3	Catechin (µL)	$CuSO_4$ (µL)	Duration (h)	Laccase-like (U/mL)	Peroxidase-like (U/mL)	Catechol oxidase-like (U/mL)	Tyrosinase-like (U/mL)
1	-1	-1	-1	100	100	24	44.96 ± 1.72	5.12 ± 0.17	10.67 ± 0.82	12.61 ± 0.92
2	1	-1	-1	500	100	24	50.98 ± 4.71	5.90 ± 0.58	11.45 ± 0.90	14.91 ± 0.06
3	-1	1	-1	100	500	24	53.68 ± 1.36	7.05 ± 0.35	15.03 ± 1.22	18.53 ± 2.12
4	1	1	-1	500	500	24	59.59 ± 5.33	7.82 ± 0.75	17.61 ± 0.88	21.58 ± 1.10
5	-1	-1	1	100	100	84	84.92 ± 4.23	9.11 ± 0.96	21.50 ± 0.65	22.59 ± 1.29
6	1	-1	1	500	100	84	82.02 ± 4.00	8.72 ± 0.73	19.29 ± 1.13	20.77 ± 2.22
7	-1	1	1	100	500	84	75.38 ± 0.88	14.09 ± 1.04	21.61 ± 3.54	18.27 ± 2.05
8	1	1	1	500	500	84	67.13 ± 0.76	10.61 ± 0.49	21.63 ± 1.06	21.91 ± 2.12
9	-1	0	0	20	333	54	39.58 ± 2.75	4.93 ± 0.18	10.16 ± 0.84	10.76 ± 0.41
10	1	0	0	646	333	54	65.46 ± 0.73	9.28 ± 1.30	18.55 ± 2.15	23.61 ± 0.69
11	0	-1	0	333	20	54	51.97 ± 1.35	5.61 ± 0.67	11.16 ± 1.41	13.34 ± 0.79
12	0	1	0	333	646	54	57.72 ± 3.12	12.69 ± 0.82	19.34 ± 1.87	20.29 ± 2.13
13	0	0	-1	333	333	12	30.38 ± 1.45	3.43 ± 0.09	6.49 ± 0.44	7.69 ± 0.52
14	0	0	1	333	333	96	89.36 ± 9.29	10.85 ± 0.16	22.85 ± 2.16	25.11 ± 2.50
15–20	0	0	0	333	333	54	71.79 ± 3.85	9.41 ± 0.85	18.43 ± 1.05	21.12 ± 1.68

Table S5.3: ANOVA for the quadratic model of ABTS-oxidizing activity in the MPLO preparation from *Alcaligenes faecalis* NZRM 836.

Source	Sum of Squares	df	Mean Square	F-value	p-value
Model	2593.63	9	288.18	5.88	0.0053
Catechin (X_1)	165.54	1	165.54	3.38	0.0959
$CuSO_4$ (X_2)	61.06	1	61.06	1.25	0.2904
Time (X_3)	1412.54	1	1412.54	28.83	0.0003
X_1X_2	3.25	1	3.25	0.07	0.8019
X_1X_3	62.16	1	62.16	1.27	0.2863
X_2X_3	140.28	1	140.28	2.86	0.1215
X_1^2	384.19	1	384.19	7.84	0.0188
X_2^2	316.45	1	316.45	6.46	0.0293
X_3^2	191.26	1	191.26	3.90	0.0764
Residual	490.01	10	49.00		
Lack of Fit	482.50	5	96.50	64.26	0.0002 (significant)
Pure Error	7.51	5	1.50		
Cor Total	3083.64	19			

Table S5.4: ANOVA for the quadratic model of pyrogallol-oxidizing activity in the MPLO preparation from *Alcaligenes faecalis* NZRM 836.

Source	Sum of Squares	df	Mean Square	F-value	p-value
Model	70.68	9	7.85	5.83	0.0055
Catechin (X_1)	0.41	1	0.41	0.14	0.7178
$CuSO_4$ (X_2)	21.43	1	21.43	15.91	0.0026
Time (X_3)	38.66	1	38.66	28.70	0.0003
X_1X_2	1.20	1	1.20	0.40	0.5398
X_1X_3	3.67	1	3.67	1.23	0.2930
X_2X_3	1.20	1	1.20	0.89	0.3672
X_1^2	2.14	1	2.14	1.59	0.2358
X_2^2	0.17	1	0.17	0.13	0.7282
X_3^2	0.21	1	0.21	0.16	0.7017
Residual	13.47	10	1.35		
Lack of Fit	13.05	5	2.61	31.07	0.0009 (significant)
Pure Error	0.42	5	0.08		
Cor Total	84.15	19			

Table S5.5: ANOVA for the quadratic model of catechol-oxidizing activity in the MPLO preparation from *Alcaligenes faecalis* NZRM 836.

Source	Sum of Squares	df	Mean Square	F-value	p-value
Model	211.41	9	23.49	4.77	0.0113
Catechin (X_1)	23.22	1	23.22	4.72	0.0550
$CuSO_4$ (X_2)	47.99	1	47.99	9.75	0.0108
Time (X_3)	122.60	1	122.60	24.90	0.0005
X_1X_2	2.31	1	2.31	0.47	0.5088
X_1X_3	3.78	1	3.78	0.77	0.4014
X_2X_3	7.03	1	7.03	1.43	0.2597
X_1^2	3.25	1	3.25	0.66	0.4358
X_2^2	0.78	1	0.78	0.16	0.6991
X_3^2	0.04	1	0.04	0.01	0.9259
Residual	49.24	10	4.92		
Lack of Fit	48.48	5	9.70	64.36	0.0002 (significant)
Pure Error	0.75	5	0.15		
Cor Total	260.65	19			

Table S5.6: ANOVA for the quadratic model of L-DOPA-oxidizing activity in the MPLO preparation from *Alcaligenes faecalis* NZRM 836.

Source	Sum of Squares	df	Mean Square	F-value	p-value
Model	210.58	9	23.40	4.09	0.0192
Catechin (X_1)	25.19	1	25.19	4.41	0.0621
$CuSO_4$ (X_2)	38.74	1	38.74	6.78	0.0263
Time (X_3)	112.60	1	112.60	19.71	0.0013
X_1X_2	2.53	1	2.53	0.44	0.5207
X_1X_3	3.78	1	3.78	0.66	0.4349
X_2X_3	5.95	1	5.95	1.04	0.3315
X_1^2	17.98	1	17.98	3.15	0.1065
X_2^2	3.33	1	3.33	0.58	0.4630
X_3^2	3.58	1	3.58	0.63	0.4472
Residual	57.14	10	5.71		
Lack of Fit	55.04	5	11.01	26.21	0.0014 (significant)
Pure Error	2.10	5	0.42		
Cor Total	267.72	19			

Table S5.7: Fitted second-order polynomial regression equations in coded units for the four enzyme activities of the MPLO preparation.

X_1 = Catechin, X_2 = $CuSO_4$, X_3 = Duration (Time), each in coded (−1 to +1, α = 1.682 at axial points) units. Regenerated from the complete individual-run raw dataset (n = 20 runs).

Response	Fitted Second-Order Polynomial Equation (coded units)
ABTS-oxidizing activity (Y_1)	$Y_1 = 78.987 + 3.481X_1 + 2.114X_2 + 10.170X_3 + 0.637X_1X_2 - 2.788X_1X_3 - 4.188X_2X_3 - 5.162X_1^2 - 4.685X_2^2 - 3.642X_3^2$
Pyrogallol-oxidizing activity (Y_2)	$Y_2 = 9.951 + 0.612X_1 + 1.253X_2 + 1.682X_3 - 0.138X_1X_2 - 0.438X_1X_3 - 0.388X_2X_3 - 0.386X_1^2 + 0.109X_2^2 - 0.120X_3^2$
Catechol-oxidizing activity (Y_3)	$Y_3 = 18.042 + 1.304X_1 + 1.874X_2 + 2.996X_3 + 0.537X_1X_2 - 0.688X_1X_3 - 0.938X_2X_3 - 0.474X_1^2 + 0.232X_2^2 + 0.056X_3^2$
L-DOPA-oxidizing activity (Y_4)	$Y_4 = 21.001 + 1.358X_1 + 1.684X_2 + 2.871X_3 + 0.562X_1X_2 - 0.688X_1X_3 - 0.863X_2X_3 - 1.117X_1^2 - 0.480X_2^2 - 0.498X_3^2$

Center-point validity check

ABTS-oxidizing activity: intercept = 78.987 vs. measured center-point average = 79.317 U/mL

Pyrogallol-oxidizing activity: intercept = 9.951 vs. measured center-point average = 10 U/mL

Catechol-oxidizing activity: intercept = 18.042 vs. measured center-point average = 18.133 U/mL

L-DOPA-oxidizing activity: intercept = 21.001 vs. measured center-point average = 21.1 U/mL

Each equation's intercept represents the model's predicted response at the design center (X_1=X_2=X_3=0); this should closely match the actual measured activity at the repeated center-point runs (n = 6) in Table S5.2, since these are independent, direct measurements at exactly that point. All four intercepts fall within 1.6 U/mL of their respective measured center-point averages, confirming these equations are correctly derived from the source design data.

Table S5.8: Desirability weights for multi-response optimization.

Enzyme	Desirability Weight	Target (U/mL)	Rationale
Laccase	0.25	Maximize (>90)	Radical oxidation for ring fission and broad phenolic transformation
Peroxidase	0.25	Maximize (>10)	H_2O_2-dependent oxidation and prevention of excessive oxidative damage
Catechol oxidase	0.20	Maximize (>20)	Quinone formation for degalloylation of galloylated catechins
Tyrosinase	0.30	Maximize (>250)	Selective oxidation of dehydroxylated catechins for stable theaflavin-like pigments and improved color/mouthfeel

Table S5.9: Pearson correlation coefficients (r) and p-values between major polyphenols, enzyme activities, and pH (* $p < 0.05$, ** $p < 0.01$).

Parameter	pH (r)	ABTS activity (r)	DOPA activity (r)
EGCG	0.90**	0.78	0.85*
EGC	0.96**	0.65	0.72
ECG	0.68	0.71	0.79*
EC	0.94**	0.74	0.81*
GCG	0.55	0.88*	0.62
Gallic acid	0.42	0.82*	0.58

Table S5.10: Time–dose optimization of enzymatic oxidation of green tea infusion by MPLO enzyme preparation.

Treatment	Time	EGCG (µg/mL)	EGC (µg/mL)	EC (µg/mL)	GCG (µg/mL)	Total TF (µg/mL)
Control	t1	866.74 ± 43.34^{a}	416.96 ± 20.85^{a}	93.32 ± 4.67^{b}	11.59 ± 0.58^{c}	1.24 ± 0.06^{c}
	t2	837.33 ± 41.87^{a}	391.83 ± 19.59^{b}	89.74 ± 4.49^{c}	14.10 ± 0.71^{b}	1.51 ± 0.08^{c}
	t3	779.34 ± 38.97^{b}	401.76 ± 20.09^{b}	95.53 ± 4.78^{b}	18.38 ± 0.92^{a}	1.72 ± 0.09^{c}
	t4	719.11 ± 35.96^{c}	387.23 ± 19.36^{b}	93.90 ± 4.70^{b}	19.81 ± 0.99^{a}	1.72 ± 0.09^{c}
	t5	736.24 ± 36.81^{c}	408.65 ± 20.43^{a}	101.33 ± 5.07^{a}	22.09 ± 1.10^{a}	1.91 ± 0.10^{c}
	t6	662.07 ± 33.10^{d}	433.46 ± 21.67^{a}	108.03 ± 5.40^{a}	19.46 ± 0.97^{a}	2.31 ± 0.12^{c}
50 µL	t1	938.52 ± 46.93^{a}	467.62 ± 23.38^{a}	105.17 ± 5.26^{a}	13.20 ± 0.66^{b}	1.31 ± 0.07^{c}
	t2	802.30 ± 40.12^{b}	420.85 ± 21.04^{b}	91.50 ± 4.58^{c}	14.73 ± 0.74^{b}	1.26 ± 0.06^{c}
	t3	760.46 ± 38.02^{b}	426.58 ± 21.33^{b}	98.12 ± 4.91^{b}	20.18 ± 1.01^{a}	2.74 ± 0.14^{b}
	t4	598.05 ± 29.90^{c}	352.49 ± 17.62^{c}	80.26 ± 4.01^{d}	14.88 ± 0.74^{b}	1.37 ± 0.07^{c}
	t5	629.07 ± 31.45^{c}	408.96 ± 20.45^{a}	101.89 ± 5.09^{a}	18.42 ± 0.92^{a}	6.63 ± 0.33^{a}
	t6	555.34 ± 27.77^{d}	403.23 ± 20.16^{a}	105.44 ± 5.27^{a}	18.91 ± 0.95^{a}	8.97 ± 0.45^{a}
100 µL	t1	834.37 ± 41.72^{b}	419.81 ± 20.99^{b}	91.45 ± 4.57^{c}	12.35 ± 0.62^{c}	1.44 ± 0.07^{c}
	t2	729.24 ± 36.46^{c}	376.69 ± 18.83^{c}	81.88 ± 4.09^{d}	11.64 ± 0.58^{c}	1.33 ± 0.07^{c}
	t3	629.17 ± 31.46^{c}	374.65 ± 18.73^{c}	87.73 ± 4.39^{c}	15.84 ± 0.79^{b}	4.96 ± 0.25^{a}
	t4	562.75 ± 28.14^{d}	365.75 ± 18.29^{c}	87.12 ± 4.36^{c}	16.19 ± 0.81^{b}	2.18 ± 0.11^{b}
	t5	561.37 ± 28.07^{d}	394.81 ± 19.74^{b}	98.99 ± 4.95^{b}	17.60 ± 0.88^{a}	3.03 ± 0.15^{b}
	t6	488.00 ± 24.40^{e}	406.82 ± 20.34^{b}	109.84 ± 5.49^{a}	19.52 ± 0.98^{a}	8.98 ± 0.45^{a}
200 µL	t1	775.42 ± 38.77^{c}	390.46 ± 19.52^{b}	83.44 ± 4.17^{d}	11.80 ± 0.59^{c}	1.38 ± 0.07^{c}
	t2	782.03 ± 39.10^{c}	460.36 ± 23.02^{a}	101.71 ± 5.09^{a}	13.20 ± 0.66^{b}	1.35 ± 0.07^{c}
	t3	677.49 ± 33.87^{c}	477.59 ± 23.88^{a}	112.22 ± 5.61^{a}	17.92 ± 0.90^{a}	2.65 ± 0.13^{b}
	t4	485.30 ± 24.27^{e}	352.54 ± 17.63^{c}	85.39 ± 4.27^{c}	15.86 ± 0.79^{b}	2.83 ± 0.14^{b}
	t5	462.19 ± 23.11^{e}	358.50 ± 17.93^{c}	90.14 ± 4.51^{c}	16.12 ± 0.81^{b}	1.41 ± 0.07^{c}
	t6	424.95 ± 21.25^{f}	398.65 ± 19.93^{b}	107.54 ± 5.38^{a}	18.73 ± 0.94^{a}	1.57 ± 0.08^{c}
500 µL	t1	811.27 ± 40.56^{b}	433.94 ± 21.70^{a}	92.87 ± 4.64^{c}	10.91 ± 0.55^{c}	1.27 ± 0.06^{c}
	t2	644.09 ± 32.20^{d}	360.33 ± 18.02^{c}	79.23 ± 3.96^{d}	11.71 ± 0.59^{c}	1.39 ± 0.07^{c}
	t3	524.36 ± 26.22^{d}	378.21 ± 18.91^{c}	88.71 ± 4.44^{c}	15.90 ± 0.80^{b}	2.42 ± 0.12^{b}
	t4	478.41 ± 23.92^{e}	387.08 ± 19.35^{b}	95.44 ± 4.77^{b}	16.94 ± 0.85^{b}	1.47 ± 0.07^{c}
	t5	743.14 ± 37.16^{c}	408.60 ± 20.43^{b}	102.81 ± 5.14^{a}	19.33 ± 0.97^{a}	1.97 ± 0.10^{c}
	t6	368.36 ± 18.42^{g}	326.29 ± 16.31^{d}	84.54 ± 4.23^{c}	15.07 ± 0.75^{b}	1.48 ± 0.07^{c}

Table S5.11: Derringer's desirability analysis identifying the optimal reaction timepoint

Individual and composite desirability scores (D) across all sampled timepoints, combining five criteria: TF:TR ratio, Briskness Index, color development (A420), gallic acid concentration, and pH stability. All D values are normalized 0–1, with 1 representing the most desirable value observed for that criterion. Composite D is calculated as the geometric mean of the five individual D values. The highest composite score (bold) identifies the optimal timepoint.

Time (h)	D (TF:TR ratio)	D (Briskness Index)	D (Color, A420)	D (Gallic acid)	D (pH)	Composite D
0	0.00	0.00	0.00	0.42	0.00	0.000
1	0.46	0.24	0.15	0.38	0.90	0.360
2	0.87	0.76	0.34	0.60	0.82	0.646
3	1.00	1.00	0.57	0.80	0.77	0.811
5	0.97	0.99	0.91	1.00	0.78	0.925
6	0.97	0.97	1.00	0.22	0.74	0.690
10	0.32	0.80	1.00	0.00	0.00	0.000

The 5 h timepoint achieves the highest composite desirability (D = 0.925), exceeding both the 3 h (D = 0.811) and 6 h (D = 0.690) timepoints. This reflects the simultaneous near-optimal performance of the oxidative pathway (TF:TR ratio, Briskness Index) and the hydrolysis pathway (gallic acid, reaching its absolute maximum at this timepoint), combined with stable, near-neutral pH — a convergence not achieved at any other sampled timepoint.

Table S5.12: Wavelength, standard assay conditions, and method reference for each of the six substrates in the substrate specificity analysis (Section 5.2.12.4, Table 5.5).

Substrate	λmax (nm)	Optimum pH	Optimum Temperature	Assay Method Reference
ABTS	420	pH 3	70 °C	Bourbonnais & Paice (1990)
L-DOPA	475	pH 7	70 °C	Zhang et al. (2006)
Catechol	410	pH 7 (0.1 M phosphate buffer)*	Not stated*	Soliva-Fortuny et al. (2001)
Pyrogallol	420	pH 6.0 (100 mM potassium phosphate buffer)	20 °C	Chance & Maehly (1955)
Syringaldazine	530	pH 6.5	30 °C	Holm et al. (1998)
Guaiacol	470	pH 6.5	25 °C	Tonami et al. (2004)

Appendix E: Supplementary data for Chapter 6

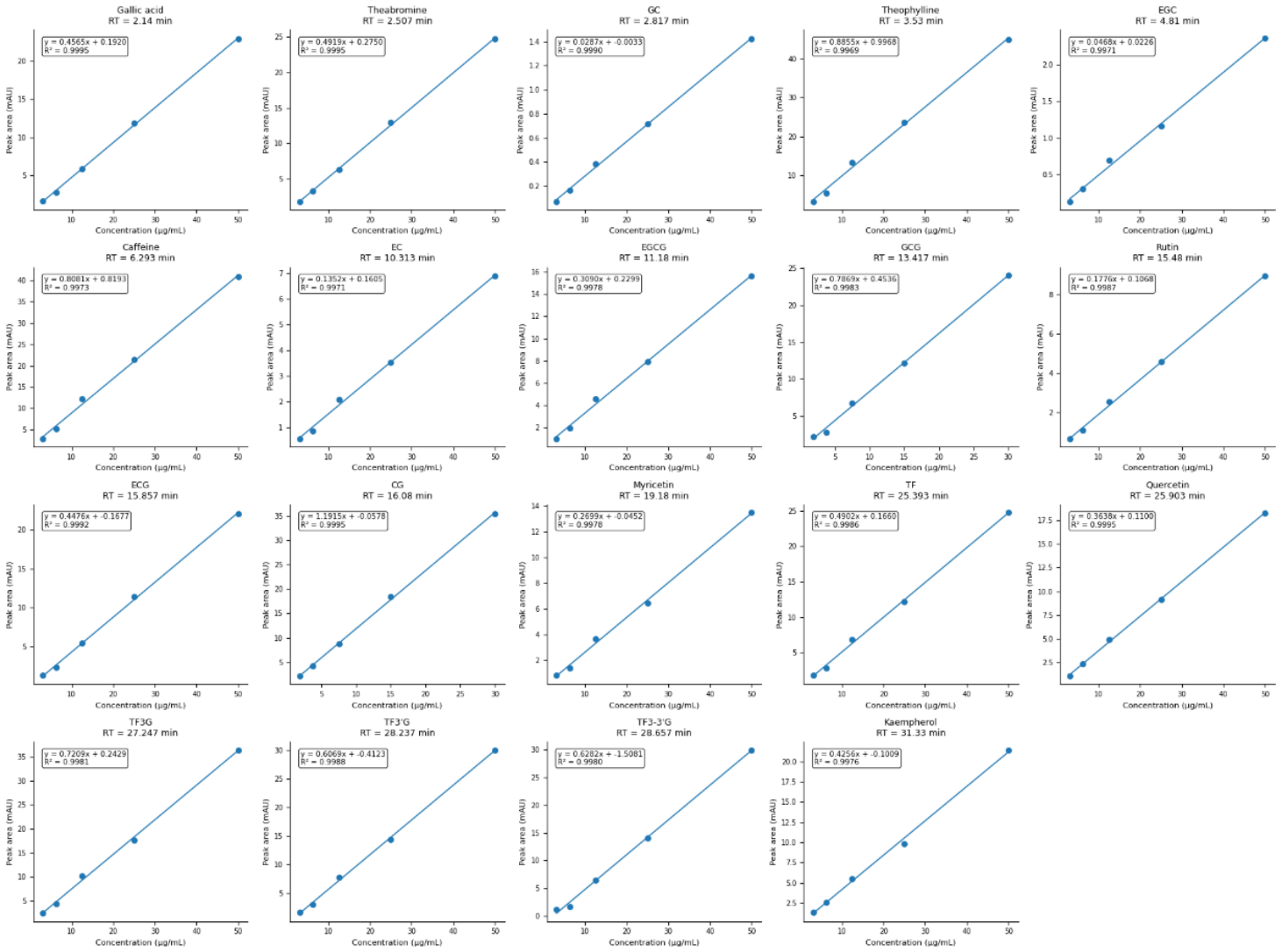

Figure S6.1: Calibration curves of the 19 standard compounds used in HPLC–DAD analysis.

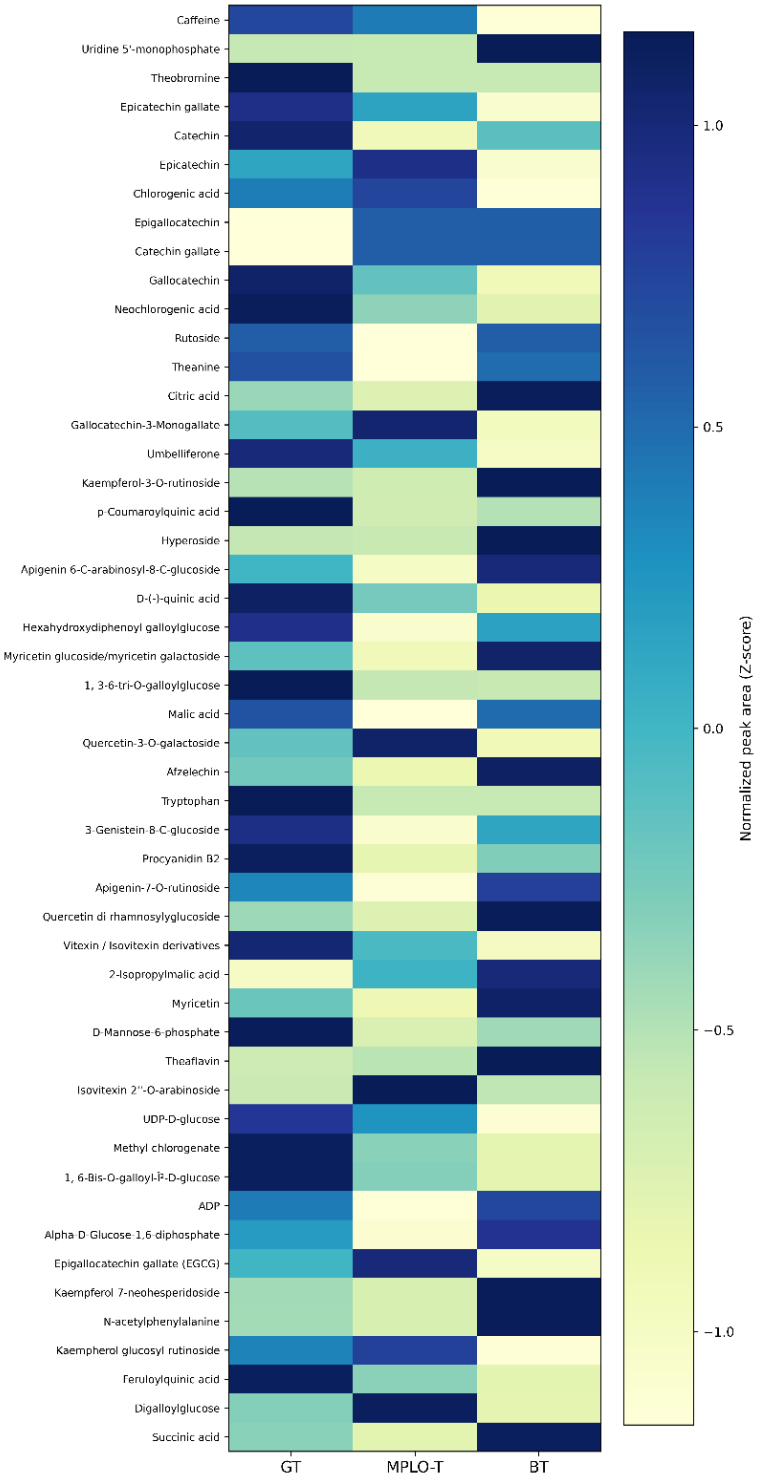

Figure S6.2: Heatmap of the top 50 discriminant metabolites identified by LC–MS across green tea (GT), MPLO-treated tea (MPLO-T), and black tea (BT). Data are presented as Z-score normalized intensities, where blue indicates higher relative abundance and yellow indicates lower abundance. Hierarchical clustering highlights distinct metabolite distribution patterns, with GT enriched in catechins, BT enriched in oxidation-associated metabolites, and MPLO-T displaying an intermediate profile.

Table S6.1: Retention times, calibration ranges, regression equations, correlation coefficients (R^2), and LOD and LOQ values of target compounds determined by HPLC–DAD at 280 nm (n=3).

Compound	RT (min)	Range (µg/mL)	Regression Equation (y = mx + c)	R^2	LOD (µg/mL)	LOQ (µg/mL)
Gallic acid	2.14	3.125–50	y = 0.4565x + 0.0106	0.9985	0.20	0.60
Theabromine	2.507	3.125–50	y = 0.4919x + 0.0187	0.9982	0.06	0.19
GC	2.817	3.125–50	y = 0.02865x + 0.0071	0.9906	0.09	0.27
Theophylline	3.53	3.125–50	y = 0.8855x + 0.0478	0.9966	0.43	1.29
EGC	4.81	3.125–50	y = 0.04684x + 0.0039	0.9964	0.46	1.42
Caffeine	6.293	3.125–50	y = 0.8081x + 0.0512	0.9973	0.37	1.13
EC	10.313	3.125–50	y = 0.1352x + 0.0108	0.9959	0.42	1.27
EGCG	11.18	3.125–50	y = 0.3090x + 0.0184	0.9971	0.81	1.45
GCG	13.417	1.875–30	y = 0.7869x + 0.0215	0.9981	0.08	0.28
Rutin	15.48	3.125–50	y = 0.1776x + 0.0082	0.9984	0.05	0.14
ECG	15.857	3.125–50	y = 0.4476x + 0.0146	0.9990	0.06	0.17
CG	16.08	1.875–30	y = 1.1915x + 0.0321	0.9979	0.84	1.53
Myricetin	19.18	3.125–50	y = 0.2699x + 0.0112	0.9977	0.83	1.50
TF	25.393	3.125–50	y = 0.4902x + 0.0203	0.9979	0.07	0.21
Quercetin	25.903	3.125–50	y = 0.3638x + 0.0157	0.9958	0.25	0.75
TF3G	27.247	3.125–50	y = 0.7209x + 0.0398	0.9961	0.11	0.34
TF3'G	28.237	3.125–50	y = 0.6069x + 0.0286	0.9973	0.19	0.59
TF3-3'G	28.657	3.125–50	y = 0.6282x + 0.0415	0.9902	0.42	0.79
Kaempferol	31.33	3.125–50	y = 0.4256x + 0.0369	0.9924	0.44	1.38

Table S6.2: Putatively annotated metabolites detected in green tea (GT), black tea (BT), and MPLO-treated tea (MPLO-T) by untargeted LC–MS analysis

Section A. Catechins and oxidation-derived products

Compound name	Ionization mode	Mean RT (min)	Mean m/z	Molecular formula	Metabolite class	MPLO-T peak area	GT peak area	BT peak area	Annotation confidence
Catechin	ESI+	5.910	291.086	C15H14O6	Catechins	198153609	1664353614	796854430	MSI Level 1
Epicatechin	ESI−	9.076	289.072	C15H14O6	Catechins	1040704874	850240711	565930215	MSI Level 2
Epigallocatechin	ESI+	9.900	307.081	C15H14O7	Catechins	741557823	569761908	740389055	MSI Level 2
Gallocatechin	ESI−	4.615	305.067	C15H14O7	Catechins	575899403	732283975	479415130	MSI Level 2
Epigallocatechin gallate (EGCG)	ESI−	9.850	457.077	C22H18O11	Catechin gallates	45678901	23456789	876543	MSI Level 1
Epicatechin gallate	ESI−	13.460	441.083	C22H18O10	Catechin gallates	1039129159	1357836611	528589707	MSI Level 1
Catechin gallate	ESI+	13.500	443.098	C22H18O10	Catechin gallates	652841864	586191709	652841864	MSI Level 2
Gallocatechin-3-monogallate	ESI−	9.767	457.078	C22H18O11	Catechin gallates	586063754	390886502	242561816	MSI Level 2
Procyanidin B2	ESI+	9.500	579.150	C30H26O12	Catechin dimers	45238912	128742563	67845219	MSI Level 2
Theaflavin	ESI−	22.580	563.120	C29H24O12	Theaflavin derivatives	7053574	45678	118419777	MSI Level 1
Theaflavin 3′-gallate	ESI−	25.532	715.131	C36H28O16	Theaflavin derivatives	11156449	ND	47564396	MSI Level 2

Theaflavin 3-gallate	ESI−	24.530	715.131	C36H28O16	Theaflavin derivatives	6311705	ND	95567424	MSI Level 2
Theaflavin digallate	ESI−	25.969	867.143	C43H32O20	Theaflavin derivatives	3850604	ND	8202668	MSI Level 2
Neotheaflavin	ESI−	10.899	563.140	C26H28O14	Theaflavin derivatives	2150871	1649564	2486571	MSI Level 2
Degalloyl-oolongtheanin	ESI−	15.436	579.172	C27H32O14	Oxidation-derived catechin products	ND	3766333	2879231	MSI Level 2
Theaflavic acid	ESI−	17.250	427.026	Putative	Oxidation-derived polyphenols	87234	112345	45678	MSI Level 3
Theacitrin A	ESI−	6.280	759.119	Putative	Oxidized catechin derivatives	45234	37890	23456	MSI Level 3
Theasinensin C	ESI−	7.890	913.182	Putative	Catechin dimers	34567	28945	12345	MSI Level 3
Theasinensin F	ESI−	8.450	911.166	Putative	Catechin dimers	45678	67890	23456	MSI Level 3

Section B. Phenolic acids, tannins, and hydrolysable tannins

Compound name	Ionization mode	Mean RT (min)	Mean m/z	Molecular formula	Metabolite class	MPLO-T peak area	GT peak area	BT peak area	Annotation confidence
Gallic acid	ESI−	3.450	169.014	C7H6O5	Phenolic acids	987654	876543	765432	MSI Level 1
Protocatechuic acid	ESI−	3.632	153.018	C7H6O4	Phenolic acids	1604232	3487439	19813719	MSI Level 1
Caffeic acid	ESI−	3.678	179.033	C9H8O4	Hydroxycinnamic acids	7244188	10724266	18518431	MSI Level 1
Chlorogenic acid	ESI−	6.640	353.088	C16H18O9	Quinic acid derivatives	997055778	860361223	219016954	MSI Level 1

Neochlorogenic acid	ESI−	3.678	353.088	C16H18O9	Quinic acid derivatives	372058801	1090812987	163424880	MSI Level 2
p-Coumaroylquinic acid	ESI−	5.329	337.094	C16H18O8	Quinic acid derivatives	132823276	399481204	154435571	MSI Level 2
Digalloylglucose	ESI−	4.314	483.078	C20H20O14	Hydrolysable tannins	16821463	13216659	11947201	MSI Level 2
1,3,6-tri-O-galloylglucose	ESI−	12.053	635.089	C27H24O18	Hydrolysable tannins	60705112	214317580	57725629	MSI Level 2
1,6-Bis-O-galloyl-β-D-glucose	ESI+	3.522	483.078	C20H20O14	Hydrolysable tannins	25504897	41237074	20049518	MSI Level 2
Hexahydroxydiphenoyl galloylglucose	ESI−	6.717	633.073	C27H22O18	Hydrolysable tannins	70929012	182708341	140364784	MSI Level 2
Ellagic acid	ESI−	12.828	300.999	C14H6O8	Hydrolysable tannins	14621311	ND	17812758	MSI Level 1

Section C. Alkaloids, amino acids, and organic acids

Compound name	Ionization mode	Mean RT (min)	Mean m/z	Molecular formula	Metabolite class	MPLO-T peak area	GT peak area	BT peak area	Annotation confidence
Caffeine	ESI+	5.580	195.088	C8H10N4O2	Xanthines	34509585153	41100332819	2137340637	MSI Level 1
Theobromine	ESI+	2.520	181.072	C7H8N4O2	Xanthines	2137340637	3886987990	2137340637	MSI Level 1
Theophylline	ESI−	3.506	179.057	C7H8N4O2	Xanthines	3142454	ND	5183701	MSI Level 1
Theanine	ESI+	1.571	175.108	C7H14N2O3	Amino acid derivatives	313393977	562608166	538618474	MSI Level 1
Tryptophan	ESI+	4.100	205.097	C11H12N2O2	Amino acid derivatives	72552016	113019315	72552016	MSI Level 1

Phenylalanine	ESI−	2.390	164.071	C9H11NO2	Amino acid derivatives	4738525	4769752	5183701	MSI Level 1
Citric acid	ESI−	1.782	191.019	C6H8O7	Organic acids	337573723	376612263	543067614	MSI Level 1
Malic acid	ESI−	1.582	133.013	C4H6O5	Organic acids	67145492	135589376	129862880	MSI Level 1
Succinic acid	ESI−	1.933	117.018	C4H6O4	Organic acids	7335385	11028274	22819079	MSI Level 1
Glutaric acid	ESI−	2.374	131.034	C5H8O4	Organic acids	2301705	1126709	1879534	MSI Level 1
Azelaic acid	ESI−	16.134	187.097	C9H16O4	Organic acids	8965855	5156530	18595078	MSI Level 2

Section D. Selected flavonoid glycosides and related flavonoids

Compound name	Ionization mode	Mean RT (min)	Mean m/z	Molecular formula	Metabolite class	MPLO-T peak area	GT peak area	BT peak area	Annotation confidence
Hyperoside	ESI−	13.387	463.088	C21H20O12	Flavonoid glycosides	11514644	18623646	535372408	MSI Level 2
Kaempferol-3-O-rutinoside	ESI−	14.071	593.152	C27H30O15	Flavonoid glycosides	59132508	117088555	868988730	MSI Level 1
Quercetin-3-O-galactoside	ESI+	13.000	465.103	C21H20O12	Flavonoid glycosides	194294544	85000000	17553140	MSI Level 2
Rutoside	ESI+	12.970	611.161	C27H30O16	Flavonoid glycosides	19271327	717838330	717838330	MSI Level 1
Myricetin	ESI+	12.500	319.045	C15H10O8	Flavonols	10049081	40709774	96892657	MSI Level 2
Kaempferol	ESI−	28.826	285.041	C15H10O6	Flavonols	212345	187654	145678	MSI Level 1
Quercetin	ESI−	22.340	301.035	C15H10O7	Flavonols	765432	654321	432198	MSI Level 1

Abbreviations: GT = green tea; BT = black tea; MPLO-T = microbial polyphenol-oxidizing-like oxidoreductase-treated tea; ND = not detected. Annotation confidence: MSI Level 1 = confirmed using authentic standards; MSI Level 2 = putatively annotated based on accurate mass, retention behavior, and database/literature comparison; MSI Level 3 = putative compound class or unresolved annotation. Analytical note: Peak areas represent relative LC–MS signal intensities and do not indicate absolute metabolite concentrations.

Table S6.3: Volumes of electrolyte stock solutions used to prepare simulated digestion fluids (SSF, SGF, SIF), for a final volume of 400 mL at 1.25× concentration.

Salt solution added	Stock concentration		SSF (pH 7)		SGF (pH 3)		SIF (pH 7)	
	g/L	M	mL added*	Final (mM)	mL added*	Final (mM)	mL added*	Final (mM)
KCl	37.3	0.5	15.1	15.1	6.9	6.9	6.8	6.8
KH2PO4	68	0.5	3.7	3.7	0.9	0.9	0.8	0.8
NaHCO3†	84	1	6.8	13.6	12.5	25	42.5	85
NaCl	117	2	–	–	11.8	47.2	9.6	38.4
MgCl2·6H2O	30.5	0.15	0.5	0.15	0.4	0.12	1.1	0.33
(NH4)2CO3†	48	0.5	0.06	0.06	0.5	0.5	–	–
HCl	–	6	0.09	1.1	1.3	15.6	0.7	8.4
CaCl2·2H2O — added before use‡	44.1	0.3	0.025	1.5	0.005	0.15	0.04	0.6

* Volume of stock solution added per 400 mL of digestion fluid prepared.

† Contributes to the bicarbonate buffer system stabilising fluid pH.

‡ CaCl2·2H2O is added immediately before use, not during stock preparation, to prevent premature precipitation with phosphate and carbonate salts.

Source: reagent volumes and concentrations reproduced from the harmonised INFOGEST static *in vitro* digestion protocol (Brodkorb et al., 2019, Nature Protocols; Minekus et al., 2014, Food & Function), used here for the simulated gastrointestinal digestion described in Section 6.2.9.

MASSEY UNIVERSITY
TE KUNENGA KI PŪREHUROA
UNIVERSITY OF NEW ZEALAND

GRADUATE RESEARCH SCHOOL

STATEMENT OF CONTRIBUTION DOCTORATE WITH PUBLICATIONS/MANUSCRIPTS

We, the student and the student's main supervisor, certify that all co-authors have consented to their work being included in the thesis and they have accepted the student's contribution as indicated below in the Statement of Originality.	
Student name:	Prishanthini Muthulingam
Name and title of main supervisor:	Associate Professor Ali Rashidinejad
In which chapter is the manuscript/published work?	Chapter 3

Describe the contribution that the student and members of the supervisory team have made to the manuscript/published work:[1]

Prishanthini Muthulingam: Writing – original draft, Visualization, Software, Resources, Project administration, Methodology, Investigation, Formal analysis, Data curation, Conceptualization; Ali Rashidinejad: Writing – review & editing, Validation, Supervision, Conceptualization. Carl H. Mesarich: Writing – review & editing, Supervision, Resources, Methodology, Conceptualization. Chandrika M. Nanayakkara: Writing – review & editing, Supervision, Resources;. Punyasiri P.A Nimal: Writing – review & editing, Validation, Supervision, Resources, Conceptualization. David G. Popovich: Writing – review & editing, Supervision, Conceptualization.

Please select one of the following three options:

- (●) **The manuscript/published work is published or in press**

  Please provide the full reference of the research output:

  Muthulingam, P., Rashidinejad, A., Popovich, D., Punyasiri, P. A. N., Nanayakkara, C. M., & Mesarich, C. H. (2025). Microbial polyphenol oxidases in tea catechin oxidation: A novel approach to tea biotransformation. Food and Bioproducts Processing, 154, 731-740. https://10.1016/j.fbp.2025.11.012

- ( ) **The manuscript is currently under review for publication**

  Please provide the name of the journal:

- ( ) **It is intended that the manuscript will be published, but it has not yet been submitted to a journal**

Student's signature:		Main supervisor's signature:	

This form should be placed at the beginning of each relevant thesis chapter.

[1] Refer to the Massey University Publishing and Authorship guidelines (OneMassey for staff, Stream for students) and/ or Contributor Roles Taxonomy (CRediT) guidelines for guidance.

MASSEY UNIVERSITY
TE KUNENGA KI PŪREHUROA
UNIVERSITY OF NEW ZEALAND

GRADUATE RESEARCH SCHOOL

STATEMENT OF CONTRIBUTION DOCTORATE WITH PUBLICATIONS/MANUSCRIPTS

We, the student and the student's main supervisor, certify that all co-authors have consented to their work being included in the thesis and they have accepted the student's contribution as indicated below in the Statement of Originality.	
Student name:	Prishanthini Muthulingam
Name and title of main supervisor:	Associate Professor Ali Rashidinejad
In which chapter is the manuscript/published work?	Chapter 4 (Paper 1)

Describe the contribution that the student and members of the supervisory team have made to the manuscript/published work:[1]

Prishanthini Muthulingam: Writing – original draft, Visualization, Software, Resources, Project administration, Methodology, Investigation, Formal analysis, Data curation, Conceptualization; Ali Rashidinejad: Writing – review & editing, Validation, Supervision, Conceptualization. Carl H. Mesarich: Writing – review & editing, Supervision, Resources, Methodology, Conceptualization. Chandrika M. Nanayakkara: Writing – review & editing, Supervision, Resources;. Punyasiri P.A Nimal: Writing – review & editing, Validation, Supervision, Resources, Conceptualization. David G. Popovich: Writing – review & editing, Supervision, Conceptualization.

Please select one of the following three options:

(●) **The manuscript/published work is published or in press**

Please provide the full reference of the research output:

Muthulingam, P., Rashidinejad, A., Popovich, D., Punyasiri, P. A. N., Nanayakkara, C. M., & Mesarich, C. H. (2025). Microbial polyphenol oxidases in tea catechin oxidation: A novel approach to tea biotransformation. Food and Bioproducts Processing, 154, 731-740. https://10.1016/j.fbp.2025.11.012

( ) **The manuscript is currently under review for publication**

Please provide the name of the journal:

( ) **It is intended that the manuscript will be published, but it has not yet been submitted to a journal**

Student's signature:		Main supervisor's signature:	

This form should be placed at the beginning of each relevant thesis chapter.

[1] Refer to the Massey University Publishing and Authorship guidelines (OneMassey for staff, Stream for students) and/ or Contributor Roles Taxonomy (CRediT) guidelines for guidance.

MASSEY UNIVERSITY
TE KUNENGA KI PŪREHUROA
UNIVERSITY OF NEW ZEALAND

GRADUATE RESEARCH SCHOOL

STATEMENT OF CONTRIBUTION
DOCTORATE WITH PUBLICATIONS/MANUSCRIPTS

We, the student and the student's main supervisor, certify that all co-authors have consented to their work being included in the thesis and they have accepted the student's contribution as indicated below in the Statement of Originality.	
Student name:	Prishanthini Muthulingam
Name and title of main supervisor:	Associate Professor Ali Rashidinejad
In which chapter is the manuscript/published work?	Chapter 4 (Paper 2)

Describe the contribution that the student and members of the supervisory team have made to the manuscript/published work:[1]

Prishanthini Muthulingam: Writing – original draft, Visualization, Software, Resources, Project administration,Methodology, Investigation, Formal analysis, Data curation, Conceptualization; Ali Rashidinejad: Writing – review & editing, Validation, Supervision, Conceptualization. Carl H. Mesarich: Writing – review & editing, Supervision, Resources, Methodology, Conceptualization. Chandrika M. Nanayakkara: Writing – review & editing, Supervision, Resources;. Punyasiri P.A Nimal: Writing – review & editing, Validation, Supervision, Resources, David G. Popovich: Writing – review & editing, Supervision.

Please select one of the following three options:

○	**The manuscript/published work is published or in press** Please provide the full reference of the research output:
◉	**The manuscript is currently under review for publication** Please provide the name of the journal: Journal of Food Science and Technology (Springer)
○	**It is intended that the manuscript will be published, but it has not yet been submitted to a journal**

Student's signature:		Main supervisor's signature:	

This form should be placed at the beginning of each relevant thesis chapter.

[1] Refer to the Massey University Publishing and Authorship guidelines (OneMassey for staff, Stream for students) and/ or Contributor Roles Taxonomy (CRediT) guidelines for guidance.

MASSEY UNIVERSITY
TE KUNENGA KI PŪREHUROA
UNIVERSITY OF NEW ZEALAND

GRADUATE RESEARCH SCHOOL

STATEMENT OF CONTRIBUTION
DOCTORATE WITH PUBLICATIONS/MANUSCRIPTS

We, the student and the student's main supervisor, certify that all co-authors have consented to their work being included in the thesis and they have accepted the student's contribution as indicated below in the Statement of Originality.	
Student name:	Prishanthini Muthulingam
Name and title of main supervisor:	Associate Professor Ali Rashidinejad
In which chapter is the manuscript/published work?	Chapter 5

Describe the contribution that the student and members of the supervisory team have made to the manuscript/published work:[1]

Prishanthini Muthulingam: Writing – original draft, Visualization, Software, Resources, Project administration, Methodology, Investigation, Formal analysis, Data curation, Conceptualization; Ali Rashidinejad: Writing – review & editing, Validation, Supervision, Conceptualization. Carl H. Mesarich: Writing – review & editing, Supervision, Resources, Methodology, Conceptualization. Chandrika M. Nanayakkara: Writing – review & editing, Supervision, Resources;. Punyasiri P.A Nimal: Writing – review & editing, Validation, Supervision, Resources, Conceptualization. David G. Popovich: Writing – review & editing, Supervision, Conceptualization.

Please select one of the following three options:

○	**The manuscript/published work is published or in press** Please provide the full reference of the research output:
○	**The manuscript is currently under review for publication** Please provide the name of the journal:
◉	**It is intended that the manuscript will be published, but it has not yet been submitted to a journal**

Student's signature:		Main supervisor's signature:	

This form should be placed at the beginning of each relevant thesis chapter.

[1] Refer to the Massey University Publishing and Authorship guidelines (OneMassey for staff, Stream for students) and/ or Contributor Roles Taxonomy (CRediT) guidelines for guidance.

MASSEY UNIVERSITY
TE KUNENGA KI PŪREHUROA
UNIVERSITY OF NEW ZEALAND

GRADUATE RESEARCH SCHOOL

STATEMENT OF CONTRIBUTION
DOCTORATE WITH PUBLICATIONS/MANUSCRIPTS

We, the student and the student's main supervisor, certify that all co-authors have consented to their work being included in the thesis and they have accepted the student's contribution as indicated below in the Statement of Originality.	
Student name:	Prishanthini Muthulingam
Name and title of main supervisor:	Associate Professor Ali Rashidinejad
In which chapter is the manuscript/published work?	Chapter 6
Describe the contribution that the student and members of the supervisory team have made to the manuscript/published work:[1] Prishanthini Muthulingam: Writing – original draft, Visualization, Software, Resources, Project administration, Methodology, Investigation, Formal analysis, Data curation, Conceptualization; Ali Rashidinejad: Writing – review & editing, Validation, Supervision, Conceptualization. Carl H. Mesarich: Writing – review & editing, Supervision, Resources, Methodology, Conceptualization. Chandrika M. Nanayakkara: Writing – review & editing, Supervision, Resources;. Punyasiri P.A Nimal: Writing – review & editing, Validation, Supervision, Resources, Conceptualization. David G. Popovich: Writing – review & editing, Supervision, Conceptualization.	
Please select one of the following three options:	
○ The manuscript/published work is published or in press Please provide the full reference of the research output:	
○ The manuscript is currently under review for publication Please provide the name of the journal:	
◉ It is intended that the manuscript will be published, but it has not yet been submitted to a journal	
Student's signature: 	Main supervisor's signature: 
This form should be placed at the beginning of each relevant thesis chapter.	

[1] Refer to the Massey University Publishing and Authorship guidelines (OneMassey for staff, Stream for students) and/ or Contributor Roles Taxonomy (CRediT) guidelines for guidance.